



Study of centrifugal and resonance effects in the asymmetric and spherical top molecules: C₂D₄, ClO₂, CD₄, SiF₄

Mariia Merkulova

► To cite this version:

Mariia Merkulova. Study of centrifugal and resonance effects in the asymmetric and spherical top molecules: C₂D₄, ClO₂, CD₄, SiF₄. Optics [physics.optics]. Université Bourgogne Franche-Comté; Université polytechnique de Tomsk (Russie), 2024. English. NNT : 2024UBFCK078 . tel-04951222

HAL Id: tel-04951222

<https://theses.hal.science/tel-04951222v1>

Submitted on 17 Feb 2025

HAL is a multi-disciplinary open access archive for the deposit and dissemination of scientific research documents, whether they are published or not. The documents may come from teaching and research institutions in France or abroad, or from public or private research centers.

L'archive ouverte pluridisciplinaire **HAL**, est destinée au dépôt et à la diffusion de documents scientifiques de niveau recherche, publiés ou non, émanant des établissements d'enseignement et de recherche français ou étrangers, des laboratoires publics ou privés.



RESEARCH SCHOOL
OF HIGH-ENERGY
PHYSICS

UNIVERSITÉ BOURGOGNE FRANCHE-COMTÉ
Laboratoire Interdisciplinaire Carnot de Bourgogne – UMR CNRS 6303
TOMSK POLYTECHNIC UNIVERSITY
Research School of High-Energy Physics

**Study of centrifugal and resonance effects
in the asymmetric and spherical top molecules: C₂D₄, ClO₂, CD₄, SiF₄**
by

Mariia MERKULOVA

A Thesis in Physics Submitted for the Degree of
Doctor of Philosophy

Date of defence: December 20, 2024

Mrs Maud ROTGER	Professor Université de Reims Champagne-Ardenne - GSMA	Reviewer President of the Jury
Mr Pierre BÉJOT	CNRS Researcher Université Bourgogne	Examiner
Mr Valery PEREVALOV	Professor Institute of Atmospheric Optics, Siberian branch of Russian Academy of Sciences	Examiner
Mrs Nina LAVRENTIEVA	Professor Institute of Atmospheric Optics, Siberian branch of Russian Academy of Sciences	Reviewer
Mrs Olga GROMOVA	Professor National Research Tomsk Polytechnic University - RSHEP	Invited
Mr Vincent BOUDON	CNRS Senior Researcher Université Bourgogne - ICB Laboratoire	Supervisor
Mr Oleg ULENIKOV	Professor National Research Tomsk Polytechnic University - RSHEP	Supervisor

Laboratoire Interdisciplinaire Carnot de Bourgogne – UMR CNRS 6303
Université Bourgogne Franche-Comté, 9 Avenue A. Savary 21078 Dijon, France

Research School of High-Energy Physics
Tomsk Polytechnic University, 30 Lenin Avenue, 634050 Tomsk, Russia

Contents

Introduction	4
Chapter 1	
Methods of theoretical study of vibrational-rotational molecular spectra	6
1.1. The vibrational-rotational Hamiltonian of a molecule	6
1.2. Elements of isotopic substitution theory.....	13
1.3. Irreducible tensor operators theory	17
1.4. The vibrational Hamiltonian considering tetrahedral splittings	20
1.5. Vibrational polyads.....	21
Chapter 2	
Theoretical study on high-resolution spectra of asymmetric tops: C₂D₄ и ClO₂ molecules.....	23
2.1. Ethylene C ₂ D ₄	23
2.1.1. Description and theoretical background of the deuterated ethylene molecule	23
2.1.2. Results of the study of the vibrational-rotational structure of the spectra of the C ₂ D ₄ molecule. v ₅ + v ₁₂ and v ₆ + v ₁₁ combination bands	26
2.2. Chlorine dioxide ClO ₂	30
2.2.1. Theoretical description of molecules in non-singlet electronic states	30
2.2.2. Analysis of the vibrational and rotational structure of the spectra of ClO ₂ molecule. Fundamental band v ₃ and combination band v ₁ + v ₃	32
Chapter 3	
Theoretical study on high-resolution spectra of spherical tops: CD₄, SiF₄ and SiH₄ molecules... 	36
3.1. Deuterated methane isotopologue CD ₄	36
3.1.1. Theoretical methods for describing the spectra of spherical top molecule methane CD ₄	36
3.1.2. Results of analysis of vibrational-rotational energies and line intensities of CD ₄ methane in the region of the v ₂ /v ₄ dyad.....	39
3.2. Silicon tetrafluoride – silane SiF ₄	44

3.2.1. Theoretical methods for describing the spectra of spherical top silane SiF ₄ molecule.....	45
3.2.2. Analysis of combination bands spectra of SiF ₄	46
3.3. Silane SiH ₄	50
3.3.1. Study of the shape and absolute intensity of the spectrum lines of silane SiH ₄	50
Conclusion.....	52
Publications on the thesis topic	54
Bibliography	57
Appendix A. Figure for Chapter 1.....	68
Appendix B. Figures for Chapter 2	69
Appendix C. Tables for Chapter 2	75
Appendix D. Tables for Chapter 3	97

Introduction

The study of rotational and vibrational-rotational spectra of polyatomic molecules in the gas phase has long been of fundamental importance for determining the exact molecular geometry in various vibrational states, for obtaining information on the internal force field, vibrational-rotational interaction parameters, dipole moments, calculating thermodynamic functions from structural and vibrational data, and, in general, for obtaining information on the relationship between the structure and physical properties of a molecule.

The importance of studying vibrational-rotational states of polyatomic molecules has recently increased markedly due to the advent of high-resolution spectroscopy and significant advances in theoretical and experimental studies of the fine structure of vibrational-rotational spectra of molecules.

The analysis of the electromagnetic spectrum of a molecule allows us to obtain information about its energy levels, and the position of these energy levels directly depends on the internal physical characteristics of the molecule. Thus, the analysis of molecular spectra makes it possible to extract a variety of physical parameters describing the internal properties of molecules. Moreover, the information obtained from spectra is characterized by a high degree of accuracy and is important for a deeper understanding of the internal properties of molecules [1].

The structure and properties of a molecule depend directly on its symmetry. This dependence is displayed in high-resolution spectra, and thus, the study of spectra of molecules of different symmetries requires the use of special methods and approaches, as well as taking into account known peculiarities and possible difficulties. For example, when studying the spectra of molecules belonging to the class of spherical top (for which all three moments of inertia are equal), traditional methods and approaches, such as the combination difference method, are inapplicable. Due to the high (e.g., tetrahedral, T_d) symmetry of spherical tops, the spectra of such molecules exhibit the so-called “tetrahedral splitting”, which greatly complicates the mathematical description of such spectra. The presence of “hot” bands in the spectra complicates the lines interpretation in the spectrum, since the spectrum becomes very dense; the lines are mixed and sometimes completely overlap.

Molecules belonging to the class of asymmetric top (all three moments of inertia are unequal) have a weak degree of symmetry. Their study can be complicated by the presence of lines belonging to the “hot” bands. A correct and complete study of such spectra requires specially selected experimental conditions capable of reducing the influence of the presence of hot bands.

Among molecules of the asymmetric top type, a particular place is occupied by molecules in degenerate electronic states. The study of such molecules requires a special approach to the description of non-singlet electronic states. At present, there is a lack of guaranteed accurate methods for describing the spectra of these molecules to fulfil the need for highly accurate quantitative information on the

parameters of spectral lines. Therefore, there is a need to develop specific methods that can theoretically justify the behaviour of the current high-resolution experimental spectra of such molecules.

These difficulties, as well as the mentioned practical significance of the information obtained by analysing spectra for various fields of physics, chemistry, materials science, biology, astronomy and atmospheric optics determine the relevance of the topic of the research carried out within the framework of the thesis. The work is devoted to obtaining new high-precision information by investigating high-resolution spectra of spherical and asymmetric top molecules, as well as developing new and improving existing methods for analysing spectra of molecules in non-singlet electronic states. Thus, **the aim of this work** was formulated:

- Obtaining theoretical data on the line positions corresponding to vibrational-rotational transitions in the spectra of SiF₄, CD₄, C₂D₄, ClO₂ molecules and their isotopologues for further solution of the inverse spectroscopic problem and obtaining the parameters of the effective Hamiltonian for excited vibrational-rotational bands.
- Obtaining theoretical spectra of the “hot” bands of the SiF₄ molecule using the obtained experimental values of the effective Hamiltonian parameters of combination bands.
- Obtaining theoretical data on the line intensities corresponding to vibrational-rotational transitions in the spectrum of SiH₄ molecules to obtain dipole moment parameters.

Achieving the set goals requires the solution of several **tasks**:

1. To analyse the line positions of vibrational-rotational spectra of combination bands of SiF₄, CD₄, C₂D₄, ClO₂ molecules and their isotopologues.
2. Solve the inverse spectroscopic problem for the studied bands.
3. Using the obtained spectroscopic parameters for the SiF₄ combination bands and XTDS software package calculate the positions of the lines and construct the theoretical spectrum of the “hot” bands of this molecule up to 14 polyad.
4. Obtain new high-precision spectra of the ground state of SiH₄ molecule, analyse the intensities of the spectra lines to improve the data on the dipole moment parameters.

The methods of quantum mechanics, group theory and the apparatus of the theory of irreducible tensor operators were used to solve the set problems.

Chapter 1

Methods of theoretical study of vibrational-rotational molecular spectra

This chapter provides fundamental information related to the theory of vibrational-rotational spectroscopy of polyatomic molecules. In particular, the fundamental principles underlying the theoretical description of a molecule as a quantum system, on which the methods of theoretical modelling of the energy structure of molecules are based, are discussed, and tools for the analysis of molecular spectra with low and high degree of symmetry are reviewed. These aspects are considered to be an essential part of the overall methodology and are the basis for understanding the results and conclusions presented hereafter.

1.1. The vibrational-rotational Hamiltonian of a molecule

Transitions between different quantum states of a molecule, which are studied in vibrational-rotational spectroscopy, represent the results of time-evolution of a molecular system during non-destructive interaction with electromagnetic radiation. For an isolated molecule, such processes can be described by the time-dependent Schrödinger equation:

$$i\hbar \frac{\partial \Psi}{\partial t} = \mathbf{H}\Psi \quad (1.1.1)$$

where Ψ is the total time-dependent wave function depending on the coordinates q of the system of particles and time t .

Typically, spectroscopy uses non-relativistic Hamiltonians that have the following form:

$$\mathbf{H} = T_{\text{nucl}} + T_{\text{el}} + V, \quad (1.1.2)$$

where T_{nucl} and T_{el} are the operators describing the kinetic energy of nuclei and electrons; V is the potential energy operator of the molecule, which includes the electric attraction energy of electrons to nuclei and the repulsion energy between electrons and nuclei. As the potential energy operator V does not depend on time, we can use the time-independent Schrödinger equation. Let us write the operators T_{nucl} , T_{el} and V as follows:

$$T_{\text{nucl}} = \frac{-\hbar^2}{2} \sum_N \frac{1}{m_N} \left(\frac{\partial^2}{\partial x_N^2} + \frac{\partial^2}{\partial y_N^2} + \frac{\partial^2}{\partial z_N^2} \right), \quad (1.1.3)$$

$$T_{el} = \frac{-\hbar^2}{2m_e} \sum_i \left(\frac{\partial^2}{\partial x_i^2} + \frac{\partial^2}{\partial y_i^2} + \frac{\partial^2}{\partial z_i^2} \right),$$

$$V = \sum_{\substack{i,j \\ i>j}} \frac{e^2}{r_{ij}} + \sum_{\substack{N,N' \\ N>N'}} \frac{Z_N Z_{N'}}{r_{NN'}} - \sum_{i,N} \frac{e Z_N}{r_{iN}},$$

where m_N and m_e are the masses of nuclei and electrons, respectively; z_N is the charge of the nuclei; r_{ab} is the distance between particles a and b . Note that x_N , x_i are the coordinates of nuclei and electrons in the Cartesian space-fixed system (SFS).

Although expression (1.1.2) for the Hamiltonian in terms of space-fixed coordinates of atomic nuclei and electrons has a simple form, its numerical integration will be very complicated even for a simple molecular system. Furthermore, we know from physical experiments that bonding electrons hold the atomic nuclei of a molecule in a configuration with approximately fixed bond lengths and valence angles. From the point of view of classical mechanics, such a system of atomic nuclei and electrons can exhibit translational and rotational motion in space: the atomic nuclei can oscillate in the configuration given by the electronic structure of the molecule; the electrons of the molecule can move around the atomic nuclei.

The quantum mechanical description of these motions should yield the vibrational, rotational and electronic energy levels and the corresponding wave functions of the Schrödinger equation for this system. The most convenient approach to solving this problem is to develop a model for the motions of a molecule which would allow for description of such a system in terms of its translation, its overall rotation, the vibration of its atomic nuclei and its electronic motions. This can be achieved by replacing the space-fixed coordinates of the atomic nuclei and electrons with a new system of coordinates that refer to a movable system of x , y , z axes fixed at the centre of mass of the molecule. The movable system of x , y , z axes will follow the movement of the whole molecule and will be bound to the rigid equilibrium configuration of the atomic nuclei, i. e. all components of the angular momentum of the equilibrium configuration with respect to the x , y , z axes will disappear. Therefore, we will call the system of x , y , z axes a molecular fixed system (MFS).

The resulting Hamiltonian then assumes a more complicated form than that corresponding to eq. (1.1.2), but a clear physical interpretation can be given to its individual terms occurring. Furthermore, successive approximations to the complete vibrational-rotational Hamiltonian can be found. This has the advantage that the Schrödinger equation in the simplest approximation frequently has a simple analytical solution which can be used in solving the problem to higher approximations by a standard perturbation or variational approach.

One of the most successful coordinate transformations, by which it becomes possible to separate different types of motions in a molecule, is the transformation [1]:

$$\begin{aligned}x_{N\alpha} &= R_\alpha + \sum_\beta k_{\alpha\beta} \tilde{r}_{N\beta}, \\x_{i\alpha} &= R_\alpha + \sum_\beta k_{\alpha\beta} \tilde{r}_{i\beta},\end{aligned}\tag{1.1.4}$$

Here $x_{N\alpha}$ and $x_{i\alpha}$ are the components of the vector describing the N^{th} atom and the i^{th} electron in the Cartesian coordinate system; R_α is the vector of the origin of the molecular-fixed coordinate system relative to the space-fixed system; $k_{\alpha\beta}$ are the directional cosines matrices of the angles between the axes of the old and new coordinate systems (also known as the Euler angle functions). The molecular-fixed coordinate system is defined so that its origin is at the centre of mass of the whole molecule, which can be written as:

$$\sum_N m_N \tilde{r}_{N\beta} + \sum_i m_e \tilde{r}_{i\beta} = 0.\tag{1.1.5}$$

Here $\tilde{r}_{i\beta}$ represents the coordinate component of the i^{th} electron in the molecularly fixed system; we give below the expression for the coordinates $\tilde{r}_{N\beta}$ of the N^{th} atom:

$$\tilde{r}_{N\beta} = \tilde{r}_{N\beta}^e + \sum_\lambda m_N^{-\frac{1}{2}} l_{N\beta\lambda} Q_\lambda,\tag{1.1.6}$$

where Q_λ represents the vibrational coordinates.

The constants $\tilde{r}_{N\beta}$ and $l_{N\beta\lambda}$ are usually arbitrary, but they are chosen based on mandatory conditions:

1. $\tilde{r}_{N\beta}$ corresponds to $\tilde{r}_{N\beta}^e$ when the configuration of the nuclei are in equilibrium;
2. the axes of the molecular fixed coordinate system coincide with the principal axes of inertia of the molecule when the configuration of the nuclei are in equilibrium;
3. the vibrations are normal;
4. the Eckart conditions are satisfied.

Since the coordinates of Q are independent, these conditions can be expressed mathematically as follows:

$$\sum_N m_N \tilde{r}_{N\beta}^e + \sum_i m_e \tilde{r}_{i\beta} = 0,\tag{1.1.7}$$

$$\sum_N m_N \tilde{r}_{N\alpha}^e \tilde{r}_{N\beta}^e = 0, \alpha \neq \beta,\tag{1.1.8}$$

$$\sum_{N,\alpha} l_{N\alpha\lambda} l_{N\alpha\mu} = \delta_{\lambda\mu}, \quad (1.1.9)$$

$$\sum_N m_N^{\frac{1}{2}} l_{N\gamma\lambda} = 0, \quad (1.1.10a)$$

$$\sum_{N\beta\gamma} \varepsilon_{\alpha\beta\gamma} m_N^{\frac{1}{2}} \tilde{r}_{N\beta}^e l_{N\gamma\lambda} = 0, \quad (1.1.10b)$$

The conditions (1.1.10a) and (1.1.10b) are called the first and the second Eckart conditions [2].

Here $\varepsilon_{\alpha\beta\gamma}$ is a completely antisymmetric tensor, i. e.:

$$\varepsilon_{\alpha\beta\gamma} = \begin{cases} 1 & \text{if } \alpha, \beta, \gamma \text{ is a cyclic permutation of indices } x, y, z; \\ 0 & \text{if } \alpha = \beta, \beta = \gamma \text{ or } \alpha = \gamma; \\ -1 & \text{for all other cases.} \end{cases}$$

Thus, the coordinate transformation (1.1.4) is given explicitly.

However, we note that the presented scheme for introducing new coordinates has a significant disadvantage: to determine the coordinates of electrons and nuclei, it is necessary at each moment to know not only the configuration of the nuclei, but also the location of all electrons with respect to the nuclei, since the position of the centre of the new coordinate system is located at the centre of mass of the entire molecule. As a result, the problem becomes much more complicated.

Therefore, the most correct definition of the new coordinates is when $r_{N\beta}$ and $r_{i\beta}$ are counted from the centre of mass of the nuclei rather than the whole molecule. In this case, the expressions for the transformation of coordinates will be written in the following form:

$$x_{N\alpha} = R_\alpha + \sum_\beta k_{\alpha\beta} \left(r_{N\beta}^e + \sum_\lambda m_N^{-\frac{1}{2}} l_{N\beta\lambda} Q_\lambda - \frac{m_0}{M} \sum_i r_{i\beta} \right), \quad (1.1.11)$$

and

$$x_{i\alpha} = R_\alpha + \sum_\beta k_{\alpha\beta} \left(r_{i\beta}^e - \frac{m_e}{M} \sum_j r_{j\beta} \right), \quad (1.1.12)$$

where $r_{N\beta}$ and $r_{i\beta}$ are the positions of electrons and nuclei relative to the centre of mass of the molecule's nuclei.

Now that we know the mathematically expressed rules (1.1.11), (1.1.12) for the coordinate transformation, we can determine the transformation law for the momentum operators $P_{N\alpha} = -i\hbar \frac{\partial}{\partial x_{N\alpha}}$ and $P_{i\alpha} = -i\hbar \frac{\partial}{\partial x_{i\alpha}}$. Let us use the fact that these formulas were obtained from the polynomial [3]:

$$L = \sum_i \frac{m_e}{2} \dot{x}_i^2 + \sum_N \frac{m_N}{2} \dot{x}_N^2 + V, \quad (1.1.13)$$

The transformations for expressing the classical quantities $P_{N\alpha}$ and $P_{i\alpha}$ through the corresponding quantities in the molecular coordinate system are shown in detail in [4]. Thus, the expressions for the operators take the following form:

$$P_{i\alpha} = \frac{m_e}{M} P_\alpha + \sum_\beta k_{\alpha\beta} P_{i\beta}, \quad (1.1.14)$$

$$\begin{aligned} P_{N\alpha} = & \frac{m_N}{M} P_\alpha + \sum_\beta k_{\alpha\beta} \left\{ \sum_\lambda m_N^{\frac{1}{2}} l_{N\beta\lambda} P_\lambda + \sum_{\gamma\delta} \sum_{\lambda\mu} m_N^{1/2} l_{N\beta\lambda} \xi_{\lambda\mu}^\gamma \mu_{\gamma\delta} Q_\mu N_\delta - \right. \\ & \left. - m_N \sum_{\gamma\delta\chi} \varepsilon_{\beta\gamma\delta} r_{N\gamma}^e \mu_{\delta\chi} N_\chi - \sum_\lambda m_N^{1/2} Q_\lambda \sum_{\gamma\delta\chi} \varepsilon_{\beta\gamma\delta} l_{N\gamma\lambda} \mu_{\delta\chi} \times N_\chi - \frac{m_e}{M_N} \sum_j P_{j\beta} \right\}. \end{aligned} \quad (1.1.15)$$

Here $M_N = \sum_N m_N$ is the total mass of all nuclei; $P_\alpha = -i\hbar \frac{\partial}{\partial R_\alpha}$, $P_\lambda = -i\hbar \frac{\partial}{\partial Q_\lambda}$; $\mu_{\gamma\delta}$ are the elements of the matrix of inverse moments of inertia; $\xi_{\lambda\mu}^\gamma$ are the Coriolis constants expressed through the constants of the oscillation forms:

$$\mu_{\alpha\beta}^{-1} = \sum_{\gamma\delta} I''_{\alpha\gamma} I_{\gamma\delta}^{e-1} I''_{\delta\beta}; \quad (1.1.16)$$

$$I''_{\alpha\beta} = \delta_{\alpha\beta} \sum_N m_N \sum_\gamma (r_{N\gamma}^e)^2 - \sum_N m_N r_{N\alpha}^e r_{N\beta}^e + \frac{1}{2} \sum_\lambda a_\lambda^{\alpha\beta} Q_\lambda; \quad (1.1.17)$$

N_α are operators having the form $N_\alpha = J_\alpha - G_\alpha - L_\alpha$, where J_α expresses the components of the total angular momentum; $G_\alpha = \sum_{\lambda\mu} \zeta_{\lambda\mu}^\alpha Q_\lambda P_\mu$ are components of the vibrational angular momentum; $L_\alpha = \sum_{\beta\gamma} \varepsilon_{\alpha\beta\gamma} \sum_i r_{i\beta} P_{i\gamma}$ are components of the electronic angular momentum. It should be noted that the appearance of the last term in eq. (1.1.15) is due to the fact that the centre of mass of the whole molecule does not coincide with the centre of mass of the nuclei. However, in the further application of the Born-Oppenheimer approximation, the masses of electrons are assumed to be infinitesimal compared to the

masses of nuclei, and thus the centre of mass of the molecule coincides with the centre of mass of nuclei, and the last term in the formula disappears.

To obtain the Hamiltonian expressed through the coordinates of the molecular-fixed coordinate system, we will use directly the eq. (1.1.11), (1.1.12), (1.1.14) and (1.1.15). After the simplification procedure, taking into account the symmetry of the matrices (1.1.16) and (1.1.17), we obtain the final expression for the operators:

$$P_{N\alpha} = \frac{m_N}{M} P_\alpha + \sum_\beta k_{\alpha\beta} \left\{ \sum_\lambda m_N^{1/2} l_{N\beta\gamma} P_\lambda - \sum_{\gamma\delta\chi} m_N \varepsilon_{\beta\gamma\chi} r_{N\gamma}^e I_{\chi\delta}^{\prime\prime-1} N_\delta \right\}. \quad (1.1.18)$$

Taking into account the fact that at transition to a new coordinate system the normalisation conditions of the wave functions change [5], the final Hamiltonian will take the following form:

$$\begin{aligned} \mathbf{H} = & \sum_\alpha \frac{P_\alpha^2}{2M} + \frac{1}{2m_{el}} \sum_{i\alpha} P_{i\alpha}^2 + \frac{1}{2M_N} \sum_\alpha \left(\sum_i P_{i\alpha} \right)^2 + \frac{1}{2} \sum_\lambda P_\lambda^2 + \\ & + \frac{1}{2} \sum_{\alpha\beta} (J_\alpha - G_\alpha - L_\alpha) \tilde{\mu}_{\alpha\beta} (J_\beta - G_\beta - L_\beta) + V. \end{aligned} \quad (1.1.19)$$

Here, the first term describes the translational motion of the molecule as a whole; the second term describes the kinetic energy of the electrons; the third term, due to the difference between the centre of nuclei mass and the whole molecule, is responsible for the mass isotopic energy shift; the fourth and fifth terms describe the vibrational motion of the nuclear frame and its rotation in space, respectively; the operator V represents the potential energy operator of the electric attraction of electrons to nuclei and the repulsion energy between electrons and nuclei.

It should be remembered that the transformations of the Hamiltonian described above are valid only for nonlinear molecules. This is due to the fact that, unlike a nonlinear molecule, a linear molecule can be defined in space not by three but only by two coordinates, which essentially affects the formulas for transforming the coordinate and momentum operators; in addition, one of the moments of inertia of a linear molecule turns to zero.

As mentioned above, a molecule can be considered as a set of electrons and nuclei bound by Coulomb forces. The Schrödinger equation for such a general model of the molecule as a whole allows one to obtain spectroscopic information on molecular states, but it turns out to be inconvenient even for preliminary evaluations and qualitative discussions. Therefore, in such cases one turns to particular model which will be discussed further below [6].

The vibrational model describes a molecule as a set of material points bound together by elastic forces. The rotational model of a molecule can be thought of as a set of material points fixed relative to

each other in an equilibrium configuration. From the point of view of such a “rotational” model, the molecule can be considered as a spinning top.

The electron model assumes that nuclei are fixed in an equilibrium configuration and electrons move in their Coulomb field. In many cases it can be considered that the states of nuclei motion corresponding to a given electronic state are determined by the Schrödinger equation for nuclei, in which the potential energy operator is taken to be the corresponding adiabatic potential. In a two-atomic molecule, the displacements of the nuclei from the equilibrium position are described by a single coordinate defining the change of the internuclear distance, and, in this case, the adiabatic potentials are described as curves in the plane (Figure 1.1(a)). For a polyatomic molecule, the space of coordinates describing the displacements of the nuclei relative to each other is multidimensional, and the adiabatic potentials are hypersurfaces in this space (Figure 1.1 (b)).

The concept of potential hypersurfaces, the intramolecular potential function (IMPF) and the equilibrium structure of a molecule in quantum mechanics is described using the Born-Oppenheimer approximation.

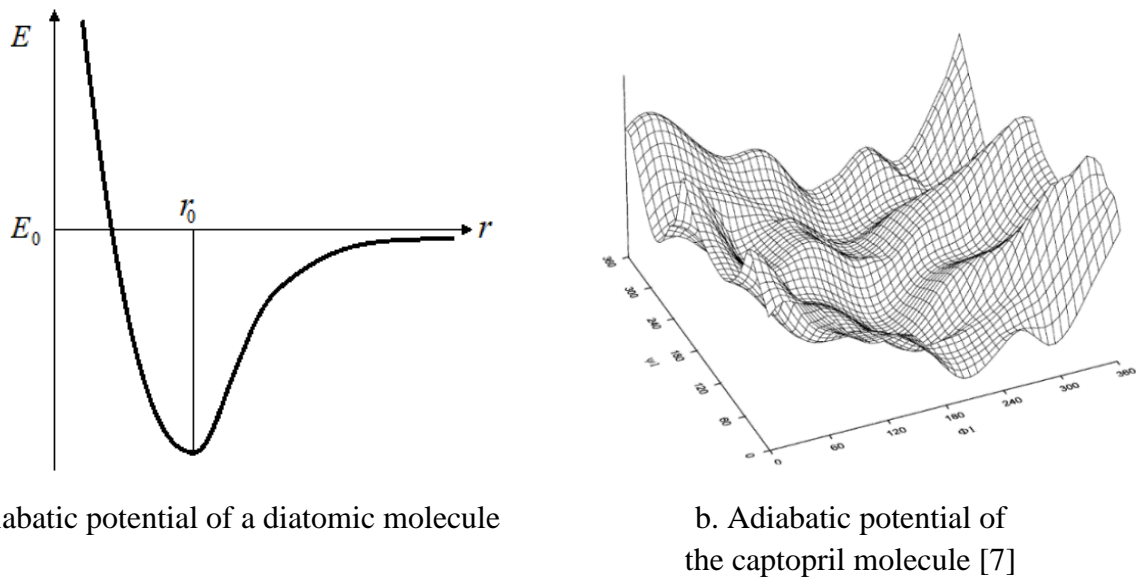


Figure 1.1 – Graphical representation of IMPF.

In this approximation, it is assumed that the molecular wave function can be written as $\Psi = \Psi_{\text{el}}\Psi_{\text{vib}}\Psi_{\text{rot}}$ and thus the energies due to each type of motion are additive:

$$E = E_{\text{el}} + E_{\text{vib}} + E_{\text{rot}} \quad (1.1.20)$$

The application of the Born-Oppenheimer approximation leads naturally to the description of the molecule as a rigid rotor – the rotation is considered separately from the vibrational motion of the nuclei,

which will be further described as a perturbation. The largest contribution to the energy of the molecule is given by the electron motion around the nuclei, followed by the contribution of nuclear vibrations and, finally, by nuclear rotation. The basis for the possibility of such a classification is the comparative values of nuclear and electronic masses.

It can be shown that the Hamiltonian in such a case breaks into parts differing by the order of smallness:

$$H = H_e + H_1 + H_2 \quad (1.1.21)$$

where

$$H_e = \frac{1}{2} m_e \sum_{j\alpha} P_{j\alpha}^2 + V_{r,Q}(r, Q), \quad (1.1.22)$$

$$H_1 = \frac{1}{2} \sum_{\alpha\beta} \mu_{\alpha\beta} (J_\alpha - P_\alpha)(J_\beta - P_\beta) + \frac{1}{2} \sum_\alpha \frac{P_\alpha}{2M} + \frac{1}{2} \sum_\lambda P_\lambda^2, \quad (1.1.23)$$

$$H_2 = \frac{1}{2M_N} \sum_\alpha \left(\sum_i P_{i\alpha} \right)^2 + \frac{1}{2} \sum_{\alpha\beta} \tilde{\mu}_{\alpha\beta} (L_\alpha L_\beta - (J_\alpha - G_\alpha)L_\beta - L_\alpha(J_\beta - G_\beta)). \quad (1.1.24)$$

Note that the obtained eigenfunctions and the values of the Hamiltonian H_e depend parametrically on the distance in Δr_{NK} of the molecule. The error introduced by using this approximation is much smaller than the errors introduced by other approximations.

The fact that in this approximation the IMPF is the same for all isotopic modifications of the molecule allows us to use experimental information on all possible isotopologues to analyse vibrational-rotational spectra, thereby increasing the accuracy of the spectroscopic problem being solved.

1.2. Elements of isotopic substitution theory

The concept of “isotopic effects” implies a change in certain properties of the molecules under study when one type of nuclei is changed from one to another. To solve many problems of vibrational-rotational spectroscopy, it is necessary to estimate spectroscopic parameters, spectral line parameters, and knowledge of molecular constants. One of the effective tools for obtaining this kind of information is the isotopic dependence of the mentioned parameters, which allows one to work under conditions with no initial data on the molecule under study.

The kinetic isotope effect arises mainly due to changes in the ground vibrational states caused by isotopic perturbation along the minimum energy path of the potential energy surface, which can only be explained by quantum mechanical treatment of the system.

The dependence of molecular parameters on atomic masses such as harmonic frequencies, anharmonic constants and others is determined in the potential function according to the fact that the normal coordinates

$$V = V_0 + \frac{1}{2} \sum_{\lambda} \omega_{\lambda} Q_{\lambda}^2 + \sum_{\lambda\mu\nu} K_{\lambda\mu\nu} Q_{\lambda} Q_{\mu} Q_{\nu} + \dots \quad (1.2.1)$$

are functions of atomic masses. Consequently, if we find the relationship between the normal coordinates of isotopic molecules, we can obtain isotopic relations for the given constants in a general form. Thus, if we find the relationship between the normal coordinates of isotopic molecules, we can obtain isotopic relations for the above constants in a general form.

Let

$$H(x) = \sum_{N\alpha} \frac{P_{N\alpha}^2}{2m_N} + V(x_{N\alpha}); \quad (1.2.2)$$

and

$$H'(x) = \sum_{N\alpha} \frac{P_{N\alpha}^2}{2m'_N} + V(x_{N\alpha}); \quad (1.2.3)$$

are the Hamiltonian of the basic molecule and its arbitrary isotopic modification, respectively. Here $x_{N\alpha}$ is the coordinates of N^{th} nuclei of the molecule with m_N mass, $P_{N\alpha} = -i\hbar \frac{\partial}{\partial x_{N\alpha}}$. The Hamiltonians given in this form are convenient at studying isotope substitution, since only the kinetic part is a function of masses. The potential energy does not depend on masses and, hence, is invariant under isotope substitution.

Thus, the Hamiltonian of an isotope-substituted molecule can be represented as:

$$H'(x) = H(x) - \sum_{N\alpha} \frac{m'_N - m_N}{2m'_N m_N} P_{N\alpha}^2 = H(x) + h, \quad (1.2.4)$$

where the contribution responsible for all isotope substitution-related effects is explicitly identified. To solve the problem, it is necessary to make a transition from the Cartesian coordinates $x_{N\alpha}$ of the space-fixed coordinate system to the system associated with the molecule.

It is convenient if the corresponding molecular coordinate system satisfies the Eckart conditions and the requirement of normality of vibrational coordinates. It was shown in [8] that such a transformation leads the Hamiltonian $H'(x)$ into the Watson Hamiltonian (see eq. (2.1.3)). Similar transformations of coordinates:

$$r'_{N\beta} = \sum_{\lambda} m'^{\frac{1}{2}}_N l'_{N\beta\lambda} Q'_{\lambda}, \quad (1.2.5)$$

$$x'_{N\alpha} = R'_{\alpha} + \sum_{\beta} K'_{\alpha\beta} r'_{N\beta}, \quad (1.2.6)$$

transform the Hamiltonian of the isotope-substituted molecule $H'(x)$ into the Hamiltonian of Watson's species. The transformation parameters (1.2.5), (1.2.6) satisfy the corresponding Eckart conditions (1.1.7)–(1.1.10) and the normality requirement of the coordinates for an isotope-substituted molecule (Q'_i).

Note that such transformation of coordinates is not the only one leading to the Hamiltonian of the isotopomer in the Watson form. First one can perform any standard coordinate transformation and express the Hamiltonian $H'(x)$ in these coordinates. The result will be the so-called “intermediate” Hamiltonian. In this case, following that the set of standard coordinate transformations forms a group, then, consequently, there will be such a transformation that will allow one to pass from the “intermediate” coordinates to a set of variables satisfying the Eckart conditions for the isotopologue of the molecule. In this case, the “intermediate” Hamiltonian is transformed to the Watson's one. Thus, the transition from the $H'(x)$ operator to a Watson's operator can be carried out in several ways with obtaining some “intermediate” Hamiltonian. The possibility of gradual transformation of the Hamiltonian with introduction of an intermediate becomes important in connection with the following circumstances. As it was shown in [8], the Hamiltonian of an isotopologue can be represented in the form (1.2.4). Therefore, if the normal coordinates of the parent molecule are chosen as “intermediate” coordinates, the operator h will depend only on the constants of the parent molecule and the atomic masses, i. e., the constants of vibration forms $l_{N\alpha\lambda}$, the parameters of equilibrium configurations $r^e_{N\alpha}$, moments of inertia, harmonic frequencies, and anharmonic constants. By defining the second transformation, one can immediately obtain the Hamiltonian of the isotope-substituted molecule in Watson form. If we preserve the dependence of the “intermediate” Hamiltonian on the constants of the basic molecule, then, when comparing it with the Watson operator of the basic modification, we obtain the desired isotopic relations.

As noted in [8], in the theory of isotope substitution it is very important to know the relations between the vibration form constants of the basic and isotope-substituted modifications. In this case, these relations take on the form:

$$l'_{K\gamma\lambda} = \sum_{\alpha\mu} K_{\alpha\gamma}^e \frac{m_N^{\frac{1}{2}}}{m'_N} l_{K\alpha\mu} \beta_{\lambda\mu}. \quad (1.2.7)$$

Here indices N, K denote atoms of the molecule; parameters belonging to the substituted molecule are marked with “'”; indices α, β, γ denote x, y or z components of the corresponding vector quantity; λ, μ, ν number different normal vibrational coordinates; m_N and m'_N represent the nuclear masses of the

original and isotope-substituted molecule, respectively. The values $K_{\alpha\gamma}^e$ (the index “*e*” corresponds to the equilibrium nuclear configuration of the molecule) are the elements of the matrix defining the rotation of the molecular coordinate system during the transition from the original to the isotope-substituted modification. The $\beta_{\lambda\mu}$ values are elements of the matrix inverse of the $\alpha_{\lambda\mu}$ matrix, where the last defines the transition from the normal coordinates of the original isotopologue to the substituted one. The elements of the matrix α can be determined from the following relations:

$$\sum_{\nu} \alpha_{\lambda\nu} \alpha_{\mu\nu} = A_{\lambda\mu} = \sum_{N_{\alpha}} \frac{m_N}{m'_N} l_{N\alpha\lambda} l_{N\alpha\mu}, \quad (1.2.8)$$

$$\sum_{\nu} A_{\lambda\nu} W_{\nu} \alpha_{\nu\mu} = \alpha_{\lambda\mu} W'_{\mu},$$

leading to the known equation:

$$\det\{AW - W'\} = 0. \quad (1.2.9)$$

Here A is a matrix with elements $A_{\lambda\nu}$; W and W' are diagonal matrices with elements $W_{\nu} = \omega_{\lambda}^2 \delta_{\lambda\nu}$ and $W'_{\nu} = \omega'_{\lambda}^2 \delta_{\lambda\nu}$, respectively; ω_{λ} and ω'_{λ} are the harmonic frequencies of the original and isotope-substituted molecules.

Using the isotope substitution theory, the Hamiltonian parameters were theoretically predicted to simplify the solution of the inverse spectroscopic problem. As an example, the parameter calculations for the vibrational state ($v_5 = v_{12} = 1$) of the C₂D₄ molecule are given.

Due to isotopic substitution, the spectroscopic parameters of the C₂D₄ molecule vibrational states undergo significant changes relative to the corresponding parameters of the main modification. To control the solution of the inverse spectroscopic problem, the values of the main rotational parameters (A , B , and C) of the vibrational state ($v_5 = v_{12} = 1$) were theoretically calculated.

Let us use the dependence [9] of rotational constants A , B and C on vibrational quantum numbers known in the literature:

$$B_{\beta} = B_{\beta}^e - \sum_{\lambda} \alpha_{\beta\lambda} \left(v_{\lambda} + \frac{d_{\lambda}}{2} \right) + \dots \quad (1.2.10)$$

The choice of axes is conditioned by the I' -representation ($I_z < I_x < I_y$) of the A -reduced Watson operator. B_{β}^e are the values of the rotational constants for the equilibrium configuration, $\alpha_{\beta\lambda}$ are the coefficients taking into account the anharmonicity corrections to the rotational constants, v_{λ} are the quantum numbers v_1, v_2, \dots, v_{12} , d_{λ} is the degeneracy multiple of the λ^{th} vibration.

Numerical values of the rotational constants $B_x^e = 0.976 \text{ cm}^{-1}$ (A parameter), $B_y^e = 0.810 \text{ cm}^{-1}$ (B parameter), $B_z^e = 4.776 \text{ cm}^{-1}$ (C parameter) for the main modification of C₂H₄, as well as $\tilde{B}_x^e =$

0.716 cm^{-1} , $\tilde{B}_y^e = 0.551 \text{ cm}^{-1}$, $\tilde{B}_z^e = 2.401 \text{ cm}^{-1}$ for the isotopologue C_2D_4 were obtained by solving the system of equations (1.10)–(1.14) from [4]. The values of the rotational constants $A = 4.90502 \text{ cm}^{-1}$, $B = 1.006238 \text{ cm}^{-1}$, $C = 0.82347 \text{ cm}^{-1}$ of the $v_5 + v_{12}$ band for the main modification were taken from [10].

Let us take into account that in case of isotopic substitution of $\text{C}_2\text{D}_4 \leftarrow \text{C}_2\text{H}_4$ the coefficient $\alpha_{\beta\lambda}$ for the C_2D_4 molecule is two times smaller than the corresponding coefficients $\alpha_{\beta\lambda}$ for the C_2H_4 molecule [10], i. e. the relation is valid:

$$\tilde{\alpha}_{\beta\lambda} = \frac{1}{2} \alpha_{\beta\lambda}. \quad (1.2.11)$$

Using equations (1.2.10), (1.2.11), as well as numerical values of equilibrium rotational constants for the main modification of C_2H_4 and isotopologue C_2D_4 , the values of rotational constants $\tilde{A} = 2.47 \text{ cm}^{-1}$, $\tilde{B} = 0.73 \text{ cm}^{-1}$, $\tilde{C} = 0.56 \text{ cm}^{-1}$ for the vibrational state ($v_5 = v_{12} = 1$) of the C_2D_4 molecule were obtained. As can be seen, the B_β parameters for the main modification differ on average by a factor of 0.6 from the corresponding \tilde{B}_β parameters for the C_2D_4 molecule, which further confirms the presence of a strong isotope substitution effect during deuterium-substitution.

1.3. Irreducible tensor operators theory

Describing quantum systems, the mathematical apparatus based on the theory of operators is used. The concept of operator is widely used in quantum mechanics and quantum field theory. For application to the problems of molecular spectroscopy, operators of physical quantities and wave functions are represented in the form of linear combinations, and such combinations can be transformed by irreducible representations from the symmetry group of the system under study. Symmetrized combinations of operators are called irreducible tensor operators. Mathematical operations with irreducible tensors differ from the rules of ordinary algebra. The greatest contribution to the development of the mathematical apparatus of irreducible tensor operators for application to the problems of molecular spectroscopy was made by K. T. Hecht [11, 12].

The set of orthonormal functions can be considered as a vector in the n -dimensional vector space L_n . At operations g from the group G of linear transformations of space L , an arbitrary vector x with components x_i ($i = 1, 2, \dots, n$) transforms into some other vector $x' = gx$, which components are related to the components of the original vector by the transformation

$$x'_i = gx_i = \sum_j T_{ij}(g)x_j. \quad (1.3.1)$$

The products of two arbitrary vectors x (x_i) and y (y_i) of space L_n for operations $g \in G$ will transform according to the law:

$$x'_i y'_i = g(x_i y_i)_i = \sum_{k,l} T_{ki}(g) T_{lj}(g) x_k y_l = \sum_{k,l} T_{kl,ij}(g) x_k y_l, \quad (1.3.2)$$

where matrix $T_{kl,ij}(g)$ is the direct product of matrices T_{kl} and T_{ij} . The set of n^2 quantities transformed by the operation g , as well as n^2 products $x_i y_i$ of the coordinates of two arbitrary vectors x and y of L_n is called a tensor of the second order. Hereafter we will denote it as A_{ij} .

A tensor A_{ij} is called symmetric if the equality $A_{ij} = A_{ji}$ holds. If $A_{ij} = -A_{ji}$, the tensor A_{ij} is called antisymmetric. Any tensor A_{ij} of the second order can be represented as the sum of its symmetric and antisymmetric parts.

Similarly, we can introduce a l^{th} order tensor $A_{i_1 i_2 \dots i_l}$, defined as a set of n' quantities $A_{i_1 i_2 \dots i_l} = \prod_{k=1}^l x_{j_k}^{(k)}$, changing at g transformations (1.3.1) of the vector space according to the law:

$$A'_{i_1 i_2 \dots i_l} = \sum_{i_1 i_2 \dots i_l} \left(\prod_{k=1}^l T_{j_k i_k}(g) \right) A_{i_1 i_2 \dots i_l}. \quad (1.3.3)$$

The entire set of transformation matrices (1.3.3) for different transformations $g \in G$ forms a representation of the group G . Such a representation is called a l^{th} order tensor representation. This representation is in general reducible since it is a product of l n -dimensional representations of (1.3.1).

The irreducible symmetry tensor Γ of a group G of linear transformations is the set $[\Gamma]$ of values ψ_i^Γ transformed under operations g of a group G by the irreducible representation T^Γ of a group G :

$$g\psi_i^\Gamma = \tilde{\psi}_i^\Gamma = \sum_j T_{ji}^\Gamma(g) \psi_i^\Gamma, \quad (1.3.4)$$

where $[\Gamma]$ is the dimension of the representation. The set $[\Gamma]$ of values ψ_i^Γ is called an irreducible tensor set of functions.

For irreducible tensors, algebraic operations such as tensor summation and tensor binding (convolution) are defined.

As a result of the summation of the tensors ϕ_i^Γ and ψ_i^Γ transformed by the same irreducible representation T^Γ of the group G , we obtain an irreducible tensor, which is transformed according to the same irreducible representation T^Γ : $\phi_i^\Gamma + \psi_i^\Gamma = \chi_i^\Gamma$.

As a result of binding (convolution) the tensors $\phi_i^{\gamma_1}$ and $\psi_i^{\gamma_2}$, we obtain an irreducible tensor transformed by an irreducible representation $T^\Gamma \in D^{\gamma_1} \times D^{\gamma_2}$ in the form of

$$\chi_k^\Gamma \equiv [\phi^{\gamma_1} \times \psi^{\gamma_2}]_k^\Gamma = \sum_{ij} \phi_i^{\gamma_1} \psi_j^{\gamma_2} F_{\Gamma k}^{\gamma_1 i \gamma_2 j}, \quad (1.3.5)$$

where $F_{\Gamma k}^{\gamma_1 i \gamma_2 j}$ are the Clebsch–Gordan coefficients [13].

Similarly to the definition (1.3.3), a tensor operator is a set of operators linearly mutually transformable under linear transformations of the space in which these operators act.

An irreducible tensor operator is a set of operators $P_i^{(\Gamma)}$ transformed under the operations R of the space symmetry group by the irreducible representation T^Γ of this group:

$$R^{-1} P_i^{(\Gamma)} R = \sum_k [T^\Gamma(R)]_i^k P_k^{(\Gamma)}. \quad (1.3.6)$$

For irreducible tensor operators, summations and combining are also defined, which have exactly the same form as for irreducible tensors, if the quantities $\phi_i^\Gamma + \psi_i^\Gamma$ and x^γ are treated as operators. It is clear that irreducible tensor operators can be multiplied by numerical constants.

Describing quantum phenomena, the advantages of using the formalism of irreducible tensor operators are largely determined by one of the main theorems of the formalism – the Wigner-Eckart theorem [14]. According to this theorem, any matrix element from the operator of any physical quantity can be divided into two factors: the Clebsch-Gordan coefficient and the so-called reduced matrix element, depending on a particular kind of operator basis:

$$\langle \Psi_{v_1 \sigma_1}^{\gamma_1} | P_s^\Gamma | \Psi_{v_2 \sigma_2}^{\gamma_2} \rangle = F_{\gamma_2 \sigma_2 \Gamma s}^{\gamma_1 \sigma_1} \langle \Psi_{v_1}^{\gamma_1} | P^\Gamma | \Psi_{v_2}^{\gamma_2} \rangle, \quad (1.3.7)$$

where v_1, v_2 are all other, except for the symmetry indices γ and σ , indices characterising the function ψ . The value $\langle \Psi_{v_1}^{\gamma_1} | P^\Gamma | \Psi_{v_2}^{\gamma_2} \rangle$ in equation (1.3.7) is called the reduced matrix element, which is the characteristic value of the set of matrix elements. Its value does not depend on the choice of the basis of the group representations. To calculate the reduced matrix element, it is enough to calculate the simplest, from the point of view of calculations, matrix element $\langle \Psi_{v_1 \sigma_1}^{\gamma_1} | P_s^\Gamma | \Psi_{v_2 \sigma_2}^{\gamma_2} \rangle$, and then, knowing the corresponding Clebsch-Gordan coefficients, by formula (1.3.7) we can calculate all other matrix elements with the given values of indices γ_1, γ_2 and Γ .

Thus, the Wigner-Eckart theorem provides a significant simplification of the procedure for computing matrix elements allowed by the symmetry of the problem and reduces this procedure to the computation of standard sums of products of Klebsch-Gordan coefficients.

1.4. The vibrational Hamiltonian considering tetrahedral splittings

In the spectra of molecules possessing a high degree of symmetry (which symmetry groups are isomorphic, for example, to the T_d group), so-called “tetrahedral” splittings are observed. When describing the spectra of such molecules, it is necessary to use a mathematical model that takes into account these splittings. The Hamiltonian of a molecule, in accordance with the general vibrational-rotational theory, can be written in the form of a set of effective operators or the so-called effective operator matrices:

$$H^{\text{vib.-rot.}} = \sum_{v,v'} |v\rangle\langle v'| H^{v,v'}, \quad (1.4.1)$$

where the operators $H^{v,v'}$ depend only on the rotational operators J_a , summing over all degenerate and interacting states; $|v\rangle$ and $\langle v'|$ are vibrational functions, which must have the properties of irreducible tensor sets belonging to the symmetry group of the molecule. In other words, the Hamiltonian can be written taking into account the symmetry properties of rotational operators and vibrational functions in the following form:

$$H^{\text{vib.-rot.}} = \sum_{vl\gamma, v'l'\gamma'} \sum_{n\Gamma} [(\langle v l \gamma | \otimes \langle v' l' \gamma' |)^{n\Gamma} \otimes H_{vl\gamma, v'l'\gamma'}^{n\Gamma}]^{A_1}, \quad (1.4.2)$$

where, according to the existence of five irreducible representations of the group T_d , the indices γ, γ' and Γ can take the values A_1, A_2, E, F_1 and F_2 . Thus, different combinations of indices γ, γ' and Γ in expression (1.4.2) lead to different kinds of rotational operators.

Further we consider in detail the problem of constructing the part of the Hamiltonian which is responsible for the tetrahedral splittings. In this case, the problem is solved using the operator perturbation theory, where the types of operators are determined from the conditions of the full symmetry of the Hamiltonian and the knowledge of the symmetry of vibrations.

From the rotational-vibrational theory, it is known that any molecule of n atoms has $3n - 6$ vibrational degrees of freedom. However, due to symmetry in XY_4 type molecules, nine vibrational degrees of freedom correspond to four normal vibrations: v_1, v_2, v_3 and v_4 (this will be shown in more detail in section 3.1.1). As shown in [15], ten parameters of the tetrahedral splittings $G_{22}, G_{33}, G_{34}, G_{44}, S_{34}, T_{33}, T_{34}, T_{44}, T_{23}$ and T_{24} are sufficient for a correct description. The required operators take the following form:

1. The operator responsible for G_{22} -type splittings:

$$H_1 = d_{2222} (Q_{2_1}^2 + Q_{2_2}^2)^2 + V_3; \quad (1.4.3)$$

2. An operator that associates splittings with the parameter G_{33} , G_{44} :

$$H_2 = B\zeta_\lambda^2 \sum_{\mu\nu} \varepsilon_{\lambda\mu\nu} (Q_\mu P_\nu + Q_\nu P_\mu) + d_{\lambda\lambda\lambda\lambda_x} (Q_{\lambda_x}^2 + Q_{\lambda_y}^2 + Q_{\lambda_z}^2) + V_3, \quad (1.4.4)$$

where $\lambda = 3$ or 4 , V_3 is the cubic part of the intramolecular potential function V^{anh} , B is the equilibrium rotational parameter, $\varepsilon_{\lambda\mu\nu}$ is a completely antisymmetric tensor, and $d_{\lambda\lambda\lambda\lambda_x}$ is one of the quartic anharmonicity parameters (see [11, 12]);

3. The splittings associated with the parameter G_{34} are represented as:

$$H_3 = \frac{B}{2} \zeta_{34}^2 + 2B\zeta_3\zeta_4 + V_3; \quad (1.4.5)$$

4. The operator responsible for the T_{33} and T_{44} splittings is signed as:

$$H_4 = d_{\lambda\lambda\lambda\lambda_x} (Q_{\lambda_x}^4 + Q_{\lambda_y}^4 + Q_{\lambda_z}^4 - 3Q_{\lambda_x}^2 Q_{\lambda_y}^2 - 3Q_{\lambda_x}^2 Q_{\lambda_z}^2 - 3Q_{\lambda_y}^2 Q_{\lambda_z}^2) + V_3; \quad (1.4.6)$$

λ takes values of 3 or 4;

5. For T_{33} and $T_{4\lambda}$ splittings, the operators take the following form ($\lambda = 3; 4$):

$$\begin{aligned} H_{5a} = & d_{3344_\lambda} [3Q_{4x}^2 Q_{3x}^2 + 3Q_{4y}^2 Q_{3y}^2 + 3Q_{4z}^2 Q_{3z}^2 - \\ & -(Q_{3x}^2 + Q_{3y}^2 + Q_{3z}^2)(Q_{4x}^2 + Q_{4y}^2 + Q_{4z}^2) - \\ & -4Q_{3x}Q_{3y}Q_{4x}Q_{4y} - 4Q_{3x}Q_{3z}Q_{4x}Q_{4z} - 4Q_{3y}Q_{3z}Q_{4y}Q_{4z}] + V_3 \end{aligned} \quad (1.4.7)$$

and

$$H_{5b} = d_{2244_t} [Q_{12}Q_{22}(Q_{\lambda_x}^2 + Q_{\lambda_y}^2) + (Q_{21}^2 - Q_{22}^2)(Q_{\lambda_x}^2 + Q_{\lambda_y}^2 - 2Q_{\lambda_z}^2)] + V_3, \quad (1.4.8)$$

respectively;

6. The operator responsible for S_{34} type splits is written out as:

$$\begin{aligned} H_6 = & d_{3344_x} [(Q_{3x}Q_{4x} + Q_{3y}Q_{4y} + Q_{3z}Q_{4z})^2 - \\ & -\frac{1}{3}(Q_{3x}^2 + Q_{3y}^2 + Q_{3z}^2)(Q_{4x}^2 + Q_{4y}^2 + Q_{4z}^2)] + V_3. \end{aligned} \quad (1.4.9)$$

1.5. Vibrational polyads

Consider a molecule with N different normal modes of vibrations (which can be degenerate). The vibrational level (v_1, v_2, \dots, v_N) belongs to the polyad P_n if the vibrational quantum numbers v_i ($i = 1, \dots, N$) satisfy the relation:

$$n = \sum_{i=1}^N i_i v_i, \quad (1.5.1)$$

where (i_1, i_2, \dots, i_N) are N integers chosen to define the polyad scheme. A simple example is the methane molecule (CH_4). This molecule has $N = 4$ normal modes of oscillation: v_1 (non-generated), v_2 (doubly degenerated), v_3 and v_4 (triply degenerated). It is known that their frequencies satisfy the approximate relation:

$$v_1 \approx v_3 \approx 2v_2 \approx 2v_4. \quad (1.5.2)$$

Thus, the vibrational levels of methane are grouped into polyads using a polyad scheme:

$$(i_1, i_2, i_3, i_4) = (2, 1, 2, 1), \quad (1.5.3)$$

In other words, the polyad P_n describes all vibrational states satisfying the condition:

$$n = 2v_1 + v_2 + 2v_3 + v_4, \quad (1.5.4)$$

which leads to the standard polyads for methane (Figure 1.2; see Figure A.1 (Appendix A) for an example of polyads for the SiF_4 molecule): P_1 with two vibrational levels (upper states of the v_2/v_4 dyad), P_2 with five levels (upper states of the $v_1/v_3/2v_2/2v_4/v_2 + v_4$ pentad), etc.

The polyad scheme, defined by a set of integers (i_1, i_2, \dots, i_N) , allows us to simplify the study of any system of vibrational levels, even for molecules that do not have a clear polyad scheme.

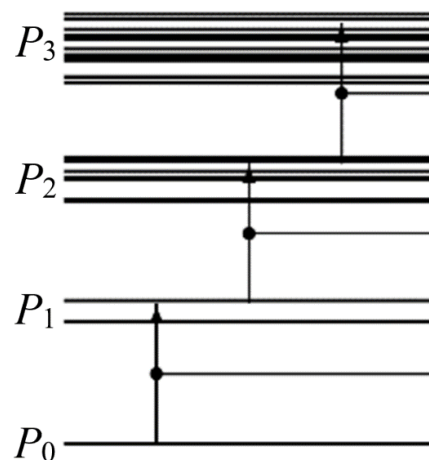


Figure 1.2 – Graphical representation of energy levels grouped into polyads $P_0 - P_3$.

Chapter 2

Theoretical study on high-resolution spectra of asymmetric tops: C₂D₄ и ClO₂ molecules

This chapter is devoted to the theoretical study of asymmetric top molecules, namely, to the study of the vibrational-rotational spectra of the fully deuterated ethylene isotopologue C₂D₄ and the molecule in the non-singlet electronic state chlorine dioxide ClO₂. At the beginning of each section, a literature review is given, as well as information from the theory necessary to describe the spectra of asymmetric top molecules.

2.1. Ethylene C₂D₄

As one of the most important objects of study in various fields of science, ethylene is of great interest for high-resolution spectroscopy. Found not only in the Earth's atmosphere, this gaseous substance has also been detected in interstellar space, planetary nebulae [16], the atmospheres of giant planets such as Saturn, Jupiter [17], and the atmosphere of Jupiter's satellite Titan [18, 19]. Ethylene plays a role as a hormone in plant biochemistry, naturally diffusing into the ambient air and affecting atmospheric chemistry and global climate [20–22]. Therefore, many laboratory studies have been devoted to analysing the positions and intensities of the spectral lines of this molecule [23–29]. Speaking of the fully deuterated ethylene isotopologue C₂D₄, along with other types of deuterated ethylene, it should always be taken into account for the correct determination of the intramolecular potential function of this molecule, as well as when analysing the distribution of H and D atoms in the process of isotopic substitution [30].

2.1.1. Description and theoretical background of the deuterated ethylene molecule

The ethylene molecule C₂D₄ is an asymmetric top molecule which asymmetry parameter is $k \approx (2B - A - C)/(A - C) = -0.817$, and the symmetry group is isomorphic to the point group D_{2h}. This group is characterised by the symmetry properties shown in Table 2.1, where columns 1–9 show the set of irreducible representations and characters of the D_{2h} group; column 10 shows the symmetries of the rotational operators J_α and the directional cosines k_{za} , and column 11 shows the symmetries of each of the 12 vibrational coordinates q_λ of the molecule C₂D₄. Absorption transitions in this molecule are possible only between vibrational states whose symmetries Γ and Γ' have different indices “u” and “g” denoting, respectively, symmetric and antisymmetric vibrations with respect to the inversion centre i . In addition, transitions from the ground vibrational state are only allowed to the upper vibrational level with symmetry type B_{1u} , B_{2u} or B_{3u} . Transitions to the upper vibrational level A_u are forbidden by

symmetry and can only occur in the spectrum as a result of Coriolis-type resonance. Column 10 also shows that transitions from the ground state to vibrational co-states like A_g , B_{1g} , B_{2g} or B_{3g} are completely forbidden due to symmetry properties and due to the absence of interaction between states with different indices “ u ” and “ g ”.

By analysing Table 2.1, we can describe the selection rules and symmetry type for different bands:

1. The $B_{1u} \leftarrow A_g$ bands belong to the c -type and are characterised by the following selection rules:

$$\Delta J = 0, \pm 1; \Delta K_a = \text{odd}; \Delta K_c = \text{even}.$$

2. The $B_{2u} \leftarrow A_g$ bands belong to the b -type and are characterised by the following selection rules:

$$\Delta J = 0, \pm 1; \Delta K_a = \Delta K_c = \text{odd}.$$

3. The $B_{3u} \leftarrow A_g$ bands belong to the a -type and are characterised by the following selection rules:

$$\Delta J = 0, \pm 1; \Delta K_a = \text{even}; \Delta K_c = \text{odd}.$$

Table 2.1 – Symmetry types and characters of irreducible representations of the D_{2h} group.

Repr.	E	σ_{xy}	σ_{xz}	σ_{yz}	i	$C_2(z)$	$C_2(y)$	$C_2(x)$	Rot.	Vibr.
I	2	3	4	5	6	7	8	9	10	11
A_g	1	1	1	1	1	1	1	1		q_1, q_2, q_3
A_u	1	-1	-1	-1	-1	1	1	1		q_4
B_{1g}	1	1	-1	-1	1	1	-1	-1	J_y, k_{zy}	q_5, q_6
B_{1u}	1	-1	1	1	-1	1	-1	-1		q_7
B_{2g}	1	-1	1	-1	1	-1	1	-1	J_x, k_{zx}	q_8
B_{2u}	1	1	-1	1	-1	-1	1	-1		q_9, q_{10}
B_{3g}	1	-1	-1	1	1	-1	-1	1	J_z, k_{zz}	
B_{3u}	1	1	1	-1	-1	-1	-1	1		q_{11}, q_{12}

Thus, the studied states must be described using a Hamiltonian that takes into account resonance interactions between different vibrational states. This model of the Hamiltonian has the following form:

$$H^{\text{rot.-vib.}} = \sum_{\nu, \tilde{\nu}}^2 |\nu\rangle\langle\tilde{\nu}| H^{\nu\tilde{\nu}}, \quad (2.1.1)$$

where the summation is over all vibrational states, and $H^{\nu\tilde{\nu}}$ is represented as follows:

$$H^{\nu\tilde{\nu}} = \begin{vmatrix} 1 & 1 & 2 & 3 \\ 2 & W & F & C \\ 3 & - & W & - \\ 3 & - & - & W \end{vmatrix}, \quad (2.1.2)$$

where W are matrix elements of the diagonal operator; F is the Fermi resonance interaction operator; C is the Coriolis interaction operator. The diagonal blocks of the Hamiltonian describing the rotational structure of unperturbed vibrational states are taken in the form of the Watson operator [31]:

$$\begin{aligned}
H^{v\tilde{v}} = & E^v + \left[A^v - \frac{1}{2}(B^v + C^v) \right] J_z^2 + \frac{1}{2}(B^v + C^v) J^2 + \frac{1}{2}(B^v + C^v) J_{xy}^2 - \\
& - \Delta_K^v J_z^4 - \Delta_{JK}^v J_z^2 J^2 - \Delta_K^v J^4 - \delta_K^v [J_z^2, J_{xy}^2]_+ - 2\delta_J^v J^2 J_{xy}^2 + \\
& + H_K^v J_z^6 + H_{KJ}^v J_z^4 J^2 + H_{JK}^v J_z^2 J^4 + H_J^v J^6 + [h_K^v J_z^4 + h_{JK}^v J_z^2 J^2 + h_J^v J^4, J_{xy}^2]_+ + \\
& + L_K^v J_z^8 + L_{KK}^v J_z^6 J^2 + L_{JK}^v J_z^4 J^4 + L_{JJ}^v J_z^2 J^6 + L_J^v J_z^8 + [J_K^v J_z^6 + J_{KJ}^v J_z^4 J^2 + J_{JK}^v J_z^2 J^4 + J_J^v J^6, J_{xy}^2]_+ + \\
& + P_K^v J_z^{10} + P_{KKJ}^v J_z^8 J^2 + P_{KJ}^v J_z^6 J^4 + P_J^v J_z^4 J^6 + S_K^v J_z^{12} + S_{KKJ}^v J_z^{10} J^2 + \dots,
\end{aligned} \tag{2.1.3}$$

where $J_{xy}^2 = J_x^2 - J_y^2$ and $[A, B]_+ = AB + BA$; $J_\alpha (\alpha = x, y, z)$ are the components of the angular momentum operator defined in the molecularly fixed coordinate system; E is the vibrational energy; A, B, C are rotational constants; $\Delta_J, \Delta_{JK}, \Delta_K, \delta_K, \delta_{JK}$ are centrifugal distortion parameters of the fourth degree and $H_K, H_{KJ}, H_{JK}, H_J, h_K, h_{JK}, h_J$ are centrifugal distortion parameters of the sixth degree.

As for non-diagonal blocks, based on symmetry considerations, it can be shown that the three operators describing the Coriolis interaction (resonance between states of different symmetries) should be written in the following form [31]:

$$\begin{aligned}
H_{v,\tilde{v}}(v \neq \tilde{v}) = & {}^{v\tilde{v}}F_0 + {}^{v\tilde{v}}F_K J_z^2 + {}^{v\tilde{v}}F_J J^2 + \dots + {}^{v\tilde{v}}F_{xy}(J_x^2 - J_y^2) + \\
& + {}^{v\tilde{v}}F_{Kxy}\{J_z^2, (J_x^2 - J_y^2)\}_+ + 2{}^{v\tilde{v}}F_{Jxy}J^2(J_x^2 - J_y^2) + \dots
\end{aligned} \tag{2.1.4}$$

1. Coriolis *a*-type interaction between the ($v_{10} = 1, B_{2u}$) and ($v_7 = 1, B_{1u}$) states:

$$\begin{aligned}
H_{v,\tilde{v}} = & iJ_z H_{v\tilde{v}}^{(1)} + [J_x, J_y]_+ H_{v\tilde{v}}^{(2)} + H_{v\tilde{v}}^{(2)} [J_x, J_y] + \\
& + [iJ_z, (J_x^2 - J_y^2)]_+ H_{v\tilde{v}}^{(3)} + H_{v\tilde{v}}^{(3)} [iJ_z, (J_x^2 - J_y^2)]_+ + \dots
\end{aligned} \tag{2.1.5}$$

2. Coriolis *b*-type interaction between the ($v_{10} = 1, B_{2u}$) and ($v_4 = 1, B_{3u}$) states:

$$\begin{aligned}
H_{v,\tilde{v}} = & iJ_x H_{v\tilde{v}}^{(1)} + H_{v\tilde{v}}^{(1)} iJ_x + [J_y, J_z]_+ H_{v\tilde{v}}^{(2)} + H_{v\tilde{v}}^{(2)} [J_y, J_z] + \\
& + [iJ_x, (J_x^2 - J_y^2)]_+ H_{v\tilde{v}}^{(3)} + H_{v\tilde{v}}^{(3)} [iJ_x, (J_x^2 - J_y^2)]_+ + \dots
\end{aligned} \tag{2.1.6}$$

3. Coriolis *c*-type interaction between the ($v_{10} = 1, B_{2u}$) and ($v_{12} = 1, B_{3u}$) states:

$$\begin{aligned}
H_{v,\tilde{v}} = & iJ_y H_{v\tilde{v}}^{(1)} + H_{v\tilde{v}}^{(1)} iJ_y + [J_x, J_z]_+ H_{v\tilde{v}}^{(2)} + H_{v\tilde{v}}^{(2)} [J_x, J_z]_+ + \\
& + [iJ_y, (J_x^2 - J_y^2)]_+ H_{v\tilde{v}}^{(3)} + H_{v\tilde{v}}^{(3)} [iJ_y, (J_x^2 - J_y^2)]_+ + \dots
\end{aligned} \tag{2.1.7}$$

2.1.2. Results of the study of the vibrational-rotational structure of the spectra of the C₂D₄ molecule. v₅ + v₁₂ and v₆ + v₁₁ combination bands

The spectra of the C₂D₄ molecule were recorded in the wavelength range 2,900–3,500 cm⁻¹ using a Bruker IFS 125 HR Fourier spectrometer (Braunschweig, Germany) based on a Michelson interferometer with a resolution of 0.0025 cm⁻¹. The investigated sample was in the gaseous state at room temperature and pressure of 1.05 mbar, the optical path length was 24 m, and the number of scans was 500. To increase the optical path length, the gas was placed in a stainless-steel White cell. The lines of the N₂O molecule were used to calibrate the spectrum. The average deviation of the N₂O line positions from the line positions published in the current HITRAN database is of the order of 10⁻⁴ cm⁻¹.

The recorded spectrum around the v₅ + v₁₂ band is shown in Figure 2.1, with the centre of the band located around the value 3,386 cm⁻¹. Figure 2.2 shows the spectrum of the band v₆ + v₁₁ with the centre near the value 3,203 cm⁻¹. Both bands belong to the *b*-type and are characterised by the presence of strong *R*- and *P*-branches and weak central *Q*-branches which lines are mostly overlapped by the lines of the neighbouring *R*- and *P*-branches. As described earlier, the following selection rules are used to analyse *b*-type bands: $\Delta J = 0, \pm 1$; $\Delta K_a = \Delta K_c = \pm (2n + 1)$, where $n = 0, 1, 2, \dots$

The spectra were analysed using the method of combination differences. Note that this method is one of the simplest, since the exact Rydberg–Ritz combination principle is the only method for line assignment without any mathematical model representation [32, 33]. The necessary data on the vibrational-rotational energies of the ground state was taken from [34]. The information on the assigned transitions was then used to determine the energy structure of the (v₅ = v₁₂ = 1) and (v₆ = v₁₁ = 1) states. The energies of excited vibrational-rotational levels were calculated as mean values of the energies of several transitions (*P*-, *Q*-, and *R*-branches) from the ground vibrational state. As an illustration, Tables C.1 and C.2 (Appendix C) present fragments from the list of assigned transitions for each studied combination band, where J' , K'_a , K'_c are quantum numbers of the ground vibrational state levels, J , K_a , K_c are quantum numbers of the excited vibrational state levels, δ is the difference between the experimental value of line positions and the theoretically calculated one.

As an illustration of the performed assignment, i. e. association of quantum numbers with lines in the spectrum in Figures 2.1 and 2.2 one can observe the structure of *R*-branches of the studied band. The intersection of *R*-branches for series with different values of the quantum number K_a is clearly tracked. Along with this, it is necessary to note the following: during the search of $JK_aJ - K_a$

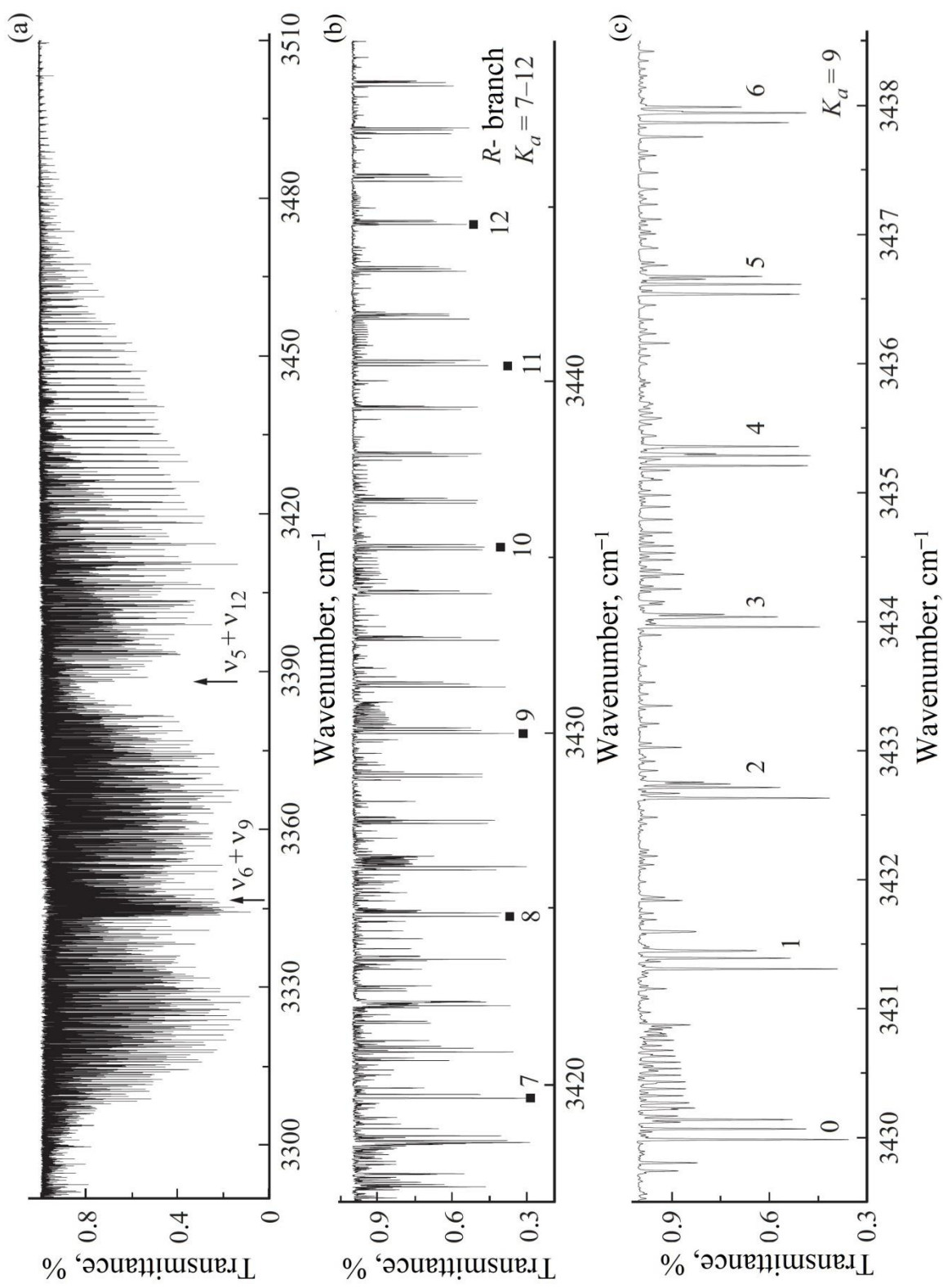


Figure 2.1 – Infrared spectra of ethylene C_2D_4 in the region 3,290–3,510 cm^{-1} (a); on the fragments (b) and (c) the part of R -branch of $v_5 + v_{12}$ band is shown.

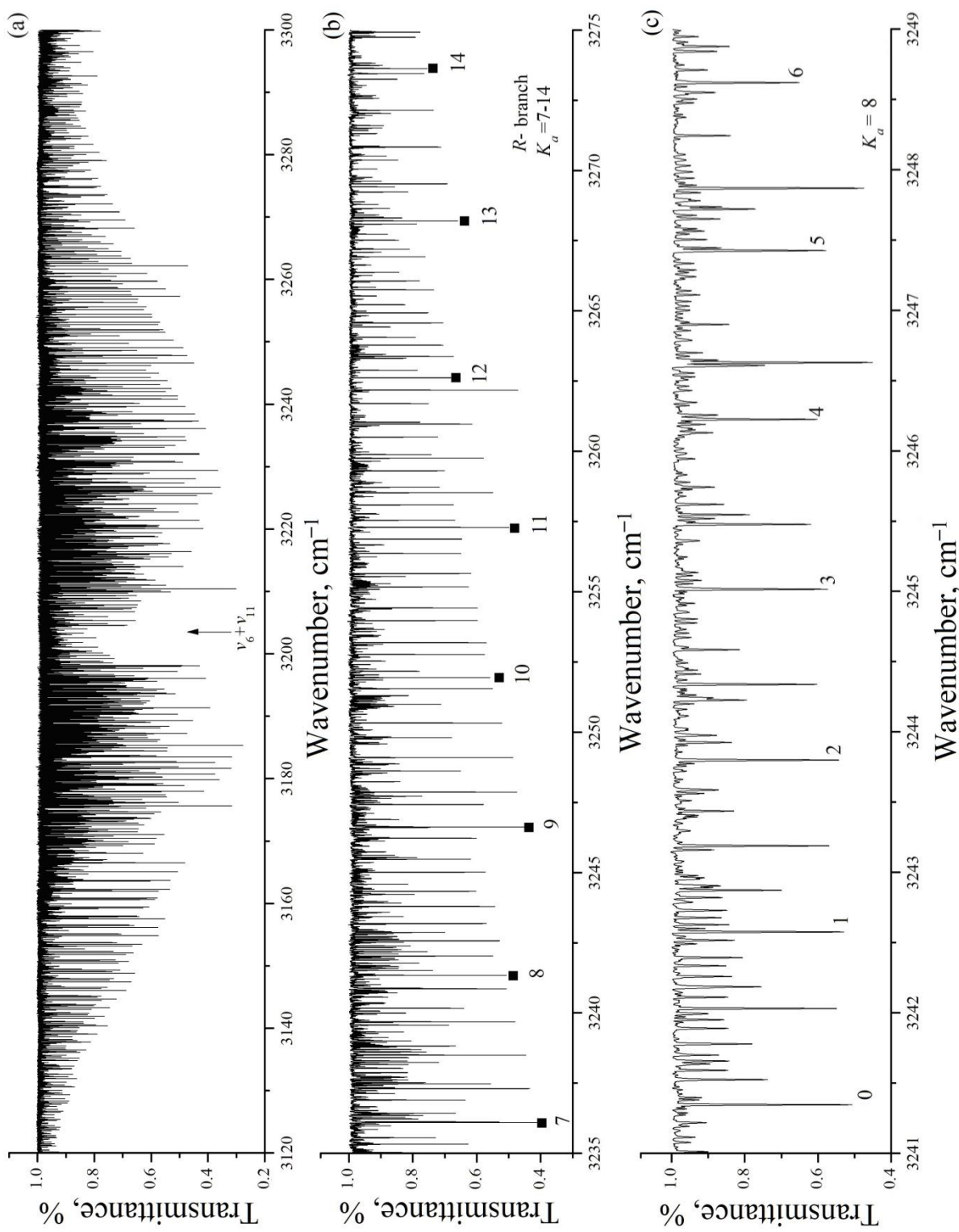


Figure 2.2 – Infrared spectra of ethylene C_2D_4 in the region $3,120\text{--}3,300 \text{ cm}^{-1}$ (a); on the fragments (b) and (c) the part of R -branch of the $v_6 + v_{11}$ band is shown.

series one could observe untypical behaviour of lines in Q -branches. For example, for series $K_a = 5$ the distance between the lines of the spectrum corresponding to small quantum numbers decreases, and at $J = 13$ the Q -branch turns back. This situation appears at close arrangement of energy levels related to different vibrational states, i. e. in the presence of resonance.

This fact emphasizes the necessity of a comprehensive consideration of correctness of the study of vibrational states ($v_5 = v_{12} = 1$) and ($v_6 = v_{11} = 1$) as isolated ones. It is known from the general principles of vibrational-rotational theory [4] that the close proximity of bands can lead to a complex spectrum picture. Based on this, we can talk about the existence of interactions between the vibrational states ($v_5 = v_{12} = 1$) and ($v_6 = v_9 = 1$), which leads to the necessity to use an effective Hamiltonian that takes resonance interactions into account.

However, without correct theoretical predictions of the parameters of non-diagonal blocks (which is a nontrivial task), the resonance model of the effective Hamiltonian turns out to be no better (since the solution of the inverse problem becomes unstable and incorrect) than the model for the isolated state. At the same time, as shown by the theoretical calculation of the rotational parameters of the band using the isotope substitution theory method (as mentioned in Section 1.2), the parameters found by solving the inverse spectroscopic problem (at quantum numbers $K_a \leq 12$, $J \leq 22$) using the Hamiltonian that does not take resonance interactions into account and the parameters calculated by the isotope substitution theory differ insignificantly. On the basis of the above, it is sufficient to consider the investigated states as isolated ones in order to obtain an appropriate set of parameters.

At the initial stage of solving the inverse spectroscopic problem, the parameters of the ground vibrational state of the C_2D_4 molecule were taken from [34] (column 3 in Tables C.3, C.4) as Hamiltonian parameters of the first approximation. Then, using a step-by-step substitution of experimental energies with a weight coefficient of 1, the optimum number of varying parameters was determined (Tables C.3, C.4, column 2). Thus, 2,080 transitions of the $v_5 + v_{12}$ band and 2,415 transitions of the $v_6 + v_{11}$ band were assigned to the values of the quantum numbers $K_a^{\max} = 12$ и $K_a^{\max} = 17$, respectively. 529 exact values of the vibrational and rotational energies of the vibrational state ($v_5 = v_{12} = 1$) and 181 values for the vibrational state ($v_6 = v_{11} = 1$) were determined. The latter ones were used in the weight fitting of the parameters of the effective Hamiltonian.

The values of 12 parameters for the $v_5 + v_{12}$ band and 8 parameters for the $v_6 + v_{11}$ band obtained by the fitting method reproduce the experimental energy values with an accuracy of $1.3 \cdot 10^{-3} \text{ cm}^{-1}$ for $v_5 + v_{12}$ and $1.5 \cdot 10^{-3} \text{ cm}^{-1}$ for $v_6 + v_{11}$, which is close to the experimental accuracy.

2.2. Chlorine dioxide ClO₂

Significant interest in the physical and chemical properties of chlorine-containing materials was observed after the discovery of extremely high concentrations of chlorine monoxide ClO at low altitudes in the stratosphere above Antarctica [35, 36]. Measurements showing the formation of ClO₂ at night-time [37] provided strong evidence that the evolution of the Antarctic ozone hole is chemically driven by chlorine. However, when viewed in another context, chlorine dioxide is of particular importance as a useful chemical. It is an oxidising agent that is one of the most effective and fast-acting disinfectants, capable of eliminating bacteria, viruses, biofilms and moulds [38]. Based on the above, chlorine dioxide ClO₂ has been the object of many laboratory studies in analysing rotational [39, 40], electronic [41–43] and low-resolution infrared vibrational spectra [44, 45]. As for the high-resolution spectra of the ClO₂ molecule, they have been considered in a number of papers [46–51], including a recent paper [52] devoted to studies of the fundamental ν_1 band.

2.2.1. Theoretical description of molecules in non-singlet electronic states

The chlorine dioxide molecule ClO₂ is a stable free radical with the ground electronic state $X(^2B_1)$, and its symmetry group in the equilibrium state is isomorphic to the point group C_{2v}. This group is characterised by the symmetry properties shown in Table 2.2.

Table 2.2 – Characters of irreducible representations of the group C_{2v}.

Repr.	<i>E</i>	<i>C</i> ₂	σ_{yz}	σ_{xz}	Basis
<i>I</i>	2	3	4	5	6
<i>A</i> ₁	1	1	1	1	<i>z</i>
<i>A</i> ₂	1	1	-1	-1	<i>R</i> _{<i>z</i>}
<i>B</i> ₁	1	-1	-1	1	<i>x, R</i> _{<i>y</i>}
<i>B</i> ₂	1	-1	1	-1	<i>y, R</i> _{<i>x</i>}

The theory and methods used to describe the vibrational-rotational structure of polyatomic molecules in singlet electronic states are well developed and widely approved in a large number of studies of high-resolution spectra. However, these methods cannot provide high accuracy of the results obtained when studying molecules in non-singlet electronic states because of the presence of strong interactions between the rotation of the molecule and the spin of the unpaired electron (or electrons). Therefore, for a correct description of the energy levels of such molecules it is necessary to use an improved, more complex model of the Hamiltonian, which takes into account spin-rotational interactions in asymmetric top molecules:

$$H^{\text{eff}} = H^{\text{rot.}} + H^{\text{sp.-rot.}} + H^{\text{sp.}}, \quad (2.2.1)$$

where $H^{\text{rot.}}$ is the usual vibrational-rotational Hamiltonian of the asymmetric top, corresponding to expressions (2.1.1)–(2.1.4). The most important in expression (2.2.1) is the second contribution, which describes various spin-rotational effects of interactions. It can be represented as summands of different order of smallness:

$$H^{\text{sp.-rot.}} = {}^{(2)}H^{\text{sp.-rot.}} + {}^{(4)}H^{\text{sp.-rot.}} + {}^{(6)}H^{\text{sp.-rot.}}, \quad (2.2.2)$$

where each of the components can be written as:

$${}^{(2)}H^{\text{sp.-rot.}} = a_0(NS) + aN_zS_z + b(N_xS_x - N_yS_y), \quad (2.2.3)$$

$$\begin{aligned} {}^{(4)}H^{\text{sp.-rot.}} = & \Delta_J^S N^2(NS) + \frac{1}{2}\Delta_{NK}^S(N^2N_zS_z + N_zS_zN^2) + \Delta_{KN}^S N_z^2(NS) + \Delta_K^S N_z^3 S_z + \\ & + \delta_N^S(N_+^2 + N_-^2)(NS) + \frac{1}{2}\delta_K^S[(N_+^2 + N_-^2), N_zS_z], \end{aligned} \quad (2.2.4)$$

$$\begin{aligned} {}^{(6)}H^{\text{sp.-rot.}} = & H_J^S N^4(NS) + \frac{1}{2}H_{NNK}^S[N^4, N_zS_z]_+ + H_{KNN}^S N_z^2 N^2(NS) + \\ & + \frac{1}{2}H_{NKK}^S[N^2N_z^2, N_zS_z]_+ + H_{KKN}^S N_z^4(NS) + H_K^S N_z^4 N_z S_z + \\ & + \frac{1}{2}h_{KN}^S[(N_+^2 + N_-^2), N_z^2(NS)]_+ + \frac{1}{2}h_{NK}^S[(N_+^2 + N_-^2)N^2, N_zS_z]_+ + h_{NN}^S(N_+^2 + N_-^2)N^2(NS). \end{aligned} \quad (2.2.5)$$

The notations correspond to those generally accepted for the description of spin-rotational interactions. Here $N_+ = (N_x - N_y)/\sqrt{2}$ and $N_- = (N_x + N_y)/\sqrt{2}$ are the rotational creation and annihilation operators, respectively; the coefficients Δ_N^S , Δ_{NK}^S , Δ_{KN}^S , Δ_K^S , δ_N^S and δ_K^S are introduced by analogy with the corresponding fourth-order centrifugal distortion coefficients of the rotational operator. The last, third component (2.2.5) depends only on the spin operators and affects only the vibrational energy, so it was not studied in this work. A more detailed derivation of the Hamiltonian and its matrix elements is described in [52].

The ^{16}O nucleus present in the molecule has zero spin and is thus a boson, and the allowed Pauli full wave function of the $^{16}\text{O}^{35}\text{Cl}^{16}\text{O}$ molecule must have A^+ or A^- symmetry [53]. If we take into account the symmetry properties of the ground and excited vibrational states, it is easy to conclude that at the combination of quantum numbers $K_a + K_c = \text{"odd"}$, only transitions of $A_2(A^+)$ symmetry are allowed, and at $K_a + K_c = \text{"even"}$, transitions of $B_2(B^+)$ symmetry are observed in the spectrum. All other levels are absent in the spectrum. Thus, in the ClO_2 molecule only transitions of the a -type are possible for the bands investigated in this work. The selection rules in this case will be written as: $\Delta N = 0, \pm 1$;

ΔK_a = “even”; ΔK_c = “odd”; $\Delta J = 0, \pm 1$; $\Delta S = 0, \pm 1$. Note that the presence of a zero value of the spin of the ^{16}O nucleus leads to the absence of half of all possible transitions.

2.2.2. Analysis of the vibrational and rotational structure of the spectra of ClO_2 molecule.

Fundamental band v_3 and combination band $v_1 + v_3$

To study the v_3 and $v_1 + v_3$ bands, two spectra in the wavelength range 700–2,100 cm^{-1} were recorded on a Bruker IFS 125 HR Fourier spectrometer (Braunschweig, Germany) with a resolution of 0.0015–0.0030 cm^{-1} . The ClO_2 sample consisted of isotopologues of $^{35}\text{ClO}_2$ and $^{37}\text{ClO}_2$ in the ratio 3/1 and was placed in a White cell in the gaseous state at room temperature and pressures of 100 and 250 Pa for the first and second spectra, respectively. The water vapour (H_2O), carbon monoxide (CO) and carbonyl sulphide (OCS) lines were used for calibration. The optical path lengths were 0.23 and 6.4 m and the number of scans were 400 and 2,000 for the first and second spectra, respectively.

Figures 2.3–2.5 show the spectra of the studied bands with the indication of their centres. As it was mentioned earlier, the studied bands are a -type bands, so they are characterised by strong R -, P -, and Q -branches. The spectra were assigned by the previously described combination difference method; the values of vibrational and rotational energies of the ground vibrational state were taken from [52]. Considering that in the recorded spectra a large number of lines are overlapped (due to numerous unresolved and weakly resolved doublets), the values of the upper spin-rotation energies were determined using only isolated, unsaturated and non-weak lines.

Thus, using the improved Hamiltonian model, 37 spectroscopic parameters of the v_3 band (vibrational energy, 3 rotational parameters, 18 centrifugal distortion parameters, and 15 spin-rotational parameters) were determined from 2,220 values of vibrational and rotational energies due to 5,200 transitions (Table C.5, Appendix C) with maximum values of quantum numbers $K_a = 21$. This set of parameters (Table C.6) allows us to reproduce the experimental values of the upper energy levels with an accuracy of $d_{\text{rms}} = 2.4 \cdot 10^{-4} \text{ cm}^{-1}$.

Using the obtained data of the fundamental v_3 band and data on the v_1 band [52], 983 energy values were similarly obtained by analysing the $v_1 + v_3$ band, due to more than 2,000 transitions with a maximum value of the quantum number $K_a = 59$. A set of 30 spectroscopic parameters (vibrational energy, 17 rotational and centrifugal and 12 spin-rotational parameters (Table C.7)) allows us to reproduce the values of experimental energies with a standard deviation $d_{\text{rms}} = 2.5 \cdot 10^{-4} \text{ cm}^{-1}$, which exceeds the data known in the literature [51] by almost 35 times.

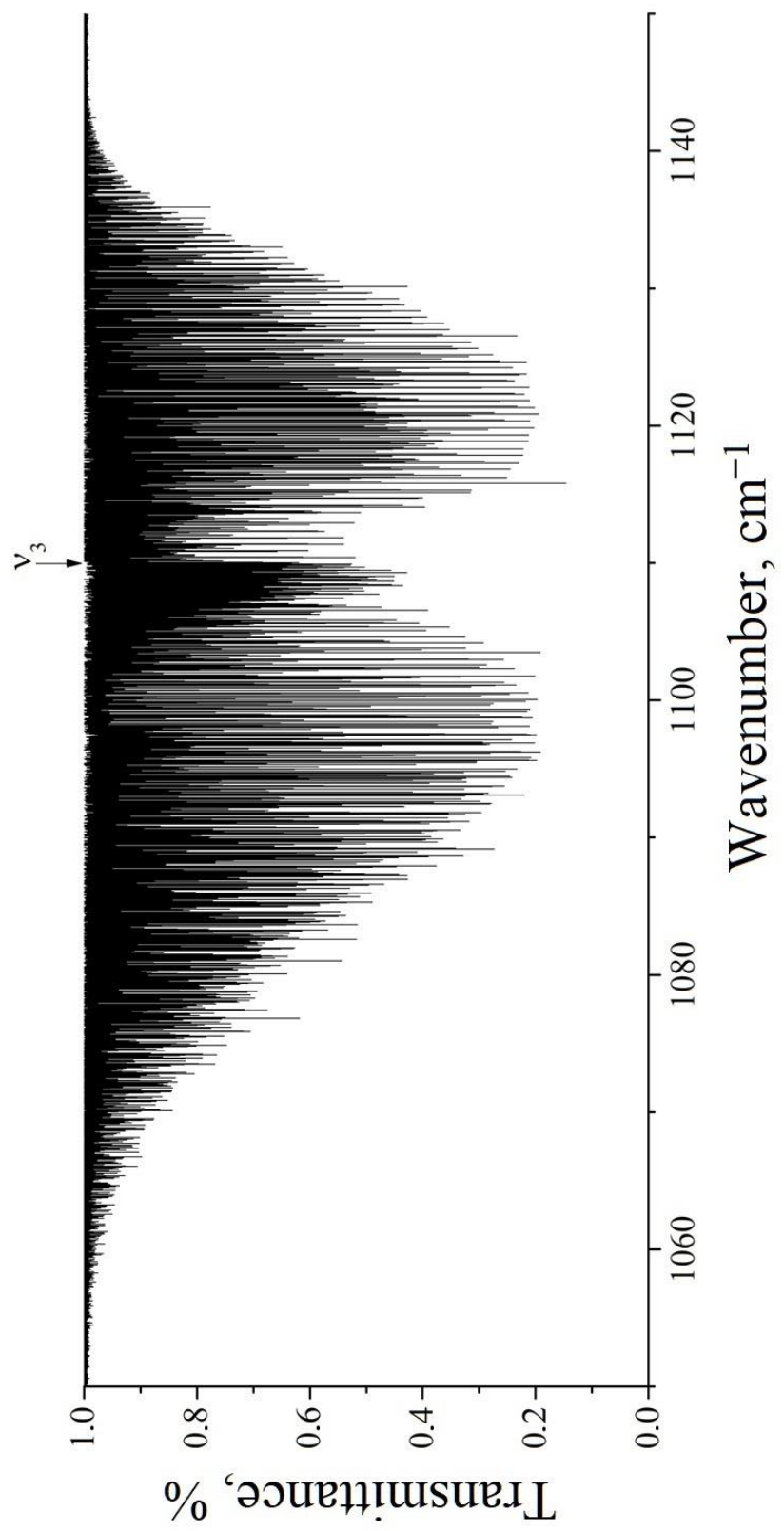


Figure 2.3 – Overview spectra of the ClO_2 molecule in the region of the v_3 band.

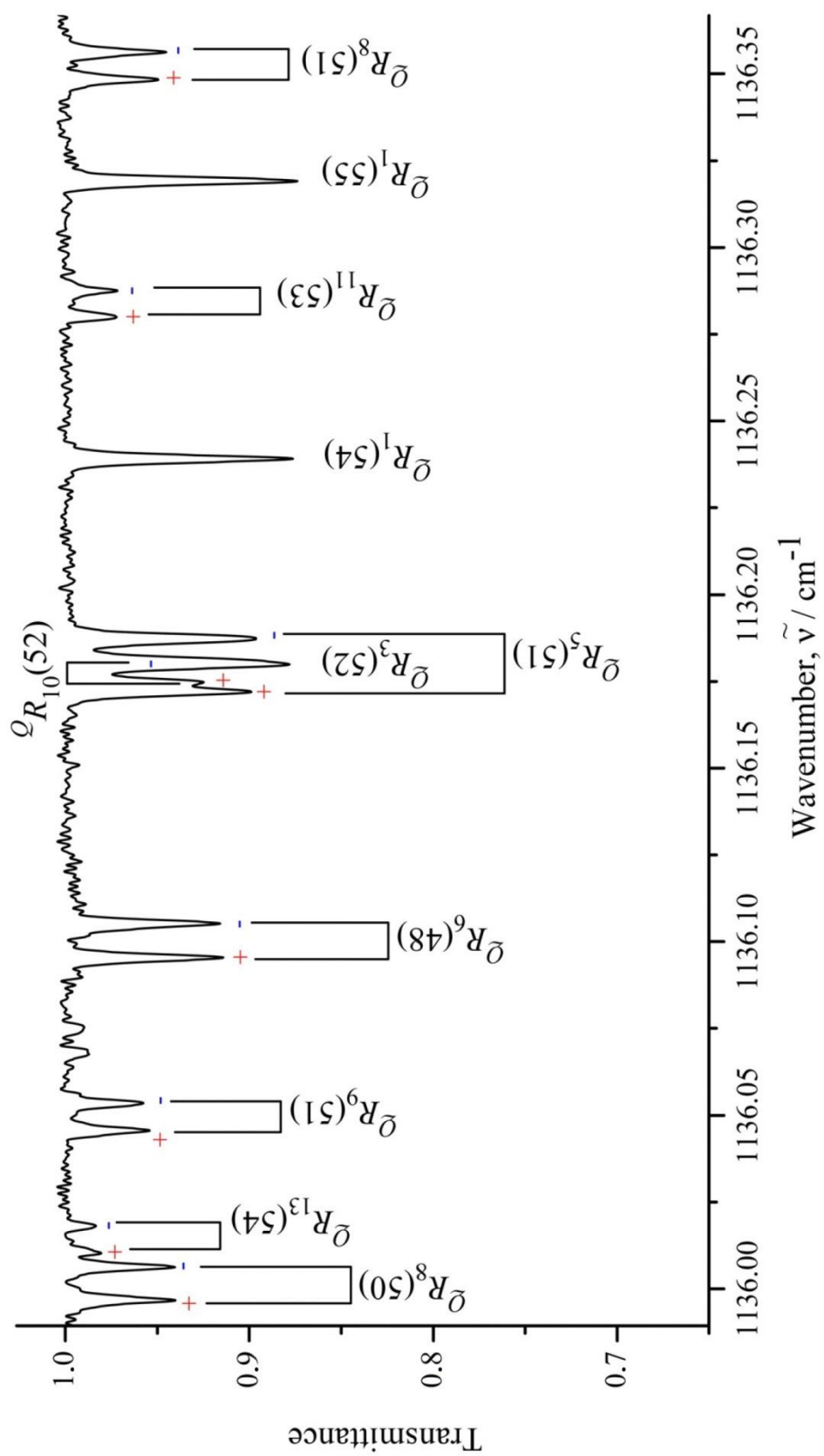


Figure 2.4 – Illustration of spin-rotation splittings in the R -branch region in the v_3 band. Symbols “+” and “-” denote symmetric and asymmetric components of doublets $J = N \pm 1/2$.

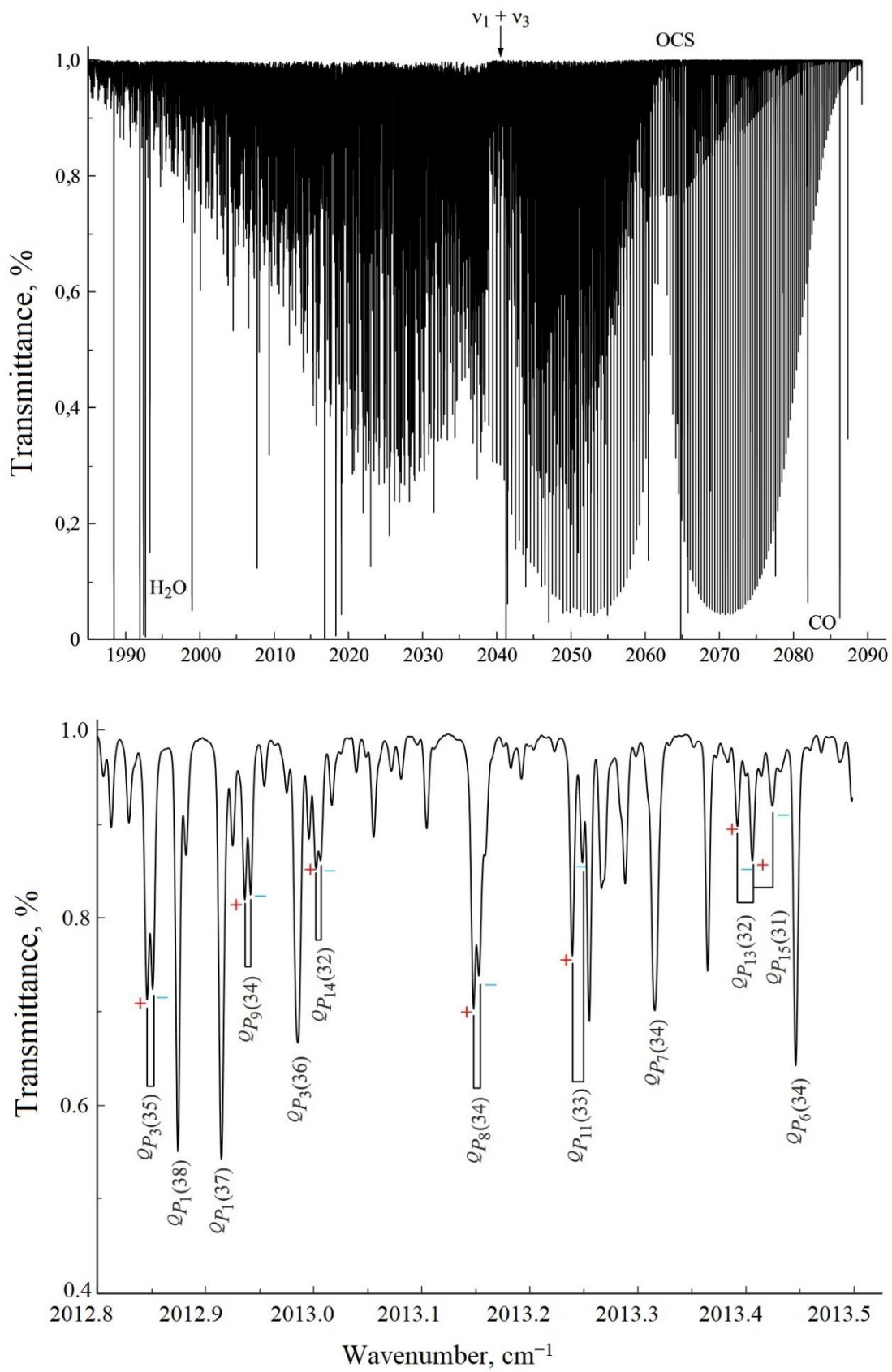


Figure 2.5 – Studied spectrum of the $v_1 + v_3$ band of the ClO_2 (upper fragment); doublet structure of the P -branch of $v_1 + v_3$ band (lower fragment).

Chapter 3

Theoretical study on high-resolution spectra of spherical tops: CD₄, SiF₄ and SiH₄ molecules

This chapter presents the results of vibrational-rotational spectra analyses of spherical top molecules CD₄, SiF₄, and SiH₄. At the beginning of each section, a literature review is given, as well as information from the theory of describing the spectra of spherical top molecules.

3.1. Deuterated methane isotopologue CD₄

The methane molecule, observed in various regions of our Universe, has been the subject of high-resolution molecular spectroscopy studies for many decades. More specifically, its spectroscopic properties play an important role in solving the problems of climate change in the Earth's atmosphere [54], in studies in astrophysics and planetology [55–60], in understanding chemical reactions in the atmospheres of exoplanets [61], and others. At the same time, many studies of the physical and chemical properties of the planets' atmospheres in the solar system and interstellar space require high-precision spectroscopic information not only about the CH₄ methane molecule itself, but also about its various isotopologues [62–64]. In the field of chemical physics, methane plays an important role as a prototype with fundamental importance for understanding the rotational dynamics of spherical top [65], for the development of chemical bonding theory [66] and intramolecular reactions [67], for understanding the structure of the potential hypersurface [68–70] and the fundamental dynamics of bimolecular reactions [71–73]. Isotopic substitution theory, being a powerful method for analysing the spectra of polyatomic molecules, initially requires highly accurate experimental data on both the basic and various isotopically substituted species of the molecule under study [74, 75].

3.1.1. Theoretical methods for describing the spectra of spherical top molecule methane CD₄

CD₄ is a spherical top molecule with a tetrahedral structure; its symmetry group is isomorphic to the T_d group. There are five representations in this symmetry group: A₁, A₂, E, F₁, F₂. All irreducible representations of the group are represented as characters in Table 3.1.

By reason of symmetry, molecules of XY₄ type have four normal vibrations: v₁, v₂, v₃ and v₄. Two of them correspond to stretching vibrations (v₁(A₁) non-generate and v₃(F₂) triply degenerate) and two to deformation vibrations (v₂(E) doubly degenerate and v₄(F₂) triply degenerate).

Based on the T_d symmetry of the CD₄ molecule, transitions in the absorption spectra of this molecule are possible only between such vibrational states ($v\Gamma$) and ($v'\Gamma'$), for which the condition is fulfilled

$$\Gamma \otimes \Gamma' \in F_2. \quad (3.1.1)$$

Transitions that do not satisfy this relation are forbidden by the symmetry of the molecule, but they can occur in the absorption spectrum due to resonance interactions between allowed transitions. In this section, the “allowed” v_4 band and the “symmetry forbidden” v_2 band are presented.

Table 3.1 – Characters of irreducible representations of the T_d group.

Repr.	E	$8C_3$	$3C_2$	$6S_4$	$6\sigma_d$	Basis
I	2	3	4	5	6	7
A_1	1	1	1	1	1	
A_2	1	1	-1	-1	-1	
E	2	-1	2	0	0	
F_1	3	0	-1	1	-1	(R_x, R_y, R_z)
F_2	3	0	-1	-1	1	x, y, z

The effective Hamiltonian (1.3.1) was used to describe the spectra of the CD_4 molecule in the region of the v_2/v_4 dyad. For the dyad of interacting bands v_2 and v_4 of a molecule of XY_4 type (T_d symmetry), the expression (1.3.1) can be represented in the form of:

$$H^{\text{vib.-rot.}} = H_{\text{GS}}^{\text{vib.-rot.}} + H_{\text{dyad}}^{\text{vib.-rot.}} \quad (3.1.2)$$

with

$$H_{\text{GS}}^{\text{vib.-rot.}} = \sum_{\Omega K} |0000, A_1\rangle \langle 0000, A_1| R^{\Omega(K, A_1)} Y_{(0000, A_1), (0000, A_1)}^{\Omega(K, A_1)} \quad (3.1.3)$$

$$\begin{aligned} H_{\text{dyad}}^{\text{vib.-rot.}} &= \sum_{\Gamma} \sum_{\Omega K} |0100, E\rangle \otimes \langle 0100, E| R^{\Omega(K, \Gamma)} Y_{(0100, E), (0100, E)}^{\Omega(K, \Gamma)} + \\ &+ \sum_{\Gamma} \sum_{\Omega K} [(|0001, F_2\rangle \otimes \langle 0001, F_2|)^{\Gamma} \otimes R^{\Omega(K, \Gamma)}]^{A_1} Y_{(0001, F_2), (0001, F_2)}^{\Omega(K, \Gamma)} + \\ &+ \sum_{\Gamma} \sum_{\Omega K} [(|0100, E\rangle \otimes \langle 0001, F_2|)^{\Gamma} \otimes R^{\Omega(K, \Gamma)}]^{A_1} Y_{(0100, E), (0001, F_2)}^{\Omega(K, \Gamma)} + \\ &+ \sum_{\Gamma} \sum_{\Omega K} [(|0001, F_2\rangle \otimes \langle 0100, E|)^{\Gamma} \otimes R^{\Omega(K, \Gamma)}]^{A_1} Y_{(0100, E), (0001, F_2)}^{*\Omega(K, \Gamma)}. \end{aligned} \quad (3.1.4)$$

All notations in equations (3.1.4)–(3.1.5) are traditional: $|0000, A_1\rangle$, $|0100, E\rangle$ and $|0001, F_2\rangle$ are the symmetrized vibrational functions of the ground and two single excited vibrational states; $R^{\Omega(K, \Gamma)}$ are symmetrized rotational operators; Ω is the total degree of the rotational operator J_α ($\alpha = x, y, z$) in the individual operator R ; K is the rank of this operator, Γ is its symmetry in the group T_d . The sign \otimes

denotes a tensor product, and the values $Y_{v_l\gamma_l, v_u\gamma_u}^{\Omega(K, \Gamma)}$ are different-type spectroscopic parameters (more details are given in [76–78]).

The shape and absolute line intensity were analysed to obtain the dipole moment parameters of the molecule. The intensity of an individual line was described as [78]:

$$S_{v_0} = \frac{8\pi^3 v_0}{4\pi\epsilon_0} \left[1 - \exp\left(-\frac{hc v_0}{k_B T}\right) \right] N \frac{g_A}{Z(T)} \exp\left(-\frac{E_A}{k_B T}\right) \mathcal{R}_A^B. \quad (3.1.5)$$

Here $v_0 = (E_B - E_A)/hc$ is the wave number of the corresponding transition; E_B and E_A represent the energies of the excited and ground vibrational-rotational states of the transition; g_A is the statistical weight of the nuclear spin (for the CD_4 molecule we have $g_{A1} = g_{A2} = 15$, $g_E = 12$, and $g_{F1} = g_{F2} = 18$ for the rotational symmetry states A_1, A_2, E, F_1 and F_2 [79]); $Z(T)$ is the distribution function. The value of

$$\mathcal{R}_A^B = |\langle A | \mu_Z' | B \rangle|^2 \quad (3.1.6)$$

in equation (3.1.6) is the square of the matrix element of the effective dipole moment operator (more details are given in [80])

$$\mu_Z' = \sum_{v_l\gamma_l, v_u\gamma_u} \sum_{\Gamma_r n\Gamma_r \Omega K \tilde{K}} \left([|v_l\gamma_l\rangle \otimes \langle v_u\gamma_u|]^{(\Gamma_r)} \otimes R^{\Omega K(\tilde{K}, n\Gamma_r)} \right)^{A_2} p_{v_l\gamma_l, v_u\gamma_u}^{\Omega K(\tilde{K}, n\Gamma_r)} \quad (3.1.7)$$

on the symmetrized lower $\langle A |$ and upper $| B \rangle$ ro-vibrational wave functions of transition; the values $p_{v_l\gamma_l, v_u\gamma_u}^{\Omega K(\tilde{K}, n\Gamma_r)}$ are the so-called effective dipole moment parameters of the band $(v_u\gamma_u) \leftarrow (v_l\gamma_l)$; indexes l and u are related to the lower and upper wave functions, and the effective operators $R^{\Omega K(\tilde{K}, n\Gamma_r)}$ have the form [81]:

$$R^{\Omega K(\tilde{K}, n\Gamma_r)} = \sum_{\mu} \tilde{K} G_{n\Gamma_r \sigma_r}^{\mu} R_{\mu}^{\Omega K(\tilde{K})} = \sum_{\mu} \tilde{K} G_{n\Gamma_r \sigma_r}^{\mu} \left(R^{\Omega(K)} \otimes \lambda^{(1)} \right)_{\mu}^{\tilde{K}}. \quad (3.1.8)$$

Here \tilde{K} takes the values $K - 1, K$ or $K + 1$. From the three k_{Zx} , k_{Zy} , and k_{Zz} direction cosines operators it is possible to easily constrain the irreducible tensorial operators $\lambda^{(1)}$, following the rules:

$$\begin{aligned} \lambda_0^{(1)} &= k_{Zz} = \cos\theta, \\ \lambda_{\mp 1}^{(1)} &= \frac{\pm(k_{Zx} \pm ik_{Zy})}{\sqrt{2}} = \mp \sin\theta e^{\frac{\mp i\chi}{\sqrt{2}}}. \end{aligned} \quad (3.1.9)$$

The matrix elements $\langle A|\mu_z'|B\rangle$ can be calculated using the results of the theory of irreducible tensor sets [82, 83]. As shown in [81], in molecules of XY₄ type (of T_d symmetry) for ro-vibrational transitions from the ground vibrational state these matrix elements can be written as:

$$\langle A|\mu_z'|B\rangle = \sum_{n_{gr}\gamma_{gr}^r n_u\gamma_u} A_{0A_1, J_{gr} n_{gr}\gamma_{gr}^r}^{C_{gr}S_{gr}} B_{\nu_u \Gamma_u, J_u n_u \gamma_u^r}^{C_u S_u} \mathcal{R}_{0A_1; J_{gr} n_{gr}\gamma_{gr}^r; C_{gr}S_{gr}}^{\nu_u \gamma_u; J_u n_u \gamma_u^r; C_u S_u} \quad (3.1.10)$$

In more details all transformations for obtaining matrix elements of dipole moment operators are presented in [82, 83].

3.1.2. Results of analysis of vibrational-rotational energies and line intensities of CD₄ methane in the region of the v₂/v₄ dyad

To analyse the positions and intensities of the lines, three spectra of gaseous CD₄ (with a percentage of the investigated gas sample more than 99 %) were recorded (Figure 3.1) using a Bruker IFS125HR Fourier Transform Infrared Spectrometer (Braunschweig, Germany) in the wavelength ranges from 800 to 1,400 cm⁻¹. For this purpose, optical single-pass (spectrum I) and multi-pass White cells (spectrum II and III) [84], both made of stainless steel, were used. For all spectra a globar multiband infrared radiation source together with a KBr beam splitter and an MCT detector have been used at an optical resolution of 0.003 cm⁻¹. The number of scans of at least 700 for each spectrum allowed to additionally improve the signal-to-noise ratio. For each of spectra I, II, and III the pressures were 80, 100, and 352 Pa, respectively; the optical path lengths were 230.500 ± 0.200 mm, 4.052 ± 0.002 m, and 24.052 ± 0.012 m, respectively; and the aperture values were 1.7, 1.3, and 1.7 mm, respectively.

The total linewidth varied between 0.0030 and 0.0049 cm⁻¹. The total line width is dominated by the Doppler effect, since the width of the pressure line can almost be neglected. Using the Beer–Bouguer–Lambert law, the line intensity S can be derived from the area of one A_{line} absorption line, the partial pressure p of the gas samples (¹²CD₄ and ¹³CD₄), the temperature T and the optical path length L :

$$S = \frac{k_B T}{PL} A_{\text{line}}, \quad (3.1.11)$$

with

$$A_{\text{line}} = \frac{1}{\log(e)} \int \log \left(\frac{I_0(\nu)}{I(\nu)} \right) d\nu. \quad (3.1.12)$$

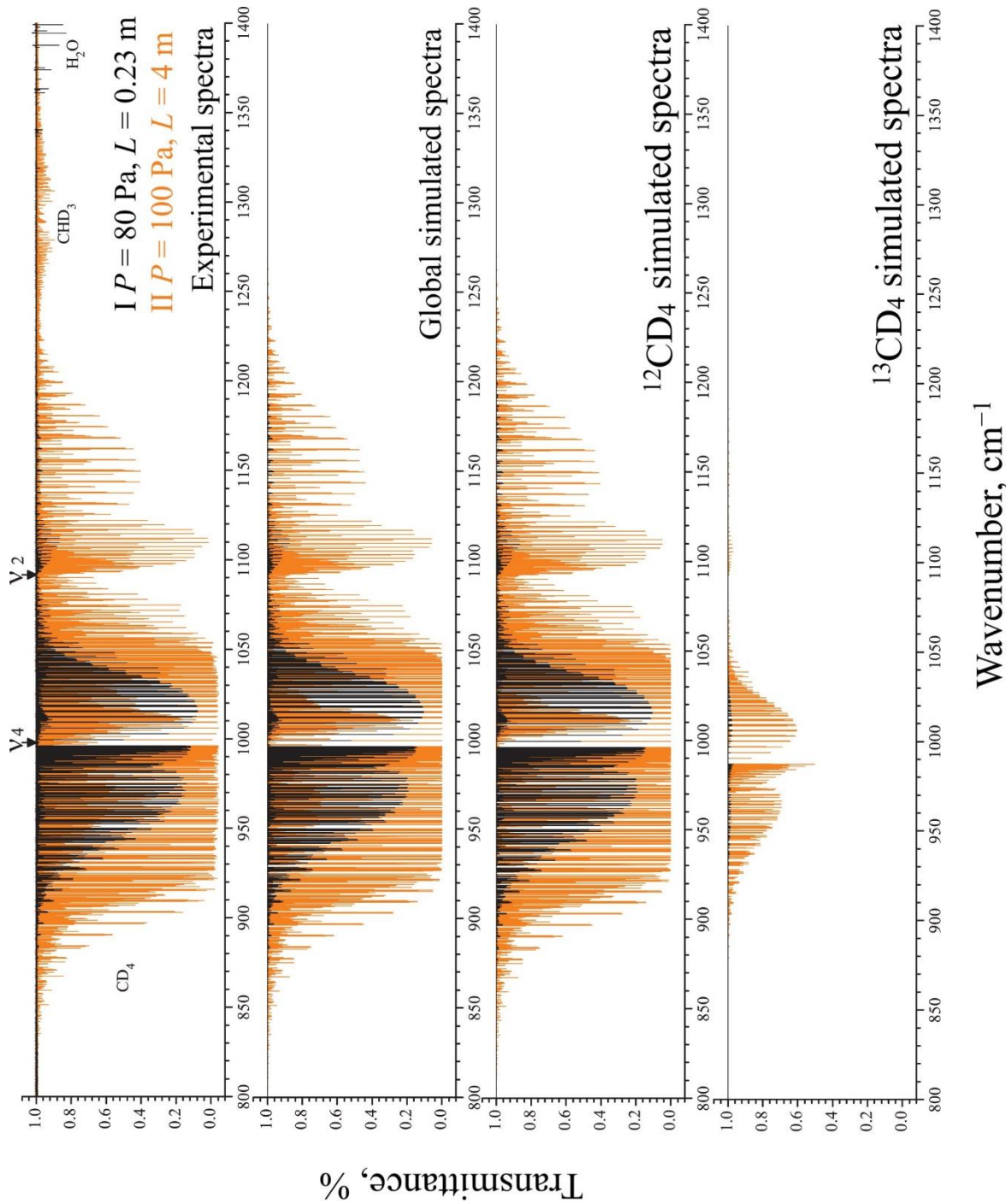


Figure 3.1 – Spectra I (black) and II (orange) of the $^{12}\text{CD}_4$ and $^{13}\text{CD}_4$ in the dyad ν_2/ν_4 region.
Upper part presents the experimental spectra. Lower part presents the calculated ones.

Line intensities were obtained by direct integration of the measured effective line absorption, which can be well fitted by the Voigt or Hartmann-Tran line profile.

Previously, a study of the CD₄ molecule spectra in the region of the strong-interacting bands of the dyad v₂/v₄ was first presented in [74]. New results on the investigation of the positions of the dyad lines of interacting states of the main modification are presented in [84]. In the process of analysis, it became clear that lines belonging to the ¹³CD₄ isotopologue are present in the spectrum. For this reason, it was possible to analyse the positions and intensities of not only the basic but also the isotopole-substituted molecule.

At the beginning of the present analysis of experimental data, assignments of the ¹³CD₄ molecule transitions have been made simultaneously with the fit of parameters $Y_{\nu l \gamma, \nu' l' \gamma'}^{\Omega(K, \Gamma)}$ of the effective Hamiltonian (3.1.2) using the SPHETOM software package [85], which was tailored specifically for such studies. In accordance with the general statements of the isotopic substitution theory, the higher order effective spectroscopic parameters of ¹³CD₄ molecule should be close to the values of corresponding parameters of ¹²CD₄ (at least, the difference between the corresponding parameters of the ¹²CD₄ and ¹³CD₄ isotopologues should be no more than 8–10 %). For this reason (taking into account that the values of higher order parameters are very small), it is suitable to put initial values of such higher order spectroscopic parameters of [84] as an initial approximation when analysing the isotopologue substituted modification. The initial values of the main spectroscopic parameters (band centres, Coriolis interaction parameter, and additions to the rotational parameters of the upper vibrational states) have been numerically estimated on the basis of formulas and relations from [8]. On this basis, as the result of the analysis, the 689 transitions were assigned with a maximum value of the quantum number $J = 23$ (compared to the results known in the literature of 171 interpreted transitions with $J^{\max} = 12$ from [74]) for the v₄ band and 212 transitions were assigned with a maximum value of the quantum number $J = 21$ for the v₂ band (no data for this band in [74]). The derived result is a considerable extension of the information known from the preceding studies about spectroscopic properties of v₂/v₄ bands of the ¹³CD₄ molecule. The complete list of assigned experimental transitions for these bands within the study of the ¹³CD₄ molecule spectra is given in the Table D.1 (Appendix D). The data are presented in the formulation of the STDS software package.

On the basis of the derived information about transition values, a weighted fit of parameters of the effective Hamiltonian was made. At the first step of the analysis both an assignment and a preliminary fit of parameters have been made by use of the SPHETOM code. However, the final fit was fulfilled using the XTDS software [86, 87]. As the result, 18 fitted parameters (1 parameter of the ground vibrational state, 8 and 4 parameters of the (0001, F₂) and (0100, E) vibrational states, and 5 Coriolis interaction parameters) were obtained and are presented in Table D.2 column 5 together with their 1σ confidence statistical intervals (the latter are shown in parentheses). For comparison, column 6 presents

parameters previously known in the literature [74]. Column 4 present the parameters from [84], were the dyad for the main isotopologue $^{12}\text{CD}_4$ was studied. The obtained spectroscopic parameters allow us to reproduce the experimental positions of the lines with an error of no more than $d_{\text{rms}} = 2.57 \cdot 10^{-4} \text{ cm}^{-1}$, which is close to the value of the experimental error, despite the weak intensity of the studied lines (Figure 3.2). The accuracy of the obtained results is also confirmed by the consistency of the parameter values for the basic $^{12}\text{CD}_4$ and isotope-substituted $^{13}\text{CD}_4$ modifications of the deuterated methane molecule.

The absolute line intensities of the v_4 band of the $^{12}\text{CD}_4$ molecule were analysed in spectrum I. Spectrum II was used to analyse the line intensities of the weaker v_2 band. In the first step of the analysis, the individual intensities of 777 unmixed unsaturated and not too weak transitions of the v_4 band and 780 transitions of the v_2 band were determined from fitting the contour of the lines to the Hartmann-Tran profile [88, 89] (as an illustration, Figure 3.3 shows a sample of the shape and intensity fit of an individual line belonging to the v_4 band). The experimental line intensities of the v_4 band of the $^{13}\text{CD}_4$ molecule were similarly investigated (the transitions belonging to the v_2 band had too low intensities even in the strong II spectrum, so it was not possible to analyse them). In the Tables D.3, D.4 the experimental values of the lines' intensities of v_2/v_4 dyad of the molecule $^{12}\text{CD}_4$ and of v_4 band of the $^{13}\text{CD}_4$ molecule, respectively, are presented. The data on the experiment absolute line intensities were then used to determine the effective dipole moment parameters $p_{v_l \gamma_l, v_u \gamma_u}^{\Omega K(\tilde{K}, n \Gamma_r)}$ of the v_4 and v_2 bands of the $^{12}\text{CD}_4$ molecule and of the v_4 band of the $^{13}\text{CD}_4$ molecule from the weighted fit procedure. The obtained values of the effective dipole moment parameters are presented in column 3 of Table D.5.

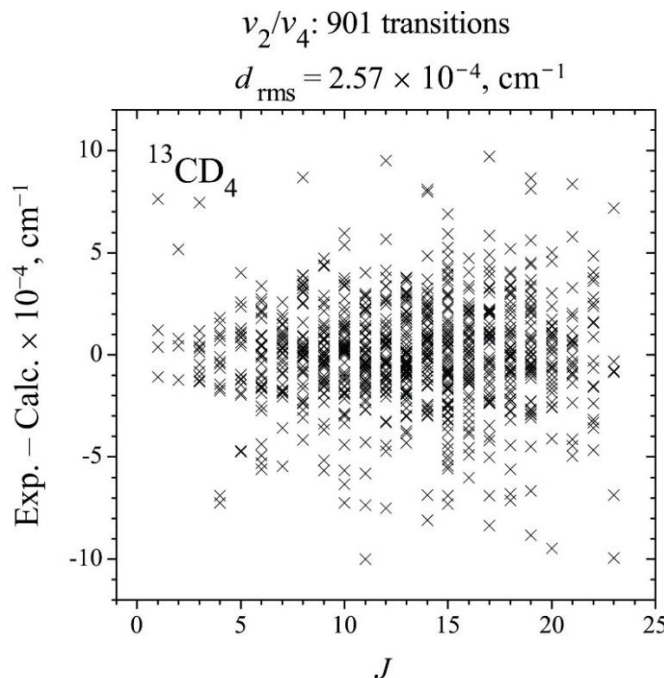


Figure 3.2 – Fit residuals for line position values and fit statistic for the v_2 and v_4 bands of $^{13}\text{CD}_4$.

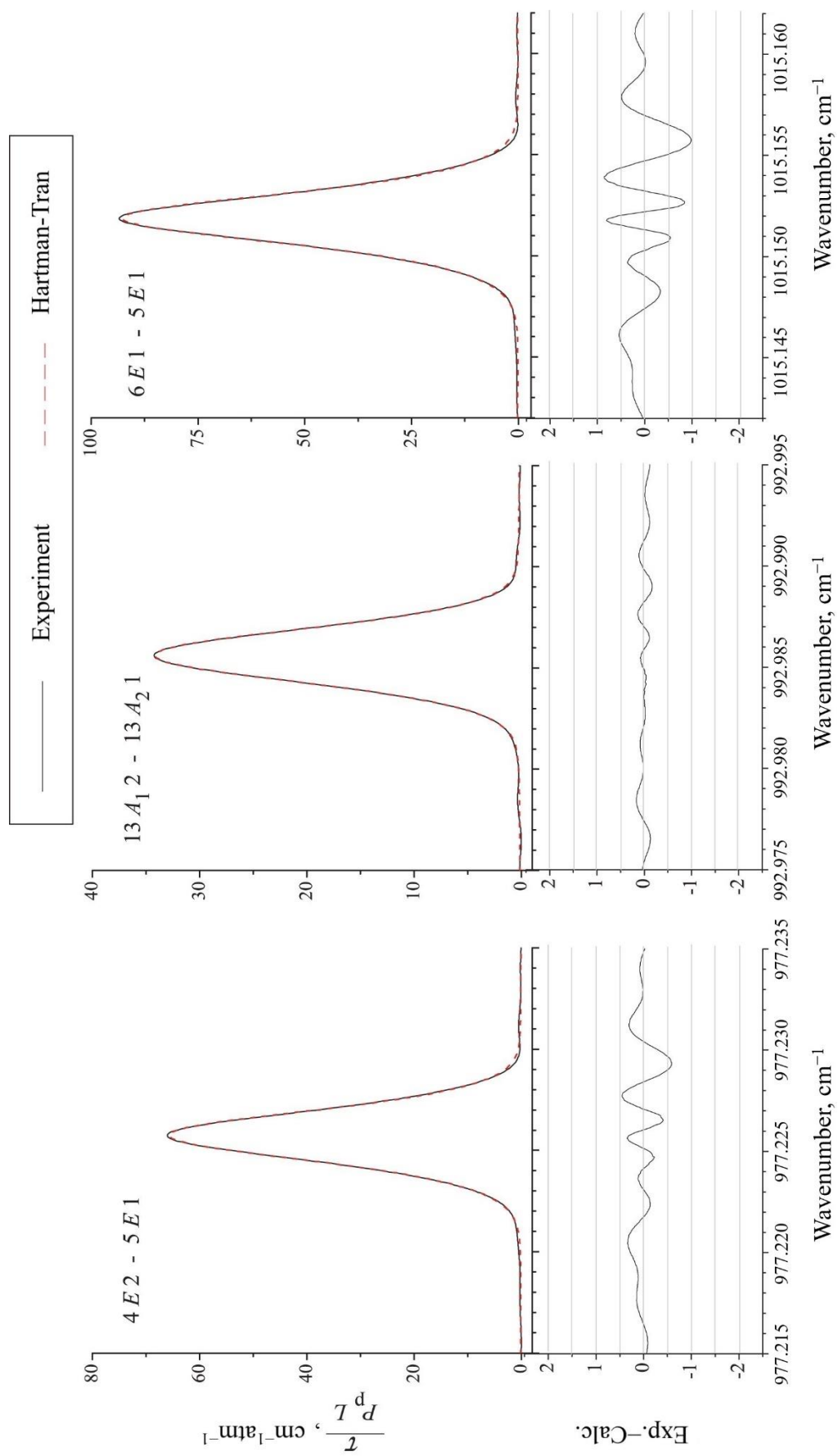


Figure 3.3 – Experimental and theoretical Hartmann-Tran profile line shapes (for the experimental spectrum I).

The lower part of the figure shows the difference between the experimental and theoretically calculated line intensities.

Thus, the individual intensity values of the 131 transitions were determined from fitting their shape using the Hartmann-Tran profile and then determining the parameters $p_{\nu_l \gamma_l, \nu_u \gamma_u}^{\Omega K(\tilde{K}, n \Gamma_r)}$ of the effective dipole moment (column 4 of Table D.5). As can be seen from the data presented in Table D.5, only the main dipole moment parameter was varied for the ν_4 band of the $^{13}\text{CD}_4$ molecule, the values of the other parameters were fixed by the values of the corresponding parameters of the ν_4 band of the $^{12}\text{CD}_4$ molecule. The error in describing the experimental contours using the obtained parameters did not exceed 5 % for all bands and all isotopologues. The exact values of the errors are presented in the last row of Table D.5.

3.2. Silicon tetrafluoride – silane SiF_4

Silicon tetrafluoride (SiF_4) is interesting from both practical and theoretical points of view. It is used as a chemical reagent to produce high quality semi-conducting silicon epitaxial coatings [90]. This molecule is formed during volcanic activity [91], and since this gas is involved in the formation of extremely poisonous hydrogen fluoride (HF) when in contact with hot water and acids [92], it is necessary to be able to detect this compound in the atmosphere with high accuracy. Geothermal infrared spectroscopy, utilising radiation from the volcano itself, allows continuous monitoring of SiF_4 content in the air [93, 94]. Thus, better knowledge of spectroscopic parameters is necessary to determine the exact concentrations of this molecule.

From the theoretical point of view, the SiF_4 molecule is a spherical top molecule (STM). The particular features of STM, which were initially seen as difficulties to be removed, became the motivation that led to original modelling methods applicable to a wide range of spectroscopic problems [86]. One of the important and challenging problems in chemical physics is the accurate determination of the intramolecular multidimensional potential surface and dipole moment surface, which can be used in a variety of numerous applications. Therefore, knowledge of highly accurate spectroscopic information not only on the basic ($^{28}\text{SiF}_4$) but also on the isotopically substituted modifications ($^{29}\text{SiF}_4$, $^{30}\text{SiF}_4$) plays an important role in the complete description of the properties of molecules in the natural isotopic mixture [95].

One of the first theoretical and experimental studies of silicon tetrafluoride was carried out more than half a century ago [96–98], and mainly concerned not so much the spectroscopic data of the molecule itself as the construction of vibrational frequencies of XY_4 type molecules, the determination of force constants, and the re-examination of the molecular structure of gaseous SiF_4 . In later papers [99–101], the authors describe the study of the fundamental ν_3 band and the $3\nu_3$ band, which were analysed using diode laser spectroscopy with Doppler confinement and sub-Doppler saturation spectroscopy, attributed to infrared and microwave transitions. The next few years of work devoted to the study of this

molecule cover some theoretical calculations, improvement of the Hamiltonian model, measurement of the double resonance and ground state enhancement with the v_3 band [102, 103]. Thus, the main attention of researchers has long been focused on the study of the v_3 band and the ground state, which has influenced the further development of theoretical and experimental methods to study this molecule.

Subsequently, the authors of [104] presented their results on the calculation of the equilibrium structure, thermodynamic and kinetic parameters of the silicon tetrafluoride molecule. With the development of experimental techniques and the theory of describing spherical top molecules [105], a number of recent works [106, 107] provided more accurate information on the spectroscopic parameters of the fundamental and overtone states and their combinations, leading to an accurate determination of the equilibrium Si-F bond length. The first fit of the dipole moment derivative for the v_3 band of the fundamental isotopologue $^{28}\text{SiF}_4$ was performed. Knowing the fundamental bands data, it became possible to investigate more complex combination bands of the molecule, which is presented in this section of the work.

3.2.1. Theoretical methods for describing the spectra of spherical top silane SiF_4 molecule

Like the CD_4 molecule described earlier in this work, the SiF_4 molecule is a spherical top molecule with a tetrahedral structure, its symmetry group is isomorphic to the T_d point group. Also, like the methane molecule, by symmetry, the SiF_4 molecule has four normal vibrations: v_1 , v_2 , v_3 and v_4 . Two of them correspond to valence vibrations ($v_1(A_1)$ non-generate and $v_3(F_2)$ triply degenerate) and two to stretching ($v_2(E)$ doubly degenerate and $v_4(F_2)$ triply degenerate).

Based on the theory of symmetry, group theory and their application to molecular spectroscopy, the basic theoretical model for the description of molecules belonging to one symmetry group (in this case a group isomorphic to the point group T_d) has the same form, and therefore we will omit the repetition of the main statements from section 3.1. Instead, we will give some peculiarities encountered in the description of the heavy highly symmetric molecule SiF_4 .

As it has been said before, the silicon tetrafluoride molecule belongs to the type of spherical top by the ratio between the moments of inertia, and therefore the results of fundamental studies of the authors [108, 109], as well as the tensor formalism and methods of group theory from [86, 105] are used for its description. For this type of molecule, there exist approximate relations between the wave numbers of its normal vibrational modes, which can then be grouped into vibrational polyads. This approximate relation can be described through vibrational states:

$$k = 6v_1 + 2v_2 + 8v_3 + 3v_4, \quad (3.2.1)$$

which, thus, leads to polyads typical to the silane molecule (and its fully fluorinated version SiF₄): P_0 (ground state), P_1 is absent in this case, P_2 for the v_2 band, etc. The complete list of vibrational levels grouped by polyads is shown graphically in Figure A.1 (Appendix A). It should also be noted that simple calculations in the first approximation by perturbation theory show that the contribution of interactions between different ro-vibrational modes is negligible for a SiF₄-type molecule. Thus, its ro-vibrational bands can initially be analysed with sufficient accuracy using the isolated state model. Despite this, the presence of high symmetry leads to another problem, namely the previously mentioned tetrahedral splittings in both vibrational and vibrational-rotational states, which make it necessary to use a more complex Hamiltonian that takes these splittings into account. The Hamiltonian model used to describe the spectra of spherical top was presented earlier in Section 3.1.1.

3.2.2. Analysis of combination bands spectra of SiF₄

The spectra were recorded using synchrotron radiation to record the far-infrared range (100–600 cm⁻¹) at the AILES station of the SOLEIL synchrotron, and using a broadband infrared source combined with a different collimator size for the mid-range (600–2,400 cm⁻¹). The spectra were recorded using a Bruker 125HR Fourier transform spectrometer. Due to the weak intensity of many of the studied bands and the large number of “hot” bands, the sample was placed in a cryogenic cell with a long optical path with a maintained temperature of 163 K. The optical path length was 3 m (93 m for the spectra recorded in the $v_2 + v_4$ band region), and the resolution varied from 0.0015 to 0.004 cm⁻¹. The sample pressure was chosen to avoid saturation in the spectra in the region of the v_2 band. The number of scans was varied from 90 to 1,920. The well-studied line data of the CO₂ and COS spectra were used for calibration.

At the initial stage of the study of combination bands spectra of the SiF₄ molecule, data on the fundamental bands [107] of this molecule were used as parameters of the effective Hamiltonian of the first approximation. The lines were assigned using the SPVEIW software package. The XTDS software package was used to analyse and calculate the energy structure of the vibrational states ($v_1 = v_2 = 1$), ($v_1 = v_3 = 1$), ($v_1 = v_4 = 1$), ($v_2 = v_3 = 1$), ($v_2 = v_4 = 1$) and ($v_3 = v_4 = 1$). Both software packages were developed at the ICB interdisciplinary laboratory of the University of Burgundy (Dijon, France) [86, 87].

The main difficulty in studying the spectra is the presence of a large number of transitions belonging to the “hot” bands of the SiF₄ molecule, despite the experimental conditions chosen in such a way as to reduce the intensity of these lines in the studied spectra. The presence of “hot” bands can be clearly seen in the spectrum of the $v_2 + v_4$ band (Figure 3.4). Despite the close location of the ro-vibrational bands centres, their interaction appears to be insignificant, and therefore all ro-vibrational bands, presented in this section, were analysed using a theoretical model for isolated states.

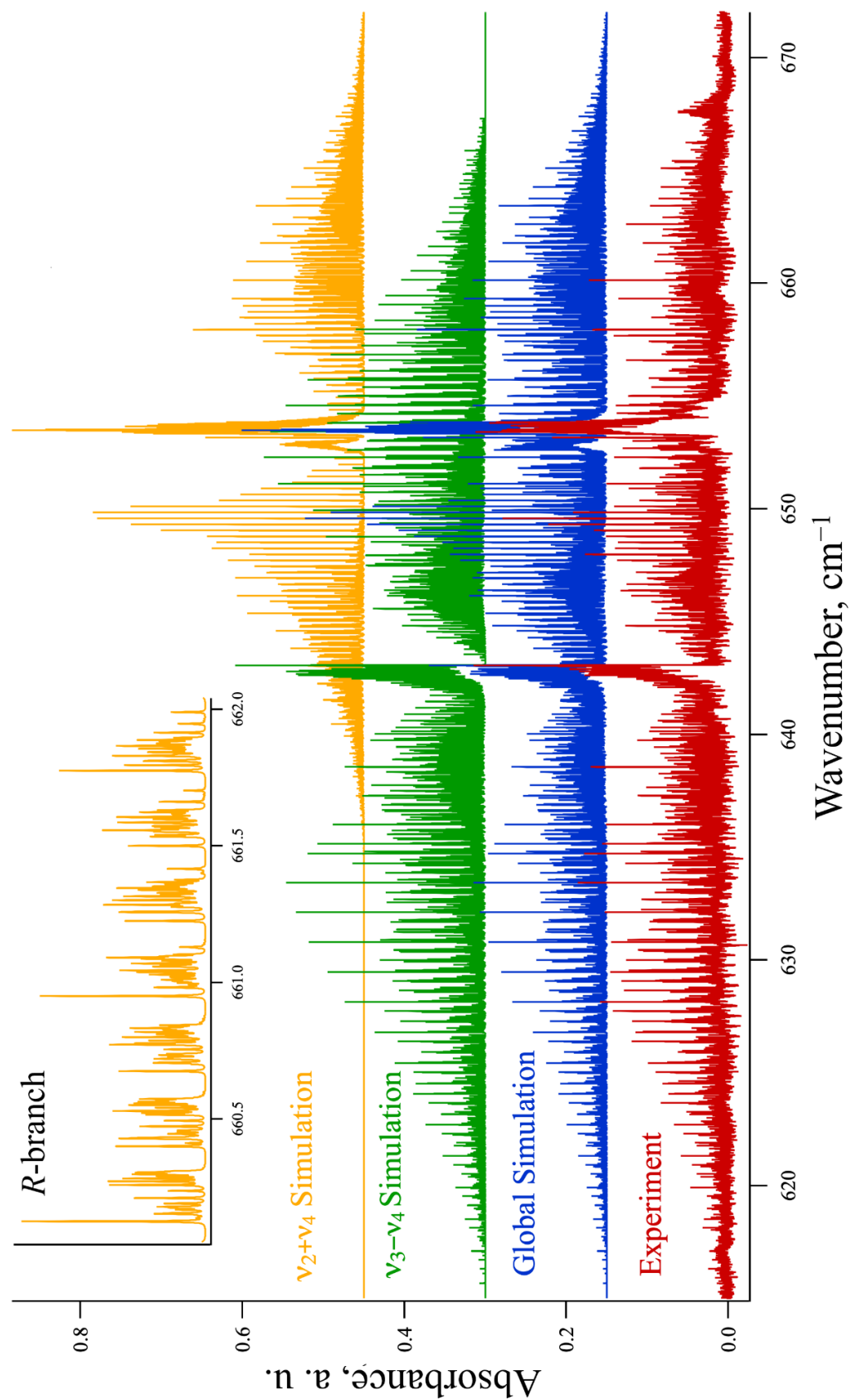


Figure 3.4 – The $v_2 + v_4$ and $v_3 - v_4$ bands. Comparison of experimental and theoretical spectra.

The detailed image of the *R*-branch is shown in the inset above.

Statistics on the results of combination bands spectra analyses are given in Table 3.2 (column 5 represents the number of parameters fitted in this work).

Table 3.2 – Statistical data on the results of combination band analysis of SiF₄ molecule.

Band	Band centre, cm ⁻¹	<i>J</i> ^{max}	<i>N</i> _{transitions}	<i>N</i> _{parameters}	<i>d</i> _{rms} · 10 ⁻³ , cm ⁻¹
<i>1</i>	<i>2</i>	<i>3</i>	<i>4</i>	<i>5</i>	<i>6</i>
v ₁ + v ₂	1064.2395	78	1,141	6	0.398
v ₁ + v ₂ + v ₄	1454.8007	16	135	16	0.429
v ₁ + v ₃	1828.3546	82	1,334	9	0.563
²⁹ v ₁ + v ₃	1819.3854	45	198	8	0.665
³⁰ v ₁ + v ₃	1810.8235	58	267	11	0.478
v ₁ + v ₄	1189.9905	58	1,131	4	0.417
v ₂ + v ₃	1294.5825	70	2,907	22	0.445
v ₂ + v ₄	653.3963	54	844	19	0.382
v ₃ + v ₄	1418.5583	60	2,194	44	0.633
Total			10,151		

For the v₁ + v₃ band (Figure B.1, Appendix B), due to its high intensity, it was possible to analyse not only the transitions belonging to the main modification of the ²⁸SiF₄ molecule, but also for the isotopologues ²⁹SiF₄ and ³⁰SiF₄. The study of the v₂ + v₄ band was complicated by the presence of closely located transitions belonging to the “hot” band v₃ – v₄ (see Figure 3.4), mixed and overlapped with the lines of the studied band. The spectrum of the v₃ + v₄ band (Figure B.2) consists of four sublevels, which makes the spectrum very dense. Thus, analysing this band required taking into account the interaction of the closely spaced four sublevels, which made the task more difficult. The v₂ + v₃ band (Figure B.3) was analysed up to a maximum value of quantum number *J* = 70; the spectra of this band do not contain lines belonging to “hot” bands or other combination bands. In the spectrum of the v₁ + v₄ band (Figure B.4) it was possible to identify a band centre belonging to the ²⁹SiF₄ isotopologue, but due to its weak intensity it was not possible to analysed. The spectrum of the weak band v₁ + v₂ (Figure B.5), which centre is located quite close to the centre of the fundamental band v₃ (less than 40 cm⁻¹), was analysed, as well as other combination bands in this study, with a theoretical model that does not take resonance interactions into account. At the same time, the spectroscopic parameters obtained by fit allow us to reproduce the experimental positions of the lines with an accuracy no worse than the experimental one.

The obtained combination band parameters allow theoretical calculations of the spectra of “hot” bands, such as v₃ + v₁ – v₁, v₃ + v₂ – v₂ and v₃ + v₄ – v₄ (Figure 3.5). The data on the positions of the lines corresponding to the “hot” transitions were recorded in the international spectroscopic database *TFSiCaSDa* [110].

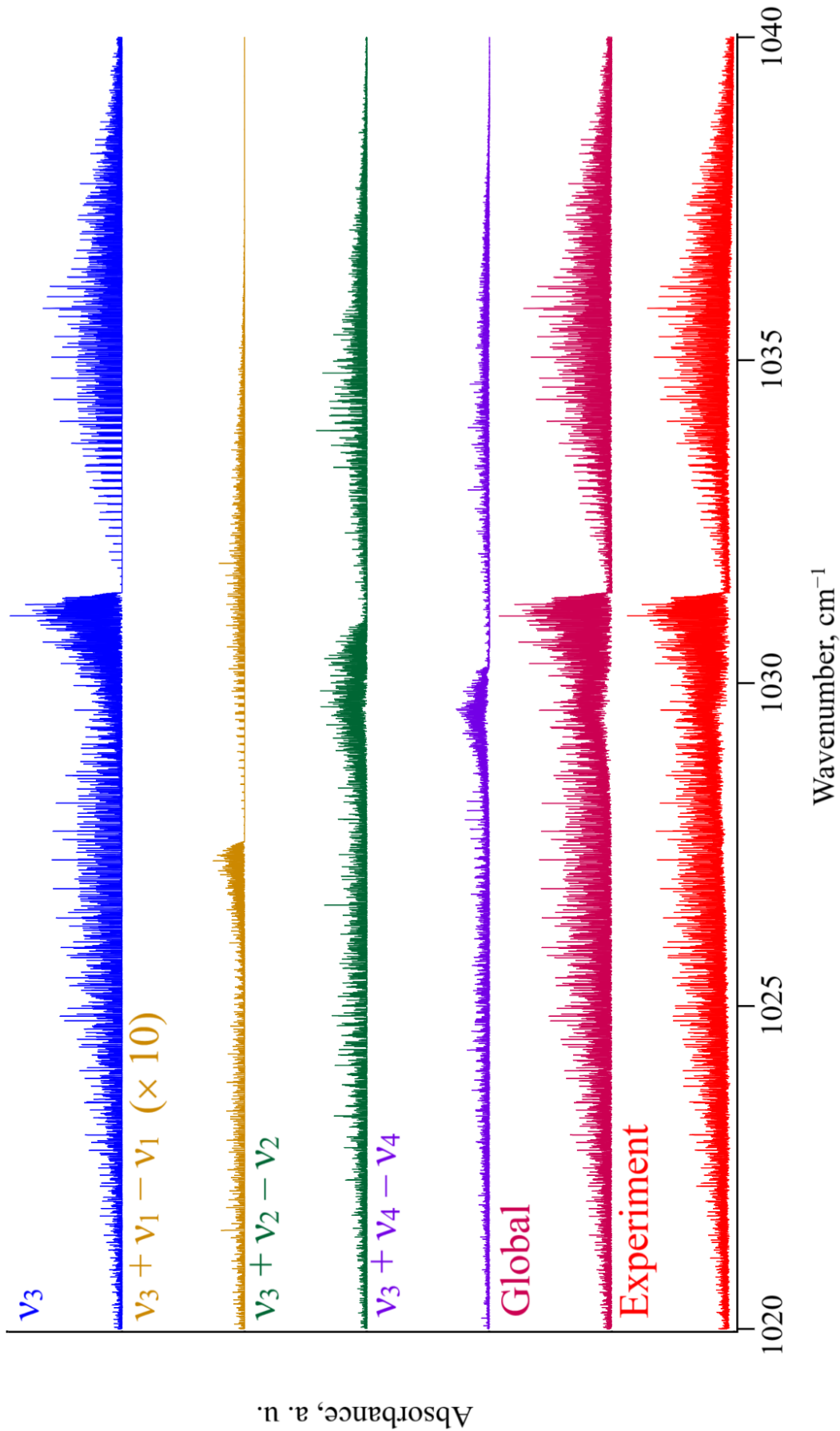


Figure 3.5 – Theoretical “hot” bands spectra in the region of the v_3 band.

Comparison with the experimental spectra. The intensity of the $v_3 + v_1 - v_1$ band is increased by a factor of 10.

Therefore, the spectra of silicon tetrafluoride were analysed in the region of combination bands, and data on the energy structure of vibrational states ($v_1 = v_2 = 1$), ($v_1 = v_3 = 1$), ($v_1 = v_4 = 1$), ($v_2 = v_3 = 1$), ($v_2 = v_4 = 1$) and ($v_3 = v_4 = 1$) were obtained. The 10,151 transitions with a value of $J^{\max} = 82$ were assigned, which allowed to solve the inverse spectroscopic problem and obtain sets of parameters of the effective Hamiltonian (Tables D.6–D.12) describing the experimental positions of the lines with a standard deviation of a few 10^{-4} cm⁻¹. Fit residuals for certain combination bands are shown in Figure B.6. The results obtained are important for further high-precision semiempirical determination of the intramolecular potency function of the SiF₄ molecule, as well as for subsequent analyses of the line intensities of this molecule.

3.3. Silane SiH₄

Interest in studies of high-resolution spectra of silane SiH₄ is due to several reasons. First, studies of the high-resolution spectra of the SiH₄ molecule can be useful in studying the composition of the atmospheres of giant planets such as Jupiter and Saturn [111–114]. The main isotopologue ²⁸SiH₄ has been reported in the interstellar dust formation surrounding the star IRC+10216 [115, 116], which emission range lies in the far infrared region. Silane, like its tetrafluorinated analogue, plays an important role as a precursor for the chemical vapour deposition of silicon layers [117]. Therefore, high purity silicon production processes require control of gaseous silane [118], more often by spectroscopic methods. On this basis, silane SiH₄, while being the lightest of all stable silicon compounds, has been the subject of numerous studies over the years [119], including high-resolution spectroscopic methods [120–125].

3.3.1. Study of the shape and absolute intensity of the spectrum lines of silane SiH₄

A large cooled multireflective absorption cell was used to record the spectrum in combination with synchrotron radiation at the “AILES” station of the SOLEIL synchrotron (France). The optical path length was 93 m. Three spectra of pure gaseous SiH₄ were recorded at different pressures (12.5, 25 and 50 mbar) and at a temperature of about 160 K. Thus, spectra of both “cold” (ground state) and “hot” ($v_3 - v_3$) rotational lines in the range 45–165 cm⁻¹ were obtained.

The absolute line intensities of silane SiH₄ were measured for this range for the first time. For this nonpolar molecule, the effective dipole moment is very small and is due to the effects of centrifugal distortion. In the initial stage of the analysis, the individual intensities of about one hundred unmixed, unsaturated, and non-weak lines were determined from fitting the contour of the lines to the Voigt profile. The experimentally derived absolute line intensity data were then used to determine the effective

dipole moment parameters from the fit procedure with weighting coefficients. The experimental values of the shape and absolute line intensities allowed us to obtain a set of effective dipole moment parameters that describe the experimental characteristics of the spectral lines corresponding to the transitions between the ground state levels and the “hot” band transitions $v_3 - v_3$ with an error of no more than 5.7 %.

Figure 3.6 shows an example of a cluster of cold transitions $R(18)$ at different pressures compared to the theoretical calculation using the obtained effective dipole moment parameters (Table 3.3).

Table 3.3 – Parameters of the effective dipole moment of SiH_4 in the far infrared range.

$(v, \gamma) (v', \gamma')$	$(\Omega, K, n\Gamma)$	Value, D
<i>I</i>	<i>2</i>	<i>3</i>
(0000, A_1) (0000, A_1)	$2(2,0F2)10^5$	0.9946(78)
	$4(2,0F2)10^7$	0.1910(31)
	$6(2,0F2)10^{10}$	0.5829(28)
d_{rms}	5,67 %	

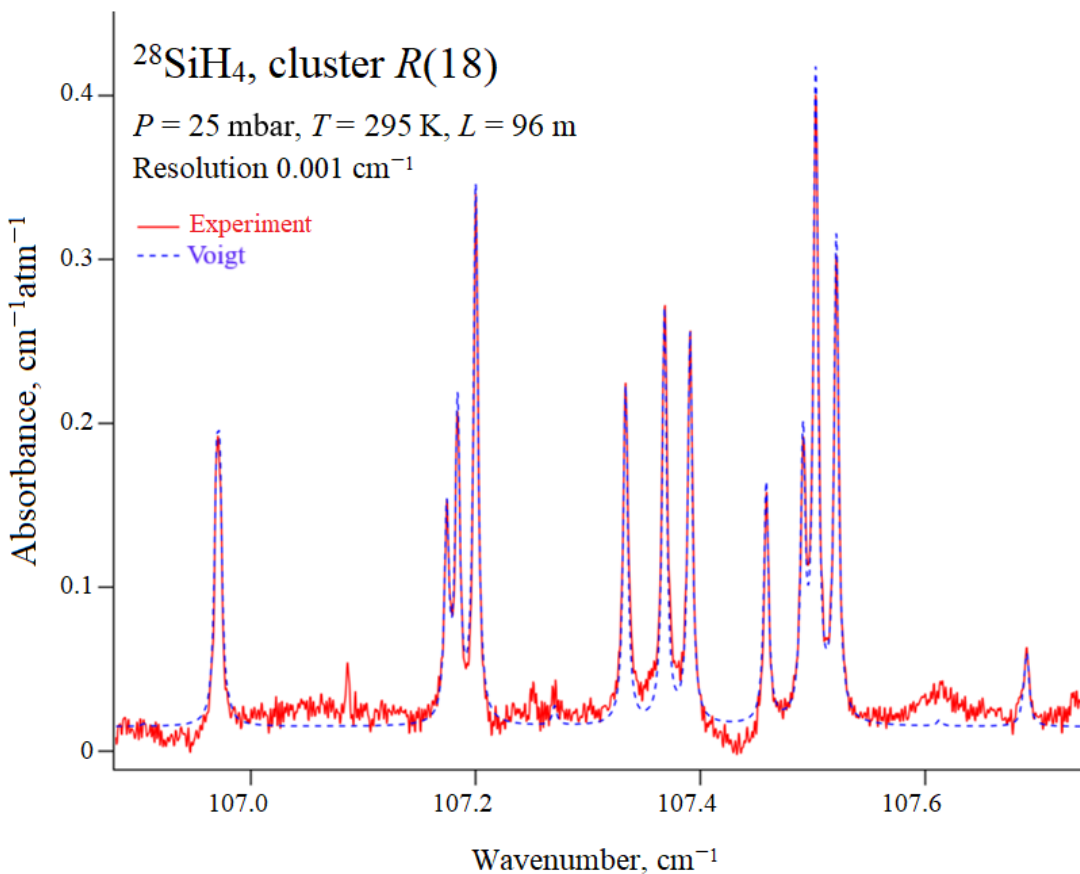


Figure 3.6 – Comparison of experimental and calculated shape and line intensities in the region of R -branch between the levels of the ground vibrational state.

Experimental conditions are presented in the upper left part of the figure.

Conclusion

This thesis presents the results of theoretical studies of the spectra of asymmetric and spherical top molecules in various regions of the far and mid-infrared ranges. An approach based on the theory of irreducible tensor operators to describe the high-resolution spectra of asymmetric wavelength molecules in doublet electronic states, which allows to improve the calculation of the positions of the spectral lines of the fundamental band of the ClO₂ molecule by more than ten times, is proposed.

The following tasks were set and solved in the work:

- For the first time, the combination band transitions of the v₅ + v₁₂ and v₆ + v₁₁ bands of the C₂D₄ molecule, about 4,500 in total, have been determined up to the maximum values of the quantum numbers K_a^{max} = 12 and K_a^{max} = 17 for the v₅ + v₁₂ and v₆ + v₁₁ bands, respectively.
- The spectroscopic parameters of the C₂D₄ molecule have been determined for the first time by analysing the high-resolution ro-vibrational spectra of the v₅ + v₁₂ and v₆ + v₁₁ bands.
- The transitions of the fundamental v₃ and combination v₁ + v₃ bands of the ClO₂ molecule have been assigned for the first time, or with much higher accuracy, using a newly proposed approach based on the theory of irreducible tensor operators for an improved description of the spectra of asymmetric top molecules in the nonsinglet electronic state, 7,200 in total, up to a maximum value of the quantum numbers K_a = 21 and K_a = 59 for the fundamental and combination bands, respectively.
- The parameters of the effective Hamiltonian of the ClO₂ molecule have been determined for the first time, or with much higher accuracy, based on the analysis of high-resolution vibrational-rotational spectra of the v₃ and v₁ + v₃ bands using the proposed approach to describe molecules in nonsinglet electronic states, which takes into account spin-rotational interactions in molecules of this type.
- The transitions corresponding to the v₂/v₄ dyad of ¹³CD₄ molecule have been assigned for the first time; the absolute intensities of the v₂/v₄ dyad transitions of ¹²CD₄ molecule have been determined with much higher accuracy, and for the first time for the v₄ band of ¹³CD₄ molecule.
- The spectroscopic parameters of the ¹³CD₄ molecule have been determined for the first time, and the parameters of the effective dipole moment of the v₂/v₄ dyad of ¹²CD₄ molecule and for the first time for the v₄ band of ¹³CD₄ molecule have been determined for the first time, or with much higher accuracy.
- More than 10,000 transition of the combination bands v₁ + v₂, v₁ + v₃, v₁ + v₄, v₂ + v₃, v₂ + v₄ and v₃ + v₄ of the SiF₄ molecule have been assigned for the first time up to J^{max} = 78, 82, 58, 58, 70, 54 and 60, respectively; v₁ + v₃ band transitions were also determined for the first time for the isotopologues ²⁹SiF₄ and ³⁰SiF₄.
- The spectroscopic parameters of the combination bands v₁ + v₂, v₁ + v₃, v₁ + v₄, v₂ + v₃, v₂ + v₄ and v₃ + v₄ of the SiF₄ molecule have been determined for the first time by analysing high-resolution vibrational-rotational spectra.

- For the first time for the SiF₄ molecule the positions of the lines were calculated and theoretical spectra of the “hot” bands $v_3 + v_1 - v_1$, $v_3 + v_2 - v_2$ and $v_3 + v_4 - v_4$ were constructed with an accuracy not worse than the experimental one.

- The absolute intensities of the lines corresponding to the transitions between the levels of the ground vibrational state, as well as transitions of the “hot” $v_3 - v_3$ band, have been determined for the SiH₄ molecule for the first time.

- For the first time, the parameters of the effective dipole moment of the SiH₄ molecule were determined in the far-infrared range, where the lines corresponding to the transitions between the ground state levels and the transitions of the “hot” $v_3 - v_3$ band are located.

Practically, the obtained results can be used as follows:

- Information on the structure of high-resolution spectra of SiH₄, SiF₄, CD₄, C₂D₄, ClO₂ and their isotopologues is an essential addition to existing databases of vibrational-rotational spectra of molecules and can be used in a wide range of practical applications of fine structure information on molecular spectra.

- The developed approach for the analysis of free radicals of the asymmetric tops in non-singlet electronic states can be used to analyse the spectra of various molecules belonging to the mentioned class.

Subsequent studies that serve to develop the selected topic include:

- The study of the combination bands $2v_3$ and $3v_3$ of the SiF₄ molecule, so the investigated range will cover 24 polyads of the SiF₄ molecule.
- Obtaining experimental values of intensities of individual lines belonging to the SiF₄ molecule, which will complete the data on the dipole moment parameters of this molecule.
- Publication of papers on new data obtained.

Publications on the thesis topic

Articles in journals included in the list of peer-reviewed scientific publications

1. Зятькова А. Г., Меркулова М. А., Конова Ю. В. Определение энергетической структуры и спектроскопических параметров колебательного состояния ($\nu_5 = \nu_{12} = 1$) молекулы C₂D₄ // Оптика и спектроскопия. – 2020. – Т. 128. – №. 5. – С. 583-588.

In the translated version, indexed by “Web of Science” and “Scopus”

Ziatkova A. G., Merkulova M. A., Konova Yu. V. Determination of the energy structure and spectroscopic parameters of the vibrational state ($\nu_5 = \nu_{12} = 1$) of the C₂D₄ molecule // Optics and Spectroscopy. – 2020. – Vol. 128. – No. 5. – P. 569-574.

2. Меркулова М. А., Каакулин А. Н., Громова О. В., Бехтерева Е. С. Анализ спектра высокого разрешения молекул в дублетных электронных состояниях: фундаментальная полоса ν_3 диоксида хлора (¹⁶O³⁵Cl¹⁶O) в основном электронном состоянии X²B₁ // Оптика и спектроскопия. – 2021. – Т. 129. – №. 8. – С. 979-984.

In the translated version, indexed by “Web of Science” and “Scopus”

Merkulova M. A., Kakaulin A. N., Gromova O. V., Bekhtereva E. S. Analysis of the high-resolution spectrum of molecules in doublet electronic states: fundamental ν_3 band of chlorine dioxide (¹⁶O³⁵Cl¹⁶O) in the ground electronic state X²B₁ // Optics and Spectroscopy. – 2021. – Vol. 129. – No. 10. – P. 1138-1144.

3. Бехтерева Е. С., Каакулин А. Н., Меркулова М. А., Громова О. В., Конова Ю. В., Зидо К. Спектроскопия высокого разрешения молекул типа асимметричного волчка в несинглетных электронных состояниях: полоса $\nu_1 + \nu_3$ молекулы ClO₂ // Оптика и спектроскопия. – 2022. – Т. 130. – №. 9. – С. 1327-1333.

In the translated version, indexed by “Web of Science” and “Scopus”

Bekhtereva E. S., Kakaulin A. N., Merkulova M. A., Gromova O. V., Konova Yu. V., Sydow C. High-resolution spectroscopy of asymmetric top molecules in non-singlet electronic states: $\nu_1 + \nu_3$ band of the ClO₂ molecule // Optics and Spectroscopy. – 2022. – Vol. 130. – No. 7. – P. 425-432.

4. Merkulova M., Boudon V., Manceron L. Analysis of high-resolution spectra of SiF₄ combination bands // Journal of Molecular Spectroscopy. – 2023. – Vol. 391. – P. 111738.

5. Ulenikov O. N., Bekhtereva E. S., Gromova O. V., Kakaulin A. N., Merkulova M. A., Sydow C., Berezkin K. B., Bauerecker S. High resolution spectroscopy of asymmetric top molecules in nonsinglet electronic states: the ν_3 fundamental of chlorine dioxide (¹⁶O³⁵Cl¹⁶O) free radical in the X²B₁ electronic ground state // Physical Chemistry Chemical Physics. – 2023. – Vol. 25. – No. 8. – P. 6270-6287.

6. Ulenikov O. N., Gromova O. V., Bekhtereva E. S., Nikolaeva N. I., Merkulova M. A., Morzhikova Y. B., Bauerecker S. Comparative line position and line strength analysis of the v_2/v_4 dyad of $^{12}\text{CD}_4$ and $^{13}\text{CD}_4$ // Journal of Quantitative Spectroscopy and Radiative Transfer. – 2023. – Vol. 311. – P. 108770.

7. Richard C., Ben Fathallah O., Hardy P., Kamel R., Merkulova M., Ulenikov O., Boudon V. Casda24: Latest updates to the Dijon calculated spectroscopic databases // Journal of Molecular Spectroscopy. – 2024. – Vol. 327. – P. 109127.

Publications in conference collections

8. Меркулова М. А. Определение энергетической структуры и спектроскопических параметров колебательного состояния ($v_5 = v_{12} = 1$) молекулы C_2D_4 / Меркулова М. А. // Перспективы развития фундаментальных наук: сборник научных трудов XVII Международной конференции студентов, аспирантов и молодых ученых, ТПУ, Томск, Россия. – Сборник трудов: Изд-во ТПУ. – 2020. – Т.1: Физика. – С. 128-130, Томск. (21-24 апреля, 2020). = Merkulova M. A. Determination of the energy structure and spectroscopic parameters of the vibrational state ($v_5 = v_{12} = 1$) of the C_2D_4 molecule / Merkulova M. A. // Prospects for the development of fundamental sciences: book of abstracts of the XVII International Conference of students, postgraduates and young scientists, TPU, Tomsk, Russia. – Book of Abstracts: TPU Publishing House. – 2020. – V. 1: Physics. – P. 128-130, Tomsk. (21-24 April, 2020).

9. Меркулова М. А., Громова О. В., Бехтерева Е. С., Уленеков О. Н. Анализ спектра высокого разрешения молекул в дублетных электронных состояниях: фундаментальная полоса v_3 дихлора ($^{16}\text{O}^{35}\text{Cl}^{16}\text{O}$) в основном электронном состоянии / Меркулова М. А., Громова О. В., Бехтерева Е. С., Уленеков О. Н. // Современные технологии, экономика и образование: сборник материалов II Всероссийской научно-методической конференции, ТПУ, Томск, Россия. – Сборник материалов: Изд-во ТПУ. – 2020. – С. 216-217, Томск. (2-4 сентября, 2020). = Merkulova M. A., Gromova O. V., Bekhtereva E. S., Ulenikov O. N. Analysis of high resolution spectra of molecules in nonsinglet electronic states: the v_3 fundamental of chlorine dioxide ($^{16}\text{O}^{35}\text{Cl}^{16}\text{O}$) electronic ground state / Merkulova M. A., Gromova O. V., Bekhtereva E. S., Ulenikov O. N. // Modern technologies, economics and education: book of abstracts of II All-Russian scientific and methodological conference, TPU, Russia. – Book of Abstracts: TPU Publishing House. – 2020. – P. 216-217, Tomsk. (2-4 September, 2020).

10. Merkulova M., Boudon V., Manceron L. Analysis of high-resolution spectra of SiF_4 combination bands // New developments in high resolution molecular spectroscopy and outreach to modern applications: international workshop, Les Houches school of physics, Haute Savoie, France. – Book of Abstracts. – 2022. – P. 51-52, Les Houches. (29 May – 3 June, 2022).

11. Merkulova M., Boudon V., Manceron L. High-resolution spectroscopy and analysis of combination bands of SiF₄ // Edifices Moléculaires Isolés et Environnés : international workshop, CNRS, Dunkerque, France. – Résumés. – 2022. – P. 76, Dunkerque. (14-17 Juin, 2022).
12. Merkulova M., Boudon V., Manceron L. High-resolution spectroscopy and analysis of combination bands of SiF₄ // 15th ASA Conference (united with 16th HITRAN Conference): international conference, URCA, Reims, France. – Book of Abstracts. – 2022. – P. 26, Reims. (24-26 August, 2022).
13. Merkulova M. Analysis of high-resolution spectra of SiF₄ combination bands / Merkulova M., Boudon V., Manceron L. // High Resolution Molecular Spectroscopy: book of abstracts of the 28th international colloquium, UBFC, Dijon, France. – Book of abstracts. – 2023. – P. 130, Dijon. (28 August – 1 september, 2023).
14. Merkulova M., Boudon V., Manceron L. New high-resolution combination bands of SiF₄. Experiment and simulation // International symposium on molecular spectroscopy: book of abstracts of the 77th international symposium, UIUC, Urbana-Champaign, USA. – 2024. – P7564, Urbana-Champaign. (17-21 June, 2024).

Bibliography

1. Макушкин Ю. С., Улеников О. Н., Чеглоков А. Е., Смирнов В. С. Симметрия и ее применения к задачам колебательно-вращательной спектроскопии молекул : в 2 Томах. Т. 2. — Изд-во Том. ун-та. — Томск, 1990. — 224 с.
2. Eckart C. Some Studies Concerning Rotating Axes and Polyatomic Molecules // Physical Review. — 1935. — Vol. 47. — No. 7. — P. 552-558.
3. Makushkin Yu. S., Ulenikov O. N. On the transformation of the complete electron-nuclear Hamiltonian of a polyatomic molecule to the intramolecular coordinates // Journal of Molecular Spectroscopy. — 1977. — Vol. 68. — No. 1. — P. 1-20.
4. Howard B. J., Moss R. E. The molecular hamiltonian: I. Non-linear molecules // Molecular Physics. — 1970. — Vol. 19. — No. 4. — P. 433-450.
5. Ландау Л. Д., Лифшиц Е. М. Квантовая механика (нерелятивистская теория) : в 10 Т. Т. III. — 4-е изд., испр. — М.: Наука, 1989. — 768 с.
6. Киселев А. А., Ляпцев А. В. Квантовомеханическая теория возмущений (диаграммный метод): Учебное пособие. — ЛГУ, 1989. — 357 с.
7. Zamarbide G., Estrada M., Zamora M., Torday L., Enriz R., Tomas-Vert F., Csizmadia I. An ab initio conformational study on captopril // Journal of Molecular Structure: THEOCHEM. — 2003. — Vol. 666. — P. 599-608.
8. Bykov A. D., Makushkin Yu. S., Ulenikov O. N. On the displacements of centres of vibration-rotation lines under isotope substitution in polyatomic molecules // Molecular Physics. — 1984. — Vol. 51. — No. 4. — P. 907-918.
9. Nielsen H. H. The Vibration-Rotation Energies of Molecules // Reviews of Modern Physics. — 1951. — Vol. 23. — No. 2. — P. 90-136.
10. Ulenikov O. N., Onopenko G. A., Bekhtereva E. S., Petrova T. M., Solodov A. M., Solodov A. A. High resolution study of the $v_5 + v_{12}$ band of C_2H_4 // Molecular Physics. — 2010. — Vol. 108. — No. 5. — P. 637-647.
11. Hecht K. T. The vibration-rotation energies of tetrahedral XY_4 molecules: Part I. Theory of spherical top molecules // Journal of Molecular Spectroscopy. — 1961. — Vol. 5. — No. 1. — P. 355-389.
12. Hecht K. T. Vibration-rotation energies of tetrahedral XY_4 molecules: Part II. The fundamental v_3 of CH_4 // Journal of Molecular Spectroscopy. — 1961. — Vol. 5. — No. 1. — P. 390-404.
13. Жилинский Б. И., Перевалов В. И., Тютерев В. Г. Метод неприводимых тензорных операторов в теории спектров молекул. — Новосибирск: Наука. — Новосибирск, 1987. — 233 с.

14. Suhonen J. Tensor Operators and the Wigner-Eckart Theorem // From Nucleons to Nucleus: Concepts of Microscopic Nuclear Theory/ ed. J. Suhonen. — Berlin, Heidelberg: Springer, 2007. — P. 23-38.
15. Распопова Н. И. Теоретическое исследование спектров молекул типа сферического волчка на основе формализма неприводимых тензорных операторов / Н. И. Распопова. — Томск: НИ ТПУ, 2018. — 162 с.
16. Kostiuk T., Romani P., Espenak F., Livengood T.A., Goldstein J. J. Temperature and abundances in the Jovian auroral stratosphere: 2. Ethylene as a probe of the microbar region // Journal of Geophysical Research: Planets. — 1993. — Vol. 98. — No. E10. — P. 18823-18830.
17. Bézard B., Moses J. I., Lacy J., Greathouse T., Richter M., Griffith C. Detection of Ethylene (C_2H_4) on Jupiter and Saturn in Non-Auroral Regions. — 2001. — Vol. 33. — P. 22.07.
18. Coustenis A., Achterberg R. K., Conrath B. J., Jennings D. E., Marten A., Gautier D., Nixon C. A., Flasar F. M., Teanby N. A., Bézard B., Samuelson R. E., Carlson R. C., Lellouch E., Bjoraker G. L., Romani P. N., Taylor F. W., Irwin P. G. J., Fouchet T., Hubert A., Orton G. S., Kunde V. G., Vinatier S., Mondellini J., Abbas M. M., Courtin R. The composition of Titan's stratosphere from Cassini / CIRS mid-infrared spectra // Icarus. — 2007. — Vol. 189. — No. 1. — P. 35-62.
19. Vervack R. J., Sandel B. R., Strobel D. F. New perspectives on Titan's upper atmosphere from a reanalysis of the Voyager 1 UVS solar occultations // Icarus. — 2004. — Vol. 170. — No. 1. — P. 91-112.
20. Abeles F. B., Heggestad H. E. Ethylene: An Urban Air Pollutant // Journal of the Air Pollution Control Association. — 1973. — Vol. 23. — No. 6. — P. 517-521.
21. Barry C. S., Giovannoni J. J. Ethylene and Fruit Ripening // Journal of Plant Growth Regulation. — 2007. — Vol. 26. — No. 2. — P. 143.
22. Lin Z., Zhong S., Grierson D. Recent advances in ethylene research // Journal of Experimental Botany. — 2009. — Vol. 60. — No. 12. — P. 3311-3336.
23. Flaud J.-M., Lafferty W. J., Sams R., Malathy Devi V. High resolution analysis of the ethylene- ^{13}C spectrum in the 8.4–14.3- μm region // Journal of Molecular Spectroscopy. — 2010. — Vol. 259. — No. 1. — P. 39-45.
24. Ben Hassen A., Kwabia Tchana F., Flaud J.-M., Lafferty W. J., Landsheere X., Aroui H. Absolute line intensities for ethylene from 1800 to 2350 cm^{-1} // Journal of Molecular Spectroscopy. — 2012. — Vol. 282. — P. 30-33.
25. Lebron G. B., Tan T. L. Integrated Band Intensities of Ethylene ($^{12}C_2H_4$) by Fourier Transform Infrared Spectroscopy // International Journal of Spectroscopy. — 2012. — Vol. 2012. — P. 5.

26. Tan T. L., Gabona M. G. Analysis of the Coriolis interaction between v_6 and v_4 bands of ethylene-*cis*- d_2 (*cis*-C₂H₂D₂) by high-resolution FTIR spectroscopy // Journal of Molecular Spectroscopy. — 2012. — Vol. 272. — No. 1. — P. 51-54.
27. Tan T. L., Lebron G. B. The v_{12} band of ethylene-1-¹³C (¹³C¹²CH₄) by high-resolution FTIR spectroscopy // Journal of Molecular Spectroscopy. — 2010. — Vol. 261. — No. 1. — P. 63-67.
28. Tan T. L., Lebron G. B. High-resolution infrared analysis of the v_7 band of *cis*-ethylene- d_2 (*cis*-C₂H₂D₂) // Journal of Molecular Spectroscopy. — 2010. — Vol. 261. — No. 2. — P. 87-90.
29. Ulenikov O. N., Bekhtereva E. S., Gromova O. V., Kakaulin A. N., Sydow C., Bauerecker S. Extended analysis of the v_{12} band of ¹²C₂H₄ for astrophysical applications: Line strengths, widths, and shifts // Journal of Quantitative Spectroscopy and Radiative Transfer. — 2019. — Vol. 233. — P. 57-66.
30. Conn G. K. T., Twigg G. H., Rideal E. K. Infra-red analysis applied to the exchange reaction between ethylene and deuterioethylene // Proceedings of the Royal Society of London. Series A. Mathematical and Physical Sciences. — 1997. — Vol. 171. — No. 944. — P. 70-78.
31. Watson J. K. G. Determination of Centrifugal Distortion Coefficients of Asymmetric-Top Molecules // The Journal of Chemical Physics. — 1967. — Vol. 46. — No. 5. — P. 1935-1949.
32. Ulenikov O. N., Gromova O. V., Bekhtereva E. S., Fomchenko A. L., Sydow C., Bauerecker S. First high resolution analysis of the $3v_1$ band of ³⁴S¹⁶O₂ // Journal of Molecular Spectroscopy. — 2016. — Vol. 319. — P. 50-54.
33. Ulenikov O. N., Bekhtereva E. S., Gromova O. V., Buttersack T., Sydow C., Bauerecker S. High resolution FTIR study of ³⁴S¹⁶O₂: The bands $2v_1$, $v_1 + v_3$, $v_1 + v_2 + v_3 - v_2$ and $v_1 + v_2 + v_3$ // Journal of Quantitative Spectroscopy and Radiative Transfer. — 2016. — Vol. 169. — P. 49-57.
34. Ulenikov O. N., Gromova O. V., Bekhtereva E. S., Fomchenko A. L., Zhang F., Sydow C., Maul C., Bauerecker S. High resolution analysis of C₂D₄ in the region of 600–1150 cm⁻¹ // Journal of Quantitative Spectroscopy and Radiative Transfer. — 2016. — Vol. 182. — P. 55-70.
35. Solomon S. The mystery of the Antarctic Ozone “Hole” // Reviews of Geophysics. — 1988. — Vol. 26. — No. 1. — P. 131-148.
36. Vaida V., Solomon S., Richard E.C., Rühl E., Jefferson A. Photoisomerization of OCIO: a possible mechanism for polar ozone depletion // Nature. — 1989. — Vol. 342. — No. 6248. — P. 405-408.
37. Carty T., Rivière E. D., Salawitch R. J., Berthet G., Renard J.-B., Pfeilsticker K., Dorf M., Butz A., Bösch H., Stimpfle R. M., Wilmouth D. M., Richard E. C., Fahey D. W., Popp P. J., Schoeberl M. R., Lait L. R., Bui T. P. Nighttime OCIO in the winter Arctic vortex // Journal of Geophysical Research: Atmospheres. — 2005. — Vol. 110. — No. D1. — P. 2004JD005035.

38. Curl R. F., Heidelberg R. F., Kinsey J. L. Microwave Spectrum of Chlorine Dioxide. II. Analysis of Hyperfine Structure and the Spectrum of $^{35}\text{Cl}^{16}\text{O}^{18}\text{O}$ // Physical Review. — 1962. — Vol. 125. — No. 6. — P. 1993-1999.
39. Curl R. F. Microwave Spectrum of Chlorine Dioxide. III. Interpretation of the Hyperfine Coupling Constants Obtained in Terms of the Electronic Structure // The Journal of Chemical Physics. — 1962. — Vol. 37. — No. 4. — P. 779-784.
40. Tolles W. M., Kinsey J. L., Curl R. F., Heidelberg R. F. Microwave Spectrum of Chlorine Dioxide. V. The Stark and Zeeman Effects // The Journal of Chemical Physics. — 1962. — Vol. 37. — No. 5. — P. 927-930.
41. Brand J. C. D., Redding R. W., Richardson A. W. The 4750-Å band system of chlorine dioxide. Rotational analysis, force field and intensity calculations // Journal of Molecular Spectroscopy. — 1970. — Vol. 34. — No. 3. — P. 399-414.
42. Curl R. F., Abe K., Bissinger J., Bennett C., Tittel F. K. Fluorescence spectrum of chlorine dioxide induced by the 4765 Å argon-ion laser line // Journal of Molecular Spectroscopy. — 1973. — Vol. 48. — No. 1. — P. 72-85.
43. Hamada Y., Merer A. J., Michielsen S., Rice S. A. Rotational analysis of bands at the long-wavelength end of the $\tilde{\text{A}}^2\text{A}_2-\tilde{\text{X}}^2\text{B}_1$ electronic transition of ClO_2 // Journal of Molecular Spectroscopy. — 1981. — Vol. 86. — No. 2. — P. 499-525.
44. Richardson A. W. Band contour analysis of the v_3 band of chlorine dioxide // Journal of Molecular Spectroscopy. — 1970. — Vol. 35. — No. 1. — P. 43-48.
45. Benner D. C., Rinsland C. P. Identification and intensities of the “forbidden” $3v_2$ band of $^{12}\text{C}^{16}\text{O}_2$ // Journal of Molecular Spectroscopy. — 1985. — Vol. 112. — No. 1. — P. 18-25.
46. Hamada Y., Tsuboi M. High Resolution Infrared Spectrum of Chlorine Dioxide: The v_2 Fundamental Band // Bulletin of the Chemical Society of Japan. — 1979. — Vol. 52. — No. 2. — P. 383-385.
47. Hamada Y., Tsuboi M. High-resolution infrared spectrum of chlorine dioxide: The v_1 fundamental band // Journal of Molecular Spectroscopy. — 1980. — Vol. 83. — No. 2. — P. 373-390.
48. Tanaka K., Tanaka T. CO_2 and N_2O laser Stark spectroscopy of the v_1 band of the ClO_2 radical // Journal of Molecular Spectroscopy. — 1983. — Vol. 98. — No. 2. — P. 425-452.
49. Ortigoso J., Escribano R., Burkholder J. B., Howard C. J., Lafferty W. J. High-resolution infrared spectrum of the v_1 band of OCIO // Journal of Molecular Spectroscopy. — 1991. — Vol. 148. — No. 2. — P. 346-370.
50. Ortigoso J., Escribano R., Burkholder J. B., Lafferty W. J. Intensities and dipole moment derivatives of the fundamental bands of $^{35}\text{ClO}_2$ and an intensity analysis of the v_1 band // Journal of Molecular Spectroscopy. — 1992. — Vol. 156. — No. 1. — P. 89-97.

51. Ortigoso J., Escribano R., Burkholder J. B., Lafferty W. J. Infrared Spectrum of OCLO in the 2000 cm^{-1} Region: The $2v_1$ and $v_1 + v_3$ Bands // Journal of Molecular Spectroscopy. — 1993. — Vol. 158. — No. 2. — P. 347-356.
52. Ulenikov O. N., Bektereva E. S., Gromova O. V., Quack M., Berezkin K. B., Sydow C., Bauerecker S. High resolution ro-vibrational analysis of molecules in doublet electronic states: the v_1 fundamental of chlorine dioxide ($^{16}\text{O}^{35}\text{Cl}^{16}\text{O}$) in the $X^2\text{B}_1$ electronic ground state // Physical Chemistry Chemical Physics. — 2021. — Vol. 23. — No. 8. — P. 4580-4596.
53. Quack M. Fundamental Symmetries and Symmetry Violations from High Resolution Spectroscopy // Handbook of High-resolution Spectroscopy / eds. M. Quack, F. Merkt. — Wiley, 2011.
54. Khalil M. a. K. Non-CO₂ greenhouse gases in the atmosphere // Annual Review of Environment and Resources. — 1999. — Vol. 24. — P. 645-661.
55. Guzmán Marmolejo A., Segura A. Methane in the Solar System // Boletín de la Sociedad Geológica Mexicana. — 2015. — Vol. 67. — No. 3. — P. 377-385.
56. Coradini A., Filacchione G., Capaccioni F., Cerroni P., Adriani A., Brown R. H., Langevin Y., Gondet B. CASSINI/VIMS-V at Jupiter: Radiometric calibration test and data results // Planetary and Space Science. — 2004. — Vol. 52. — No. 7. — P. 661-670.
57. Formisano V., Atreya S., Encrenaz T., Ignatiev N., Giuranna M. Detection of Methane in the Atmosphere of Mars // Science. — 2004. — Vol. 306. — No. 5702. — P. 1758-1761.
58. Irwin P. G. J., Sihra K., Bowles N., Taylor F. W., Calcutt S. B. Methane absorption in the atmosphere of Jupiter from 1800 to 9500 cm^{-1} and implications for vertical cloud structure // Icarus. — 2005. — Vol. 176. — No. 2. — P. 255-271.
59. Negrão A., Coustenis A., Lellouch E., Maillard J.-P., Rannou P., Schmitt B., McKay C. P., Boudon V. Titan's surface albedo variations over a Titan season from near-infrared CFHT/FTS spectra: Surfaces and Atmospheres of the Outer Planets, their Satellites and Ring Systems from Cassini-Huygens Data // Planetary and Space Science. — 2006. — Vol. 54. — No. 12. — P. 1225-1246.
60. Hand E. NASA rover yet to find methane on Mars // Nature. — 2012. — Vol. 452. — P. 296-297.
61. Showman A. P. A whiff of methane // Nature. — 2008. — Vol. 452. — No. 7185. — P. 296-297.
62. Griffith C. A., Penteado P., Rannou P., Brown R., Boudon V., Baines K. H., Clark R., Drossart P., Buratti B., Nicholson P., McKay C. P., Coustenis A., Negrão A., Jaumann R. Evidence for a Polar Ethane Cloud on Titan // Science. — 2006. — Vol. 313. — No. 5793. — P. 1620-1622.
63. Coustenis A., Negrão A., Salama A., Schulz B., Lellouch E., Rannou P., Drossart P., Encrenaz T., Schmitt B., Boudon V., Nikitin A. Titan's 3-micron spectral region from ISO high-resolution spectroscopy // Icarus. — 2006. — Vol. 180. — No. 1. — P. 176-185.

64. Fowler M. M., Barr S. A long-range atmospheric tracer field test // Atmospheric Environment (1967). — 1983. — Vol. 17. — No. 9. — P. 1677-1685.
65. Zare R. N., Harter W. G. Angular Momentum: Understanding Spatial Aspects in Chemistry and Physics // Physics Today. — 1989. — Vol. 42. — No. 12. — P. 68-70.
66. Pauling L. The nature of the chemical bond. II. The one-electron bond and the three-electron bond // ACS Publications. — 1931. — Vol. 53. — No. 9. — P. 3225-3237.
67. Quack M. Quantitative comparison between detailed (state selected) relative rate data and averaged (thermal) absolute rate data for complex forming reactions // ACS Publications. — 1979. — Vol. 83. — No. 1. — P. 150-158.
68. Marquardt R., Quack M. Global analytical potential hypersurfaces for large amplitude nuclear motion and reactions in methane. I. Formulation of the potentials and adjustment of parameters to ab initio data and experimental constraints // The Journal of Chemical Physics. — 1998. — Vol. 109. — No. 24. — P. 10628-10643.
69. Schwenke D. W. Towards accurate ab initio predictions of the vibrational spectrum of methane // Spectrochimica Acta Part A: Molecular and Biomolecular Spectroscopy. — 2002. — Vol. 58. — No. 4. — P. 849-861.
70. Marquardt R., Quack M. Global Analytical Potential Hypersurface for Large Amplitude Nuclear Motion and Reactions in Methane II. Characteristic Properties of the Potential and Comparison to Other Potentials and Experimental Information // The Journal of Physical Chemistry A. — 2004. — Vol. 108. — No. 15. — P. 3166-3181.
71. Camden J. P., Bechtel H. A., Ankeny Brown D. J., Zare R. N. Comparing reactions of H and Cl with C-H stretch-excited CHD₃ // The Journal of Chemical Physics. — 2006. — Vol. 124. — No. 3. — P. 034311.
72. Hu W., Lendvay G., Troya D., Schatz G. C., Camden J. P., Bechtel H. A., Brown D. J. A., Martin M. R., Zare R. N. H + CD₄ Abstraction Reaction Dynamics: Product Energy Partitioning // The Journal of Physical Chemistry A. — 2006. — Vol. 110. — No. 9. — P. 3017-3027.
73. Camden J. P., Bechtel H. A., Ankeny Brown D. J., Martin M. R., Zare R. N., Hu W., Lendvay G., Troya D., Schatz G. C. A Reinterpretation of the Mechanism of the Simplest Reaction at an sp₃-Hybridized Carbon Atom: H + CD₄ → CD₃ + HD // Journal of the American Chemical Society. — 2005. — Vol. 127. — No. 34. — P. 11898-11899.
74. Loëte M., Hilico J. C., Valentin A., Chazelas J., Henry L. Analysis of the v₂ and v₄ infrared bands of CD₄ // Journal of Molecular Spectroscopy. — 1983. — Vol. 99. — No. 1. — P. 63-86.
75. Touzani L., Loëte M., Lavorel B., Millot G. Measurement and Analysis of the Raman Intensities of ¹²CD₄ // Journal of Molecular Spectroscopy. — 1995. — Vol. 171. — No. 1. — P. 58-85.

76. Boudon V., Champion J.-P., Gabard T., Loëte M., Michelot F., Pierre G., Rotger M., Wenger Ch., Rey M. Symmetry-adapted tensorial formalism to model rovibrational and rovibronic spectra of molecules pertaining to various point groups: Special Issue Dedicated to Dr. Jon T. Hougen on the Occasion of His 68th Birthday // Journal of Molecular Spectroscopy. — 2004. — Vol. 228. — No. 2. — P. 620-634.
77. Cheglokov A., Ulenikov O., Zhilyakov A., Cherepanov V., Makushkin Y., Malikova A. On the determination of spectroscopic constants as functions of intramolecular parameters // Journal of Physics B: Atomic, Molecular and Optical Physics. — 1989. — Vol. 22. — No. 7. — P. 997.
78. Flaud J. M., Camy-Peyret C. Vibration-rotation intensities in H₂O-type molecules application to the 2v₂, v₁, and v₃ bands of H₂¹⁶O // Journal of Molecular Spectroscopy. — 1975. — Vol. 55. — No. 1. — P. 278-310.
79. Herzberg G. Molecular spectra and molecular structure. Vol. 2: Infrared and Raman spectra of polyatomic molecules : in 2 Vol. Vol. 2. Molecular spectra and molecular structure. Vol.2. — Van Noststrand. — New York, 1956. — 644 p.
80. McDowell R. S. Rotational partition functions for spherical-top molecules // Journal of Quantitative Spectroscopy and Radiative Transfer. — 1987. — Vol. 38. — No. 5. — P. 337-346.
81. Saveliev V., Ulenikov O. Calculation of vibration-rotation line intensities of polyatomic molecules based on the formalism of irreducible tensorial sets // Journal of Physics B: Atomic and Molecular Physics. — 1987. — Vol. 20. — No. 1. — P. 67.
82. Fano U., Racah G. Irreducible Tensorial Sets. — First Edition. — New York: Academic Press, 1959. — 171 p.
83. Wigner E.P. Quantum theory of angular momentum. — New York: Academic Press, 1965.
84. Bauerecker S., Sydow C., Maul C., Gromova O. V., Bekhtereva E. S., Nikolaeva N. I., Ulenikov O. N. Expanded ro-vibrational analysis of the dyad region of CD₄: Line positions and energy levels // Journal of Quantitative Spectroscopy and Radiative Transfer. — 2022. — Vol. 288. — P. 108275.
85. Ulenikov O. N., Gromova O. V., Bekhtereva E. S., Raspopova N. I., Sennikov P. G., Koshelev M. A., Velmuzhova I. A., Velmuzhov A. P., Bulanov A. D. High resolution study of ^MGeH₄ (*M* = 76, 74) in the dyad region // Journal of Quantitative Spectroscopy and Radiative Transfer. — 2014. — Vol. 144. — P. 11-26.
86. Wenger Ch., Boudon V., Rotger M., Sanzharov M., Champion J.-P. XTDS and SPVIEW: Graphical tools for the analysis and simulation of high-resolution molecular spectra: Special issue dedicated to the pioneering work of Drs. Edward A. Cohen and Herbert M. Pickett on spectroscopy relevant to the Earth's atmosphere and astrophysics // Journal of Molecular Spectroscopy. — 2008. — Vol. 251. — No. 1. — P. 102-113.

87. Wenger Ch., Champion J. P. Spherical top data system (STDS) software for the simulation of spherical top spectra: Atmospheric Spectroscopy Applications 96 // Journal of Quantitative Spectroscopy and Radiative Transfer. — 1998. — Vol. 59. — No. 3. — P. 471-480.
88. Tran H., Ngo N. H., Hartmann J.-M. Efficient computation of some speed-dependent isolated line profiles // Journal of Quantitative Spectroscopy and Radiative Transfer. — 2013. — Vol. 129. — P. 199-203.
89. Tran H., Ngo N. H., Hartmann J.-M., Gamache R. R., Mondelain D., Kassi S., Campargue A., Gianfrani L., Castrillo A., Fasci E., Rohart F. Velocity effects on the shape of pure H₂O isolated lines: Complementary tests of the partially correlated speed-dependent Keilson-Storer model // The Journal of Chemical Physics. — 2013. — Vol. 138. — No. 3. — P. 034302.
90. Rana T., Chandrashekhar M. V. S., Daniels K., Sudarshan T. SiC Homoepitaxy, Etching and Graphene Epitaxial Growth on SiC Substrates Using a Novel Fluorinated Si Precursor Gas (SiF₄) // Journal of Electronic Materials. — 2016. — Vol. 45. — No. 4. — P. 2019-2024.
91. Taquet N., Meza Hernández I., Stremme W., Bezanilla A., Grutter M., Campion R., Palm M., Boulesteix T. Continuous measurements of SiF₄ and SO₂ by thermal emission spectroscopy: Insight from a 6-month survey at the Popocatépetl volcano // Journal of Volcanology and Geothermal Research. — 2017. — Vol. 341. — P. 255-268.
92. Ignatov S. K., Sennikov P. G., Chuprova L. A., Razuvayev A. G. Thermodynamic and kinetic parameters of elementary steps in gas-phase hydrolysis of SiF₄. Quantum-chemical and FTIR spectroscopic studies // Russian Chemical Bulletin. — 2003. — Vol. 52. — No. 4. — P. 837-845.
93. Krueger A., Stremme W., Harig R., Grutter M. Volcanic SO₂ and SiF₄ visualization using 2-D thermal emission spectroscopy; Part 2: Wind propagation and emission rates // Atmospheric Measurement Techniques. — 2013. — Vol. 6. — No. 1. — P. 47-61.
94. Stremme W., Krueger A., Harig R., Grutter M. Volcanic SO₂ and SiF₄ visualization using 2-D thermal emission spectroscopy; Part 1: Slant-columns and their ratios // Atmospheric Measurement Techniques. — 2012. — Vol. 5. — No. 2. — P. 275-288.
95. Etim E. E., Olagboye S. A., Godwin O. E., Atiatah I. M. Quantum Chemical studies on Silicon tetrafluoride and its protonated analogues // International Journal of Modern Chemistry — 2020. — Vol. 12. — No. 1. — P. 26-45.
96. Shimanouchi T., Nakagawa I., Hiraishi J., Ishii M. Force constants of CF₄, SiF₄, BF₃, CH₄, SiH₄, NH₃, and PH₃ // Journal of Molecular Spectroscopy. — 1966. — Vol. 19. — No. 1. — P. 78-107.
97. Hagen K., Hedberg K. Interatomic distances and rms amplitudes of vibration of gaseous SiF₄ from electron diffraction // The Journal of Chemical Physics. — 2003. — Vol. 59. — No. 3. — P. 1549-1550.

98. Königer F., Müller A. Molecular constants of SiF₄, GeF₄, and RuO₄ // Journal of Molecular Spectroscopy. — 1977. — Vol. 65. — No. 3. — P. 339-344.
99. Patterson C. W., McDowell R. S., Nereson N. G., Krohn B. J., Wells J. S., Petersen F. R. Tunable laser diode study of the v₃ band of SiF₄ near 9.7 μm // Journal of Molecular Spectroscopy. — 1982. — Vol. 91. — No. 2. — P. 416-423.
100. Patterson C. W., Pine A. S. Doppler-limited spectrum and analysis of the 3v₃ manifold of SiF₄ // Journal of Molecular Spectroscopy. — 1982. — Vol. 96. — No. 2. — P. 404-421.
101. Takami M., Kuze H. Infrared–microwave double resonance spectroscopy of the SiF₄ v₃ fundamental using a tunable diode laser // The Journal of Chemical Physics. — 1983. — Vol. 78. — No. 5. — P. 2204-2209.
102. Halonen L. Stretching vibrational overtone and combination states in silicon tetrafluoride // Journal of Molecular Spectroscopy. — 1986. — Vol. 120. — No. 1. — P. 175-184.
103. Jörissen L., Kreiner W.A., Chen Y.-T., Oka T. Observation of ground state rotational transitions in silicon tetrafluoride // Journal of Molecular Spectroscopy. — 1986. — Vol. 120. — No. 1. — P. 233-235.
104. Breidung J., Demaison J., Margulès L., Thiel W. Equilibrium structure of SiF₄ // Chemical Physics Letters. — 1999. — Vol. 313. — No. 3. — P. 713-717.
105. Boudon V., Champion J.-P., Gabard T., Loëte M., Rotger M., Wenger C. Spherical Top Theory and Molecular Spectra // Handbook of High-resolution Spectroscopy. — John Wiley & Sons, Ltd, 2011.
106. Boudon V., Manceron L., Richard C. High-resolution spectroscopy and analysis of the v₃, v₄ and 2v₄ bands of SiF₄ in natural isotopic abundance // Journal of Quantitative Spectroscopy and Radiative Transfer. — 2020. — Vol. 253. — P. 107114.
107. Boudon V., Richard C., Manceron L. High-Resolution spectroscopy and analysis of the fundamental modes of ²⁸SiF₄. Accurate experimental determination of the Si–F bond length // Journal of Molecular Spectroscopy. — 2022. — Vol. 383. — P. 111549.
108. Herranz J. The rotational structure of the fundamental infrared bands of methane-type molecules // Journal of Molecular Spectroscopy. — 1961. — Vol. 6. — P. 343-359.
109. Robiette A. G., Gray D. L., Birss F. W. The effective vibration-rotation hamiltonian for triply-degenerate fundamentals of tetrahedral XY₄ molecules // Molecular Physics. — 1976. — Vol. 32. — No. 6. — P. 1591-1607.
110. Richard C., Ben Fathallah O., Hardy P., Kamel R., Merkulova M., Rotger M., Ulenikov O. N., Boudon V. TFSiCaSDa data base : Calculated spectroscopic databases. — URL: <https://vamdc.icb.cnrs.fr/PHP/SiF4.php> (дата обращения: 28.08.2024).

111. Treffers R. R., Larson H. P., Fink U., Gautier T. N. Upper limits to trace constituents in Jupiter's atmosphere from an analysis of its 5- μm spectrum // Icarus. — 1978. — Vol. 34. — No. 2. — P. 331-343.
112. Larson H. P., Fink U., Smith H. A., Davis D. S. The middle-infrared spectrum of Saturn - Evidence for phosphine and upper limits to other trace atmospheric constituents // The Astrophysical Journal. — 1980. — Vol. 240. — P. 327.
113. Fegley B., Lodders K. Chemical Models of the Deep Atmospheres of Jupiter and Saturn // Icarus. — 1994. — Vol. 110. — No. 1. — P. 117-154.
114. Cochran A. L. Solar System Science Enabled with the Next Generation Space Telescope: ASP Conference Series // Science With The NGST (Next Generation of Space Telescope). — 1998. — Vol. 133. — P. 188.
115. Goldhaber D. M., Betz A. L. Silane in IRC +10216. // The Astrophysical Journal. — 1984. — Vol. 279. — P. L55-L58.
116. Monnier J. D., Danchi W. C., Hale D. S., Tuthill P. G., Townes C. H. Mid-Infrared Interferometry on Spectral Lines. III. Ammonia and Silane around IRC +10216 and VY Canis Majoris // The Astrophysical Journal. — 2000. — Vol. 543. — No. 2. — P. 868.
117. Allen W. D., Schaefer H. F. Geometrical structures, force constants, and vibrational spectra of SiH, SiH₂, SiH₃, and SiH₄ // Chemical Physics. — 1986. — Vol. 108. — No. 2. — P. 243-274.
118. Chuprov L. A., Sennikov P. G., Tokhadze K. G., Ignatov S. K., Schrems O. High-resolution Fourier-transform IR spectroscopic determination of impurities in silicon tetrafluoride and silane prepared from it // Inorganic Materials. — 2006. — Vol. 42. — No. 8. — P. 924-931.
119. Bartlome R., Feltrin, A., Ballif, C. Infrared laser-based monitoring of the silane dissociation during deposition of silicon thin films // Applied Physics Letters. — 2009. — Vol. 94. — No. 20. — P. 201501.
120. Boutahar A., Touzani L., Loëte M., Millot G., Lavorel B. Raman Intensities of the v₁/v₃ Dyad of ²⁸SiH₄ // Journal of Molecular Spectroscopy. — 1995. — Vol. 169. — No. 1. — P. 38-57.
121. Terki-Hassaïne M., Claveau Ch., Valentin A., Pierre G. Analysis of the Infrared Fourier Transform Spectrum of the Spectra of Silane in the Range 2930–3300 cm⁻¹ // Journal of Molecular Spectroscopy. — 1999. — Vol. 197. — No. 2. — P. 307-321.
122. van Helden J. H., Lopatik D., Nave A., Lang N., Davies P.B., Röpcke J. High resolution spectroscopy of silane with an external-cavity quantum cascade laser: Absolute line strengths of the v₃ fundamental band at 4.6 μm // Journal of Quantitative Spectroscopy and Radiative Transfer. — 2015. — Vol. 151. — P. 287-294.
123. Ulenikov O. N., Gromova O. V., Bekhtereva E.S., Raspopova N. I., Fomchenko A. L., Sydow C., Bauerecker S. High resolution study of strongly interacting v₃(F₂)/v₁(A₁) bands of ^MSiH₄ ($M = 28$,

29, 30) // Journal of Quantitative Spectroscopy and Radiative Transfer. — 2017. — Vol. 201. — P. 35-44.

124. Ulenikov O. N., Gromova O. V., Bektereva E. S., Raspopova N. I., Sklyarova E. A., Sydow C., Berezkin K., Maul C., Bauerecker S. Line strengths, widths and shifts analysis of the $2v_2$, $v_2 + v_4$ and $2v_4$ bands in $^{28}\text{SiH}_4$, $^{29}\text{SiH}_4$ and $^{30}\text{SiH}_4$ // Journal of Quantitative Spectroscopy and Radiative Transfer. — 2021. — Vol. 270. — P. 107683.

125. Pierre G., Valentin A., Henry L. Étude par transformée de Fourier, du spectre, du silane dans la région de 1000 cm^{-1} . Analyse de la diade v_2 et v_4 // Canadian Journal of Physics. — 1986. — Vol. 64. — No. 3. — P. 341-350.

Appendix A. Figure for Chapter 1

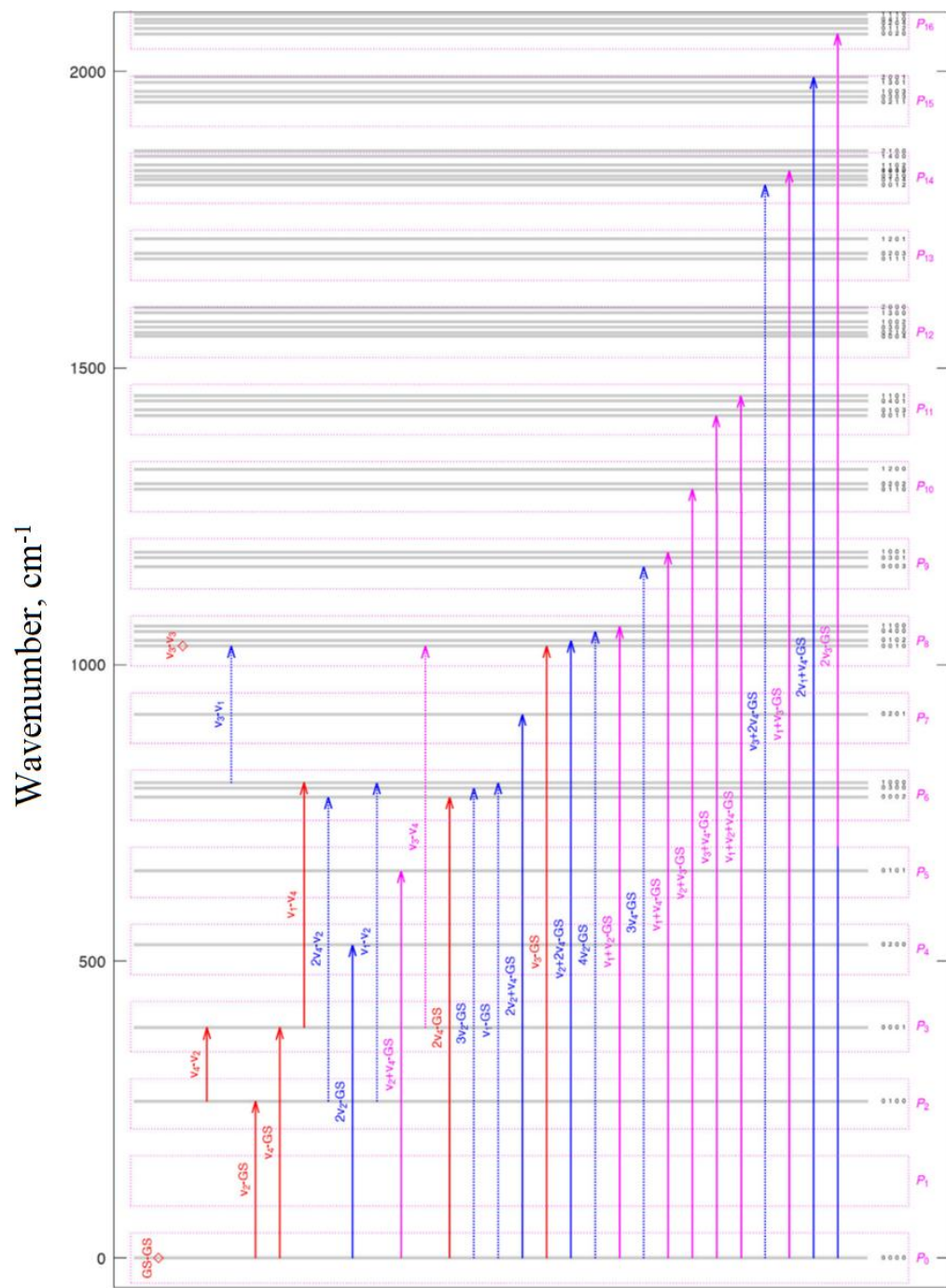


Figure A.1 – Vibrational levels of SiF_4 molecule.

The red solid line indicates the previously investigated bands; the blue solid line – the bands that are planned to be investigated in the future; the dashed blue line – the transitions that cannot be investigated in the spectra registered for this work due to their weak intensity; the pink solid line – the bands investigated in this work and the dashed pink line – the theoretically calculated bands for which the spectroscopic parameters were not varied.

Appendix B. Figures for Chapter 2

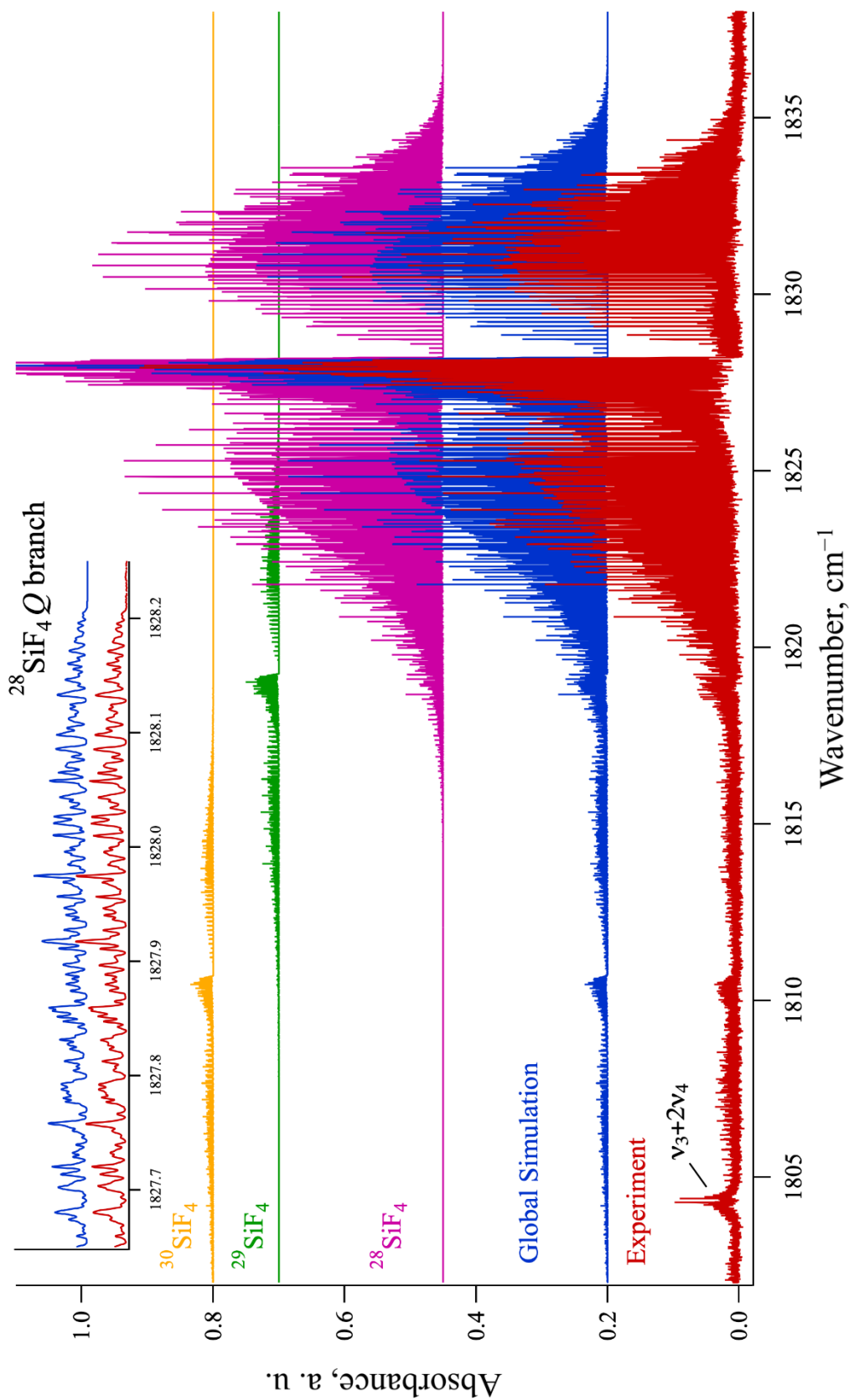


Figure B.1 – Theoretical and experimental spectra of the $\nu_1 + \nu_3$ band for three isotopologues: $^{28}\text{SiF}_4$, $^{29}\text{SiF}_4$ and $^{30}\text{SiF}_4$. The insert shows part of a Q -branch.

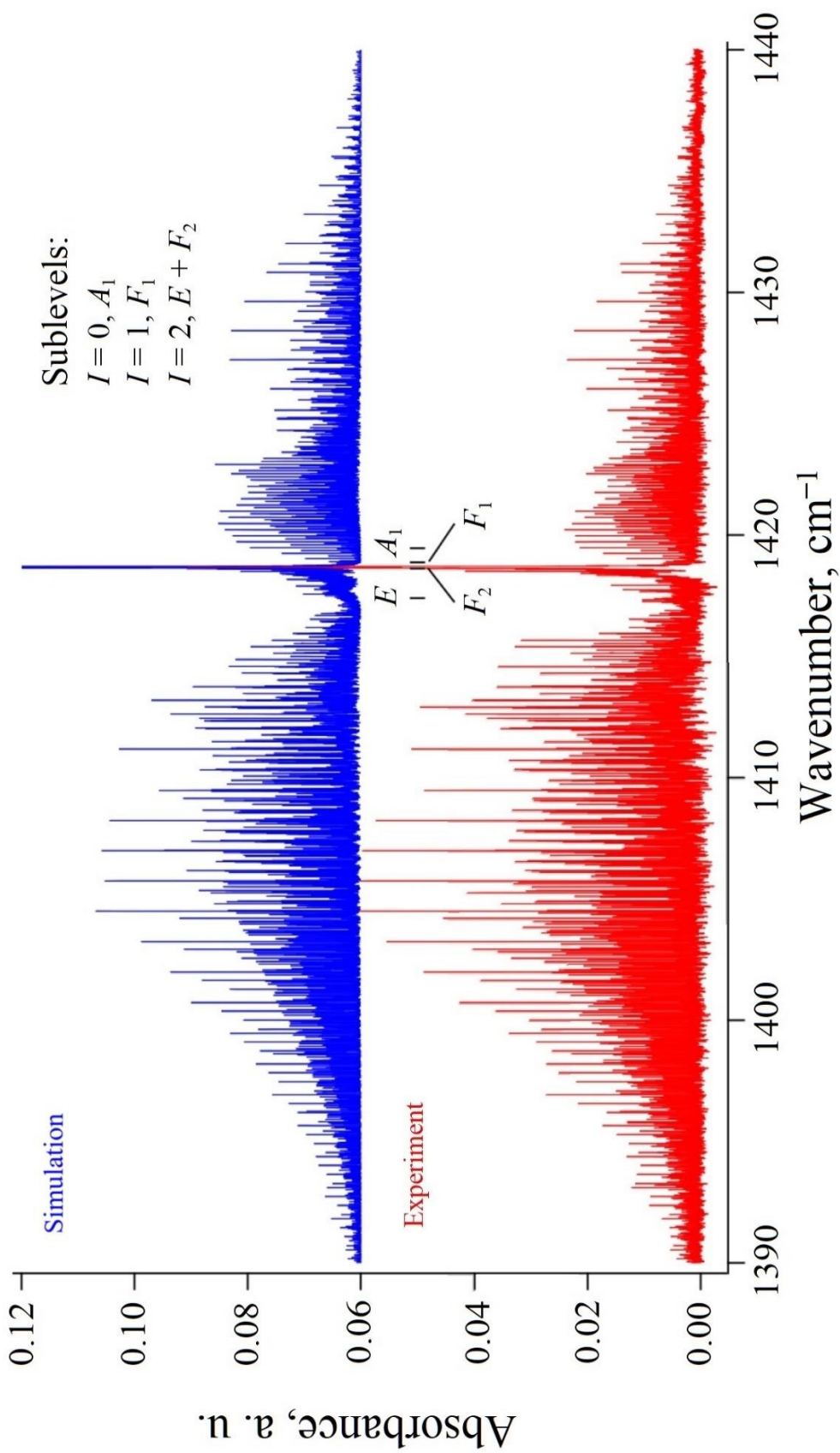


Figure B.2 – Theoretical and experiment spectra of the $v_3 + v_4$ band.

The centres of the four sub-levels are located within 2.06 cm^{-1} .

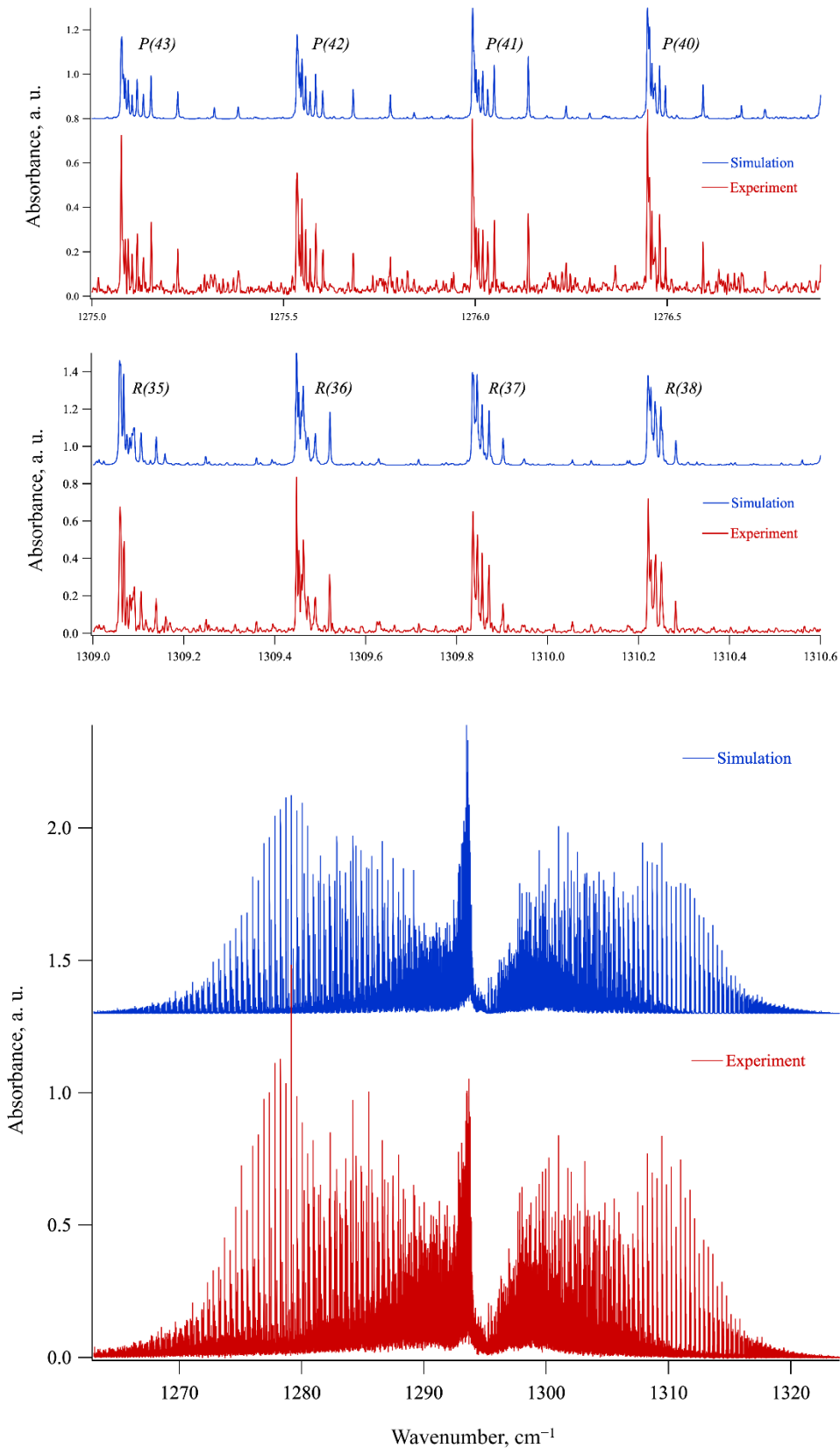


Figure B.3 – Comparison of the theoretically calculated and experimental spectra of the $v_2 + v_3$ band.
The lower part shows a fragment of the P -branch.

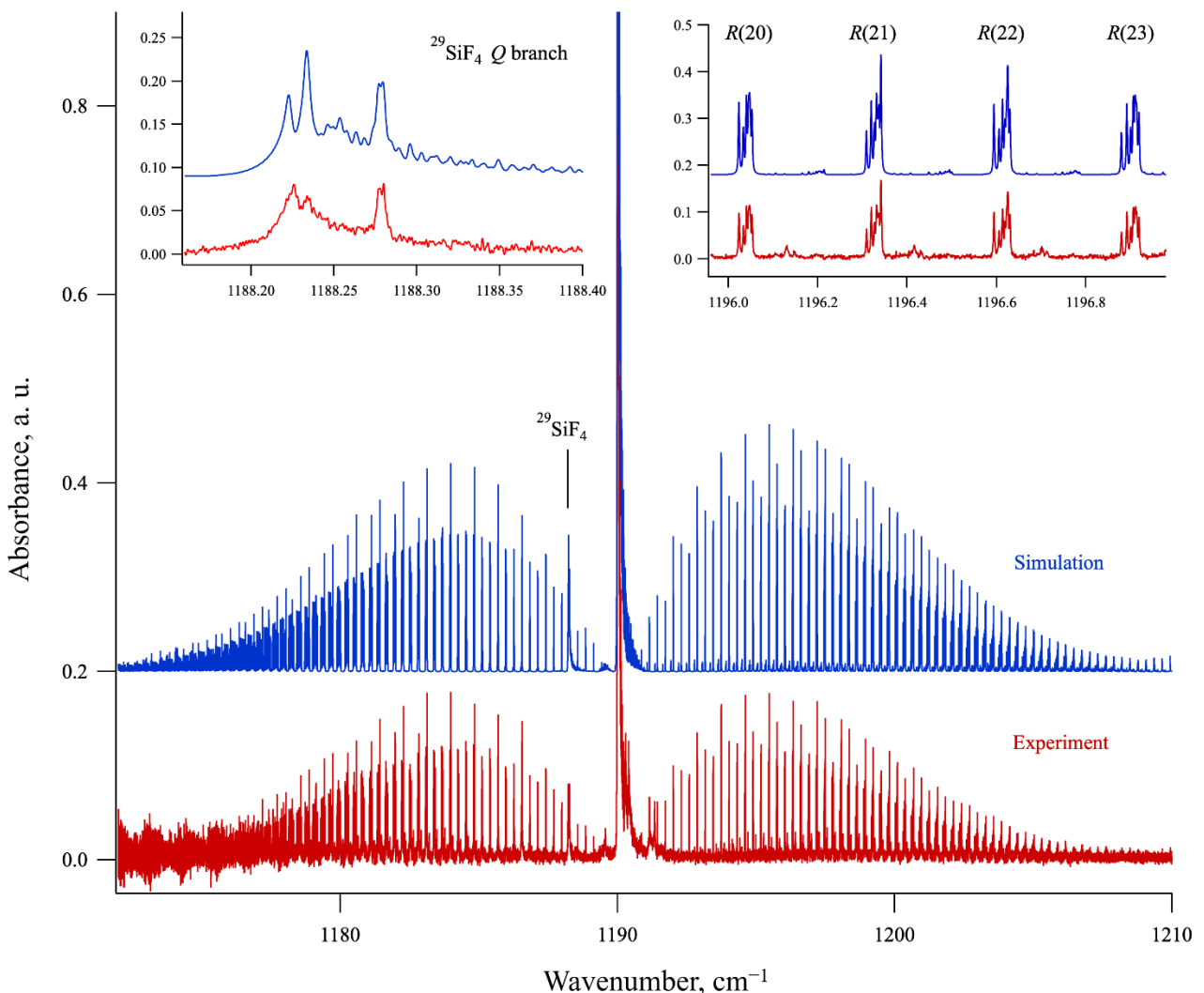


Figure B.4 – Theoretical and experimental spectra of the $v_1 + v_4$ band. The fragments show a part of the *R*-branch and the centre of the band belonging to the $^{29}\text{SiF}_4$ isotopologue.

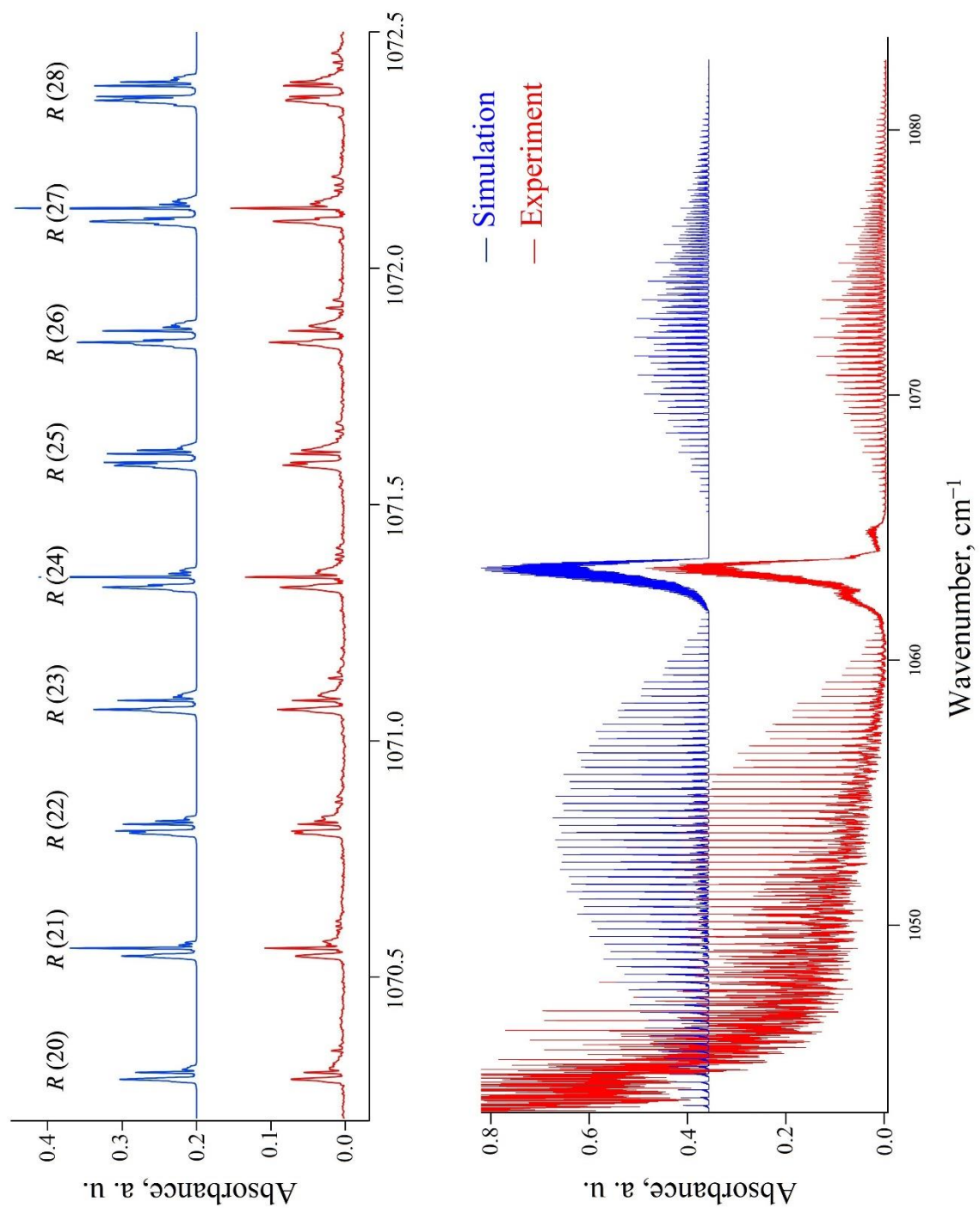


Figure B.5 – Theoretical and experimental spectra of the $v_1 + v_2$ band.

The R -branch of the v_3 band can be seen in the left part of the experimental spectrum.

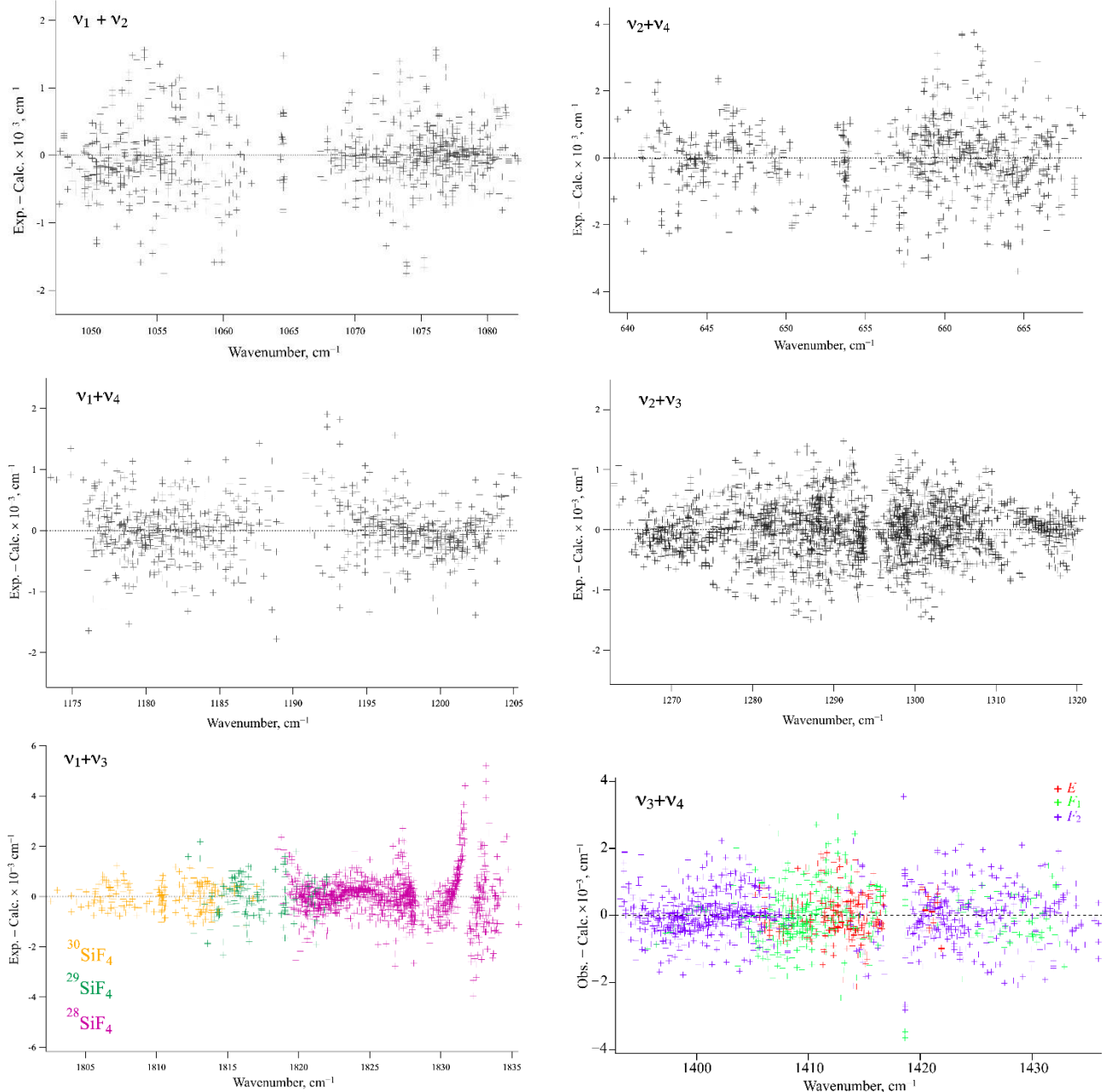


Figure B.6 – Fit residuals for line positions for certain combination bands of SiF_4 .

Appendix C. Tables for Chapter 2
Table C.1 – *B*-type transitions corresponding to the $v_5 + v_{12}$ band of the C_2D_4 molecule (part).

JK_aK_c	$J'K'_aK'_c$	Transition, cm^{-1}	Transmittance, %	Energy, cm^{-1}	Mean value, cm^{-1}	$\delta \cdot 10^{-4},$ cm^{-1}
13 7 6	12 6 7	3427.5131	43.3	3593.7163	3593.7164	4
	14 8 7	3342.3511	51.4	3593.7165		
14 7 7	13 6 8	3428.8283	48.3	3612.0575	3612.0586	9
	14 6 8	3410.4701	54.8	3612.0589		
	15 8 8	3341.0911	54.1	3612.0579		
15 7 8	14 6 9	3430.1396	52.9	3631.7258	3631.7265	9
	16 8 9	3339.8375	55.4	3631.7272		
16 7 9	16 6 10	3410.4049	68.0	3652.7289	3652.7287	3
	16 8 8	3360.8389	59.5	3652.7287		
	17 8 10	3338.5913	57.9	3652.7284		
12 8 4	11 7 5	3430.0677	48.7	3603.7548	3603.7547	-2
	12 9 3	3357.2948	80.3	3603.7547		
	13 9 5	3340.3448	56.3	3603.7544		
13 8 5	12 7 6	3431.3909	53.5	3620.7491	3620.7490	1
	14 9 6	3339.0774	61.3	3620.7489		
14 8 6	13 7 7	3432.7139	56.6	3639.0619	3639.0619	5
	14 9 5	3357.3902	73.4	3639.0618		
	15 9 7	3337.8139	62.1	3639.0619		
10 9 1	9 8 2	3431.3075	39.0	3604.4008	3604.4008	-7
	11 10 2	3339.6535	48.3	3604.4007		
11 9 2	10 8 3	3432.6323	41.5	3618.7562	3618.7558	-11
	11 10 1	3354.0082	82.6	3618.7555		
	12 10 3	3338.3795	50.1	3618.7559		
12 9 3	11 8 4	3433.9584	44.6	3634.4227	3634.4227	-7
	12 10 2	3354.0464	80.5	3634.4227		
	13 10 4	3337.1089	50.9	3634.4226		
11 10 1	10 9 2	3436.5359	50.8	3653.0268	3653.0268	-2
	11 9 2	3422.2062	79.6	3653.0271		
	12 11 2	3335.1695	59.8	3653.0264		

Table C.2 – *B*-type transitions corresponding to the $v_6 + v_{11}$ band of the C₂D₄ molecule (part).

JK_aK_c	$J'K'_aK'_c$	Transition, cm ⁻¹	Transmittance, %	Energy, cm ⁻¹	Mean value, cm ⁻¹	$\delta \cdot 10^{-4}$, cm ⁻¹
12 9 3	11 8 4	3250.3321	52.1	3450.7964	3450.7963	1
	12 10 2	3170.4201	58.2	3450.7964		
	13 10 4	3153.4827	63.3	3450.7963		
13 9 4	12 8 5	3251.5536	55.1	3467.6702	3467.6701	-3
	13 10 3	3170.3564	83.5	3467.6701		
	14 10 5	3152.1095	66.2	3467.6697		
14 9 5	13 8 6	3252.7683	57.5	3485.8511	3485.8510	-5
	14 10 4	3170.1901	82.4	3485.8510		
	15 10 6	3150.7324	67.9	3485.8510		
11 10 1	10 9 2	3253.1920	56.8	3469.6828	3469.6826	2
	11 11 0	3167.4468	94.0	3469.6824		
	12 11 2	3151.8256	68.9	3469.6825		
12 10 2	11 9 3	3254.4283	59.8	3485.2493	3485.2491	2
	12 11 1	3167.3919	91.7	3485.2489		
	13 11 3	3150.4645	71.5	3485.2490		
13 10 3	12 9 4	3255.6585	61.7	3502.1184	3502.1181	-1
	13 11 2	3167.3336	87.2	3502.1181		
	14 11 4	3149.0986	73.6	3502.1182		
13 11 2	12 10 3	3259.7588	57.8	3540.1351	3540.1350	-2
	13 12 1	3164.3211	91.9	3540.1348		
	14 12 3	3146.0957	68.7	3540.1349		
14 11 3	13 10 4	3260.9769	61.5	3558.2905	3558.2904	-1
	14 12 2	3164.2512	91.5	3558.2904		
	15 12 4	3144.7188	72.2	3558.2902		
15 11 4	14 10 5	3262.1860	62.3	3577.7465	3577.7469	-2
	15 12 3	3164.1755	89.5	3577.7470		
	16 12 5	3143.3354	74.5	3577.7469		

Table C.3 – Spectroscopic parameters of the vibrational state ($v_5 = v_{12} = 1$).

Parameter	$(v_5 = v_{12} = 1) \text{C}_2\text{D}_4, \text{cm}^{-1}$ *	$(v_{\text{GS}} = 1) \text{C}_2\text{D}_4, \text{cm}^{-1}$ [34]
<i>I</i>	2	3
E	3386.14881(69)	-
A	2.46485(25)	2.44158560
B	0.737601(80)	0.73492916
C	0.562587(93)	0.5635243
$\Delta_K \cdot 10^4$	0.4648(28)	0.208659
$\Delta_{JK} \cdot 10^4$	0.0049(13)	0.026825
$\Delta_J \cdot 10^4$	0.01156(86)	0.0080394
$H_K \cdot 10^8$	0.08354	0.08354
$H_{KJ} \cdot 10^8$	-0.01244	-0.01244
$H_{JK} \cdot 10^8$	0.004030	0.004030
$H_J \cdot 10^8$	0.105(23)	0.00008339
$L_K \cdot 10^{12}$	-0.02792	-0.02792
$L_{JK} \cdot 10^{12}$	-0.0005615	-0.0005615
$L_{JJK} \cdot 10^{11}$	-0.87(11)	-
$L_J \cdot 10^{12}$	-0.00000430	-0.00000430
$P_K \cdot 10^{11}$	-0.2370(62)	-
$P_{KKJ} \cdot 10^{11}$	0.2407(37)	-
$\delta_K \cdot 10^4$	0.038845	0.038845
$\delta_J \cdot 10^4$	0.0064(16)	0.00214769
$h_K \cdot 10^8$	0.06732	0.06732
$h_{JK} \cdot 10^8$	0.002895	0.002895
$h_J \cdot 10^8$	0.00004948	0.00004948
d_{rms}	0.0013	
N_{energy}	176	

*Here and further in the text: in brackets in columns 2 and 3 are statistical confidence intervals of 1σ relative to the last indicated numbers. The parameter values given without confidence intervals were fixed at the values of the corresponding parameters of the ground vibrational state and were not fit in the fitting procedure.

Table C.4 – Spectroscopic parameters of the vibrational state ($v_6 = v_{11} = 1$).

Parameter	$(v_6 = v_{11} = 1) \text{C}_2\text{D}_4, \text{cm}^{-1}$	$(v_{\text{GS}} = 1) \text{C}_2\text{D}_4, \text{cm}^{-1}$ [34]
<i>I</i>	2	3
<i>E</i>	3203.354284(77)	-
<i>A</i>	2.457560(84)	2.44158560
<i>B</i>	0.762142(91)	0.73492916
<i>C</i>	0.5991597(24)	0.5635243
$\Delta_K \cdot 10^4$	0.23854(90)	0.208659
$\Delta_{JK} \cdot 10^4$	0.0301(25)	0.026825
$\Delta_J \cdot 10^4$	0.00782(27)	0.0080394
$H_K \cdot 10^8$	0.08354	0.08354
$H_{KJ} \cdot 10^8$	-0.01244	-0.01244
$H_{JK} \cdot 10^8$	0.00354(45)	0.004030
$H_J \cdot 10^8$	0.00008339	0.00008339
$L_K \cdot 10^{12}$	-0.02792	-0.02792
$L_{JK} \cdot 10^{12}$	-0.0005615	-0.0005615
$L_{JJK} \cdot 10^{11}$	-	-
$L_J \cdot 10^{12}$	-0.00000430	-0.00000430
$P_K \cdot 10^{11}$	-	-
$P_{KKJ} \cdot 10^{11}$	-	-
$\delta_K \cdot 10^4$	0.038845	0.038845
$\delta_J \cdot 10^4$	0.00214769	0.00214769
$h_K \cdot 10^8$	0.06732	0.06732
$h_{JK} \cdot 10^8$	0.002895	0.002895
$h_J \cdot 10^8$	0.00004948	0.00004948
d_{rms}	0.0015	
N_{energy}	181	

Table C.5 – Ro-vibrational term values for the v_3 band of the ClO₂ molecule (in cm⁻¹).

N	K_a	K_c	J	E	Δ	δ	N	K_a	K_c	J	E	Δ	δ	N	K_a	K_c	J	E	Δ	δ	N	K_a	K_c	J	E	Δ	δ	N	K_a	K_c	J	E	Δ	δ
				2	3	4	I				2	3	4	I				2	3	4	I				2	3	4	I				2	3	4
1	1	1	+	1112.0921		-2	10	8	2	-	1234.1396	2	0	14	14	0	-	1449.6311		0	18	4	14	-	1237.1718		0	20	20	0	-	1795.3224		-1
2	0	2	-	1111.9306	2	0	10	8	2	+	1233.8316	1	0	14	14	0	+	1448.9879	0	1	18	4	14	+	1237.0579	1	-1	20	20	0	+	1794.3961	2	0
2	0	2	+	1111.9219	1	0	10	9	1	-	1258.1144	1	1	15	1	15	-	1180.4505	2	0	18	5	13	-	1249.6795	2	0	21	1	21	-	1243.4513	1	0
2	1	1	-	1113.4440		-3	10	9	1	+	1257.7366	1	0	15	1	15	+	1180.4310	0	0	18	5	13	+	1249.5478	2	0	21	1	21	+	1243.4318	1	-1
2	1	1	+	1113.4121	1	0	10	10	0	-	1284.8649	1	0	15	2	14	-	1188.0529	5	-1	18	6	12	-	1265.1554		0	21	2	20	-	1253.9089		-1
2	2	0	+	1117.5655		1	10	10	0	+	1284.4100	1	0	15	2	14	+	1187.9948	2	1	18	6	12	+	1264.9985	3	1	21	2	20	+	1253.8459	2	0
3	1	3	-	1115.0140	2	0	11	1	11	-	1149.5856	2	-1	15	3	13	-	1195.9747		0	18	7	11	-	1283.4860	1	0	21	3	19	-	1263.4667	2	0
3	1	3	+	1114.9951		1	11	1	11	+	1149.5669	1	0	15	3	13	+	1195.8896		-1	18	7	11	+	1283.2984	1	1	21	3	19	+	1263.3700	2	-1
3	2	2	-	1119.4538		-3	11	2	10	-	1155.6881		1	15	4	12	-	1205.8932	2	-1	18	8	10	-	1304.6383	1	1	21	4	18	-	1273.7561	3	1
3	2	2	+	1119.3895	3	-2	11	2	10	+	1155.6343	1	-2	15	4	12	+	1205.7877	1	1	18	8	10	+	1304.4147	1	0	21	4	18	+	1273.6375	4	-1
3	3	1	+	1126.4481	1	0	11	3	9	-	1163.0618		0	15	5	11	-	1218.5697		0	18	9	9	-	1328.5911	1	1	21	5	17	-	1286.3258	1	0
4	0	4	+	1116.1446	2	-1	11	3	9	+	1162.9835	2	1	15	5	11	+	1218.4392	2	2	18	9	9	+	1328.3269	2	0	21	5	17	+	1286.1897	2	0
4	1	3	-	1117.8745	0	-1	11	4	8	-	1172.9633	0	0	15	6	10	-	1234.0974	1	1	18	10	8	-	1355.3265	1	0	21	6	16	-	1301.7373	0	0
4	1	3	+	1117.8403	2	0	11	4	8	+	1172.8578	1	-1	15	6	10	+	1233.9355	1	0	18	10	8	+	1355.0171	1	0	21	6	16	+	1301.5801	2	1
4	2	2	-	1121.8978	1	0	11	5	7	-	1185.6932	2	0	15	7	9	-	1252.4552	1	1	18	11	7	-	1384.8272	1	0	21	7	15	-	1320.0246	1	0
4	2	2	+	1121.8403	1	0	11	5	7	+	1185.5533	1	0	15	7	9	+	1252.2562	1	-1	18	11	7	+	1384.4679	1	0	21	7	15	+	1319.8413	2	0
4	3	1	+	1128.8862		0	11	6	6	-	1201.2549	1	0	15	8	8	-	1273.6233	1	0	18	12	6	-	1417.0757	1	0	21	8	14	-	1341.1511	1	0
4	4	0	-	1138.9400		-1	11	6	6	+	1201.0728	1	0	15	8	8	+	1273.3819	1	0	18	12	6	+	1416.6619	2	1	21	8	14	+	1340.9372	0	0
4	4	0	+	1138.7662	2	0	11	7	5	-	1219.6335	1	0	15	9	7	-	1297.5859	1	0	18	13	5	-	1452.0534	1	0	21	9	13	-	1365.0886	1	0
5	1	5	-	1120.2225	0	0	11	7	5	+	1219.4016	1	0	15	9	7	+	1297.2960	1	-1	18	13	5	+	1451.5806	1	1	21	9	13	+	1364.8399	1	0
5	1	5	+	1120.2055	2	0	11	8	4	-	1240.8153		-2	15	10	6	-	1324.3270	2	0	18	14	4	-	1489.7412	0	0	21	10	12	-	1391.8154	1	0
5	2	4	-	1124.9022	1	1	11	8	4	+	1240.5266	1	1	15	10	6	+	1323.9834	1	0	18	14	4	+	1489.2049	0	0	21	10	12	+	1391.5277		1
5	2	4	+	1124.8497	0	-1	11	9	3	-	1264.7876	1	0	15	11	5	-	1353.8306	1	0	18	15	3	-	1530.1187	2	0	21	11	11	-	1421.3120	0	0
5	3	3	-	1132.0232		0	11	9	3	+	1264.4345	2	0	15	11	5	+	1353.4278		-1	18	15	3	+	1529.5148	0	0	21	11	11	+	1420.9809	2	-1
5	3	3	+	1131.9296	1	0	11	10	2	-	1291.5357		0	15	12	4	-	1386.0800	2	1	18	16	2	-	1573.1647	1	-1	21	12	10	-	1453.5594	1	0
5	4	2	-	1141.9628	1	-1	11	10	2	+	1291.1116	1	0	15	12	4	+	1385.6128	2	0	18	16	2	+	1572.4889	1	0	21	12	10	+	1453.1813	1	0
5	4	2	+	1141.8133	1	0	11	11	1	-	1321.0446	2	-1	15	13	3	-	1421.0568	2	-1	18	17	1	-	1618.8571	1	0	21	13	9	-	1488.5385	2	-1

Table C.5 – Continued.

<i>N</i>	<i>K_a</i>	<i>K_c</i>	<i>J</i>	<i>E</i>	Δ	δ	<i>N</i>	<i>K_a</i>	<i>K_c</i>	<i>J</i>	<i>E</i>	Δ	δ	<i>N</i>	<i>K_a</i>	<i>K_c</i>	<i>J</i>	<i>E</i>	Δ	δ	<i>N</i>	<i>K_a</i>	<i>K_c</i>	<i>J</i>	<i>E</i>	Δ	δ							
<i>I</i>				2	3	4	<i>I</i>				2	3	4	<i>I</i>				2	3	4	<i>I</i>				2	3	4							
5	5	1	-	1154.7344	1	0	11	11	1	+	1320.5427	1	0	15	13	3	+	1420.5203	1	0	18	17	1	+	1618.1052		0	21	13	9	+	1488.1094	1	0
5	5	1	+	1154.5142	1	2	12	0	12	-	1156.1672	4	1	15	14	2	-	1458.7429	2	2	18	18	0	-	1667.1726		-1	21	14	8	-	1526.2298		0
6	0	6	+	1122.7340	2	-2	12	0	12	+	1156.1446	1	1	15	14	2	+	1458.1316	1	-1	18	18	0	+	1666.3407		0	21	14	8	+	1525.7455	1	0
6	1	5	-	1124.8265	1	1	12	1	11	-	1160.5319		0	15	15	1	-	1499.1173	1	0	19	1	19	-	1220.2331	0	0	21	15	7	-	1566.6123	1	0
6	1	5	+	1124.7850	0	-1	12	1	11	+	1160.4694		-1	15	15	1	+	1498.4268		0	19	1	19	+	1220.2135	0	0	21	15	7	+	1566.0691	0	0
6	2	4	-	1128.6409	3	0	12	2	10	-	1164.1767	1	0	16	0	16	-	1189.4614	2	0	19	2	18	-	1229.6794		0	21	16	6	-	1609.6646	1	-1
6	2	4	+	1128.5864	3	0	12	2	10	+	1164.1001	1	0	16	0	16	+	1189.4403	2	0	19	2	18	+	1229.6176	2	1	21	16	6	+	1609.0589	2	0
6	3	3	-	1135.6692	2	1	12	3	9	-	1170.5059	1	0	16	1	15	-	1196.2337		-5	19	3	17	-	1238.5787	0	0	21	17	5	-	1655.3648	2	1
6	3	3	+	1135.5828	1	0	12	3	9	+	1170.4227	0	-1	16	1	15	+	1196.1647	2	1	19	3	17	+	1238.4859	3	-1	21	17	5	+	1654.6924	2	0
6	4	2	-	1145.5996	1	0	12	4	8	-	1180.2788	1	-3	16	2	14	-	1200.7204	2	1	19	4	16	-	1248.6729	3	2	21	18	4	-	1703.6889	2	1
6	4	2	+	1145.4658	2	0	12	4	8	+	1180.1748	0	3	16	2	14	+	1200.6246	1	0	19	4	16	+	1248.5595	1	-1	21	18	4	+	1702.9466		0
6	5	1	-	1158.3642	2	0	12	5	7	-	1192.9936	1	1	16	3	13	-	1206.3586	1	0	19	5	15	-	1261.2736	1	0	21	19	3	-	1754.6131		0
6	5	1	+	1158.1700	0	0	12	5	7	+	1192.8575		0	16	3	13	+	1206.2596	1	0	19	5	15	+	1261.1409	2	0	21	19	3	+	1753.7972	1	0
6	6	0	-	1173.9519	1	0	12	6	6	-	1208.5487	1	0	16	4	12	-	1215.7121	2	1	19	6	14	-	1276.7349	4	2	21	20	2	-	1808.1123		-2
6	6	0	+	1173.6848	1	0	12	6	6	+	1208.3738	1	0	16	4	12	+	1215.6035	3	0	19	6	14	+	1276.5780	1	0	21	20	2	+	1807.2196		1
7	1	7	-	1127.7315	2	-1	12	7	5	-	1226.9230	2	0	16	5	11	-	1228.3239		-5	19	7	13	-	1295.0530	3	-1	21	21	1	-	1864.1613		-1
7	1	7	+	1127.7143	1	0	12	7	5	+	1226.7023	1	0	16	5	11	+	1228.1937		-1	19	7	13	+	1294.8675	2	1	21	21	1	+	1863.1879		0
7	2	6	-	1132.7687	0	-2	12	8	4	-	1248.1020	0	0	16	6	10	-	1243.8371	2	-1	19	8	12	-	1316.1980	0	0	22	0	22	-	1255.8738	1	0
7	2	6	+	1132.7190	3	0	12	8	4	+	1247.8285	1	0	16	6	10	+	1243.6778	2	1	19	8	12	+	1315.9784	1	0	22	0	22	+	1255.8541	0	-1
7	3	5	-	1139.9222	1	0	12	9	3	-	1272.0717	1	0	16	7	9	-	1262.1875		1	19	9	11	-	1340.1466		1	22	1	21	-	1266.4776		0
7	3	5	+	1139.8405	0	0	12	9	3	+	1271.7389	4	0	16	7	9	+	1261.9932	0	0	19	9	11	+	1339.8884		0	22	1	21	+	1266.4095	3	1
7	4	4	-	1149.8484	1	0	12	10	2	-	1298.8178	0	0	16	8	8	-	1283.3511	1	0	19	10	10	-	1366.8795	1	0	22	2	20	-	1274.0502	2	-2
7	4	4	+	1149.7254	2	0	12	10	2	+	1298.4192	1	0	16	8	8	+	1283.1168	1	0	19	10	10	+	1366.5784	3	0	22	2	20	+	1273.9356	1	0
7	5	3	-	1162.6072	1	1	12	11	1	-	1328.3250	1	0	16	9	7	-	1307.3109	2	1	19	11	9	-	1396.3791	1	0	22	3	19	-	1279.7305	1	0
7	5	3	+	1162.4313	1	0	12	11	1	+	1327.8542	0	0	16	9	7	+	1307.0311	1	0	19	11	9	+	1396.0305	0	0	22	3	19	+	1279.5975	1	0
7	6	2	-	1178.1890	1	-1	12	12	0	-	1360.5767		0	16	10	6	-	1334.0502	0	0	19	12	8	-	1428.6273	1	0	22	4	18	-	1287.7373	1	0
7	6	2	+	1177.9495	1	0	12	12	0	+	1360.0277	0	0	16	10	6	+	1333.7198	0	0	19	12	8	+	1428.2269	2	0	22	4	18	+	1287.6066	1	0
7	7	1	-	1196.5841		0	13	1	13	-	1163.8985	2	-1	16	11	5	-	1363.5529	1	0	19	13	7	-	1463.6055	2	0	22	5	17	-	1299.8206	0	0
7	7	1	+	1196.2702		0	13	1	13	+	1163.8793	1	0	16	11	5	+	1363.1668	2	0	19	13	7	+	1463.1489	1	-1	22	5	17	+	1299.6812	2	-1

Table C.5 – Continued.

<i>N</i>	<i>K_a</i>	<i>K_c</i>	<i>J</i>	<i>E</i>	Δ	δ	<i>N</i>	<i>K_a</i>	<i>K_c</i>	<i>J</i>	<i>E</i>	Δ	δ	<i>N</i>	<i>K_a</i>	<i>K_c</i>	<i>J</i>	<i>E</i>	Δ	δ	<i>N</i>	<i>K_a</i>	<i>K_c</i>	<i>J</i>	<i>E</i>	Δ	δ	<i>N</i>	<i>K_a</i>	<i>K_c</i>	<i>J</i>	<i>E</i>	Δ	δ		
<i>I</i>				2	3	4	<i>I</i>				2	3	4	<i>I</i>				2	3	4	<i>I</i>				2	3	4	<i>I</i>				2	3	4		
8	0	8	-	1131.6550			1	13	2	12	-	1170.7011			2	16	12	4	-	1395.8020	2	2	19	14	6	-	1501.2943	1	0	22	6	16	-	1315.1638	4	-1
8	0	8	+	1131.6335	3	2	13	2	12	+	1170.6450	2	-1	16	12	4	+	1395.3551	2	1	19	14	6	+	1500.7774	2	0	22	6	16	+	1315.0056	4	1		
8	1	7	-	1134.2766	1	0	13	3	11	-	1178.2998	2	1	16	13	3	-	1430.7789	1	0	19	15	5	-	1541.6732	2	-1	22	7	15	-	1333.4302	1	0		
8	1	7	+	1134.2273	1	-1	13	3	11	+	1178.2189	1	0	16	13	3	+	1430.2665	2	1	19	15	5	+	1541.0919	1	0	22	7	15	+	1333.2473	1	1		
8	2	6	-	1137.9124	1	0	13	4	10	-	1188.1986		-3	16	14	2	-	1468.4652	0	0	19	16	4	-	1584.7213	1	0	22	8	14	-	1354.5451	1	0		
8	2	6	+	1137.8535	1	0	13	4	10	+	1188.0950	3	4	16	14	2	+	1467.8822	1	-1	19	16	4	+	1584.0713	1	0	22	8	14	+	1354.3332	0	1		
8	3	5	-	1144.8022		2	13	5	9	-	1200.9058	1	0	16	15	1	-	1508.8402		-2	19	17	3	-	1630.4158	1	-1	22	9	13	-	1378.4757	0	0		
8	3	5	+	1144.7222	4	-1	13	5	9	+	1200.7723	2	-2	16	15	1	+	1508.1824	1	0	19	17	3	+	1629.6936	1	2	22	9	13	+	1378.2305	2	0		
8	4	4	-	1154.7092	1	0	13	6	8	-	1216.4535	2	0	16	16	0	-	1551.8835	1	0	19	18	2	-	1678.7341	2	1	22	10	12	-	1405.1985	0	0		
8	4	4	+	1154.5935	2	0	13	6	8	+	1216.2842	1	0	16	16	0	+	1551.1459		0	19	18	2	+	1677.9351	1	0	22	10	12	+	1404.9160	2	1		
8	5	3	-	1167.4616	1	-1	13	7	7	-	1234.8231	0	0	17	1	17	-	1199.2311	1	0	19	19	1	-	1729.6515	2	0	22	11	11	-	1434.6931	2	1		
8	5	3	+	1167.2993	1	0	13	7	7	+	1234.6113	1	0	17	1	17	+	1199.2115	1	0	19	19	1	+	1728.7723		0	22	11	11	+	1434.3692	0	0		
8	6	2	-	1183.0388	0	0	13	8	6	-	1255.9989	1	1	17	2	16	-	1207.7204	3	1	20	0	20	-	1231.5346	1	1	22	12	10	-	1466.9399	1	0		
8	6	2	+	1182.8193	2	-4	13	8	6	+	1255.7381	1	0	17	2	16	+	1207.6598		-2	20	0	20	+	1231.5145	1	-1	22	12	10	+	1466.5709	1	0		
8	7	1	-	1201.4292	1	0	13	9	5	-	1279.9663	1	1	17	3	15	-	1216.0738		-1	20	1	19	-	1240.8879	3	-2	22	13	9	-	1501.9195	0	0		
8	7	1	+	1201.1436	2	-2	13	9	5	+	1279.6503	1	0	17	3	15	+	1215.9852	2	0	20	1	19	+	1240.8190	3	1	22	13	9	+	1501.5015	0	-1		
8	8	0	-	1222.6215	1	1	13	10	4	-	1306.7105	1	0	17	4	14	-	1226.0509	1	1	20	2	18	-	1247.2226		-2	22	14	8	-	1539.6120	2	1		
8	8	0	+	1222.2604		-1	13	10	4	+	1306.3334	2	0	17	4	14	+	1225.9418	1	-1	20	2	18	+	1247.1126		0	22	14	8	+	1539.1413		0		
9	1	9	-	1137.5247	2	-1	13	11	3	-	1336.2163	1	0	17	5	13	-	1238.6900	3	-3	20	3	17	-	1252.6539	0	-1	22	15	7	-	1579.9964	1	0		
9	1	9	+	1137.5068	1	0	13	11	3	+	1335.7719	1	0	17	5	13	+	1238.5597	2	2	20	3	17	+	1252.5324	1	0	22	15	7	+	1579.4695	1	1		
9	2	8	-	1143.0372		2	13	12	2	-	1368.4671	2	1	17	6	12	-	1254.1897	1	1	20	4	16	-	1261.1668	1	0	22	16	6	-	1623.0514	1	1		
9	2	8	+	1142.9868		0	13	12	2	+	1367.9495	1	0	17	6	12	+	1254.0318	1	1	20	4	16	+	1261.0456	2	0	22	16	6	+	1622.4642		0		
9	3	7	-	1150.2684	2	0	13	13	1	-	1403.4447		0	17	7	11	-	1272.5310	1	1	20	5	15	-	1273.5071	2	0	22	17	5	-	1668.7542		0		
9	3	7	+	1150.1906	3	2	13	13	1	+	1402.8486		0	17	7	11	+	1272.3404	1	0	20	5	15	+	1273.3723	1	-1	22	17	5	+	1668.1034	1	-1		
9	4	6	-	1160.1814	1	0	14	0	14	-	1171.7191	2	0	17	8	10	-	1293.6893		0	20	6	14	-	1288.9290		-1	22	18	4	-	1717.0819	2	1		
9	4	6	+	1160.0707	1	0	14	0	14	+	1171.6974	2	0	17	8	10	+	1293.4609	1	-1	20	6	14	+	1288.7723		1	22	18	4	+	1716.3639	1	0		
9	5	5	-	1172.9276	1	0	14	1	13	-	1177.2342	1	0	17	9	9	-	1317.6457	2	-1	20	7	13	-	1307.2326	2	1	22	19	3	-	1768.0099	1	0		
9	5	5	+	1172.7751	1	0	14	1	13	+	1177.1675	2	-1	17	9	9	+	1317.3746	1	0	20	7	13	+	1307.0483		1	22	19	3	+	1767.2214		1		
9	6	4	-	1188.5000	0	1	14	2	12	-	1181.1774	2	-1	17	10	8	-	1344.3834	1	0	20	8	12	-	1328.3688	1	0	22	20	2	-	1821.5135	0	0		

Table C.5 – Continued.

<i>N</i>	<i>K_a</i>	<i>K_c</i>	<i>J</i>	<i>E</i>	Δ	δ	<i>N</i>	<i>K_a</i>	<i>K_c</i>	<i>J</i>	<i>E</i>	Δ	δ	<i>N</i>	<i>K_a</i>	<i>K_c</i>	<i>J</i>	<i>E</i>	Δ	δ	<i>N</i>	<i>K_a</i>	<i>K_c</i>	<i>J</i>	<i>E</i>	Δ	δ	<i>N</i>	<i>K_a</i>	<i>K_c</i>	<i>J</i>	<i>E</i>	Δ	δ
<i>I</i>				2	3	4	<i>I</i>				2	3	4	<i>I</i>				2	3	4	<i>I</i>				2	3	4	<i>I</i>				2	3	4
9	6	4	+	1188.2964	1	-1	14	2	12	+	1181.0910	1	0	17	10	8	+	1344.0643	1	0	20	8	12	+	1328.1525	1	0	22	20	2	+	1820.6509	1	0
9	7	3	-	1206.8864	1	2	14	3	11	-	1187.1424	1	0	17	11	7	-	1373.8852	0	0	20	9	11	-	1352.3123	2	0	22	21	1	-	1877.5670		0
9	7	3	+	1206.6230	1	0	14	3	11	+	1187.0526	2	0	17	11	7	+	1373.5133	2	-1	20	9	11	+	1352.0593	2	0	22	21	1	+	1876.6272		2
9	8	2	-	1228.0746		0	14	4	10	-	1196.7554	1	-1	17	12	6	-	1406.1339	2	1	20	10	10	-	1379.0425	1	1	22	22	0	-	1936.1439	2	1
9	8	2	+	1227.7432	1	0	14	4	10	+	1196.6503	1	1	17	12	6	+	1405.7046	1	0	20	10	10	+	1378.7485	1	0	22	22	0	+	1935.1230		0
9	9	1	-	1252.0527	2	2	14	5	9	-	1209.4316	3	1	17	13	5	-	1441.1112	0	0	20	11	9	-	1408.5406	1	0	22	0	22	-	1255.8738	1	0
9	9	1	+	1251.6446		0	14	5	9	+	1209.2999	2	0	17	13	5	+	1440.6198	1	0	20	11	9	+	1408.2014	1	-1	22	0	22	+	1255.8541	0	-1
10	0	10	-	1142.8058		3	14	6	8	-	1224.9695	1	-1	17	14	4	-	1478.7980	1	-1	20	12	8	-	1440.7885	1	0	22	1	21	-	1266.4776		0
10	0	10	+	1142.7840	1	2	14	6	8	+	1224.8047		1	17	14	4	+	1478.2399	1	0	20	12	8	+	1440.4001	1	1	22	1	21	+	1266.4094		0
10	1	9	-	1146.1932	2	0	14	7	7	-	1243.3337	1	0	17	15	3	-	1519.1743	1	0	20	13	7	-	1475.7673	1	0	22	2	20	-	1274.0502	2	-2
10	1	9	+	1146.1370	2	1	14	7	7	+	1243.1291	1	0	17	15	3	+	1518.5451	1	1	20	13	7	+	1475.3251	1	-1	22	2	20	+	1273.9356	1	0
10	2	8	-	1149.7515	1	0	14	8	6	-	1264.5060	1	1	17	16	2	-	1562.2188	1	0	20	14	6	-	1513.4572	1	0	22	3	19	-	1279.7305	1	0
10	2	8	+	1149.6846	1	0	14	8	6	+	1264.2558	1	0	17	16	2	+	1561.5138	1	0	20	14	6	+	1512.9575	1	0	22	3	19	+	1279.5975	1	0
10	3	7	-	1156.4053	4	1	14	9	5	-	1288.4711	1	1	17	17	1	-	1607.9092	0	0	20	15	5	-	1553.8379	1	0	22	4	18	-	1287.7373	2	0
10	3	7	+	1156.3258	3	0	14	9	5	+	1288.1692	1	-1	17	17	1	+	1607.1244	1	0	20	15	5	+	1553.2767	1	0	22	4	18	+	1287.6067	2	1
10	4	6	-	1166.2673	2	1	14	10	4	-	1315.2137	1	0	18	0	18	-	1209.3982	1	0	20	16	4	-	1596.8880	1	0	22	5	17	-	1299.8206	0	0
10	4	6	+	1166.1598	1	1	14	10	4	+	1314.8547	2	0	18	0	18	+	1209.3777	2	-1	20	16	4	+	1596.2613		0	22	5	17	+	1299.6812		-1
10	5	5	-	1179.0048	2	1	14	11	3	-	1344.7184	3	1	18	1	17	-	1217.4663	1	-4	20	17	3	-	1642.5851	1	0	22	6	16	-	1315.1638		-1
10	5	5	+	1178.8595	1	0	14	11	3	+	1344.2963	0	0	18	1	17	+	1217.3972	1	3	20	17	3	+	1641.8890	1	-1	22	6	16	+	1315.0055		0
10	6	4	-	1194.5720	1	0	14	12	2	-	1376.9682	1	1	18	2	16	-	1222.7559	2	1	20	18	2	-	1690.9061	0	0	22	7	15	-	1333.4302	1	0
10	6	4	+	1194.3805	1	-1	14	12	2	+	1376.4777		0	18	2	16	+	1222.6520	1	0	20	18	2	+	1690.1370	1	0	22	7	15	+	1333.2473	2	1
10	7	3	-	1212.9545	1	0	14	13	1	-	1411.9453	1	-1	18	3	15	-	1228.1911	1	-1	20	19	1	-	1741.8266	2	-3	22	8	14	-	1354.5451	2	0
10	7	3	+	1212.7087	1	0	14	13	1	+	1411.3811	1	0	18	3	15	+	1228.0813	0	0	20	19	1	+	1740.9809	2	0	22	8	14	+	1354.3332	1	1
22	9	13	-	1378.4757	1	0	24	17	7	-	1697.3629	2	1	26	23	3	-	2056.9938	1	1	28	23	5	+	2089.6235		0	30	22	8	-	2065.4151		1
22	9	13	+	1378.2305	1	0	24	17	7	+	1696.7493	3	2	26	23	3	+	2056.0191	1	0	28	24	4	-	2154.1296	1	0	30	22	8	+	2064.5988	2	0
22	10	12	-	1405.1985	1	0	24	18	6	-	1745.6979	2	0	26	24	2	-	2120.5612	0	1	28	24	4	+	2153.1353		1	30	23	7	-	2126.5419		1
22	10	12	+	1404.9160	2	1	24	18	6	+	1745.0222	1	0	26	24	2	+	2119.5111	0	0	28	25	3	-	2220.1546	1	1	30	24	6	-	2190.1403		-1
22	11	11	-	1434.6931	2	1	24	19	5	-	1796.6344	0	-1	26	25	1	-	2186.5701		-1	28	25	3	+	2219.0869		1	30	24	6	+	2189.1939		1
22	11	11	+	1434.3692	0	0	24	19	5	+	1795.8933	1	0	26	25	1	+	2185.4419	2	-1	28	26	2	+	2287.4493		-3	30	25	5	-	2256.1825	2	1

Table C.5 – Continued.

<i>N</i>	<i>K_a</i>	<i>K_c</i>	<i>J</i>	<i>E</i>	Δ	δ	<i>N</i>	<i>K_a</i>	<i>K_c</i>	<i>J</i>	<i>E</i>	Δ	δ	<i>N</i>	<i>K_a</i>	<i>K_c</i>	<i>J</i>	<i>E</i>	Δ	δ	<i>N</i>	<i>K_a</i>	<i>K_c</i>	<i>J</i>	<i>E</i>	Δ	δ							
<i>I</i>				2	3	4	<i>I</i>				2	3	4	<i>I</i>				2	3	4	<i>I</i>				2	3	4							
22	12	10	-	1466.9399	1	0	24	20	4	-	1850.1474	1	0	26	26	0	-	2254.9922	2	-1	28	27	1	-	2359.4167		1	30	25	5	+	2255.1671	1	2
22	12	10	+	1466.5709	1	0	24	20	4	+	1849.3376	1	0	26	26	0	+	2253.7829		-2	28	27	1	+	2358.1944		-1	30	26	4	-	2324.6393	4	1
22	13	9	-	1501.9196	1	1	24	21	3	+	1905.3294	2	1	27	1	27	-	1326.3743	1	0	28	28	0	-	2432.5951		-1	30	27	3	-	2395.4819		3
22	13	9	+	1501.5015	0	-1	24	22	2	-	1964.7984	2	0	27	1	27	+	1326.3555	2	0	28	28	0	+	2431.2919		-3	31	1	31	-	1392.6970	1	0
22	14	8	-	1539.6120	2	1	24	22	2	+	1963.8421	1	0	27	2	26	-	1340.0537	0	0	29	1	29	-	1358.4324	1	1	31	1	31	+	1392.6785	1	-1
22	14	8	+	1539.1410	3	-3	24	23	1	-	2025.8830	3	1	27	2	26	+	1339.9892	2	2	29	1	29	+	1358.4137	1	-1	31	2	30	-	1408.5902	0	-1
22	15	7	-	1579.9964	1	0	24	23	1	+	2024.8487	3	0	27	3	25	-	1352.1681	1	0	29	2	28	-	1373.2158	1	-2	31	2	30	+	1408.5256	1	1
22	15	7	+	1579.4695	1	1	24	24	0	-	2089.4367		1	27	3	25	+	1352.0629	0	0	29	2	28	+	1373.1513	0	1	31	3	29	-	1422.7454	1	3
22	16	6	-	1623.0514	1	1	24	24	0	+	2088.3215	2	-1	27	4	24	-	1363.6620	2	1	29	3	27	-	1386.3276	1	0	31	3	29	+	1422.6369		0
22	16	6	+	1622.4641	3	-1	25	1	25	-	1296.5239	1	0	27	4	24	+	1363.5277	2	-2	29	3	27	+	1386.2208	0	1	31	4	28	-	1435.6082	2	1
22	17	5	-	1668.7542		0	25	1	25	+	1296.5049	1	0	27	5	23	-	1376.3371		0	29	4	26	-	1398.4513	2	1	31	4	28	+	1435.4651	2	-1
22	17	5	+	1668.1034	3	-1	25	2	24	-	1309.1090	1	-2	27	5	23	+	1376.1852	3	-1	29	4	26	+	1398.3123	1	-2	31	5	27	-	1448.7089		1
22	18	4	-	1717.0819	2	1	25	2	24	+	1309.0449	2	1	27	6	22	-	1391.5485	1	1	29	5	25	-	1411.2915	3	2	31	5	27	+	1448.5441		0
22	18	4	+	1716.3639	1	0	25	3	23	-	1320.2881	2	0	27	6	22	+	1391.3808	1	0	29	5	25	+	1411.1329	1	-1	31	6	26	-	1463.8153	1	3
22	19	3	-	1768.0099	1	0	25	3	23	+	1320.1851	0	-1	27	7	21	-	1409.6754		0	29	6	24	-	1426.4393	2	0	31	6	26	+	1463.6359		0
22	19	3	+	1767.2214		1	25	4	22	-	1331.2677	3	1	27	7	21	+	1409.4889		0	29	6	24	+	1426.2661	3	-1	31	7	25	-	1481.7703	2	0
22	20	2	-	1821.5135	0	0	25	4	22	+	1331.1385	3	-1	27	8	20	-	1430.7027	0	0	29	7	23	-	1444.4865	2	-1	31	7	25	+	1481.5758	1	0
22	20	2	+	1820.6509	1	0	25	5	21	-	1343.8559	2	0	27	8	20	+	1430.4932	1	0	29	7	23	+	1444.2966	2	1	31	8	24	-	1502.6791		1
22	21	1	-	1877.5670		0	25	5	21	+	1343.7099		0	27	9	19	-	1454.5797	1	0	29	8	22	-	1465.4609	1	0	31	8	24	+	1502.4656		1
22	21	1	+	1876.6270	2	1	25	6	20	-	1359.1382	2	0	27	9	19	+	1454.3435	1	0	29	8	22	+	1465.2499	2	0	31	9	23	-	1526.4814		0
22	22	0	-	1936.1437		-1	25	6	20	+	1358.9752	1	1	27	10	18	-	1481.2706		4	29	9	21	-	1489.3051	2	2	31	9	23	+	1526.2453	0	0
22	22	0	+	1935.1230		0	25	7	19	-	1377.3312	1	-2	27	10	18	+	1481.0038	1	0	29	9	21	+	1489.0693	0	0	31	10	22	-	1553.1253	0	0
23	1	23	-	1268.8823	1	0	25	7	19	+	1377.1474	1	1	27	11	17	-	1510.7466	3	-2	29	10	20	-	1515.9749	1	0	31	10	22	+	1552.8631	0	0
23	1	23	+	1268.8631	1	0	25	8	18	-	1398.4005	4	0	27	11	17	+	1510.4467	1	0	29	10	20	+	1515.7113	1	-1	31	11	21	-	1582.5736	1	0
23	2	22	-	1280.3905		0	25	8	18	+	1398.1913	1	0	27	12	16	-	1542.9859	2	1	29	11	19	-	1545.4393	1	0	31	11	21	+	1582.2824	2	1
23	2	22	+	1280.3267	1	1	25	9	17	-	1422.3034	1	0	27	12	16	+	1542.6488		1	29	11	19	+	1545.1444	1	0	31	12	20	-	1614.7971	2	0
23	3	21	-	1290.7122	1	1	25	9	17	+	1422.0650	1	0	27	13	15	-	1577.9651		0	29	12	18	-	1577.6717	0	-1	31	12	20	+	1614.4736	1	0
23	3	21	+	1290.6120	1	-1	25	10	16	-	1449.0093		-4	27	13	15	+	1577.5877	3	-1	29	12	18	+	1577.3427	2	1	31	13	19	-	1649.7702	2	0
23	4	20	-	1301.2925	3	1	25	11	15	-	1478.4953	1	0	27	14	14	-	1615.6629	2	-1	29	13	17	-	1612.6489		0	31	13	19	+	1649.4116	2	-1

Table C.5 – Continued.

<i>N</i>	<i>K_a</i>	<i>K_c</i>	<i>J</i>	<i>E</i>	Δ	δ	<i>N</i>	<i>K_a</i>	<i>K_c</i>	<i>J</i>	<i>E</i>	Δ	δ	<i>N</i>	<i>K_a</i>	<i>K_c</i>	<i>J</i>	<i>E</i>	Δ	δ	<i>N</i>	<i>K_a</i>	<i>K_c</i>	<i>J</i>	<i>E</i>	Δ	δ							
<i>I</i>				2	3	4	<i>I</i>				2	3	4	<i>I</i>				2	3	4	<i>I</i>				2	3	4							
23	4	20	+	1301.1686	4	-2	25	11	15	+	1478.1878	3	0	27	14	14	+	1615.2423	2	0	29	13	17	+	1612.2822	1	0	31	14	18	-	1687.4691	1	0
23	5	19	-	1313.8522	2	0	25	12	14	-	1510.7386	0	0	27	15	13	-	1656.0578	3	2	29	14	16	-	1650.3479	0	0	31	14	18	+	1687.0727	3	0
23	5	19	+	1313.7114	2	-1	25	12	14	+	1510.3913	2	1	27	15	13	+	1655.5905	1	2	29	14	16	+	1649.9407	3	1	31	15	17	-	1727.8704	1	0
23	6	18	-	1329.2033	5	1	25	13	13	-	1545.7189	4	2	27	16	12	-	1699.1266	3	0	29	15	15	-	1690.7461		0	31	15	17	+	1727.4332		0
23	6	18	+	1329.0437	2	1	25	13	13	+	1545.3281		1	27	16	12	+	1698.6096	0	0	29	15	15	+	1690.2955	1	1	31	16	16	-	1770.9503		-4
23	7	17	-	1347.4493	0	0	25	14	12	-	1583.4151		3	27	17	11	-	1744.8468	1	0	29	16	14	-	1733.8209	0	0	31	16	16	+	1770.4701	3	2
23	7	17	+	1347.2664	0	0	25	14	12	+	1582.9774		1	27	17	11	+	1744.2769	7	-2	29	16	14	+	1733.3237	3	0	31	17	15	-	1816.6861	1	0
23	8	16	-	1368.5512	1	1	25	15	11	-	1623.8054	2	0	27	18	10	-	1793.1946	2	0	29	17	13	-	1779.5486	2	0	31	17	15	+	1816.1590	1	0
23	8	16	+	1368.3405	2	1	25	15	11	+	1623.3178	2	0	27	18	10	+	1792.5691	1	0	29	17	13	+	1779.0021	3	-1	31	19	13	-	1916.0245	1	-1
23	9	15	-	1392.4737	1	0	25	16	10	-	1666.8687	1	2	27	19	9	-	1844.1459		4	29	18	12	-	1827.9054		-1	31	19	13	+	1915.3968	2	-1
23	9	15	+	1392.2313	1	0	25	16	10	+	1666.3274	3	-1	27	19	9	+	1843.4613	0	0	29	18	12	+	1827.3069	2	0	31	20	12	-	1969.5773		0
23	10	14	-	1419.1917	1	-1	25	17	9	-	1712.5814	2	-1	27	20	8	-	1897.6741	2	-1	29	19	11	-	1878.8668		0	31	20	12	+	1968.8953	2	0
23	10	14	+	1418.9138	1	1	25	17	9	+	1711.9839	1	1	27	20	8	+	1896.9283	1	0	29	19	11	+	1878.2132	0	0	31	21	11	-	2025.6845		1
23	11	13	-	1448.6839	2	0	25	18	8	-	1760.9207	1	0	27	21	7	-	1953.7548		-1	29	20	10	-	1932.4072	1	0	31	21	11	+	2024.9456	1	2
23	11	13	+	1448.3662	2	-1	25	18	8	+	1760.2632	1	0	27	21	7	+	1952.9445	2	1	29	20	10	+	1931.6958	1	0	31	22	10	-	2084.3195		5
23	12	12	-	1480.9300	2	1	25	19	7	-	1811.8618	1	0	27	22	6	-	2012.3611	2	1	29	21	9	-	1988.5007	1	0	31	22	10	+	2083.5206	2	1
23	12	12	+	1480.5690	1	0	25	19	7	+	1811.1413	0	0	27	22	6	+	2011.4832	1	1	29	22	8	-	2047.1206	0	1	31	23	9	-	2145.4538	2	0
23	13	11	-	1515.9099		1	25	20	6	-	1865.3802		5	27	23	5	-	2073.4653	1	0	29	23	7	-	2108.2396	0	1	31	23	9	+	2144.5932		-1
23	13	11	+	1515.5021	2	0	25	20	6	+	1864.5931	2	0	27	23	5	+	2072.5171	2	0	29	23	7	+	2107.3384	1	0	31	24	8	-	2209.0611	1	1
23	14	10	-	1553.6035	1	0	25	21	5	+	1920.5928	1	0	27	24	4	-	2137.0403	2	3	29	24	6	-	2171.8299	1	1	31	24	8	+	2208.1360	1	1
23	14	10	+	1553.1452	0	0	25	22	4	-	1980.0425		4	27	24	4	+	2136.0189	2	1	29	24	6	+	2170.8604	1	2	31	25	7	-	2275.1120	3	-1
23	15	9	-	1593.9900	2	0	25	22	4	+	1979.1142		1	27	25	3	-	2203.0563		-5	29	25	5	-	2237.8630	5	-2	31	25	7	+	2274.1200	1	0
23	15	9	+	1593.4775	1	0	25	23	3	-	2041.1329		1	27	25	3	+	2201.9598	1	-1	29	25	5	+	2236.8226	1	1	31	26	6	-	2343.5785		0
23	16	8	-	1637.0476	1	0	25	24	2	-	2104.6931	1	-1	27	26	2	-	2271.4872	2	2	29	26	4	-	2306.3103		-4	31	26	6	+	2342.5170	0	0
23	16	8	+	1636.4771		-3	25	24	2	+	2103.6120		0	27	26	2	+	2270.3118		0	29	27	3	+	2375.9529		-1	31	27	5	-	2414.4312		3
23	17	7	-	1682.7536	1	-1	25	25	1	-	2170.6947		-2	27	27	1	-	2342.3016		1	29	27	3	-	2377.1432	3	-2	31	27	5	+	2413.2980		5
23	17	7	+	1682.1224	1	0	25	25	1	+	2169.5328		-1	27	27	1	+	2341.0453	2	-1	29	28	2	+	2449.0624		-3	32	0	32	-	1410.6558	0	0
23	18	6	-	1731.0848	2	-1	26	0	26	-	1311.1685	1	0	28	0	28	-	1342.1251	1	1	29	28	2	-	2450.3317	2	0	32	0	32	+	1410.6374	1	-1
23	18	6	+	1730.3889	2	-2	26	0	26	+	1311.1495	1	0	28	0	28	+	1342.1063	1	0	29	29	1	+	2524.4956		-4	32	1	31	-	1427.0804		-1

Table C.5 – Continued.

<i>N</i>	<i>K_a</i>	<i>K_c</i>	<i>J</i>	<i>E</i>	Δ	δ	<i>N</i>	<i>K_a</i>	<i>K_c</i>	<i>J</i>	<i>E</i>	Δ	δ	<i>N</i>	<i>K_a</i>	<i>K_c</i>	<i>J</i>	<i>E</i>	Δ	δ	<i>N</i>	<i>K_a</i>	<i>K_c</i>	<i>J</i>	<i>E</i>	Δ	δ								
<i>I</i>				2	3	4	<i>I</i>				2	3	4	<i>I</i>				2	3	4	<i>I</i>				2	3	4								
23	19	5	-	1782.0171	3	0	26	1	25	-	1324.1644			1	28	1	27	-	1356.2777	2	-1	30	0	30	-	1375.2878	1	1	32	1	31	+	1427.0153		0
23	19	5	+	1781.2533	2	0	26	1	25	+	1324.0979	1	1	28	1	27	+	1356.2120	1	1	30	0	30	+	1375.2691	1	-1	32	2	30	-	1441.3950	1	-2	
23	20	4	-	1835.5253	2	1	26	2	24	-	1334.4887	4	-2	28	2	26	-	1367.9819	3	0	30	1	29	-	1390.5815	1	-1	32	2	30	+	1441.2816	1	0	
23	20	4	+	1834.6902	1	0	26	2	24	+	1334.3723	1	4	28	2	26	+	1367.8660	3	3	30	1	29	+	1390.5161	1	0	32	3	29	-	1452.3066		0	
23	21	3	-	1891.5839		4	26	3	23	-	1341.5359		-1	28	3	25	-	1376.1310	3	-1	30	2	28	-	1403.6177		-2	32	3	29	+	1452.1415		0	
23	21	3	+	1890.6741		1	26	3	23	+	1341.3841	2	1	28	3	25	+	1375.9726		0	30	2	28	+	1403.5032		2	32	4	28	-	1460.1654	1	0	
23	22	2	-	1950.1655	2	0	26	4	22	-	1348.7689		0	28	4	24	-	1383.2747	2	0	30	3	27	-	1413.0825	2	0	32	4	28	+	1459.9738	0	0	
23	22	2	+	1949.1784		0	26	4	22	+	1348.6141	3	-1	28	4	24	+	1383.1070	0	0	30	3	27	+	1412.9196	2	0	32	5	27	-	1469.5771	1	0	
23	23	1	-	2011.2439		-2	26	5	21	-	1359.9862	5	-1	28	5	23	-	1393.8977	1	0	30	4	26	-	1420.4232		-1	32	5	27	+	1469.3907	1	0	
23	23	1	+	2010.1761		-1	26	5	21	+	1359.8332	2	-1	28	5	23	+	1393.7352		-1	30	4	26	+	1420.2430		0	32	6	26	-	1483.5800		0	
24	0	24	-	1282.4181	1	0	26	6	20	-	1375.0471	1	0	28	6	22	-	1408.7154	1	0	30	5	25	-	1430.4137	0	0	32	6	26	+	1483.3947	2	0	
24	0	24	+	1282.3988	1	-1	26	6	20	+	1374.8815	0	0	28	6	22	+	1408.5444	3	0	30	5	25	+	1430.2401	1	0	32	7	25	-	1501.3514	0	0	
24	1	23	-	1294.2338		-1	26	7	19	-	1393.1961	4	2	28	7	21	-	1426.7735		-5	30	6	24	-	1444.8867	3	3	32	7	25	+	1501.1542	1	1	
24	1	23	+	1294.1667	2	1	26	7	19	+	1393.0107		0	28	7	21	+	1426.5858	1	1	30	6	24	+	1444.7089	2	0	32	8	24	-	1522.2124		1	
24	2	22	-	1303.1617	2	-2	26	8	18	-	1414.2448	2	0	28	8	20	-	1447.7746	1	0	30	7	23	-	1462.8232	1	-1	32	8	24	+	1521.9972	2	0	
24	2	22	+	1303.0453	2	1	26	8	18	+	1414.0357	1	1	28	8	20	+	1447.5645	1	0	30	7	23	+	1462.6311	1	0	32	9	23	-	1545.9899	2	0	
24	3	21	-	1309.3781	2	0	26	9	17	-	1438.1356		0	28	9	19	-	1471.6361	1	1	30	8	22	-	1483.7625	0	1	32	9	23	+	1545.7530	1	0	
24	3	21	+	1309.2348		0	26	9	17	+	1437.8985	2	0	28	9	19	+	1471.4003	1	0	30	8	22	+	1483.5503	1	0	32	10	22	-	1572.6183		1	
24	4	20	-	1316.9266	1	-1	26	10	16	-	1464.8342		-3	28	10	18	-	1498.3170	0	0	30	9	21	-	1507.5867	1	1	32	10	22	+	1572.3563	2	1	
24	4	20	+	1316.7847	2	1	26	10	16	+	1464.5659	2	-1	28	10	18	+	1498.0522	1	0	30	9	21	+	1507.3509	1	0	32	11	21	-	1602.0568	0	0	
24	5	19	-	1328.6385	0	0	26	11	15	-	1494.3159	3	-1	28	11	17	-	1527.7879	2	0	30	10	20	-	1534.2443	1	0	32	11	21	+	1601.7667	1	0	
24	5	19	+	1328.4931	1	0	26	11	15	+	1494.0125	1	0	28	12	16	-	1560.0239		0	30	10	20	+	1533.9815	1	-1	32	12	20	-	1634.2746	1	0	
24	6	18	-	1343.8670		0	26	12	14	-	1526.5573	3	-1	28	12	16	+	1559.6910	1	0	30	11	19	-	1563.7011	1	0	32	12	20	+	1633.9533	2	-1	
24	6	18	+	1343.7056	2	-1	26	12	14	+	1526.2156		1	28	13	15	-	1595.0023		0	30	11	19	+	1563.4083	1	0	32	13	19	-	1669.2449	2	-1	
24	7	17	-	1362.0831	1	0	26	13	13	-	1561.5372	0	0	28	13	15	+	1594.6306		0	30	12	18	-	1595.9294	2	-1	32	13	19	+	1668.8900	2	2	
24	7	17	+	1361.8997	2	0	26	13	13	+	1561.1535	1	-1	28	14	14	-	1632.7009	1	0	30	12	18	+	1595.6034	2	0	32	14	18	-	1706.9432	2	-1	
24	8	16	-	1383.1694	1	0	26	14	12	-	1599.2343	1	0	28	14	14	+	1632.2872	2	0	30	13	17	-	1630.9048		-1	32	14	18	+	1706.5514	2	0	
24	8	16	+	1382.9597	1	0	26	14	12	+	1598.8058	0	2	28	15	13	-	1673.0973	0	-1	30	13	17	+	1630.5426	1	1	32	15	17	-	1747.3456		-2	
24	9	15	-	1407.0829		1	26	15	11	-	1639.6272		3	28	15	13	+	1672.6388	1	0	30	14	16	-	1668.6039	1	-1	32	15	17	+	1746.9146	2	2	

Table C.5 – Continued.

<i>N</i>	<i>K_a</i>	<i>K_c</i>	<i>J</i>	<i>E</i>	Δ	δ	<i>N</i>	<i>K_a</i>	<i>K_c</i>	<i>J</i>	<i>E</i>	Δ	δ	<i>N</i>	<i>K_a</i>	<i>K_c</i>	<i>J</i>	<i>E</i>	Δ	δ	<i>N</i>	<i>K_a</i>	<i>K_c</i>	<i>J</i>	<i>E</i>	Δ	δ							
<i>I</i>				2	3	4	<i>I</i>				2	3	4	<i>I</i>				2	3	4	<i>I</i>				2	3	4							
24	9	15	+	1406.8432		5	26	15	11	+	1639.1498	1	-2	28	16	12	-	1716.1693		1	30	14	16	+	1668.2026	3	2	32	16	16	-	1790.4286		-1
24	10	14	-	1433.7955	2	0	26	16	10	-	1682.6929	0	0	28	16	12	+	1715.6625		-1	30	15	15	-	1709.0038		0	32	16	16	+	1789.9550	6	0
24	10	14	+	1433.5213	2	1	26	16	10	+	1682.1645	1	0	28	17	11	-	1761.8932	1	0	30	15	15	+	1708.5600	1	-2	32	17	15	-	1836.1679	4	1
24	11	13	-	1463.2846	0	0	26	17	9	-	1728.4096		1	28	17	11	+	1761.3357	0	1	30	16	14	-	1752.0814	2	0	32	17	15	+	1835.6494	3	1
24	11	13	+	1462.9725	1	1	26	17	9	+	1727.8265	1	0	28	18	10	-	1810.2452	2	-3	30	16	14	+	1751.5928	1	0	32	19	13	-	1935.5169		1
24	12	12	-	1495.5295	2	1	26	18	8	-	1776.7529	1	0	28	18	10	+	1809.6339	2	-1	30	17	13	-	1797.8130	1	0	32	19	13	+	1934.9004	1	-1
24	12	12	+	1495.1757	3	0	26	18	8	+	1776.1121	1	-1	28	19	9	-	1861.2014	0	-1	30	17	13	+	1797.2766	1	0	32	20	12	-	1989.0759	3	0
24	13	11	-	1530.5096	1	0	26	19	7	-	1827.6988	0	0	28	19	9	+	1860.5331	3	-1	30	18	12	-	1846.1743	2	-2	32	20	12	+	1988.4069	3	0
24	13	11	+	1530.1109	2	1	26	19	7	+	1826.9973		0	28	20	8	-	1914.7359	1	-1	30	18	12	+	1845.5877	5	0	32	21	11	-	2045.1903		3
24	14	10	-	1568.2045	0	0	26	20	6	-	1881.2221	2	0	28	20	8	+	1914.0081	1	1	30	19	11	-	1897.1412	1	-1	32	21	11	+	2044.4655		-2
24	14	10	+	1567.7572	0	1	26	20	6	+	1880.4567	1	0	28	21	7	-	1970.8231		1	30	19	11	+	1896.5009	1	-2	32	22	10	-	2103.8325	1	2
24	15	9	-	1608.5930	1	0	26	21	5	-	1937.2967	2	0	28	21	7	+	1970.0326	1	1	30	20	10	-	1950.6877		0	32	22	10	+	2103.0503	0	0
24	15	9	+	1608.0936	1	0	26	21	5	+	1936.4646	1	1	28	22	6	-	2029.4358		0	30	20	10	+	1949.9914	4	-2	32	23	9	-	2164.9758	4	3
24	16	8	-	1651.6532	1	-1	26	22	4	-	1995.8963	2	0	28	22	6	+	2028.5801	1	0	30	21	9	-	2006.7879		0	32	23	9	+	2164.1330		-1
24	16	8	+	1651.0986	0	1	26	22	4	+	1994.9945	0	1	28	23	5	-	2090.5470		-3	30	21	9	+	2006.0330		0	32	24	8	-	2228.5914		-1
32	24	8	+	2227.6867		3	34	23	11	-	2205.8467	3	0	37	5	33	-	1575.5605	1	1	39	16	24	-	1943.8121	3	2	42	10	32	-	1801.2569	1	0
32	25	7	-	2294.6520		0	34	23	11	+	2205.0370	3	-1	37	5	33	+	1575.3784	1	-1	39	16	24	+	1943.3726		2	42	10	32	+	1800.9838	1	0
32	25	7	+	2293.6819	1	1	34	24	10	-	2269.4813	3	1	37	6	32	-	1590.8548	2	2	39	17	23	-	1989.5745		1	42	11	31	-	1830.5141	1	0
32	26	6	-	2363.1281		-1	34	24	10	+	2268.6124	1	2	37	6	32	+	1590.6547		-1	39	18	22	-	2037.9781	1	1	42	11	31	+	1830.2208	1	0
32	26	6	+	2362.0904		-1	34	27	7	-	2474.9427		-1	37	7	31	-	1608.5105	5	0	39	18	22	+	2037.4620	3	-2	42	12	30	-	1862.6158	1	-1
32	27	5	-	2433.9912		2	34	27	7	+	2473.8823		2	37	7	31	+	1608.2983	1	0	39	19	21	-	2088.9964	3	1	42	12	30	+	1862.2997	2	-1
32	27	5	+	2432.8836		1	35	1	35	-	1467.8422	0	1	37	8	30	-	1629.1356	1	-1	39	20	20	+	2142.0015		-2	42	13	29	-	1897.5167	1	-1
32	29	3	+	2581.5039		0	35	1	35	+	1467.8240	1	0	37	8	30	+	1628.9093	2	0	39	21	19	-	2198.7699	1	-3	42	13	29	+	1897.1754		0
32	31	1	-	2740.7147		2	35	2	34	-	1485.9608	1	0	37	9	29	-	1652.7481		0	39	21	19	+	2198.1232	2	-2	42	14	28	-	1935.1802		-1
32	31	1	+	2739.3054		1	35	2	34	+	1485.8961	1	0	37	9	29	+	1652.5041	1	0	39	22	18	-	2257.4712		-3	42	14	28	+	1934.8113		1
33	1	33	-	1429.1673	1	1	35	3	33	-	1502.2870	3	-2	37	10	28	-	1679.2693	1	0	39	23	17	-	2318.6785		-2	42	15	27	-	1975.5747	3	1
33	1	33	+	1429.1489	0	-1	35	3	33	+	1502.1777	3	1	37	10	28	+	1679.0044	0	0	39	24	16	-	2382.3633		-1	42	15	27	+	1975.1755	2	0
33	2	32	-	1446.1728	0	0	35	4	32	-	1516.9096	2	0	37	11	27	-	1708.6391	1	1	39	24	16	+	2381.5660		-2	42	16	26	-	2018.6704	2	0
33	2	32	+	1446.1081	1	0	35	4	32	+	1516.7605	2	0	37	11	27	+	1708.3503	1	0	39	25	15	+	2447.6460	4	4	42	16	26	+	2018.2395	1	3

Table C.5 – Continued.

<i>N</i>	<i>K_a</i>	<i>K_c</i>	<i>J</i>	<i>E</i>	Δ	δ	<i>N</i>	<i>K_a</i>	<i>K_c</i>	<i>J</i>	<i>E</i>	Δ	δ	<i>N</i>	<i>K_a</i>	<i>K_c</i>	<i>J</i>	<i>E</i>	Δ	δ	<i>N</i>	<i>K_a</i>	<i>K_c</i>	<i>J</i>	<i>E</i>	Δ	δ							
<i>I</i>				2	3	4	<i>I</i>				2	3	4	<i>I</i>				2	3	4	<i>I</i>				2	3	4							
33	3	31	-	1461.4029	1	0	35	5	31	-	1530.8666	1	1	37	12	26	-	1740.8142	1	0	39	26	14	-	2517.0509	1	0	42	23	19	+	2392.9596		-3
33	3	31	+	1461.2941		2	35	5	31	+	1530.6899	5	1	37	12	26	+	1740.4991	1	1	40	0	40	-	1574.1683	0	0	42	21	21	+	2273.0855	3	-2
33	4	30	-	1475.1037	1	0	35	6	30	-	1546.0264	3	2	37	13	25	-	1775.7608	1	-1	40	0	40	+	1574.1502	0	-1	42	24	18	-	2457.3924	3	0
33	4	30	+	1474.9573	1	-1	35	6	30	+	1545.8335	4	0	37	13	25	+	1775.4164		0	40	1	39	+	1595.0011	1	1	42	24	18	+	2456.6285		0
33	5	29	-	1488.5742	3	1	35	7	29	-	1563.7773	1	1	37	14	24	-	1813.4496	1	-1	40	1	39	-	1595.0658	1	1	43	1	43	-	1644.5684	0	0
33	5	29	+	1488.4032		-1	35	7	29	+	1563.5715	1	-1	37	14	24	+	1813.0736	1	1	40	2	38	+	1614.0178	2	0	43	1	43	+	1644.5503	0	-1
33	6	28	-	1503.6778	1	0	35	8	28	-	1584.5117	2	-1	37	15	23	-	1853.8537	3	2	40	2	38	-	1614.1287	3	-1	43	2	42	-	1667.1336	0	1
33	6	28	+	1503.4923	3	2	35	8	28	+	1584.2905	3	0	37	15	23	+	1853.4433	0	1	40	3	37	+	1630.6129	3	0	43	2	42	+	1667.0688	1	0
33	7	27	-	1521.5321	1	0	35	9	27	-	1608.1999	1	0	37	16	22	-	1896.9466	0	0	40	3	37	-	1630.7735	2	0	43	3	41	-	1687.9226	1	-1
33	7	27	+	1521.3323	1	0	35	9	27	+	1607.9594		0	37	16	22	+	1896.4999	1	3	40	4	36	+	1643.3122	1	0	43	3	41	+	1687.8125	0	2
33	8	26	-	1542.3610	4	-2	35	10	26	-	1634.7704	1	-1	37	19	19	+	2041.5337	3	0	40	4	36	-	1643.5265	1	-1	43	4	40	-	1706.7523	5	2
33	8	26	+	1542.1443	3	1	35	10	26	+	1634.5075	2	0	37	20	18	+	2095.0803	1	0	40	5	35	-	1652.9613		-1	43	4	40	+	1706.5976	4	3
33	9	25	-	1566.1120		-1	35	11	25	-	1664.1722	2	0	37	21	17	-	2151.8489		0	40	5	35	+	1652.7213		1	43	5	39	-	1723.7601	4	0
33	9	25	+	1565.8742	1	0	35	11	25	+	1663.8838	0	0	37	21	17	+	2151.1840	2	2	40	6	34	+	1663.9877	0	0	43	5	39	+	1723.5666	3	0
33	10	24	-	1592.7232	0	0	35	12	24	-	1696.3676	3	0	37	22	16	+	2209.8170	4	0	40	6	34	-	1664.2190		0	43	6	38	-	1740.0835		0
33	10	24	+	1592.4611	0	0	35	12	24	+	1696.0509	2	0	37	23	15	-	2271.7205		0	40	7	33	+	1680.2491		0	43	6	38	+	1739.8633	2	-2
33	11	23	-	1622.1510	1	1	35	13	23	-	1731.3260		0	37	23	15	+	2270.9522		0	40	7	33	-	1680.4758	1	1	43	7	37	-	1757.6581	2	1
33	11	23	+	1621.8616	2	0	35	13	23	+	1730.9783	0	0	37	24	14	-	2335.3842		-4	40	8	32	-	1700.7358	0	0	43	7	37	+	1757.4233	3	-1
33	12	22	-	1654.3621	1	0	35	14	22	-	1769.0201	2	0	37	24	14	+	2334.5614		0	40	8	32	+	1700.5001		-1	43	8	36	-	1777.8955	0	0
33	12	22	+	1654.0428	1	0	35	14	22	+	1768.6388		-1	37	25	13	-	2401.4961		0	40	9	31	-	1724.1922		1	43	8	36	+	1777.6499		-2
33	13	21	-	1689.3291	1	-1	35	15	21	-	1809.4245	1	0	37	25	13	+	2400.6159		0	40	9	31	+	1723.9417		2	43	9	35	-	1801.1908		0
33	13	21	+	1688.9769	0	0	35	15	21	+	1809.0072		1	37	27	11	-	2540.9460		1	40	10	30	+	1750.3497	0	-1	43	9	35	+	1800.9321		0
33	14	20	-	1727.0265		-1	35	16	20	-	1852.5141	0	-1	37	26	12	+	2469.0869	2	0	40	10	30	-	1750.6190	1	0	43	10	34	-	1827.4980	3	-1
33	14	20	+	1726.6387	0	0	35	16	20	+	1852.0581	1	0	38	0	38	-	1529.9860	0	0	40	11	29	-	1779.9274	1	0	43	10	34	+	1827.2229	1	0
33	15	19	-	1767.4298		-2	35	19	17	-	1997.6444	3	-2	38	0	38	+	1529.9679	1	-1	40	11	29	+	1779.6366	1	0	43	11	33	-	1856.7264	1	1
33	15	19	+	1767.0037	3	-1	35	19	17	+	1997.0576	1	-1	38	1	37	-	1549.7698	0	0	40	12	28	-	1812.0630	2	0	43	11	33	+	1856.4317	1	1
33	16	18	-	1810.5152	2	-1	35	20	16	-	2051.2235		-1	38	1	37	+	1549.7051	0	0	40	12	28	+	1811.7479		0	43	12	32	-	1888.8088	1	0
33	16	18	+	1810.0482		1	35	20	16	+	2050.5880		-2	38	2	36	-	1567.6809	2	-2	40	13	27	-	1846.9853	1	0	43	12	32	+	1888.4919	1	0
33	17	17	-	1856.2583	3	1	35	21	15	-	2107.3599	3	0	38	2	36	+	1567.5699	1	1	40	13	27	+	1846.6435	1	0	43	13	31	-	1923.6972	1	-1

Table C.5 – Continued.

<i>N</i>	<i>K_a</i>	<i>K_c</i>	<i>J</i>	<i>E</i>	Δ	δ	<i>N</i>	<i>K_a</i>	<i>K_c</i>	<i>J</i>	<i>E</i>	Δ	δ	<i>N</i>	<i>K_a</i>	<i>K_c</i>	<i>J</i>	<i>E</i>	Δ	δ	<i>N</i>	<i>K_a</i>	<i>K_c</i>	<i>J</i>	<i>E</i>	Δ	δ	<i>N</i>	<i>K_a</i>	<i>K_c</i>	<i>J</i>	<i>E</i>	Δ	δ	
<i>I</i>				2	3	4	<i>I</i>				2	3	4	<i>I</i>				2	3	4	<i>I</i>				2	3	4	<i>I</i>				2	3	4	
33	17	17	+	1855.7475			1	35	21	15	+	2106.6737	2	0	38	3	35	-	1582.9760	3	-1	40	14	26	-	1884.6612	1	0	43	13	31	+	1923.3558	1	0
33	19	15	-	1955.6174	1	-2	35	22	14	-	2166.0265	1	-1	38	3	35	+	1582.8140		2	40	14	26	+	1884.2901	1	0	43	14	30	-	1961.3533	3	1	
33	19	15	+	1955.0119	2	0	35	22	14	+	2165.2871	0	0	38	4	34	-	1594.2024		2	40	15	25	-	1925.0609		0	43	14	30	+	1960.9848	0	0	
33	20	14	-	2009.1832		0	35	23	13	-	2227.1960		1	38	4	34	+	1593.9900	3	2	40	15	25	+	1924.6584		1	43	15	29	-	2001.7438	1	0	
33	20	14	+	2008.5263	1	0	35	23	13	+	2226.4011		1	38	5	33	-	1603.1511	1	-1	40	16	24	-	1968.1568	1	0	43	15	29	+	2001.3464	3	2	
33	21	13	-	2065.3050	5	4	35	24	12	-	2290.8403	3	2	38	6	32	-	1615.1004	1	-1	40	16	24	+	1967.7204	3	0	43	16	28	-	2044.8391	1	2	
33	21	13	+	2064.5940		0	35	25	11	-	2356.9306	3	2	38	6	32	+	1614.8831	0	0	41	1	41	-	1597.0850	0	0	43	16	28	+	2044.4105	1	6	
33	22	12	-	2123.9551	3	2	35	25	11	+	2356.0178	1	1	38	7	31	-	1631.9116		0	41	1	41	+	1597.0669	0	-1	43	20	24	-	2243.7038		-3	
33	22	12	+	2123.1880	3	0	35	26	10	-	2425.4385	3	4	38	7	31	+	1631.6939		0	41	2	40	-	1618.5400	0	0	43	23	21	-	2419.8886	1	-3	
33	23	11	-	2185.1065		0	35	26	10	+	2424.4631	3	0	38	8	30	-	1652.3841	1	0	41	2	40	+	1618.4753	0	0	43	23	21	+	2419.1821	1	-2	
33	23	11	+	2184.2811	1	0	35	27	9	+	2495.2946		0	38	8	30	+	1652.1548	1	1	41	3	39	-	1638.2097		-1	43	24	20	-	2483.6172	3	-2	
33	24	10	-	2248.7317	0	1	35	29	7	-	2645.1723		3	38	9	29	-	1675.9464	1	1	41	3	39	+	1638.0996		1	43	24	20	+	2482.8629		-3	
33	24	10	+	2247.8452		0	35	29	7	+	2643.9972	1	-1	38	9	29	+	1675.7002		0	41	4	38	-	1655.9385	2	3	43	25	19	+	2548.9943	2	0	
33	25	9	-	2314.8021		3	36	0	36	-	1488.0059	1	0	38	10	28	-	1702.4386	1	-1	41	4	38	+	1655.7840	1	-2	43	26	18	-	2618.4017		0	
33	25	9	+	2313.8521		0	36	0	36	+	1487.9877	0	-1	38	10	28	+	1702.1725	1	0	41	5	37	-	1672.0374	2	1	44	0	44	-	1669.1350	0	0	
33	26	8	-	2383.2885		3	36	1	35	-	1506.6736	1	-1	38	11	27	-	1731.7899	2	0	41	5	37	+	1671.8469	2	0	44	0	44	+	1669.1169	0	0	
33	26	8	+	2382.2730		2	36	1	35	+	1506.6089	1	0	38	11	27	+	1731.5007	2	0	41	6	36	-	1687.9024	1	1	44	1	43	-	1692.2541	1	0	
33	27	7	-	2454.1618		1	36	2	34	-	1523.4151		-2	38	12	26	-	1763.9532	2	0	41	6	36	+	1687.6885	3	-1	44	1	43	+	1692.1894	0	0	
33	27	7	+	2453.0782		-1	36	2	34	+	1523.3036	1	2	38	12	26	+	1763.6382	1	0	41	7	35	-	1705.4517	1	1	44	2	42	-	1713.5874	2	0	
33	29	5	-	2602.9515		-1	36	3	33	-	1537.2936		1	38	13	25	-	1798.8927	1	0	41	8	34	-	1725.8228	0	0	44	2	42	+	1713.4769	1	2	
33	28	6	+	2526.2390		-2	36	3	33	+	1537.1295	3	0	38	13	25	+	1798.5494	0	0	41	8	34	+	1725.5842	1	-1	44	3	41	-	1732.7610	1	0	
33	30	4	-	2680.8084		0	36	4	32	-	1547.1405		-1	38	14	24	-	1836.5779	2	0	41	9	33	-	1749.2397		1	44	3	41	+	1732.6029	3	0	
33	31	3	-	2760.9330		-3	36	4	32	+	1546.9327	1	0	38	14	24	+	1836.2037	2	0	41	9	33	+	1748.9863	4	-2	44	4	40	-	1748.6612	3	0	
33	31	3	+	2759.5563		1	36	5	31	-	1555.9531	2	0	38	15	23	-	1876.9808	0	-1	41	10	32	-	1775.6305	0	0	44	4	40	+	1748.4489	3	-1	
34	0	34	-	1448.2288	1	0	36	5	31	+	1555.7385	0	1	38	15	23	+	1876.5736	2	1	41	10	32	+	1775.3595	1	0	44	5	39	-	1760.1040		0	
34	0	34	+	1448.2106	1	-1	36	6	30	-	1568.6492	1	0	38	16	22	-	1920.0752	0	0	41	11	31	-	1804.9145	1	0	44	5	39	+	1759.8463		0	
34	1	33	-	1465.7773	1	-1	36	6	30	+	1568.4441	1	0	38	16	22	+	1919.6322	1	1	41	11	31	+	1804.6224		-2	44	6	38	-	1770.5628	1	-1	
34	1	33	+	1465.7124	0	0	36	7	29	-	1585.8822		0	38	19	19	+	2064.6826	5	-1	41	12	30	-	1837.0339	0	-1	44	6	38	+	1770.3012	1	0	
34	2	32	-	1481.3235	2	0	36	7	29	+	1585.6722		0	38	20	18	+	2118.2373	3	-1	41	12	30	+	1836.7185	1	0	44	7	37	-	1785.3238	1	1	

Table C.5 – Continued.

<i>N</i>	<i>K_a</i>	<i>K_c</i>	<i>J</i>	<i>E</i>	Δ	δ	<i>N</i>	<i>K_a</i>	<i>K_c</i>	<i>J</i>	<i>E</i>	Δ	δ	<i>N</i>	<i>K_a</i>	<i>K_c</i>	<i>J</i>	<i>E</i>	Δ	δ	<i>N</i>	<i>K_a</i>	<i>K_c</i>	<i>J</i>	<i>E</i>	Δ	δ								
<i>I</i>				2	3	4	<i>I</i>				2	3	4	<i>I</i>				2	3	4	<i>I</i>				2	3	4								
34	2	32	+	1481.2110			1	36	8	28	-	1606.5176	3	0	38	21	17	+	2174.3499	3	-1	41	13	29	-	1871.9462	2	0	44	7	37	+	1785.0754	1	1
34	3	31	-	1493.7282	2	0	36	8	28	+	1606.2938	2	1	38	22	16	+	2232.9932		0	41	13	29	+	1871.6047	1	0	44	8	36	-	1804.9334	1	1	
34	3	31	+	1493.5631	2	1	36	9	27	-	1630.1665		1	38	23	15	-	2294.8953		-2	41	14	28	-	1909.6162	0	-1	44	8	36	+	1804.6826	2	-4	
34	4	30	-	1502.4317		0	36	9	27	+	1629.9242	1	0	38	23	15	+	2294.1395	4	2	41	14	28	+	1909.2464	2	0	44	9	35	-	1828.0996		0	
34	4	30	+	1502.2309	1	0	36	10	26	-	1656.7133	0	0	38	24	14	-	2358.5697	3	-1	41	15	27	-	1950.0136	1	0	44	9	35	+	1827.8378		0	
34	5	29	-	1511.4204	2	-2	36	10	26	+	1656.4495	2	0	38	24	14	+	2357.7601		1	41	15	27	+	1949.6130	1	1	44	10	34	-	1854.3547		-3	
34	5	29	+	1511.2202	1	0	36	11	25	-	1686.0999	1	0	39	1	39	-	1551.8021	1	0	41	16	26	-	1993.1095	3	-1	44	10	34	+	1854.0777		2	
34	6	28	-	1524.8228	2	0	36	11	25	+	1685.8114	2	0	39	1	39	+	1551.7839	0	-1	41	16	26	+	1992.6758	3	-2	44	11	33	-	1883.5514	2	0	
34	6	28	+	1524.6283	2	-1	36	12	24	-	1718.2857	0	0	39	2	38	-	1572.1459	1	1	41	20	22	+	2191.3514		-1	44	11	33	+	1883.2549		-2	
34	7	27	-	1542.3673	1	1	36	12	24	+	1717.9698	1	-1	39	2	38	+	1572.0812	0	0	41	21	21	-	2248.1222		-2	44	12	32	-	1915.6128		0	
34	7	27	+	1542.1639	1	-1	36	13	23	-	1753.2386	0	-1	39	3	37	-	1590.6969	2	-1	41	21	21	+	2247.4914		0	44	12	32	+	1915.2952	1	2	
34	8	26	-	1563.1291		1	36	13	23	+	1752.8928	1	0	39	3	37	+	1590.5869	1	2	41	22	20	-	2306.8417	5	0	44	13	31	-	1950.4875	0	0	
34	8	26	+	1562.9099	1	0	36	14	22	-	1790.9304		0	39	4	36	-	1607.3485	3	0	41	22	20	+	2306.1649	2	0	44	13	31	+	1950.1455		-3	
34	9	25	-	1586.8488	1	0	36	14	22	+	1790.5519	1	0	39	4	36	+	1607.1951	1	1	41	23	19	-	2368.0687	2	0	44	14	30	-	1988.1351	1	0	
34	9	25	+	1586.6097	1	1	36	15	21	-	1831.3347	2	0	39	5	35	-	1622.6273	1	-1	41	23	19	+	2367.3441		0	44	14	30	+	1987.7671	1	0	
34	10	24	-	1613.4405	0	0	36	15	21	+	1830.9212	1	1	39	5	35	+	1622.4407	0	-2	41	24	18	-	2431.7748		-2	44	15	29	-	2028.5214		1	
34	10	24	+	1613.1781	2	0	36	16	20	-	1874.4262	1	0	39	6	34	-	1638.1523	2	2	41	24	18	+	2431.0005	4	-1	44	15	29	+	2028.1252		4	
34	11	23	-	1642.8560		0	36	16	20	+	1873.9750	2	1	39	6	34	+	1637.9450	3	-2	41	25	17	+	2497.1057		1	44	16	28	-	2071.6155	3	2	
34	11	23	+	1642.5672	5	0	36	19	17	+	2018.9919	2	-1	39	7	33	-	1655.7350	3	0	42	0	42	-	1620.5517	1	0	44	16	28	+	2071.1886	1	5	
34	12	22	-	1675.0600		2	36	20	16	-	2073.1561	3	-2	39	7	33	+	1655.5157	1	0	42	0	42	+	1620.5336	1	-1	45	1	45	-	1694.2513	0	0	
34	12	22	+	1674.7420	2	1	36	20	16	+	2072.5303		-2	39	8	32	-	1676.2378	1	0	42	1	41	-	1642.5608	0	1	45	1	45	+	1694.2331	1	0	
34	13	21	-	1710.0227	2	-1	36	21	15	-	2129.3001	4	-2	39	8	32	+	1676.0056	1	0	42	1	41	+	1642.4960	0	0	45	2	44	-	1717.9253	0	0	
34	13	21	+	1709.6730		-1	36	21	15	+	2128.6251	3	1	39	9	31	-	1699.7601		0	42	2	40	-	1662.7633	3	0	45	2	44	+	1717.8606	0	0	
34	14	20	-	1747.7188	3	-1	36	22	14	-	2187.9753		-1	39	9	31	+	1699.5118		0	42	2	40	+	1662.6526	1	1	45	3	43	-	1739.8330	3	0	
34	14	20	+	1747.3345	1	0	36	23	13	-	2249.1539		0	39	10	30	-	1726.2219	2	1	42	3	39	-	1680.6967	3	0	45	3	43	+	1739.7227		1	
34	15	19	-	1788.1229	1	0	36	23	13	+	2248.3729	1	1	39	10	30	+	1725.9542	1	0	42	3	39	+	1680.5375	2	-1	45	4	42	-	1759.7782	6	0	
34	15	19	+	1787.7014	1	0	36	24	12	-	2312.8080		1	39	11	29	-	1755.5527	2	1	42	4	38	-	1695.0327	1	0	45	4	42	+	1759.6231		0	
34	16	18	-	1831.2105	0	0	36	24	12	+	2311.9706	1	1	39	11	29	+	1755.2626	0	-1	42	4	38	+	1694.8186	4	1	45	5	41	-	1777.7678	3	2	
34	16	18	+	1830.7491	1	0	37	1	37	-	1508.7208	1	0	39	12	28	-	1787.7028		0	42	5	37	+	1705.0585	1	0	45	5	41	+	1777.5718	5	2	

Table C.5 – Continued.

<i>N</i>	<i>K_a</i>	<i>K_c</i>	<i>J</i>	<i>E</i>	Δ	δ	<i>N</i>	<i>K_a</i>	<i>K_c</i>	<i>J</i>	<i>E</i>	Δ	δ	<i>N</i>	<i>K_a</i>	<i>K_c</i>	<i>J</i>	<i>E</i>	Δ	δ	<i>N</i>	<i>K_a</i>	<i>K_c</i>	<i>J</i>	<i>E</i>	Δ	δ	<i>N</i>	<i>K_a</i>	<i>K_c</i>	<i>J</i>	<i>E</i>	Δ	δ
<i>I</i>				2	3	4	<i>I</i>				2	3	4	<i>I</i>				2	3	4	<i>I</i>				2	3	4	<i>I</i>				2	3	4
34	17	17	-	1876.9571	1	1	37	1	37	+	1508.7026	0	-1	39	12	28	+	1787.3878	1	0	42	6	36	-	1716.0369	3	-1	45	6	40	-	1794.6695	3	1
34	19	15	-	1976.3267	1	-2	37	2	36	-	1527.9523	0	0	39	13	27	-	1822.6342	2	0	42	6	36	+	1715.7906	1	0	45	6	40	+	1794.4436	1	-1
34	19	15	+	1975.7306		-4	37	2	36	+	1527.8877	0	1	39	13	27	+	1822.2918	2	1	42	7	35	-	1731.6016	2	0	45	7	39	-	1812.3477	0	3
34	21	13	-	2086.0279	1	-1	37	3	35	-	1545.3878	4	1	39	14	26	-	1860.3150	1	-1	42	8	34	-	1751.5818	1	1	45	7	39	+	1812.1051	3	-1
34	21	13	+	2085.3299	1	-1	37	3	35	+	1545.2777	1	0	39	14	26	+	1859.9428	3	2	42	8	34	+	1751.3391	3	0	45	8	38	-	1832.4595		1
34	22	12	-	2144.6867		4	37	4	34	-	1560.9991	2	0	39	15	25	-	1900.7167	1	0	42	9	33	-	1774.9081	2	-2	45	8	38	+	1832.2067		-1
34	22	12	+	2143.9335		-2	37	4	34	+	1560.8478	2	0	39	15	25	+	1900.3118	2	0	42	9	33	+	1774.6522	2	-2	45	9	37	-	1855.6177		1
45	9	37	+	1855.3529		0	48	15	33	+	2141.3189	2	4	52	10	42	-	2091.4158		-2	56	7	49	-	2163.9251	1	-1	60	8	52	-	2324.8998	3	0
45	10	36	-	1881.8270	1	-1	48	16	32	-	2184.7963	3	0	52	10	42	+	2091.1152	3	-3	56	7	49	+	2163.5881	2	1	60	8	52	+	2324.5453	4	-1
45	10	36	+	1881.5471		-2	49	1	49	-	1800.2100	0	-1	52	11	41	-	2120.2453		-1	56	8	48	-	2178.9191	3	-1	60	9	51	+	2343.5243	0	1
45	11	35	-	1910.9896	1	0	49	1	49	+	1800.1918	0	0	52	11	41	+	2119.9312	2	0	56	8	48	+	2178.5982	5	1	60	10	50	-	2368.1803	5	-1
45	11	35	+	1910.6914	1	-1	49	2	48	-	1826.0985	0	1	52	12	40	-	2152.0611	1	-1	56	9	47	-	2199.6657	3	3	60	10	50	+	2367.8491	3	-4
45	12	34	-	1943.0282	1	1	49	2	48	+	1826.0338	1	0	52	12	40	+	2151.7303	1	0	56	9	47	+	2199.3553	3	2	60	11	49	-	2396.3233		1
45	12	34	+	1942.7090		-2	49	3	47	-	1850.2378	3	-1	52	13	39	-	2186.7709		3	56	10	46	-	2224.8082		-2	60	11	49	+	2395.9848	4	-1
45	13	33	-	1977.8877	1	0	49	3	47	+	1850.1278	1	0	52	13	39	+	2186.4204	2	-1	56	10	46	+	2224.4936	1	0	60	12	48	+	2427.3526	1	0
45	13	33	+	1977.5455	0	0	49	4	46	+	1872.2789		-1	52	14	38	-	2224.3104	0	1	56	11	45	+	2253.0243	3	-1	60	13	47	-	2462.1148	4	1
45	14	32	-	2015.5259	3	0	49	5	45	-	1892.5386	2	-2	52	14	38	+	2223.9393	2	4	56	12	44	-	2284.9777	2	2	60	13	47	+	2461.7497	1	1
45	14	32	+	2015.1582	1	1	49	5	45	+	1892.3398	2	-2	52	15	37	-	2264.6321		5	56	12	44	+	2284.6374	1	-1	60	14	46	-	2499.4503	1	2
45	15	31	-	2055.9073	3	2	49	6	44	-	1910.9363	6	0	52	15	37	+	2264.2371		3	56	13	43	-	2319.5580	3	-1	61	1	61	-	2170.7326	1	0
45	15	31	+	2055.5115	3	1	49	6	44	+	1910.7017	1	0	53	1	53	-	1914.9509	1	0	56	13	43	+	2319.2013	2	2	61	1	61	+	2170.7146	2	0
45	16	30	-	2098.9996	2	3	49	7	43	-	1929.1230	2	1	53	1	53	+	1914.9326	1	0	56	14	42	-	2357.0102	3	1	61	2	60	-	2203.2350		3
45	16	30	+	2098.5734		-3	49	7	43	+	1928.8657		-3	53	2	52	-	1943.0488	2	0	56	14	42	+	2356.6342	2	4	61	2	60	+	2203.1733		-1
46	0	46	-	1719.9170	0	0	49	8	42	-	1949.0677	1	1	53	2	52	+	1942.9846	1	0	57	1	57	-	2038.4627	2	1	61	3	59	+	2233.9136		1
46	0	46	+	1719.8989	1	0	49	8	42	+	1948.7986		0	53	3	51	-	1969.4117	3	0	57	1	57	+	2038.4443		1	61	4	58	-	2262.9429		-2
46	1	45	-	1744.1448	1	1	49	9	41	+	1971.6372		1	53	3	51	+	1969.3023	1	0	57	2	56	-	2068.7651	3	0	61	4	58	+	2262.7932	3	-2
46	1	45	+	1744.0801	1	1	49	10	40	-	1997.8823	2	0	53	4	50	-	1993.8616	2	-1	57	2	56	+	2068.7017	0	-2	61	5	57	-	2289.8138		0
46	2	44	-	1766.6024	1	-1	49	10	40	+	1997.5913	4	-1	53	4	50	+	1993.7070	2	-1	57	3	55	+	2097.2351		2	61	5	57	+	2289.6183	1	-3
46	2	44	+	1766.4921	0	1	49	11	39	-	2026.8783	1	-1	53	5	49	+	2015.9945		-3	57	4	54	-	2124.0368		3	61	7	55	-	2336.8657		0
46	3	43	-	1786.9802	1	1	49	11	39	+	2026.5719		0	53	6	48	+	2036.2172	1	-1	57	4	54	+	2123.8838		1	61	7	55	+	2336.5839	3	2

Table C.5 – Continued.

<i>N</i>	<i>K_a</i>	<i>K_c</i>	<i>J</i>	<i>E</i>	Δ	δ	<i>N</i>	<i>K_a</i>	<i>K_c</i>	<i>J</i>	<i>E</i>	Δ	δ	<i>N</i>	<i>K_a</i>	<i>K_c</i>	<i>J</i>	<i>E</i>	Δ	δ	<i>N</i>	<i>K_a</i>	<i>K_c</i>	<i>J</i>	<i>E</i>	Δ	δ							
<i>I</i>				2	3	4	<i>I</i>				2	3	4	<i>I</i>				2	3	4	<i>I</i>				2	3	4							
46	3	43	+	1786.8224		-4	49	12	38	-	2058.8042	1	-1	53	7	47	-	2055.6220		3	57	5	53	-	2148.6373	9	1	61	8	54	-	2358.2277		-3
46	4	42	-	1804.3826	2	-1	49	12	38	+	2058.4793	0	-1	53	7	47	+	2055.3524		-1	57	5	53	+	2148.4389	5	1	61	8	54	+	2357.9172	2	0
46	4	42	+	1804.1723	4	-1	49	13	37	-	2093.5883	2	-2	53	8	46	-	2075.6319	1	1	57	6	52	+	2170.7669		-1	61	10	52	-	2405.4616		-3
46	5	41	-	1817.2511		1	49	13	37	+	2093.2427	1	0	53	8	46	+	2075.3472	1	0	57	7	51	-	2191.6203	4	3	61	10	52	+	2405.1288		-4
46	6	40	-	1827.7726	1	-2	49	14	36	-	2131.1781	1	0	53	9	45	-	2098.1635	2	0	57	7	51	+	2191.3420	2	0	61	11	51	-	2433.5993	2	-1
46	6	40	+	1827.4965	2	0	49	14	36	+	2130.8093	1	2	53	9	45	+	2097.8701		0	57	8	50	-	2212.0720		4	61	11	51	+	2433.2578	3	-3
46	7	39	-	1841.6829		-2	49	15	35	-	2171.5307		0	53	10	44	+	2123.5184	3	0	57	8	50	+	2211.7724		0	61	12	50	-	2464.9171	6	-3
46	7	39	+	1841.4214	1	0	49	15	35	+	2171.1366	4	1	53	11	43	-	2152.5970		-1	57	9	49	-	2234.3770	5	1	61	12	50	+	2464.5644	1	-1
46	8	38	-	1860.8059		1	49	16	34	-	2214.6100		0	53	11	43	+	2152.2802	3	0	57	9	49	+	2234.0672		0	61	13	49	-	2499.2804	2	-3
46	8	38	+	1860.5468		0	50	0	50	-	1828.0723	1	0	53	12	42	-	2184.3711	2	-1	57	10	48	-	2259.6739	3	-2	61	13	49	+	2498.9137	2	2
46	9	37	-	1883.7717	1	0	50	0	50	+	1828.0541	1	0	53	12	42	+	2184.0382		0	57	10	48	+	2259.3561	3	-1	61	14	48	-	2536.5819		0
46	9	37	+	1883.5034	4	-1	50	1	49	-	1854.5135	2	1	53	13	41	-	2219.0519		1	57	11	47	-	2288.1636	7	-3	61	14	48	+	2536.1976		-3
46	10	36	-	1909.9160		-4	50	1	49	+	1854.4489	1	0	53	13	41	+	2218.7002	1	0	57	11	47	+	2287.8353	2	0	62	0	62	-	2205.1670	1	0
46	10	36	+	1909.6340		1	50	2	48	-	1879.2069	1	-1	53	14	40	-	2256.5720	3	0	57	12	46	-	2319.7385		-1	62	0	62	+	2205.1493	2	0
46	11	35	-	1939.0411		-1	50	2	48	+	1879.0970	1	1	53	14	40	+	2256.1999	2	3	57	12	46	+	2319.3959		-2	62	1	61	-	2238.2180	3	-2
46	11	35	+	1938.7412		0	50	4	46	-	1922.0986	3	-1	53	15	39	-	2296.8809	6	1	57	13	45	-	2354.2812	2	0	62	1	61	+	2238.1574	1	-1
46	12	34	-	1971.0547	2	-1	50	4	46	+	1921.8925	4	-4	54	0	54	-	1945.0071		1	57	13	45	+	2353.9224	1	1	62	2	60	+	2269.4482		0
46	12	34	+	1970.7345	1	0	50	5	45	-	1938.2250	4	-1	54	0	54	+	1944.9889		2	57	14	44	-	2391.7070	2	0	62	3	59	-	2299.0310	2	2
46	13	33	-	2005.8980	2	1	50	5	45	+	1937.9612	3	-2	54	1	53	-	1973.6566	2	1	57	15	43	+	2431.5550		4	62	3	59	+	2298.8819		-3
46	13	33	+	2005.5549	1	0	50	6	44	-	1949.9992		-2	54	1	53	+	1973.5926	1	1	58	0	58	-	2070.7094	0	0	62	4	58	-	2326.4419	3	0
46	14	32	-	2043.5256	1	0	50	6	44	+	1949.6991	1	0	54	2	52	-	2000.5731	2	0	58	0	58	+	2070.6913	1	1	62	4	58	+	2326.2474	3	0
46	14	32	+	2043.1580	1	2	50	7	43	-	1962.4719	2	0	54	2	52	+	2000.4640	1	0	58	1	57	-	2101.5624		1	62	5	57	-	2351.3519		0
46	15	31	-	2083.9013		4	50	7	43	+	1962.1795	2	1	54	3	51	-	2025.5697		0	58	1	57	+	2101.4996	1	0	62	5	57	+	2363.6681		3
46	15	31	+	2083.5064		5	50	8	42	-	1980.2008		0	54	3	51	+	2025.4154	3	2	58	2	56	-	2130.6922	7	1	62	7	55	-	2388.3397	6	3
47	1	47	-	1746.1322	1	0	50	8	42	+	1979.9212	2	-1	54	4	50	+	2048.0761	4	2	58	2	56	+	2130.5848	3	-1	62	7	55	+	2387.9785	6	0
47	1	47	+	1746.1140	0	0	50	9	41	-	2002.5879		2	54	5	49	-	2067.6440	3	-1	58	3	55	-	2157.9397	5	-1	62	8	54	-	2401.9634		1
47	2	46	-	1770.9140	1	0	50	9	41	+	2002.3050		2	54	5	49	+	2067.3864	2	3	58	3	55	+	2157.7875	2	0	62	8	54	+	2401.5930		0
47	2	46	+	1770.8493	1	0	50	10	40	-	2028.4428		0	54	6	48	-	2082.0386	2	1	58	4	54	-	2183.0376		-2	62	11	51	-	2471.5203		1
47	3	45	-	1793.9386		0	50	10	40	+	2028.1488	3	0	54	6	48	+	2081.7262	2	1	58	4	54	+	2182.8390	3	0	62	11	51	+	2471.1751	3	-2

Table C.5 – Continued.

<i>N</i>	<i>K_a</i>	<i>K_c</i>	<i>J</i>	<i>E</i>	Δ	δ	<i>N</i>	<i>K_a</i>	<i>K_c</i>	<i>J</i>	<i>E</i>	Δ	δ	<i>N</i>	<i>K_a</i>	<i>K_c</i>	<i>J</i>	<i>E</i>	Δ	δ	<i>N</i>	<i>K_a</i>	<i>K_c</i>	<i>J</i>	<i>E</i>	Δ	δ							
<i>I</i>				2	3	4	<i>I</i>				2	3	4	<i>I</i>				2	3	4	<i>I</i>				2	3	4							
47	3	45	+	1793.8283	3	0	50	11	39	-	2057.3861	1	0	54	7	47	-	2094.1127	3	-1	58	5	53	-	2205.3207		-1	62	12	50	-	2502.7481	2	2
47	4	44	-	1815.0077	5	-1	50	11	39	+	2057.0769	1	-2	54	7	47	+	2093.7890	3	2	58	6	52	+	2222.7832	2	1	62	12	50	+	2502.3922		-1
47	4	44	+	1814.8525	3	1	50	12	38	-	2089.2777	2	-1	54	8	46	-	2110.0097	5	-2	58	7	51	-	2236.3006		0	62	13	49	-	2537.0575		-2
47	5	43	-	1834.0344	3	1	50	12	38	+	2088.9509		-1	54	8	46	+	2109.7042	3	0	58	7	51	+	2235.9519	1	1	62	13	49	+	2536.6885	2	1
47	5	43	+	1833.8366		0	50	13	37	-	2124.0389	0	-1	54	9	45	-	2131.4373	4	-1	58	8	50	-	2250.5452	5	0	62	14	48	-	2574.3225		2
47	6	42	-	1851.6309	4	2	50	13	37	+	2123.6919	1	1	54	9	45	+	2131.1371		0	58	8	50	+	2250.2076	3	0	63	1	63	-	2240.1479	1	-1
47	6	42	+	1851.4000	1	-1	50	14	36	-	2161.6136	1	3	54	10	44	-	2156.8692	3	1	58	9	49	-	2270.4616		3	63	1	63	+	2240.1302	1	0
47	7	41	-	1869.5082	1	1	50	14	36	+	2161.2438	2	1	54	10	44	+	2156.5617		0	58	9	49	+	2270.1399		0	63	2	62	+	2273.6876		-1
47	7	41	+	1869.2583		0	50	15	35	-	2201.9566	4	1	54	11	43	-	2185.5660	3	2	58	10	48	-	2295.2418	3	-2	63	3	61	+	2305.5286	2	1
47	8	40	-	1889.5170	1	2	50	15	35	+	2201.5625	4	2	54	11	43	+	2185.2460	3	0	58	10	48	+	2294.9190	3	-4	63	4	60	-	2335.6667	8	1
47	8	40	+	1889.2567	4	0	51	1	51	-	1856.4834	1	0	54	12	42	-	2217.2938	2	-1	58	11	47	-	2323.6013		0	63	4	60	+	2335.5191	2	0
47	9	39	-	1912.5245	1	0	51	1	51	+	1856.4651	1	0	54	12	42	+	2216.9586	1	-1	58	11	47	+	2323.2691		-3	63	5	59	+	2363.4749	2	-1
47	9	39	+	1912.2532		0	51	2	50	-	1883.4771	1	0	54	13	41	-	2251.9434	1	0	58	12	46	-	2355.1132	2	-1	63	7	57	+	2412.5995		1
47	10	38	-	1938.6207		-1	51	2	50	+	1883.4126	0	0	54	13	41	+	2251.5902	1	1	58	12	46	+	2354.7682	1	0	63	10	54	-	2482.0850		-4
47	10	38	+	1938.3355	1	-2	51	3	49	-	1908.7295	3	1	54	14	40	-	2289.4428	1	2	58	13	45	-	2389.6151	3	1	63	11	53	-	2510.0241		-4
47	11	37	-	1967.7063	1	-1	51	3	49	+	1908.6197	3	1	54	14	40	+	2289.0690	4	0	58	13	45	+	2389.2538	3	-2	63	11	53	+	2509.6766	2	-2
47	11	37	+	1967.4042	0	-1	51	4	48	+	1931.8982		-1	54	15	39	-	2329.7380		4	59	1	59	-	2103.5036	1	0	63	12	52	+	2540.8316		-2
47	12	36	-	1999.6929	1	-1	51	5	47	-	1953.2634		0	55	1	55	-	1975.6110	0	-2	59	1	59	+	2103.4855	1	1	63	13	51	-	2575.4453	3	-3
47	12	36	+	1999.3713	1	0	51	5	47	+	1953.0638		-2	55	1	55	+	1975.5928	1	0	59	2	58	-	2134.9066	4	1	63	13	51	+	2575.0743	1	2
47	13	35	-	2034.5181	2	1	51	6	46	+	1972.3170	3	-2	55	2	54	-	2004.8121	2	1	59	2	58	+	2134.8442	1	0	63	14	50	-	2612.6712	2	-1
47	13	35	+	2034.1742	2	-1	51	7	45	-	1991.1697	3	0	55	2	54	+	2004.7483	1	1	59	3	57	-	2164.5882	4	-2	63	14	50	+	2612.2841		0
47	14	34	-	2072.1342	1	0	51	7	45	+	1990.9061	1	-1	55	3	53	-	2032.2834		1	59	3	57	+	2164.4816	2	-1	64	0	64	-	2275.6749	1	0
47	14	34	+	2071.7663	1	1	51	8	44	-	2011.1085	2	0	55	3	53	+	2032.1746	3	0	59	4	56	-	2192.3991	4	-1	64	0	64	+	2275.6575	1	0
47	15	33	-	2112.5030	1	2	51	8	44	+	2010.8317	2	-1	55	4	52	-	2057.8568	3	0	59	4	56	+	2192.2477	3	0	64	1	63	+	2309.7640		2
47	15	33	+	2112.1088	2	5	51	9	43	-	2033.7944	1	2	55	4	52	+	2057.7030	2	1	59	5	55	-	2218.1357	1	-3	64	2	62	+	2342.1543	0	1
47	16	32	-	2155.5902	3	3	51	9	43	+	2033.5086	1	1	55	5	51	-	2081.3210		-5	59	5	55	+	2217.9389	2	0	64	3	61	+	2372.6980	1	0
48	0	48	-	1772.8966	1	0	51	10	42	-	2059.6148		-1	55	5	51	+	2081.1225	5	2	59	6	54	-	2241.6162		2	64	4	60	+	2401.2021	3	-3
48	0	48	+	1772.8784	0	0	51	10	42	+	2059.3177	2	-1	55	6	50	-	2102.6165	5	-1	59	6	50	+	2241.3741	3	0	64	5	59	+	2427.3044	4	-1
48	1	47	-	1798.2316	1	0	51	11	41	-	2088.5076	1	-3	55	6	50	+	2102.3748		-2	59	7	53	-	2263.1027		2	64	7	57	+	2491.1253	3	1

Table C.5 – Continued.

<i>N</i>	<i>K_a</i>	<i>K_c</i>	<i>J</i>	<i>E</i>	Δ	δ	<i>N</i>	<i>K_a</i>	<i>K_c</i>	<i>J</i>	<i>E</i>	Δ	δ	<i>N</i>	<i>K_a</i>	<i>K_c</i>	<i>J</i>	<i>E</i>	Δ	δ	<i>N</i>	<i>K_a</i>	<i>K_c</i>	<i>J</i>	<i>E</i>	Δ	δ							
<i>I</i>				2	3	4	<i>I</i>				2	3	4	<i>I</i>				2	3	4	<i>I</i>				2	3	4							
48	1	47	+	1798.1669	1	-1	51	11	41	+	2088.1963	2	-1	55	7	49	+	2122.1748	2	-1	59	7	53	+	2262.8219		1	64	5	59	+	2427.3044	4	-1
48	2	46	-	1821.8094	5	1	51	12	40	-	2120.3633	1	-1	55	8	48	-	2142.6254	5	1	59	8	52	+	2283.6425	4	-1	64	10	54	-	2521.6319		-1
48	2	46	+	1821.6989	1	0	51	12	40	+	2120.0346		0	55	8	48	+	2142.3330	2	-2	59	9	51	-	2306.2157		-1	64	10	54	+	2521.2828		0
48	3	45	-	1843.3643	3	-2	51	13	39	-	2155.0996	2	0	55	9	47	-	2165.0248	4	0	59	9	51	+	2305.8984		1	64	11	53	-	2549.1980		1
48	3	45	+	1843.2081	2	1	51	13	39	+	2154.7512	4	1	55	9	47	+	2164.7235	4	-3	59	10	50	-	2331.3250	4	1	64	11	53	+	2548.8459	3	-4
48	4	44	-	1862.1913	1	0	51	14	38	-	2192.6574	1	0	55	10	46	-	2190.5073		-1	59	10	50	+	2330.9993	4	-4	64	12	52	+	2579.8897	7	0
48	4	44	+	1861.9833	5	-1	51	14	38	+	2192.2872	2	3	55	10	46	+	2190.1966	2	-2	59	11	49	-	2359.6467		0	64	13	51	-	2614.4448		0
48	5	43	-	1876.6535		-1	51	15	37	-	2232.9903	3	1	55	11	45	-	2219.1482		0	59	11	49	+	2359.3115		-3	64	14	50	-	2651.6289	2	-1
48	5	43	+	1876.3892		-2	51	15	37	+	2232.5958	5	1	55	11	45	+	2218.8256	3	0	59	12	48	-	2391.1010	2	2	65	1	65	-	2311.7480	1	0
48	6	42	-	1887.6109	2	0	52	0	52	-	1885.4430	1	0	55	12	44	-	2250.8293	1	1	59	12	48	+	2390.7531	1	-1	65	1	65	+	2311.7305	0	0
48	6	42	+	1887.3221		1	52	0	52	+	1885.4248	1	1	55	12	44	+	2250.4914	2	-2	59	13	47	-	2425.5595	4	1	65	2	64	-	2346.4440	7	1
48	7	41	-	1900.7216	2	-1	52	1	51	-	1912.9890	1	1	55	13	43	-	2285.4456		1	59	13	47	+	2425.1966	3	2	65	2	64	+	2346.3853	6	-1
48	7	41	+	1900.4452	2	0	52	1	51	+	1912.9246	1	1	55	13	43	+	2285.0905	3	1	59	14	46	+	2462.5465	2	2	65	3	63	-	2379.4258		-2
48	8	40	-	1919.2195		1	52	2	50	-	1938.7953	3	0	55	14	42	-	2322.9219	5	-1	60	0	60	-	2136.8445	2	-1	65	3	63	+	2379.3248		-1
48	8	40	+	1918.9507		0	52	2	50	+	1938.6857	1	0	55	14	42	+	2322.5475	2	5	60	0	60	+	2136.8265	0	-1	65	4	62	+	2410.4230		-1
48	9	39	-	1941.9315	3	0	52	3	49	-	1962.6558		-1	55	15	41	-	2363.2019		-1	60	1	59	-	2168.7975	4	1	65	5	61	-	2439.6950		-2
48	9	39	+	1941.6563	2	0	52	3	49	+	1962.5006		0	56	0	56	-	2006.7630	1	0	60	1	59	+	2168.7355	1	0	65	5	61	+	2439.5054		-1
48	10	38	-	1967.9443	3	-1	52	4	48	-	1984.1219	3	-2	56	0	56	+	2006.7448	2	0	60	2	58	+	2198.9246	3	1	65	9	57	+	2490.8442		1
48	10	38	+	1967.6565	3	1	52	4	48	+	1983.9182		0	56	1	55	-	2036.5150	2	1	60	3	57	-	2227.3958		2	65	10	56	-	2561.1934	3	-1
48	11	37	-	1996.9854		0	52	5	47	-	2001.9005	5	-1	56	1	55	+	2036.4515	1	1	60	3	57	+	2227.2447	1	-2	65	11	55	-	2588.9250		5
48	11	37	+	1996.6813	3	1	52	5	47	+	2001.6391	5	-1	56	2	54	+	2064.4310		1	60	4	56	-	2253.6569	4	-2	65	11	55	+	2588.5700	2	-5
48	12	36	-	2028.9427	1	-1	52	6	46	-	2014.8417	3	-2	56	3	53	+	2090.5112	3	4	60	4	56	+	2253.4603	1	0	65	12	54	-	2619.9204		1
48	12	36	+	2028.6195	1	0	52	6	46	+	2014.5343		1	56	4	52	-	2114.5799	3	-3	60	5	55	-	2277.2829		3	65	12	54	+	2619.5567		-2
48	13	35	-	2063.7481	1	-1	52	7	45	-	2026.9431		-1	56	4	52	+	2114.3796		-1	60	5	55	+	2277.0355		2	66	0	66	-	2348.3665	1	0
48	13	35	+	2063.4035	1	0	52	8	44	-	2043.7842	2	0	56	5	51	-	2135.4476		2	60	6	54	-	2296.7926	6	2	66	0	66	+	2348.3494	2	0
48	14	34	-	2101.3517		0	52	8	44	+	2043.4922	2	-2	56	5	51	+	2135.1933		3	60	6	54	+	2296.4834		0	66	1	65	+	2383.5524		0
48	14	34	+	2100.9833		0	52	9	43	-	2065.7515	3	1	56	6	50	-	2151.4874	2	2	60	7	53	-	2311.1403	2	0	66	2	64	-	2417.1407		3
48	15	33	-	2141.7130	1	2	52	9	43	+	2065.4602	0	0	56	6	50	+	2151.1732	3	-1	60	7	53	+	2310.7839		2	66	2	64	+	2417.0407		1
66	3	63	+	2448.6909		0	68	0	68	+	2423.2233	1	-1	70	0	70	+	2500.2772	2	-1	72	1	71	-	2618.0451	1	-2	76	1	75	-	2785.2099		-2

Table C.5 – Continued.

<i>N</i>	<i>K_a</i>	<i>K_c</i>	<i>J</i>	<i>E</i>	Δ	δ	<i>N</i>	<i>K_a</i>	<i>K_c</i>	<i>J</i>	<i>E</i>	Δ	δ	<i>N</i>	<i>K_a</i>	<i>K_c</i>	<i>J</i>	<i>E</i>	Δ	δ	<i>N</i>	<i>K_a</i>	<i>K_c</i>	<i>J</i>	<i>E</i>	Δ	δ	<i>N</i>	<i>K_a</i>	<i>K_c</i>	<i>J</i>	<i>E</i>	Δ	δ		
<i>I</i>				2	3	4	<i>I</i>				2	3	4	<i>I</i>				2	3	4	<i>I</i>				2	3	4	<i>I</i>				2	3	4		
66	4	62	+	2478.3261			1	68	1	67	-	2459.5775			0	70	1	69	-	2537.7230		-2	72	1	71	+	2617.9924	1	1	76	1	75	+	2785.1580	8	-1
66	5	61	-	2505.8724	1	2	68	1	67	+	2459.5214			0	70	1	69	+	2537.6689	1	1	72	2	70	+	2654.7628		3	77	1	77	-	2787.1233	1	-2	
66	5	61	+	2505.6363	6	-1	68	2	66	-	2494.2028			3	70	2	68	-	2573.4411	5	2	73	1	73	-	2619.9583	2	0	77	1	77	+	2787.1047		0	
66	6	60	-	2530.1226	3	0	68	2	66	+	2494.1052			-4	70	2	68	+	2573.3470	1	1	73	1	73	+	2619.9413		0	78	0	78	-	2830.2724	2	1	
66	7	59	-	2536.2106	1	-2	68	3	65	-	2526.9987			1	70	5	65	+	2668.7368	1	1	74	0	74	-	2660.9343	2	1	78	0	78	+	2830.2531	1	0	
66	7	59	+	2571.5753	3	-2	68	3	65	+	2526.8593	2	1	70	7	63	-	2701.9176		1	74	0	74	+	2660.9174		0	79	1	79	-	2873.9643	3	0		
66	10	56	-	2602.1879		-4	68	5	63	-	2617.8640	1	2	71	1	71	-	2539.6378	2	-1	74	1	73	-	2700.5414		-2	79	1	79	+	2873.9436		3		
67	1	67	-	2385.5308		0	68	7	61	+	2654.2160	2	3	71	1	71	+	2539.6209	2	-1	74	1	73	+	2700.4895	4	0	80	0	80	-	2918.1982	2	0		
67	1	67	+	2385.5136	2	0	69	1	69	-	2461.4948			0	71	2	70	+	2577.5588		2	74	2	72	+	2738.3501		2	80	0	80	+	2918.1764		2	
67	2	66	+	2421.2645		0	69	1	69	+	2461.4778			0	71	3	69	-	2613.8756	3	1	75	1	75	-	2702.4541	2	0	81	1	81	-	2962.9748	4	0	
67	3	65	+	2455.3010		1	69	2	68	+	2498.3230			1	71	3	69	+	2613.7829	3	-1	75	1	75	+	2702.4366		0	81	1	81	+	2962.9504		2	
67	4	64	+	2487.5036		0	69	3	67	+	2533.4545			2	72	0	72	-	2579.5260		2	76	0	76	-	2744.5171	1	1	83	1	83	+	3054.1230	4	0	
67	5	63	+	2517.7080		-1	69	5	65	+	2598.0808			0	72	0	72	+	2579.5093		-1	76	0	76	+	2744.4995		1	84	0	84	-	3100.5542		4	
68	0	68	-	2423.2402	1	1	70	0	70	-	2500.2939	2	1																							

In Table C.5, Δ is the experimental uncertainty of the energy value, equal to one standard uncertainty in units of 10^{-4} cm^{-1} ; δ is the difference, $E^{\text{exp}} - E^{\text{calc}}$ also in units of 10^{-4} cm^{-1} . When the Δ -value is absent, the corresponding energy level was obtained from a single transition; J is the quantum number of the ground vibrational state ($J = N + 1/2$ is denoted as “+”, $J = N - 1/2$ is denoted as “-”).

Table C.6 – Spectroscopic parameters of the ($v_3 = 1$) vibrational state.

Parameter	$(v_3 = 1) \text{ ClO}_2, \text{cm}^{-1}$	$(v_{\text{GS}} = 1) \text{ ClO}_2, \text{cm}^{-1}$ [52]
<i>I</i>	2	3
<i>E</i>	1110.106659(12)	
<i>A</i>	1.72118217(28)	1.7372487(18)
<i>B</i>	0.330166907(53)	0.33198801(36)
<i>C</i>	0.276569335(54)	0.27799915(31)
$\Delta_K/10^{-4}$	0.684340(22)	0.68542(14)
$\Delta_{NK}/10^{-4}$	-0.0412950(42)	-0.038169(38)
$\Delta_N/10^{-4}$	0.00299496(29)	0.0029576(29)
$\delta_K/10^{-4}$	0.0093636(48)	0.010435(66)
$\delta_N/10^{-4}$	0.00078045(13)	0.00077094(54)
$H_K/10^{-8}$	0.92520(70)	0.9449(61)
$H_{KN}/10^{-8}$	-0.073301(93)	-0.0867(35)
$H_{NK}/10^{-8}$	-0.006162(32)	0.00664(92)
$H_N/10^{-8}$	0.00013197(77)	0.0001349(98)
$h_K/10^{-8}$	0.27125(71)	0.294(35)
$h_N/10^{-8}$	0.00003913(22)	0.0000391(23)
$L_K/10^{-12}$	-1.9486(92)	-2.001(90)
$L_{KKN}/10^{-12}$	0.1063	0.1063(66)
$L_{KNN}/10^{-12}$	0.000168(38)	
$L_N/10^{-12}$	-0.00003727(73)	-0.0000401(83)
$l_K/10^{-12}$	-0.1703(61)	-0.251(70)
$l_{KN}/10^{-12}$		
$l_{NK}/10^{-12}$	0.009753(28)	0.01054(91)
$l_N/10^{-12}$		
$P_K/10^{-16}$	3.570(42)	4.22(56)
$P_{KKN}/10^{-16}$	0.3792(96)	
$a_0/10^{-2}$	-0.355150(92)	-0.35128(57)
$a/10^{-2}$	-4.35940(37)	-4.2778(12)
$b/10^{-2}$	0.375633(60)	0.369986(60)
$\Delta^S_K/10^{-5}$	0.3975(17)	0.4023(87)
$\Delta^S_{KN}/10^{-5}$	-5.821(23)	-5.882(91)
$\Delta^S_{NK}/10^{-5}$	5.406(22)	5.465(85)
$\Delta^S_N/10^{-5}$	-0.004518(88)	-0.00315(34)
$\delta^S_K/10^{-5}$	-0.1847(76)	
$\delta^S_N/10^{-5}$		
$H^S_K/10^{-8}$		
$H^S_{KKN}/10^{-8}$	-0.2236(19)	-0.2471(79)
$H^S_{NKK}/10^{-8}$		
$H^S_{KNN}/10^{-8}$	0.2577(30)	0.2588(86)
$H^S_{NNK}/10^{-8}$	-0.00935(24)	
$H^S_N/10^{-8}$	0.000152(17)	
$h^S_{KN}/10^{-8}$	-0.5209(43)	-0.491(29)
$h^S_{NK}/10^{-8}$	0.5313(25)	0.512(25)
$h^S_{NN}/10^{-8}$	0.0000151(26)	

Table C.7 – Spectroscopic parameters of the ($v_1 = v_3 = 1$) vibrational state.

Parameter	($v_1 = v_3 = 1$) ClO ₂ , cm ⁻¹	($v_{\text{GS}} = 1$) ClO ₂ , cm ⁻¹ [52]
<i>I</i>	2	3
<i>E</i>	2038.933801(30)	
<i>A</i>	1.7191685(18)	1.7372487(18)
<i>B</i>	0.32817231(29)	0.33198801(36)
<i>C</i>	0.27474737(23)	0.27799915(31)
$\Delta_K/10^{-4}$	0.693(29)	0.68542(14)
$\Delta_{NK}/10^{-4}$	-0.040123(22)	-0.038169(38)
$\Delta_N/10^{-4}$	0.0030229(21)	0.0029576(29)
$\delta_K/10^{-4}$	0.010185(13)	0.010435(66)
$\delta_N/10^{-4}$	0.00078647(19)	0.00077094(54)
$H_K/10^{-8}$	1.0290(92)	0.9449(61)
$H_{KN}/10^{-8}$	-0.06223(28)	-0.0867(35)
$H_{NK}/10^{-8}$		0.00664(92)
$H_N/10^{-8}$	0.0003534(87)	0.0001349(98)
$h_K/10^{-8}$	0.294	0.294(35)
$h_{NK}/10^{-8}$	0.00432	0.00432
$h_N/10^{-8}$	0.0001140(81)	0.0000391(23)
$L_K/10^{-12}$	-2.49(33)	-2.001(90)
$L_{KKN}/10^{-12}$	0.524(88)	0.1063(66)
$L_N/10^{-12}$	-0.000622(20)	-0.0000401(83)
$l_{NK}/10^{-12}$	-0.0143	-0.0143(28)
$l_N/10^{-12}$	-0.000237(16)	
$P_{KKN}/10^{-16}$	0.0913	0.0913
$P_{KKN}/10^{-16}$	-0.0299(13)	
$P_K/10^{-16}$	4.22	4.22(56)
$a_0/10^{-2}$	-0.36125(27)	-0.35128(57)
$a/10^{-2}$	-4.3890(15)	-4.2778(12)
$b/10^{-2}$	0.38215(15)	0.369986(60)
$\Delta^S_K/10^{-5}$	0.490(18)	0.4023(87)
$\Delta^S_{KN}/10^{-5}$	-6.683(93)	-5.882(91)
$\Delta^S_{NK}/10^{-5}$	6.194(82)	5.465(85)
$\Delta^S_N/10^{-5}$	-0.003272(76)	-0.00315(34)
$\delta^S_K/10^{-5}$	-0.2739(84)	
$\delta^S_N/10^{-5}$		
$H^S_K/10^{-8}$		
$H^S_{KKN}/10^{-8}$	-0.281(30)	-0.2471(79)
$H^S_{NKK}/10^{-8}$		
$H^S_{KNN}/10^{-8}$	0.3325(79)	0.2588(86)
$H^S_{NNK}/10^{-8}$		
$H^S_N/10^{-8}$		
$h^S_{KN}/10^{-8}$	-0.797(37)	-0.491(29)
$h^S_{NK}/10^{-8}$	0.922(52)	0.512(25)

Appendix D. Tables for Chapter 3

Table D.1 – Experimental values of v_2/v_4 dyad line positions of $^{13}\text{CD}_4$ molecule.

<i>J</i>	γ	<i>n</i>	<i>J'</i>	γ'	<i>n'</i>	$v^{\text{exp}}, \text{cm}^{-1}$	Transmittance, %	$\delta \cdot 10^{-4}, \text{cm}^{-1}$	Band	Spectra
<i>I</i>			<i>2</i>			<i>3</i>	<i>4</i>	<i>5</i>	<i>6</i>	<i>7</i>
19	F ₂	6	20	F ₁	3	869.02016	97.8	-2.8	v ₄	III
18	F ₁	6	19	F ₂	3	870.41776	97.1	-0.7	v ₄	III
19	A ₂	3	20	A ₁	2	873.72646	98.0	-0.1	v ₄	III
18	A ₂	2	19	A ₁	1	875.95377	98.0	-1.7	v ₄	III
18	F ₂	7	19	F ₁	3	876.02580	98.0	-1.7	v ₄	III
18	E	5	19	E	2	876.05385	98.1	-3.2	v ₄	III
17	F ₂	6	18	F ₁	2	877.60614	97.2	0.9	v ₄	III
17	A ₂	3	18	A ₁	1	877.61941	97.8	4.4	v ₄	III
18	F ₂	8	19	F ₁	4	880.38255	97.2	1.7	v ₄	III
19	F ₂	9	20	F ₁	4	881.09433	98.2	-4.5	v ₄	III
23	F ₁	15	24	F ₂	4	882.02471	97.6	7.2	v ₄	III
17	F ₂	7	18	F ₁	3	882.88062	96.9	-2.2	v ₄	III
17	F ₁	6	18	F ₂	3	882.98258	96.0	-0.7	v ₄	III
13	F ₁	3	14	F ₂	3	884.27607	94.3	-1.1	v ₄	III
16	F ₁	5	17	F ₂	2	884.72092	96.5	-3.5	v ₄	III
16	F ₂	6	17	F ₁	3	884.74118	96.4	0.5	v ₄	III
18	A ₁	3	19	A ₂	2	884.75148	95.8	1.1	v ₄	III
22	F ₁	13	23	F ₂	5	885.49071	97.1	1.6	v ₄	III
18	F ₂	9	19	F ₁	4	886.26416	97.4	-0.1	v ₄	III
17	F ₁	7	18	F ₂	4	886.81760	98.2	-2.3	v ₄	III
22	A ₁	5	23	A ₂	2	887.02960	96.9	3.6	v ₄	III
17	E	5	18	E	3	887.05425	97.6	0.5	v ₄	III
22	F ₁	14	23	F ₂	4	888.15222	96.6	1.6	v ₄	III
22	F ₂	14	23	F ₁	4	888.65975	95.6	0.9	v ₄	III
21	A ₂	5	22	A ₁	2	889.58122	95.4	0.4	v ₄	III
16	F ₁	6	17	F ₂	3	889.75071	94.7	-4.9	v ₄	III
16	A ₁	3	17	A ₂	1	889.90776	95.9	1.5	v ₄	III
21	F ₂	13	22	F ₁	4	889.99905	95.1	1.2	v ₄	III
21	F ₁	12	22	F ₂	5	890.50439	95.0	-0.9	v ₄	III
12	F ₂	2	13	F ₁	4	891.34041	97.3	-1.1	v ₄	III
22	A ₂	5	23	A ₁	1	891.38936	97.1	3.8	v ₄	III
21	A ₁	4	22	A ₂	2	891.43602	95.9	1.9	v ₄	III
14	F ₁	4	15	F ₂	2	891.50952	94.0	-2.9	v ₄	III
14	A ₁	2	15	A ₂	1	891.51457	95.6	2.6	v ₄	III
19	F ₁	11	20	F ₂	5	891.52234	86.5	2.3	v ₄	III
22	F ₂	15	23	F ₁	3	891.56500	96.5	2.5	v ₄	III
22	E	10	23	E	2	891.64111	97.0	4.1	v ₄	III
15	F ₁	6	16	F ₂	2	891.78815	95.3	1.6	v ₄	III
15	E	4	16	E	2	891.80349	95.3	-1.6	v ₄	III
17	F ₂	9	18	F ₁	3	891.89203	96.7	3.3	v ₄	III
19	F ₂	10	20	F ₁	5	891.99271	85.5	2.9	v ₄	III

Table D.1 – Continued.

<i>J</i>	γ	<i>n</i>	<i>J'</i>	γ'	<i>n'</i>	ν^{exp} , cm^{-1}	Transmittance, %	$\delta \cdot 10^{-4}$, cm^{-1}	Band	Spectra
<i>I</i>		<i>2</i>		<i>3</i>		<i>4</i>		<i>5</i>		<i>7</i>
12	A ₁	1	13	A ₂	1	892.00148	96.3	0.4	v ₄	III
21	F ₁	13	22	F ₂	4	892.94963	94.5	0.7	v ₄	III
21	E	9	22	E	3	893.26307	95.3	-0.1	v ₄	III
21	F ₁	14	22	F ₂	3	895.94707	93.7	-1.4	v ₄	III
16	F ₂	8	17	F ₁	4	896.19918	96.3	0.9	v ₄	III
15	F ₂	5	16	F ₁	3	896.35804	96.6	1.1	v ₄	III
18	F ₂	10	19	F ₁	5	897.63350	79.3	1.1	v ₄	III
18	E	7	19	E	3	897.88238	83.3	0.4	v ₄	III
20	F ₂	13	21	F ₁	4	897.90568	91.2	-1.0	v ₄	III
18	F ₁	10	19	F ₂	5	898.13426	78.3	3.4	v ₄	III
14	F ₁	5	15	F ₂	3	898.73465	94.3	0.7	v ₄	III
14	F ₂	5	15	F ₁	2	898.78884	93.8	1.0	v ₄	III
13	F ₂	4	14	F ₁	1	898.94651	92.7	1.8	v ₄	III
13	F ₁	4	14	F ₂	2	898.95371	93.4	1.6	v ₄	III
11	A ₂	1	12	A ₁	2	899.15957	96.0	4.0	v ₄	III
11	F ₁	2	12	F ₂	3	899.60406	97.3	-1.8	v ₄	III
21	F ₂	15	22	F ₁	2	899.67384	90.7	2.0	v ₄	III
20	E	9	21	E	2	899.87352	94.0	0.2	v ₄	III
20	F ₁	13	21	F ₂	3	900.08900	87.5	1.1	v ₄	III
19	F ₁	12	20	F ₂	4	900.26373	86.9	-1.1	v ₄	III
20	A ₁	5	21	A ₂	1	900.42939	89.9	-0.6	v ₄	III
22	E	11	23	E	1	900.53645	91.4	4.8	v ₄	III
15	A ₂	2	16	A ₁	2	900.86026	91.0	-1.3	v ₄	III
19	E	8	20	E	3	900.94577	90.9	-0.6	v ₄	III
15	F ₁	8	16	F ₂	3	902.40210	96.5	-0.7	v ₄	III
23	A ₂	6	24	A ₁	1	902.71557	93.5	-0.8	v ₄	III
23	E	12	24	E	1	902.71557	93.5	-0.8	v ₄	III
23	F ₂	17	24	F ₁	1	902.71557	93.5	-0.8	v ₄	III
14	A ₂	2	15	A ₁	1	902.73720	96.8	1.1	v ₄	III
19	A ₂	4	20	A ₁	2	902.76640	86.9	-2.3	v ₄	III
15	A ₁	3	16	A ₂	1	902.84797	97.0	4.9	v ₄	III
14	F ₂	6	15	F ₁	3	903.06270	96.3	0.7	v ₄	III
14	E	4	15	E	2	903.24069	95.6	2.4	v ₄	III
17	A ₂	4	18	A ₁	2	903.51036	73.6	0.7	v ₄	III
20	F ₂	14	21	F ₁	3	903.74568	90.6	0.1	v ₄	III
17	F ₂	10	18	F ₁	4	903.76501	69.9	0.7	v ₄	III
17	F ₁	9	18	F ₂	5	904.03248	70.0	1.0	v ₄	III
19	F ₂	12	20	F ₁	3	904.14154	87.0	-0.7	v ₄	III
17	A ₁	3	18	A ₂	2	904.31790	70.5	2.1	v ₄	III
21	F ₂	16	22	F ₁	1	904.36703	89.7	8.4	v ₄	III
19	F ₁	13	20	F ₂	3	904.60042	85.8	-2.3	v ₄	III
18	A ₁	4	19	A ₂	2	905.28158	81.9	0.0	v ₄	III
13	F ₂	5	14	F ₁	2	905.64102	92.3	3.7	v ₄	III
18	F ₁	11	19	F ₂	4	905.78362	80.0	0.3	v ₄	III
12	F ₂	4	13	F ₁	2	906.29301	92.5	2.8	v ₄	III

Table D.1 – Continued.

<i>J</i>	γ	<i>n</i>	<i>J'</i>	γ'	<i>n'</i>	ν^{exp} , cm^{-1}	Transmittance, %	$\delta \cdot 10^{-4}$, cm^{-1}	Band	Spectra
<i>I</i>			<i>2</i>			<i>3</i>	<i>4</i>	<i>5</i>	<i>6</i>	<i>7</i>
12	E	3	13	E	1	906.29852	94.2	-0.8	ν_4	III
22	F ₁	17	23	F ₂	1	906.31602	91.7	-1.5	ν_4	III
22	F ₂	17	23	F ₁	1	906.31602	91.7	-1.6	ν_4	III
14	F ₂	7	15	F ₁	3	906.72865	93.8	1.9	ν_4	III
10	F ₂	2	11	F ₁	3	907.20321	96.4	-2.9	ν_4	III
10	E	1	11	E	2	907.27464	97.1	-2.0	ν_4	III
18	A ₂	4	19	A ₁	1	907.58032	81.4	0.0	ν_4	III
14	E	5	15	E	2	907.60879	94.6	2.5	ν_4	III
19	A ₁	5	20	A ₂	1	907.64439	87.9	-0.4	ν_4	III
19	E	9	20	E	2	907.81666	90.2	-0.1	ν_4	III
10	F ₁	2	11	F ₂	3	908.21076	95.6	-4.4	ν_4	III
18	F ₂	12	19	F ₁	3	908.72432	78.2	-0.9	ν_4	III
18	E	8	19	E	2	909.00490	84.3	-1.4	ν_4	III
13	F ₂	6	14	F ₁	3	909.30802	93.2	2.8	ν_4	III
16	F ₂	9	17	F ₁	5	909.52165	58.4	0.4	ν_4	III
13	F ₁	5	14	F ₂	3	909.73880	93.6	0.3	ν_4	III
16	E	6	17	E	3	909.79049	69.1	0.4	ν_4	III
21	A ₁	5	22	A ₂	1	909.91244	82.5	-0.6	ν_4	III
21	E	11	22	E	1	909.91244	82.5	-1.0	ν_4	III
21	F ₁	16	22	F ₂	1	909.91244	82.5	-0.9	ν_4	III
16	F ₁	9	17	F ₂	4	910.09866	54.8	-0.4	ν_4	III
17	E	7	18	E	3	911.10884	78.0	-2.0	ν_4	III
18	F ₁	12	19	F ₂	3	911.72330	78.7	-0.7	ν_4	III
18	F ₂	13	19	F ₁	2	911.90765	78.5	-1.1	ν_4	III
19	F ₂	13	20	F ₁	2	912.01786	83.5	-0.4	ν_4	III
19	F ₁	15	20	F ₂	1	912.02675	83.4	-0.9	ν_4	III
17	F ₂	11	18	F ₁	3	912.24062	71.6	-1.3	ν_4	III
13	E	4	14	E	2	912.72022	96.3	-1.7	ν_4	III
17	F ₁	11	18	F ₂	3	913.44277	70.7	-1.5	ν_4	III
11	F ₂	3	12	F ₁	2	913.51542	90.1	2.3	ν_4	III
15	F ₁	9	16	F ₂	4	915.27422	38.5	-1.3	ν_4	III
15	E	6	16	E	3	915.58060	49.7	-0.8	ν_4	III
17	E	8	18	E	2	915.74657	78.3	-0.7	ν_4	III
12	F ₁	5	13	F ₂	3	915.80593	96.7	3.4	ν_4	III
18	E	9	19	E	1	915.83812	82.5	-0.6	ν_4	III
18	F ₁	13	19	F ₂	2	915.84681	75.3	-0.1	ν_4	III
18	A ₁	5	19	A ₂	1	915.86373	78.7	-0.8	ν_4	III
17	F ₂	12	18	F ₁	2	915.88759	64.1	-0.7	ν_4	III
15	F ₂	8	16	F ₁	4	915.89353	37.8	1.1	ν_4	III
17	A ₂	5	18	A ₁	1	916.12110	72.8	-1.0	ν_4	III
16	E	7	17	E	2	916.63567	68.7	-2.0	ν_4	III
12	A ₁	2	13	A ₂	1	916.73439	89.2	0.5	ν_4	III
19	A ₂	5	20	A ₁	1	917.09136	63.7	-2.9	ν_4	III
19	F ₂	14	20	F ₁	1	917.09136	63.7	-0.5	ν_4	III
19	E	10	20	E	1	917.09136	63.7	0.7	ν_4	III

Table D.1 – Continued.

<i>J</i>	γ	<i>n</i>	<i>J'</i>	γ'	<i>n'</i>	ν^{exp} , cm^{-1}	Transmittance, %	$\delta \cdot 10^{-4}$, cm^{-1}	Band	Spectra
<i>I</i>			<i>2</i>			<i>3</i>	<i>4</i>	<i>5</i>	<i>6</i>	<i>7</i>
16	F ₁	10	17	F ₂	3	917.13093	59.9	-1.2	v ₄	III
16	A ₁	4	17	A ₂	1	918.08524	64.3	-1.4	v ₄	III
12	F ₂	6	13	F ₁	3	918.39127	95.0	-2.1	v ₄	III
11	F ₁	5	12	F ₂	2	919.04799	92.2	0.4	v ₄	III
11	E	3	12	E	2	919.15579	92.0	0.9	v ₄	III
17	F ₂	13	18	F ₁	1	919.65378	67.0	-0.5	v ₄	III
17	F ₁	12	18	F ₂	2	919.68437	67.2	-0.4	v ₄	III
16	F ₁	11	17	F ₂	2	919.78887	58.5	-0.9	v ₄	III
16	F ₂	11	17	F ₁	3	920.12198	57.2	-0.9	v ₄	III
10	E	2	11	E	1	920.61801	92.6	1.6	v ₄	III
15	A ₂	3	16	A ₁	2	920.62521	54.3	-1.3	v ₄	III
10	F ₁	3	11	F ₂	2	920.63509	90.2	3.4	v ₄	III
10	A ₁	2	11	A ₂	1	920.66853	89.7	3.8	v ₄	III
18	F ₂	14	19	F ₁	1	920.67335	54.4	-2.7	v ₄	III
18	F ₁	14	19	F ₂	1	920.67335	54.4	3.0	v ₄	III
14	A ₁	3	15	A ₂	2	920.75524	39.0	0.0	v ₄	III
14	F ₂	8	15	F ₁	4	921.38274	32.5	0.1	v ₄	III
14	A ₂	3	15	A ₁	1	921.76923	39.3	0.3	v ₄	III
11	F ₁	6	12	F ₂	2	922.63783	90.8	-0.7	v ₄	III
15	A ₁	4	16	A ₂	1	923.37635	49.1	-2.5	v ₄	III
16	F ₂	12	17	F ₁	2	923.49006	55.2	-0.4	v ₄	III
16	E	8	17	E	1	923.51552	66.1	-0.4	v ₄	III
15	F ₁	11	16	F ₂	2	924.06498	41.2	1.0	v ₄	III
17	A ₁	4	18	A ₂	1	924.24966	39.0	9.7	v ₄	III
17	E	9	18	E	1	924.24966	39.0	-8.4	v ₄	III
17	F ₁	13	18	F ₂	1	924.24966	39.0	-2.3	v ₄	III
15	E	7	16	E	2	924.27259	58.8	-0.9	v ₄	III
10	F ₁	4	11	F ₂	3	925.40465	93.1	2.1	v ₄	III
10	F ₂	4	11	F ₁	2	925.69167	89.6	0.4	v ₄	III
14	F ₂	9	15	F ₁	3	925.93735	29.6	1.4	v ₄	III
14	E	6	15	E	2	926.29655	48.3	-0.6	v ₄	III
13	F ₁	7	14	F ₂	4	926.38676	90.7	-1.9	v ₄	II
13	E	5	14	E	3	926.69385	33.7	-0.8	v ₄	III
15	F ₂	10	16	F ₁	2	927.26655	41.5	-0.2	v ₄	III
15	F ₁	12	16	F ₂	1	927.35075	42.1	-0.3	v ₄	III
9	F ₁	3	10	F ₂	2	927.63436	85.5	1.4	v ₄	III
14	F ₁	9	15	F ₂	3	927.69223	33.1	-0.6	v ₄	III
10	F ₂	5	11	F ₁	2	928.21584	93.4	1.1	v ₄	III
14	F ₂	10	15	F ₁	2	928.44738	32.5	-0.8	v ₄	III
10	E	3	11	E	2	928.58996	96.3	0.7	v ₄	III
13	F ₁	8	14	F ₂	3	930.73671	91.3	-1.2	v ₄	II
14	E	7	15	E	1	931.06375	45.0	-0.1	v ₄	III
14	F ₁	10	15	F ₂	2	931.12896	25.0	-2.7	v ₄	III
14	A ₁	4	15	A ₂	1	931.24559	36.6	-0.2	v ₄	III
15	F ₂	11	16	F ₁	1	931.38541	31.3	-5.1	v ₄	III

Table D.1 – Continued.

<i>J</i>	γ	<i>n</i>	<i>J'</i>	γ'	<i>n'</i>	ν^{exp} , cm^{-1}	Transmittance, %	$\delta \cdot 10^{-4}$, cm^{-1}	Band	Spectra
<i>I</i>			<i>2</i>			<i>3</i>	<i>4</i>	<i>5</i>	<i>6</i>	<i>7</i>
15	A ₂	4	16	A ₁	1	931.39035	45.0	0.7	v ₄	III
12	F ₂	7	13	F ₁	4	931.71156	88.1	-0.2	v ₄	II
13	E	6	14	E	2	931.78949	93.7	0.5	v ₄	II
12	E	5	13	E	2	932.08807	91.6	-1.0	v ₄	II
13	F ₂	9	14	F ₁	2	932.18109	90.5	-1.4	v ₄	II
12	F ₁	7	13	F ₂	3	932.46976	88.0	-1.8	v ₄	II
13	A ₂	4	14	A ₁	1	932.79643	92.2	-1.9	v ₄	II
9	F ₁	4	10	F ₂	3	934.28000	93.6	-1.4	v ₄	III
8	F ₂	3	9	F ₁	2	934.42435	88.0	3.3	v ₄	III
8	E	2	9	E	1	934.47099	90.5	3.1	v ₄	III
13	F ₂	10	14	F ₁	1	934.85747	90.3	-0.5	v ₄	II
14	F ₁	11	15	F ₂	1	934.94141	23.0	3.0	v ₄	III
14	F ₂	11	15	F ₁	1	934.94885	26.0	0.4	v ₄	III
13	F ₁	9	14	F ₂	2	935.03143	79.4	-0.9	v ₄	II
12	A ₁	3	13	A ₂	1	935.32572	90.1	-1.2	v ₄	II
12	F ₁	8	13	F ₂	3	935.97834	97.1	-0.5	v ₄	III
12	F ₁	8	13	F ₂	2	936.01528	88.6	-1.2	v ₄	II
12	F ₂	8	13	F ₁	3	936.54830	88.1	-1.5	v ₄	II
11	A ₂	2	12	A ₁	2	936.74235	86.1	0.9	v ₄	II
11	F ₂	6	12	F ₁	3	937.07443	85.4	-0.8	v ₄	II
11	F ₁	7	12	F ₂	3	937.46769	85.3	-0.3	v ₄	II
11	A ₁	3	12	A ₂	1	938.00684	87.1	-0.4	v ₄	II
8	F ₂	4	9	F ₁	3	938.42141	87.2	2.5	v ₄	III
13	A ₁	3	14	A ₂	1	938.48430	87.5	-3.0	v ₄	II
12	F ₂	9	13	F ₁	2	938.77114	87.4	-0.7	v ₄	II
12	E	6	13	E	1	938.88598	91.1	0.6	v ₄	II
8	F ₁	4	9	F ₂	2	939.77191	88.8	3.9	v ₄	III
20	A ₁	2	20	A ₂	1	940.13302	97.9	-1.2	v ₄	III
20	F ₁	4	20	F ₂	2	940.13985	97.5	-2.6	v ₄	III
21	A ₂	2	21	A ₁	1	940.14859	96.1	5.8	v ₄	III
21	F ₂	5	21	F ₁	2	940.14859	96.1	-0.5	v ₄	III
11	F ₁	8	12	F ₂	2	940.43168	85.5	-0.8	v ₄	II
11	E	5	12	E	2	940.73307	88.8	-0.4	v ₄	II
7	F ₂	2	8	F ₁	2	941.00296	90.0	0.3	v ₄	III
7	F ₁	3	8	F ₂	1	941.14602	85.6	1.8	v ₄	III
10	F ₂	6	11	F ₁	3	941.94000	81.8	0.0	v ₄	II
12	F ₂	10	13	F ₁	1	942.05498	86.8	0.6	v ₄	II
10	E	4	11	E	2	942.25919	87.3	0.4	v ₄	II
11	F ₁	9	12	F ₂	1	942.75111	84.9	-0.6	v ₄	II
10	F ₁	6	11	F ₂	3	942.80837	81.9	0.0	v ₄	II
7	F ₁	4	8	F ₂	1	944.12504	95.1	-0.6	v ₄	III
18	A ₂	1	18	A ₁	1	945.22215	96.9	2.0	v ₄	III
11	E	6	12	E	1	945.56736	88.3	0.4	v ₄	II
11	F ₂	8	12	F ₁	1	945.58446	83.3	0.5	v ₄	II
11	A ₂	3	12	A ₁	1	945.61700	85.4	0.1	v ₄	II

Table D.1 – Continued.

<i>J</i>	γ	<i>n</i>	<i>J'</i>	γ'	<i>n'</i>	ν^{exp} , cm^{-1}	Transmittance, %	$\delta \cdot 10^{-4}$, cm^{-1}	Band	Spectra
<i>I</i>			<i>2</i>			<i>3</i>	<i>4</i>	<i>5</i>	<i>6</i>	<i>7</i>
10	E	5	11	E	1	946.16753	84.8	-2.9	ν_4	II
10	F ₁	7	11	F ₂	2	946.39984	81.0	0.4	ν_4	II
10	A ₁	3	11	A ₂	1	946.73987	84.2	-0.4	ν_4	II
9	F ₁	5	10	F ₂	3	946.79047	78.4	-0.1	ν_4	II
9	E	4	10	E	2	947.23554	85.0	-0.3	ν_4	II
6	E	2	7	E	1	947.43426	94.5	0.0	ν_4	III
6	F ₁	2	7	F ₂	2	947.53463	89.1	-2.5	ν_4	III
9	F ₂	6	10	F ₁	2	947.65293	78.6	0.1	ν_4	II
10	F ₁	8	11	F ₂	1	949.09212	80.5	0.5	ν_4	II
10	F ₂	8	11	F ₁	1	949.14290	80.1	0.8	ν_4	II
9	A ₂	3	10	A ₁	1	949.16915	81.8	-0.4	ν_4	II
9	F ₂	7	10	F ₁	2	949.98682	93.1	0.8	ν_4	III
9	F ₂	7	10	F ₁	1	950.00536	78.5	0.0	ν_4	II
16	E	2	16	E	2	950.23874	94.0	-0.2	ν_4	III
16	F ₁	3	16	F ₂	2	950.24420	93.5	4.1	ν_4	III
16	A ₁	2	16	A ₂	1	950.24876	94.2	3.2	ν_4	III
9	F ₁	6	10	F ₂	2	950.39625	78.5	-0.1	ν_4	II
8	A ₁	2	9	A ₂	1	951.35457	78.8	-0.1	ν_4	II
8	F ₁	5	9	F ₂	2	951.70074	75.5	0.0	ν_4	II
8	F ₂	5	9	F ₁	3	952.11998	75.5	0.1	ν_4	II
16	F ₂	4	16	F ₁	2	952.21465	86.5	3.4	ν_4	III
16	F ₁	4	16	F ₂	1	952.21465	86.5	-2.0	ν_4	III
21	F ₂	6	21	F ₁	1	952.47540	82.4	-4.5	ν_4	III
21	F ₁	6	21	F ₂	1	952.47540	82.4	-4.2	ν_4	III
9	A ₁	2	10	A ₂	1	952.56266	80.4	0.4	ν_4	II
9	F ₁	7	10	F ₂	1	952.64544	77.0	0.4	ν_4	II
9	E	5	10	E	1	952.68205	84.1	1.2	ν_4	II
15	F ₁	3	15	F ₂	3	952.74486	91.3	-5.4	ν_4	III
8	A ₂	2	9	A ₁	1	952.86729	78.7	0.1	ν_4	II
8	F ₂	6	9	F ₁	2	954.03985	75.8	0.3	ν_4	II
8	E	4	9	E	1	954.25349	81.3	0.6	ν_4	II
15	E	3	15	E	1	954.56648	79.1	-6.9	ν_4	III
15	F ₁	4	15	F ₂	2	954.56648	79.1	-3.2	ν_4	III
15	A ₁	1	15	A ₂	1	954.56648	79.1	6.9	ν_4	III
20	F ₂	6	20	F ₁	1	955.18050	66.9	-1.4	ν_4	III
20	E	4	20	E	1	955.18050	66.9	-1.2	ν_4	III
20	A ₂	2	20	A ₁	1	955.18050	66.9	-1.9	ν_4	III
7	F ₁	5	8	F ₂	2	956.09243	73.0	0.1	ν_4	II
8	F ₂	7	9	F ₁	1	956.21923	74.2	0.9	ν_4	II
7	E	3	8	E	2	956.37919	81.1	0.3	ν_4	II
7	F ₂	4	8	F ₁	2	957.07130	73.0	0.4	ν_4	II
13	F ₂	2	13	F ₁	3	957.64147	86.8	-1.9	ν_4	III
19	F ₁	6	19	F ₂	1	957.83888	61.8	-0.5	ν_4	III
19	F ₂	5	19	F ₁	1	957.83888	61.8	-1.0	ν_4	III
7	F ₁	6	8	F ₂	1	958.09755	72.8	0.8	ν_4	II

Table D.1 – Continued.

<i>J</i>	γ	<i>n</i>	<i>J'</i>	γ'	<i>n'</i>	ν^{exp} , cm^{-1}	Transmittance, %	$\delta \cdot 10^{-4}$, cm^{-1}	Band	Spectra
<i>I</i>			<i>2</i>			<i>3</i>	<i>4</i>	<i>5</i>	<i>6</i>	<i>7</i>
13	E	2	13	E	1	959.20870	88.7	-0.7	ν_4	III
13	F ₂	3	13	F ₁	2	959.21289	87.3	-1.1	ν_4	III
13	A ₂	2	13	A ₁	1	959.22051	89.3	1.1	ν_4	III
7	F ₂	5	8	F ₁	1	959.68042	71.9	0.9	ν_4	II
7	A ₂	2	8	A ₁	1	959.80984	75.5	0.7	ν_4	II
4	F ₂	2	5	F ₁	2	959.87264	94.3	-0.1	ν_4	III
4	E	1	5	E	1	960.08583	93.0	1.8	ν_4	III
18	F ₁	5	18	F ₂	1	960.44484	32.4	0.4	ν_4	III
18	A ₁	2	18	A ₂	1	960.44484	32.4	0.8	ν_4	III
18	E	4	18	E	1	960.44484	32.4	0.2	ν_4	III
6	F ₂	4	7	F ₁	2	960.46108	71.0	0.4	ν_4	II
6	E	3	7	E	1	960.96652	79.3	0.4	ν_4	II
6	F ₁	4	7	F ₂	2	961.32867	71.4	0.5	ν_4	II
6	A ₁	2	7	A ₂	1	962.02922	75.1	0.5	ν_4	II
17	F ₁	5	17	F ₂	1	962.99170	33.0	1.1	ν_4	III
17	F ₂	5	17	F ₁	1	962.99170	33.0	1.3	ν_4	III
6	F ₁	5	7	F ₂	1	963.08787	70.7	1.0	ν_4	II
6	F ₂	5	7	F ₁	1	963.27069	69.7	0.4	ν_4	II
11	A ₁	1	11	A ₂	1	963.75574	85.3	0.4	ν_4	III
11	F ₁	3	11	F ₂	2	963.78450	85.5	-1.3	ν_4	III
5	A ₂	2	6	A ₁	1	964.57778	74.8	0.5	ν_4	II
5	F ₂	4	6	F ₁	1	964.92409	70.8	0.8	ν_4	II
5	F ₁	3	6	F ₂	2	965.30443	70.7	0.9	ν_4	II
16	F ₂	5	16	F ₁	1	965.47194	88.9	0.0	ν_4	II
16	E	3	16	E	1	965.47194	88.9	-1.0	ν_4	II
16	A ₂	2	16	A ₁	1	965.47194	88.9	2.1	ν_4	II
10	F ₁	2	10	F ₂	2	966.01996	84.2	-7.2	ν_4	III
10	F ₂	3	10	F ₁	1	966.06464	89.6	0.2	ν_4	III
5	A ₁	1	6	A ₂	1	966.29970	74.7	1.0	ν_4	II
5	F ₁	4	6	F ₂	1	966.68849	70.4	0.6	ν_4	II
9	F ₂	1	9	F ₁	3	967.22275	94.7	4.4	ν_4	III
19	A ₁	3	19	A ₂	1	967.79295	50.8	-2.7	ν_4	III
19	E	4	19	E	1	967.79295	50.8	2.7	ν_4	III
19	F ₁	7	19	F ₂	2	967.79295	50.8	0.8	ν_4	III
15	F ₁	5	15	F ₂	1	967.87782	87.6	-2.4	ν_4	II
15	F ₂	4	15	F ₁	1	967.87782	87.6	4.2	ν_4	II
9	F ₂	2	9	F ₁	2	968.28547	85.5	0.2	ν_4	III
9	A ₂	1	9	A ₁	1	968.33830	98.8	-1.5	ν_4	II
4	F ₂	3	5	F ₁	2	968.87144	72.0	0.7	ν_4	II
4	E	2	5	E	1	969.09716	79.4	1.6	ν_4	II
18	F ₂	6	18	F ₁	1	969.85631	48.3	-1.9	ν_4	III
18	F ₁	6	18	F ₂	2	969.85631	48.3	4.1	ν_4	III
4	F ₁	3	5	F ₂	1	969.92662	71.7	1.0	ν_4	II
4	F ₂	4	5	F ₁	1	970.31147	70.7	0.9	ν_4	II
13	F ₂	4	13	F ₁	1	972.42680	87.6	0.8	ν_4	II

Table D.1 – Continued.

<i>J</i>	γ	<i>n</i>	<i>J'</i>	γ'	<i>n'</i>	ν^{exp} , cm^{-1}	Transmittance, %	$\delta \cdot 10^{-4}$, cm^{-1}	Band	Spectra
<i>I</i>			<i>2</i>			<i>3</i>	<i>4</i>	<i>5</i>	<i>6</i>	<i>7</i>
13	F ₁	4	13	F ₂	1	972.43066	87.7	1.7	v ₄	II
3	F ₁	3	4	F ₂	1	972.78515	73.7	0.3	v ₄	II
3	E	2	4	E	1	973.38536	81.8	0.4	v ₄	II
3	F ₂	2	4	F ₁	1	973.60651	74.0	1.2	v ₄	II
19	F ₁	8	19	F ₂	3	973.61585	73.9	-2.8	v ₄	III
16	F ₁	5	16	F ₂	1	973.79832	46.8	0.2	v ₄	III
16	F ₂	6	16	F ₁	2	973.80669	41.5	1.3	v ₄	III
3	A ₂	1	4	A ₁	1	973.88983	66.4	7.5	v ₄	II
12	A ₂	1	12	A ₁	1	974.54511	86.6	1.5	v ₄	II
12	F ₂	4	12	F ₁	1	974.55285	84.4	0.8	v ₄	II
12	E	3	12	E	1	974.55684	89.0	1.4	v ₄	II
23	F ₁	10	23	F ₂	4	975.27430	92.8	-0.3	v ₄	III
18	A ₂	2	18	A ₁	1	975.40627	67.8	-6.8	v ₄	III
18	F ₂	7	18	F ₁	2	975.43282	51.4	-7.1	v ₄	III
15	A ₁	2	15	A ₂	1	975.64626	40.9	0.5	v ₄	III
15	F ₁	6	15	F ₂	2	975.66482	33.3	0.4	v ₄	III
15	E	4	15	E	1	975.67382	41.1	-3.1	v ₄	III
20	F ₁	8	20	F ₂	3	976.37759	86.0	1.0	v ₄	III
20	F ₂	8	20	F ₁	3	976.43936	81.9	-2.6	v ₄	III
2	A ₁	1	3	A ₂	1	976.48305	76.6	5.2	v ₄	II
11	F ₂	3	11	F ₁	1	976.55293	79.6	1.3	v ₄	II
2	F ₁	2	3	F ₂	1	976.88222	79.1	0.5	v ₄	II
22	A ₁	4	22	A ₂	2	977.06210	89.7	2.4	v ₄	III
17	F ₂	7	17	F ₁	3	977.14099	48.5	3.9	v ₄	III
19	F ₂	7	19	F ₁	3	978.06922	72.8	0.7	v ₄	III
19	A ₂	3	19	A ₁	1	978.20556	77.1	-0.7	v ₄	III
10	E	2	10	E	1	978.42441	84.0	0.6	v ₄	II
10	F ₁	3	10	F ₂	1	978.43863	76.8	0.2	v ₄	II
10	A ₁	2	10	A ₂	1	978.46776	80.9	0.5	v ₄	II
16	A ₁	3	16	A ₂	1	978.92617	31.3	-4.6	v ₄	III
13	F ₂	5	13	F ₁	2	979.10668	88.4	-0.6	v ₄	II
13	A ₂	3	13	A ₁	1	979.17889	90.2	-0.3	v ₄	II
20	A ₂	3	20	A ₁	2	979.71492	84.2	-0.6	v ₄	III
18	F ₂	8	18	F ₁	3	979.74992	65.1	-0.9	v ₄	III
20	F ₂	9	20	F ₁	4	980.05731	84.0	2.4	v ₄	III
9	F ₂	3	9	F ₁	1	980.14776	73.9	-0.3	v ₄	II
9	F ₁	3	9	F ₂	1	980.19933	74.1	0.0	v ₄	II
15	F ₂	5	15	F ₁	2	980.23407	91.7	-0.5	v ₄	II
1	F ₁	1	2	F ₂	1	980.43462	74.3	7.6	v ₄	II
12	F ₁	4	12	F ₂	1	980.59813	85.0	-0.4	v ₄	II
1	E	1	2	E	1	980.62295	89.2	-1.1	v ₄	II
12	F ₂	5	12	F ₁	2	980.72082	85.2	-1.1	v ₄	II
19	F ₂	8	19	F ₁	4	981.17372	74.0	1.8	v ₄	III
17	E	5	17	E	2	981.25017	63.4	-2.4	v ₄	III
19	F ₂	8	19	F ₁	3	981.25572	93.6	-6.7	v ₄	III

Table D.1 – Continued.

<i>J</i>	γ	<i>n</i>	<i>J'</i>	γ'	<i>n'</i>	ν^{exp} , cm^{-1}	Transmittance, %	$\delta \cdot 10^{-4}$, cm^{-1}	Band	Spectra
<i>I</i>			<i>2</i>			<i>3</i>	<i>4</i>	<i>5</i>	<i>6</i>	<i>7</i>
14	A ₂	2	14	A ₁	1	981.45684	91.9	0.8	v ₄	II
8	A ₂	1	8	A ₁	1	981.66614	74.9	0.4	v ₄	II
14	F ₂	6	14	F ₁	2	981.72474	90.9	-1.5	v ₄	II
8	F ₂	3	8	F ₁	1	981.74936	69.9	0.3	v ₄	II
8	E	2	8	E	1	981.79391	79.6	-0.6	v ₄	II
11	F ₁	5	11	F ₂	2	982.07399	79.4	2.1	v ₄	II
16	F ₁	7	16	F ₂	3	982.10394	37.7	0.0	v ₄	III
11	E	3	11	E	1	982.17551	79.6	-0.6	v ₄	II
20	F ₁	9	20	F ₂	4	982.21120	67.7	1.4	v ₄	III
18	F ₁	8	18	F ₂	5	982.48988	93.8	1.7	v ₄	III
13	F ₂	6	13	F ₁	3	982.79683	87.5	-0.9	v ₄	II
19	A ₁	4	19	A ₂	2	982.91588	77.1	-0.9	v ₄	III
7	F ₂	2	7	F ₁	1	983.08560	67.1	1.2	v ₄	II
13	F ₁	5	13	F ₂	3	983.14627	84.9	2.7	v ₄	III
15	E	5	15	E	2	983.15649	93.0	-0.9	v ₄	II
13	F ₁	5	13	F ₂	2	983.18292	88.2	-0.9	v ₄	II
10	F ₁	4	10	F ₂	2	983.21380	76.5	-1.2	v ₄	II
7	F ₁	3	7	F ₂	1	983.22284	68.9	-0.4	v ₄	II
17	F ₂	8	17	F ₁	4	983.23346	50.3	-0.3	v ₄	III
10	F ₂	4	10	F ₁	2	983.46447	80.4	3.6	v ₄	III
20	F ₂	10	20	F ₁	5	983.81357	81.4	-2.6	v ₄	III
16	A ₂	3	16	A ₁	2	983.86897	41.7	2.5	v ₄	III
18	A ₁	3	18	A ₂	2	984.01094	63.3	0.9	v ₄	III
6	E	2	6	E	1	984.26513	62.9	-1.6	v ₄	II
9	E	3	9	E	1	984.26513	62.9	2.6	v ₄	II
6	F ₁	2	6	F ₂	1	984.36414	66.9	-0.1	v ₄	II
9	F ₂	4	9	F ₁	2	984.43734	74.3	-0.4	v ₄	II
19	F ₁	10	19	F ₂	4	984.45982	88.7	3.7	v ₄	III
6	A ₁	1	6	A ₂	1	984.61411	72.0	-0.1	v ₄	II
13	A ₁	2	13	A ₂	1	984.64161	88.2	-0.6	v ₄	II
15	A ₂	2	15	A ₁	1	984.64944	33.2	-3.2	v ₄	III
20	E	7	20	E	4	984.66285	87.0	1.4	v ₄	III
11	F ₂	4	11	F ₁	2	984.69215	62.0	0.8	v ₄	II
17	F ₁	8	17	F ₂	4	984.76637	53.0	-0.8	v ₄	III
12	A ₁	2	12	A ₂	1	984.94664	86.1	-3.3	v ₄	II
9	A ₂	2	9	A ₁	1	984.97752	78.1	-1.0	v ₄	II
8	F ₁	3	8	F ₂	1	985.13595	70.0	-0.1	v ₄	II
16	F ₂	8	16	F ₁	4	985.14894	41.4	-0.7	v ₄	III
5	F ₂	2	5	F ₁	1	985.23486	67.2	-1.2	v ₄	II
14	F ₂	7	14	F ₁	3	985.32563	89.8	-0.4	v ₄	II
19	F ₂	9	19	F ₁	5	985.41895	75.6	0.2	v ₄	III
18	F ₂	9	18	F ₁	4	985.47673	48.4	-1.9	v ₄	III
17	E	6	17	E	3	985.59857	34.4	3.3	v ₄	III
11	F ₁	6	11	F ₂	3	985.62888	79.1	-1.3	v ₄	II
13	F ₁	6	13	F ₂	3	985.65919	87.5	-1.0	v ₄	II

Table D.1 – Continued.

<i>J</i>	γ	<i>n</i>	<i>J'</i>	γ'	<i>n'</i>	ν^{exp} , cm^{-1}	Transmittance, %	$\delta \cdot 10^{-4}$, cm^{-1}	Band	Spectra
<i>I</i>			<i>2</i>			<i>3</i>	<i>4</i>	<i>5</i>	<i>6</i>	<i>7</i>
15	F ₂	7	15	F ₁	4	985.66611	87.1	3.0	v ₄	II
7	A ₁	2	7	A ₂	1	985.70648	71.0	0.1	v ₄	II
8	F ₂	4	8	F ₁	2	985.74113	70.0	-0.7	v ₄	II
15	F ₂	7	15	F ₁	2	985.77435	40.2	5.9	v ₄	III
4	A ₂	1	4	A ₁	1	985.88461	73.2	-0.4	v ₄	II
17	F ₂	9	17	F ₁	5	985.93803	53.9	-0.1	v ₄	III
10	F ₂	5	10	F ₁	2	985.98791	71.4	-3.0	v ₄	II
10	F ₂	5	10	F ₁	1	986.00686	77.2	0.3	v ₄	III
7	F ₁	4	7	F ₂	2	986.19223	61.9	-5.5	v ₄	II
10	E	3	10	E	2	986.37920	74.0	-5.7	v ₄	II
7	E	2	7	E	1	986.50591	71.7	2.0	v ₄	II
12	F ₂	6	12	F ₁	3	986.57349	82.9	-0.4	v ₄	II
11	E	4	11	E	2	986.58128	85.0	-2.7	v ₄	II
3	F ₂	1	3	F ₁	1	986.64045	69.6	-1.1	v ₄	II
13	F ₂	7	13	F ₁	4	986.69028	85.4	0.2	v ₄	II
9	F ₁	4	9	F ₂	2	986.83790	72.6	-0.5	v ₄	II
8	E	3	8	E	2	986.84592	78.5	-0.8	v ₄	II
11	F ₂	5	11	F ₁	3	986.86354	52.6	-1.7	v ₄	II
12	A ₂	2	12	A ₁	2	986.96172	79.0	9.5	v ₄	II
3	F ₁	2	3	F ₂	1	986.97416	71.8	0.2	v ₄	II
6	F ₂	3	6	F ₁	1	986.98632	63.2	-1.5	v ₄	II
5	E	2	5	E	1	987.01667	75.6	-1.0	v ₄	II
2	E	1	2	E	1	987.04211	84.2	0.4	v ₄	II
2	F ₁	1	2	F ₂	1	987.20802	48.6	0.8	v ₄	II
7	F ₂	3	7	F ₁	2	987.20802	48.6	-1.5	v ₄	II
5	F ₂	3	5	F ₁	2	987.21414	66.9	-1.2	v ₄	II
9	A ₁	1	9	A ₂	1	987.22208	76.0	-0.5	v ₄	II
1	F ₂	1	1	F ₁	1	987.30138	85.0	1.2	v ₄	II
4	F ₁	2	4	F ₂	1	987.32172	64.6	-0.7	v ₄	II
6	A ₂	1	6	A ₁	1	987.38212	70.7	-1.0	v ₄	II
3	A ₁	1	3	A ₂	1	987.45508	76.4	-0.8	v ₄	II
1	A ₂	1	0	A ₁	1	990.69485	86.0	0.4	v ₄	II
2	F ₂	1	1	F ₁	1	993.94075	76.1	-1.2	v ₄	II
3	F ₁	1	2	F ₂	1	997.09968	71.0	-1.3	v ₄	II
3	E	1	2	E	1	997.14339	79.5	-1.3	v ₄	II
6	F ₂	4	6	F ₁	1	997.28734	94.5	0.0	v ₄	III
6	E	3	6	E	1	997.79760	92.8	0.9	v ₄	III
6	F ₁	4	6	F ₂	1	998.15810	71.7	2.1	v ₄	III
5	E	3	5	E	1	998.36065	95.2	4.0	v ₄	III
7	E	3	7	E	1	998.45423	91.6	0.5	v ₄	III
17	A ₁	3	17	A ₂	1	998.65605	94.2	1.0	v ₄	III
6	A ₁	2	6	A ₂	1	998.85498	78.7	2.6	v ₄	III
7	F ₂	4	7	F ₁	1	999.15397	86.1	1.5	v ₄	III
9	F ₁	5	9	F ₂	2	999.34834	95.0	0.4	v ₄	III
10	F ₂	6	10	F ₁	2	999.73540	95.6	1.4	v ₄	III

Table D.1 – Continued.

<i>J</i>	γ	<i>n</i>	<i>J'</i>	γ'	<i>n'</i>	ν^{exp} , cm^{-1}	Transmittance, %	$\delta \cdot 10^{-4}$, cm^{-1}	Band	Spectra
<i>I</i>			<i>2</i>			<i>3</i>	<i>4</i>	<i>5</i>	<i>6</i>	<i>7</i>
9	E	4	9	E	1	999.80633	92.8	0.1	ν_4	III
4	A ₁	1	3	A ₂	1	1000.08859	71.0	-1.8	ν_4	II
7	F ₁	6	7	F ₂	2	1000.16525	89.5	1.1	ν_4	III
7	F ₁	6	7	F ₂	1	1000.17449	81.4	-0.2	ν_4	III
4	F ₁	1	3	F ₂	1	1000.20129	66.2	-1.5	ν_4	II
9	F ₂	6	9	F ₁	2	1000.21959	90.3	4.7	ν_4	III
4	F ₂	1	3	F ₁	1	1000.29873	66.4	-1.7	ν_4	II
11	F ₁	7	11	F ₂	2	1000.52037	84.7	3.0	ν_4	III
13	F ₂	8	13	F ₁	3	1000.59634	92.7	2.6	ν_4	III
10	F ₁	6	10	F ₂	2	1000.61766	81.9	-1.9	ν_4	III
12	F ₁	7	12	F ₂	1	1000.76229	86.8	-1.5	ν_4	III
11	A ₁	3	11	A ₂	1	1001.05607	88.8	0.1	ν_4	III
8	F ₂	6	8	F ₁	2	1001.34764	65.5	0.3	ν_4	III
8	E	4	8	E	2	1001.55594	93.5	3.6	ν_4	III
9	F ₂	7	9	F ₁	1	1002.57482	85.2	0.4	ν_4	III
10	F ₂	7	10	F ₁	2	1002.66426	81.7	0.3	ν_4	III
10	F ₂	7	10	F ₁	1	1002.68288	84.0	0.3	ν_4	III
9	F ₁	6	9	F ₂	2	1002.92592	92.4	2.9	ν_4	III
9	F ₁	6	9	F ₂	1	1002.96161	79.0	2.5	ν_4	III
5	F ₁	1	4	F ₂	1	1003.08626	58.7	-4.7	ν_4	II
5	E	1	4	E	1	1003.29493	73.9	-2.0	ν_4	II
5	F ₂	1	4	F ₁	1	1003.37419	59.4	-1.5	ν_4	II
11	F ₁	8	11	F ₂	3	1003.42288	82.8	0.1	ν_4	III
11	F ₁	8	11	F ₂	2	1003.45746	88.5	-1.3	ν_4	III
5	A ₂	1	4	A ₁	1	1003.48926	68.9	-1.9	ν_4	II
11	E	5	11	E	2	1003.71488	91.2	-1.6	ν_4	III
11	E	5	11	E	1	1003.75313	54.5	1.7	ν_4	III
13	F ₁	8	13	F ₂	3	1004.14404	81.4	-0.1	ν_4	III
10	F ₁	7	10	F ₂	2	1004.17469	94.2	1.3	ν_4	III
10	F ₁	7	10	F ₂	1	1004.20381	80.9	1.4	ν_4	III
15	A ₂	3	15	A ₁	1	1004.41506	77.5	3.5	ν_4	III
12	F ₂	8	12	F ₁	2	1004.79187	80.8	1.8	ν_4	III
15	F ₂	9	15	F ₁	4	1004.98182	86.0	-2.8	ν_4	III
13	E	6	13	E	1	1005.26381	86.8	3.0	ν_4	III
17	E	7	17	E	2	1005.30502	95.8	-2.3	ν_4	III
15	F ₁	10	15	F ₂	4	1005.55560	83.7	-1.7	ν_4	III
16	E	7	16	E	3	1005.55560	83.7	-3.8	ν_4	III
13	F ₂	9	13	F ₁	2	1005.64728	86.2	-0.5	ν_4	III
16	E	7	16	E	2	1005.70942	93.4	2.0	ν_4	III
11	F ₁	9	11	F ₂	1	1005.78364	78.2	-2.3	ν_4	III
19	F ₂	11	19	F ₁	5	1005.78364	78.2	3.3	ν_4	III
6	F ₂	1	5	F ₁	2	1005.99350	63.0	-1.6	ν_4	II
6	E	1	5	E	1	1006.05538	70.0	-1.3	ν_4	II
16	F ₁	10	16	F ₂	2	1006.18696	87.5	-2.4	ν_4	III
13	A ₂	4	13	A ₁	1	1006.24824	79.8	-3.7	ν_4	III

Table D.1 – Continued.

<i>J</i>	γ	<i>n</i>	<i>J'</i>	γ'	<i>n'</i>	ν^{exp} , cm^{-1}	Transmittance, %	$\delta \cdot 10^{-4}$, cm^{-1}	Band	Spectra
<i>I</i>		<i>2</i>		<i>3</i>		<i>4</i>		<i>5</i>		<i>7</i>
17	F ₂	11	17	F ₁	5	1006.28675	90.9	-3.5	v ₄	III
6	F ₁	1	5	F ₂	1	1006.38471	63.0	-1.9	v ₄	II
6	F ₂	2	5	F ₁	1	1006.53847	50.3	-2.7	v ₄	II
12	A ₂	3	12	A ₁	1	1006.72718	82.2	-1.1	v ₄	III
16	A ₁	4	16	A ₂	1	1007.10425	89.2	-1.4	v ₄	III
14	F ₂	10	14	F ₁	1	1007.11534	78.5	3.0	v ₄	III
12	E	6	12	E	1	1007.14355	86.2	-4.7	v ₄	III
15	A ₁	4	15	A ₂	1	1007.27005	85.1	-2.1	v ₄	III
18	F ₂	12	18	F ₁	2	1008.13169	93.0	-2.7	v ₄	III
15	E	7	15	E	1	1008.14306	92.1	-1.0	v ₄	III
18	E	8	18	E	2	1008.39726	95.1	-2.2	v ₄	III
13	F ₁	9	13	F ₂	1	1008.50846	87.6	0.1	v ₄	III
19	F ₂	12	19	F ₁	2	1008.72908	95.0	0.8	v ₄	III
7	A ₂	1	6	A ₁	1	1008.76393	67.7	-1.7	v ₄	II
7	F ₂	1	6	F ₁	1	1008.85849	63.7	-1.8	v ₄	II
7	F ₁	1	6	F ₂	2	1008.97025	64.0	-1.8	v ₄	II
7	A ₁	1	6	A ₂	1	1009.39510	68.8	-1.9	v ₄	II
7	F ₁	2	6	F ₂	1	1009.54529	63.7	-2.0	v ₄	II
7	E	1	6	E	1	1009.59447	74.1	-1.8	v ₄	II
14	E	7	14	E	1	1009.75526	92.1	-1.5	v ₄	III
14	F ₁	10	14	F ₂	1	1009.81912	88.6	-2.4	v ₄	III
17	F ₂	12	17	F ₁	2	1010.14416	78.2	-0.7	v ₄	III
15	F ₂	10	15	F ₁	1	1011.16168	82.2	-2.8	v ₄	III
18	F ₁	12	18	F ₂	2	1011.16168	82.2	2.4	v ₄	III
8	F ₂	1	7	F ₁	2	1011.55494	61.7	2.5	v ₄	II
8	F ₁	1	7	F ₂	2	1011.80317	62.8	-0.9	v ₄	II
8	A ₁	1	7	A ₂	1	1012.00620	68.7	0.3	v ₄	II
8	F ₁	2	7	F ₂	1	1012.54399	65.0	-2.4	v ₄	II
16	E	8	16	E	1	1012.60450	28.1	-3.1	v ₄	III
8	F ₂	2	7	F ₁	1	1012.62758	65.1	-1.4	v ₄	II
20	F ₂	14	20	F ₁	2	1013.50067	95.2	3.0	v ₄	III
15	E	9	16	E	1	1013.67357	84.9	-3.8	v ₂	III
15	A ₂	5	16	A ₁	1	1013.67357	84.9	-7.3	v ₂	III
15	F ₂	13	16	F ₁	1	1013.67357	84.9	-5.0	v ₂	III
9	F ₁	1	8	F ₂	2	1014.26298	68.3	-1.3	v ₄	II
9	E	1	8	E	2	1014.32754	77.2	-1.6	v ₄	II
9	F ₂	1	8	F ₁	2	1014.54223	64.4	-1.2	v ₄	II
9	F ₁	2	8	F ₂	1	1014.81533	57.8	0.7	v ₄	II
15	F ₂	14	16	F ₁	2	1015.26652	83.5	-1.6	v ₂	III
9	E	2	8	E	1	1015.57535	77.6	-2.3	v ₄	II
9	F ₂	2	8	F ₁	1	1015.61058	68.3	-1.9	v ₄	II
10	F ₁	1	9	F ₂	2	1016.94448	71.5	-1.1	v ₄	II
10	F ₂	1	9	F ₁	3	1017.04361	72.1	-1.0	v ₄	II
10	A ₂	1	9	A ₁	1	1017.28592	75.8	-1.3	v ₄	II
19	F ₂	23	20	F ₁	2	1017.47317	96.7	-0.8	v ₂	III

Table D.1 – Continued.

<i>J</i>	γ	<i>n</i>	<i>J'</i>	γ'	<i>n'</i>	ν^{exp} , cm^{-1}	Transmittance, %	$\delta \cdot 10^{-4}$, cm^{-1}	Band	Spectra
<i>I</i>		<i>2</i>		<i>3</i>		<i>4</i>		<i>5</i>		<i>7</i>
10	F ₂	2	9	F ₁	2	1017.56480	71.8	-1.5	v ₄	II
10	E	1	9	E	1	1017.63531	80.2	-1.6	v ₄	II
6	F ₁	3	5	F ₂	1	1018.17619	83.1	-0.9	v ₄	III
10	F ₂	3	9	F ₁	1	1018.63384	72.4	-2.1	v ₄	II
11	F ₁	1	10	F ₂	3	1019.49596	75.3	-0.5	v ₄	II
11	E	1	10	E	2	1019.59807	72.8	10.0	v ₄	II
11	F ₂	1	10	F ₁	2	1019.69233	73.2	-0.2	v ₄	II
14	A ₁	5	15	A ₂	1	1019.86411	94.5	4.8	v ₂	III
11	A ₂	1	10	A ₁	1	1019.98004	79.0	-0.4	v ₄	II
11	F ₂	2	10	F ₁	1	1020.30777	75.6	-1.4	v ₄	II
11	F ₁	2	10	F ₂	2	1020.43122	75.5	-1.3	v ₄	II
11	A ₁	1	10	A ₂	1	1021.55514	79.2	-1.2	v ₄	II
11	F ₁	3	10	F ₂	1	1021.58831	75.8	-1.8	v ₄	II
11	E	2	10	E	1	1021.60373	83.1	-1.9	v ₄	II
12	F ₂	1	11	F ₁	3	1022.05576	79.7	-0.3	v ₄	II
12	E	1	11	E	2	1022.11298	82.0	0.3	v ₄	II
12	F ₁	1	11	F ₂	3	1022.25119	79.6	-0.4	v ₄	II
7	A ₁	2	6	A ₂	1	1022.53184	86.4	-1.8	v ₄	III
12	F ₂	2	11	F ₁	2	1022.61270	41.8	0.8	v ₄	II
7	F ₁	4	6	F ₂	1	1023.02196	90.2	-0.9	v ₄	III
12	E	2	11	E	1	1023.10121	85.9	-0.4	v ₄	II
12	F ₁	2	11	F ₂	2	1023.16390	78.5	1.2	v ₄	II
12	A ₁	1	11	A ₂	1	1023.26313	82.7	-1.2	v ₄	II
7	E	2	6	E	1	1023.33689	91.1	1.5	v ₄	III
13	F ₂	12	14	F ₁	1	1024.29898	93.6	1.9	v ₂	III
12	F ₁	3	11	F ₂	1	1024.53255	80.3	-1.6	v ₄	II
13	A ₂	1	12	A ₁	2	1024.54122	79.4	2.1	v ₄	II
12	F ₂	3	11	F ₁	1	1024.55258	80.0	-1.5	v ₄	II
16	E	12	17	E	3	1024.57801	87.4	-1.2	v ₂	III
13	F ₂	1	12	F ₁	3	1024.59955	83.4	0.2	v ₄	II
13	A ₁	1	12	A ₂	1	1024.81810	79.5	-4.3	v ₄	II
13	F ₁	2	12	F ₂	2	1025.18458	83.9	0.1	v ₄	II
16	F ₁	20	17	F ₂	2	1025.28032	87.3	-1.1	v ₂	III
13	F ₂	2	12	F ₁	2	1025.88486	84.0	-0.4	v ₄	II
13	F ₁	3	12	F ₂	1	1025.97588	83.6	-0.3	v ₄	II
14	F ₂	1	13	F ₁	4	1027.04695	87.0	1.8	v ₄	II
8	F ₁	3	7	F ₂	1	1027.21284	80.6	-1.6	v ₄	III
15	F ₁	17	16	F ₂	4	1027.40888	86.2	2.3	v ₂	III
13	F ₂	3	12	F ₁	1	1027.47300	78.4	-0.4	v ₄	II
14	A ₁	1	13	A ₂	1	1027.53749	89.4	0.9	v ₄	II
15	F ₂	18	16	F ₁	4	1027.66384	87.9	3.9	v ₂	III
12	F ₁	11	13	F ₂	1	1027.69329	82.3	-3.3	v ₂	III
15	F ₁	18	16	F ₂	3	1027.72905	86.9	2.2	v ₂	III
15	F ₂	18	16	F ₁	3	1027.73467	86.4	-3.5	v ₂	III
14	F ₁	2	13	F ₂	2	1027.75471	87.2	0.2	v ₄	II

Table D.1 – Continued.

<i>J</i>	γ	<i>n</i>	<i>J'</i>	γ'	<i>n'</i>	ν^{exp} , cm^{-1}	Transmittance, %	$\delta \cdot 10^{-4}$, cm^{-1}	Band	Spectra
<i>I</i>			<i>2</i>			<i>3</i>	<i>4</i>	<i>5</i>	<i>6</i>	<i>7</i>
8	F ₂	4	7	F ₁	1	1027.82377	74.5	0.2	ν_4	III
14	F ₂	2	13	F ₁	3	1027.88281	85.0	1.4	ν_4	II
15	A ₁	6	16	A ₂	1	1028.12667	87.5	-0.7	ν_2	III
15	F ₁	19	16	F ₂	2	1028.13187	85.4	-2.8	ν_2	III
15	E	13	16	E	2	1028.13187	85.4	-4.6	ν_2	III
14	A ₂	1	13	A ₁	1	1028.61774	89.3	-0.1	ν_4	II
14	F ₂	3	13	F ₁	2	1028.68300	87.1	0.3	ν_4	II
14	E	2	13	E	1	1028.71104	87.3	1.9	ν_4	II
12	A ₂	4	13	A ₁	1	1028.78153	82.7	2.5	ν_2	III
15	F ₁	1	14	F ₂	4	1029.50070	89.6	1.5	ν_4	II
15	F ₂	1	14	F ₁	3	1029.63653	89.9	1.7	ν_4	II
15	F ₁	2	14	F ₂	3	1030.03827	90.1	-0.1	ν_4	II
14	A ₁	6	15	A ₂	2	1030.33992	79.0	8.1	ν_2	III
14	F ₁	3	13	F ₂	1	1030.37440	86.9	-1.1	ν_4	II
14	F ₂	4	13	F ₁	1	1030.38146	87.5	-1.1	ν_4	II
14	F ₂	16	15	F ₁	4	1030.42246	85.1	1.0	ν_2	III
15	F ₂	2	14	F ₁	2	1030.44518	90.4	0.0	ν_4	II
15	A ₂	1	14	A ₁	1	1030.56270	91.5	0.4	ν_4	II
15	F ₂	3	14	F ₁	1	1031.39307	90.4	0.7	ν_4	II
15	F ₁	3	14	F ₂	2	1031.42970	90.3	0.0	ν_4	II
9	E	3	8	E	1	1031.58810	81.4	-0.6	ν_4	III
16	A ₁	1	15	A ₂	2	1031.90211	30.2	2.2	ν_4	III
16	F ₁	1	15	F ₂	4	1031.94600	26.6	2.2	ν_4	III
16	F ₂	1	15	F ₁	4	1032.00222	26.8	2.4	ν_4	III
16	A ₂	1	15	A ₁	1	1032.09211	26.0	4.0	ν_4	III
16	F ₂	2	15	F ₁	3	1032.48557	20.6	-0.5	ν_4	III
16	E	1	15	E	2	1032.55428	36.0	2.2	ν_4	III
16	F ₁	2	15	F ₂	3	1032.99121	25.9	1.3	ν_4	III
16	F ₂	3	15	F ₁	2	1033.10543	26.6	0.2	ν_4	III
15	A ₁	1	14	A ₂	1	1033.25317	91.6	0.7	ν_4	II
15	F ₁	4	14	F ₂	1	1033.25745	87.1	5.3	ν_4	II
13	F ₁	15	14	F ₂	4	1033.42840	79.5	3.6	ν_2	III
13	E	10	14	E	3	1033.46449	83.3	3.0	ν_2	III
13	F ₂	15	14	F ₁	3	1033.59034	32.0	0.0	ν_2	III
13	F ₁	16	14	F ₂	3	1033.72703	77.1	-0.8	ν_2	III
13	E	11	14	E	2	1034.07163	95.3	-2.1	ν_2	II
16	E	2	15	E	1	1034.10933	32.9	0.9	ν_4	III
16	F ₁	3	15	F ₂	2	1034.12060	25.8	0.1	ν_4	III
16	A ₁	2	15	A ₂	1	1034.14221	34.1	1.2	ν_4	III
17	F ₁	1	16	F ₂	4	1034.32142	35.4	3.0	ν_4	III
17	E	1	16	E	3	1034.37275	51.4	2.1	ν_4	III
17	F ₂	1	16	F ₁	4	1034.42582	93.9	2.0	ν_4	II
17	A ₂	1	16	A ₁	2	1034.78080	47.4	2.2	ν_4	III
17	F ₂	2	16	F ₁	3	1034.93622	35.0	-1.9	ν_4	III
17	F ₁	3	16	F ₂	2	1035.64381	34.0	0.8	ν_4	III

Table D.1 – Continued.

<i>J</i>	γ	<i>n</i>	<i>J'</i>	γ'	<i>n'</i>	ν^{exp} , cm^{-1}	Transmittance, %	$\delta \cdot 10^{-4}$, cm^{-1}	Band	Spectra
<i>I</i>			<i>2</i>			<i>3</i>	<i>4</i>	<i>5</i>	<i>6</i>	<i>7</i>
17	E	2	16	E	2	1035.67618	13.6	2.1	ν_4	III
10	F ₁	4	9	F ₂	1	1035.77914	73.9	1.2	ν_4	III
10	F ₂	4	9	F ₁	1	1036.05275	69.4	6.0	ν_4	III
18	F ₂	1	17	F ₁	5	1036.70258	48.8	1.3	ν_4	III
18	E	1	17	E	3	1036.73742	53.2	-2.8	ν_4	III
12	A ₁	5	13	A ₂	1	1036.91729	78.4	-0.3	ν_2	III
18	F ₂	2	17	F ₁	4	1037.18318	46.7	-1.4	ν_4	III
10	F ₂	10	11	F ₁	1	1037.26915	92.2	-1.8	ν_2	III
18	F ₁	2	17	F ₂	3	1037.49461	50.9	5.2	ν_4	III
18	F ₂	3	17	F ₁	3	1038.23633	53.8	2.6	ν_4	III
19	A ₂	1	18	A ₁	2	1039.04656	69.9	1.4	ν_4	III
19	F ₂	1	18	F ₁	4	1039.08022	62.2	2.1	ν_4	III
19	F ₁	1	18	F ₂	5	1039.12299	43.6	4.5	ν_4	III
19	A ₁	1	18	A ₂	2	1039.18857	66.9	0.1	ν_4	III
18	A ₂	1	17	A ₁	1	1039.46878	57.8	2.2	ν_4	III
19	F ₁	2	18	F ₂	4	1039.54409	61.9	5.6	ν_4	III
19	E	1	18	E	3	1039.59978	70.5	2.9	ν_4	III
11	F ₁	5	10	F ₂	1	1039.87768	77.8	0.4	ν_4	III
19	F ₂	2	18	F ₁	3	1039.92591	58.4	8.1	ν_4	III
11	E	3	10	E	1	1039.98206	84.3	0.0	ν_4	III
11	F ₂	13	12	F ₁	3	1039.99983	67.1	-4.3	ν_2	III
19	F ₁	3	18	F ₂	3	1040.03319	65.6	3.4	ν_4	III
11	F ₁	13	12	F ₂	3	1040.08381	76.1	2.5	ν_2	III
11	A ₁	5	12	A ₂	1	1040.33155	82.1	2.8	ν_2	III
11	F ₁	14	12	F ₂	2	1040.45252	67.9	0.0	ν_2	III
11	E	9	12	E	2	1040.48700	86.3	2.9	ν_2	III
8	A ₁	2	7	A ₂	1	1040.75367	87.7	-2.2	ν_4	III
19	F ₂	3	18	F ₁	2	1040.77375	62.1	-3.1	ν_4	III
20	E	1	19	E	3	1041.44607	70.8	0.9	ν_4	III
20	F ₁	1	19	F ₂	5	1041.48706	74.0	-0.4	ν_4	III
18	F ₂	5	17	F ₁	1	1041.72800	28.3	-0.4	ν_4	III
18	F ₁	4	17	F ₂	1	1041.72800	28.3	3.0	ν_4	III
20	A ₁	1	19	A ₂	2	1041.78923	71.9	-0.7	ν_4	III
20	F ₁	2	19	F ₂	4	1041.91207	72.7	0.3	ν_4	III
20	F ₂	2	19	F ₁	4	1041.99747	77.3	1.7	ν_4	III
20	A ₂	1	19	A ₁	1	1042.38745	64.0	-1.6	ν_4	III
20	F ₂	4	19	F ₁	2	1043.32152	73.7	0.9	ν_4	III
10	E	8	11	E	2	1043.49954	49.4	3.4	ν_2	III
12	F ₁	4	11	F ₂	1	1043.63011	38.3	-7.5	ν_4	III
12	F ₂	5	11	F ₁	1	1043.75887	32.5	3.3	ν_4	III
10	F ₂	13	11	F ₁	2	1043.86994	77.6	3.4	ν_2	III
21	F ₁	2	20	F ₂	4	1044.11751	82.4	-0.5	ν_4	III
10	E	9	11	E	1	1044.40936	86.5	2.3	ν_2	III
10	A ₁	5	11	A ₂	1	1044.43690	71.6	1.7	ν_2	III
19	A ₁	2	18	A ₂	1	1044.49373	40.1	2.1	ν_4	III

Table D.1 – Continued.

<i>J</i>	γ	<i>n</i>	<i>J'</i>	γ'	<i>n'</i>	ν^{exp} , cm^{-1}	Transmittance, %	$\delta \cdot 10^{-4}$, cm^{-1}	Band	Spectra
<i>I</i>			<i>2</i>			<i>3</i>	<i>4</i>	<i>5</i>	<i>6</i>	<i>7</i>
19	F ₁	5	18	F ₂	1	1044.49373	40.1	0.9	ν_4	III
19	E	3	18	E	1	1044.49373	40.1	0.4	ν_4	III
21	F ₁	3	20	F ₂	3	1044.93440	69.7	3.3	ν_4	III
22	A ₂	1	21	A ₁	2	1046.17088	87.2	-4.7	ν_4	III
9	F ₁	5	8	F ₂	1	1046.67550	87.9	0.4	ν_4	III
22	F ₂	3	21	F ₁	4	1046.79847	84.2	-3.6	ν_4	III
8	F ₂	8	9	F ₁	1	1046.90624	89.9	3.9	ν_2	III
12	F ₁	5	11	F ₂	2	1047.08936	77.6	5.7	ν_4	III
9	E	8	10	E	2	1047.21945	83.4	2.1	ν_2	III
20	F ₂	5	19	F ₁	1	1047.22937	62.1	0.5	ν_4	III
20	F ₁	5	19	F ₂	1	1047.22937	62.1	0.8	ν_4	III
8	A ₂	3	9	A ₁	1	1047.25768	92.2	3.4	ν_2	III
21	F ₁	5	20	F ₂	1	1047.33892	67.2	-5.0	ν_4	III
21	F ₂	4	20	F ₁	2	1047.33892	67.2	-0.4	ν_4	III
13	F ₂	5	12	F ₁	1	1047.36652	74.8	-2.6	ν_4	III
13	A ₂	3	12	A ₁	1	1047.44332	95.3	-3.0	ν_4	II
9	F ₂	12	10	F ₁	1	1047.86350	74.5	-3.7	ν_2	III
9	F ₁	12	10	F ₂	2	1047.89281	83.6	-5.7	ν_2	III
23	F ₂	1	22	F ₁	4	1048.61490	88.9	-0.9	ν_4	III
23	A ₂	1	22	A ₁	2	1048.61490	88.9	-9.9	ν_4	III
23	F ₁	4	22	F ₂	3	1049.81922	85.1	-6.9	ν_4	III
22	E	3	21	E	1	1049.91470	74.3	-2.4	ν_4	III
22	A ₂	2	21	A ₁	1	1049.91470	74.3	2.8	ν_4	III
22	F ₂	5	21	F ₁	2	1049.91470	74.3	-0.7	ν_4	III
21	A ₂	2	20	A ₁	1	1049.93439	68.6	0.5	ν_4	III
21	E	4	20	E	1	1049.93439	68.6	0.7	ν_4	III
21	F ₂	5	20	F ₁	1	1049.93439	68.6	0.7	ν_4	III
8	A ₁	4	9	A ₂	1	1050.78260	70.5	1.6	ν_2	III
8	F ₁	10	9	F ₂	2	1050.89571	60.6	8.7	ν_2	III
14	F ₁	5	13	F ₂	1	1050.89571	60.6	-1.1	ν_4	III
8	F ₂	10	9	F ₁	3	1050.99915	75.9	-3.1	ν_2	III
13	F ₂	6	12	F ₁	2	1051.04034	83.1	1.8	ν_4	III
22	F ₁	5	21	F ₂	1	1052.60790	77.8	-3.2	ν_4	III
22	F ₂	6	21	F ₁	1	1052.60790	77.8	-3.3	ν_4	III
15	A ₁	2	14	A ₂	1	1054.33342	74.3	-1.0	ν_4	III
15	F ₁	6	14	F ₂	1	1054.35496	81.3	0.4	ν_4	III
7	F ₁	9	8	F ₂	2	1054.76663	79.4	2.6	ν_2	III
14	A ₂	2	13	A ₁	1	1054.90899	85.1	2.3	ν_4	III
7	F ₂	9	8	F ₁	2	1055.17986	78.5	-3.6	ν_2	III
14	F ₂	6	13	F ₁	2	1055.19104	87.4	0.6	ν_4	III
11	A ₂	2	10	A ₁	1	1057.56308	91.5	-0.9	ν_4	III
6	F ₂	8	7	F ₁	2	1058.81828	81.8	2.2	ν_2	III
6	E	6	7	E	1	1059.07982	86.5	-5.6	ν_2	III
15	F ₁	7	14	F ₂	2	1059.12175	85.6	3.6	ν_4	III
6	F ₁	8	7	F ₂	2	1059.13014	85.8	3.4	ν_2	III

Table D.1 – Continued.

<i>J</i>	γ	<i>n</i>	<i>J'</i>	γ'	<i>n'</i>	ν^{exp} , cm^{-1}	Transmittance, %	$\delta \cdot 10^{-4}$, cm^{-1}	Band	Spectra
<i>I</i>			<i>2</i>			<i>3</i>	<i>4</i>	<i>5</i>	<i>6</i>	<i>7</i>
6	A ₁	3	7	A ₂	1	1059.19761	79.5	2.1	ν_2	III
17	F ₂	6	16	F ₁	1	1060.95241	84.1	-4.0	ν_4	III
17	A ₂	3	16	A ₁	1	1060.95770	88.8	-0.4	ν_4	III
11	F ₁	8	10	F ₂	2	1061.23213	93.4	-2.2	ν_4	III
5	A ₁	2	6	A ₂	1	1061.24025	93.7	2.4	ν_2	III
15	E	5	14	E	2	1061.80620	92.3	4.0	ν_4	III
5	A ₂	3	6	A ₁	1	1063.01011	76.3	-4.7	ν_2	III
5	F ₁	7	6	F ₂	2	1063.25173	85.1	1.1	ν_2	III
17	F ₂	7	16	F ₁	2	1066.20644	88.6	4.1	ν_4	III
17	F ₁	6	16	F ₂	1	1066.27697	82.6	2.2	ν_4	III
4	F ₁	5	5	F ₂	1	1066.51270	93.1	-6.9	ν_2	III
19	F ₁	7	18	F ₂	1	1067.24953	81.2	1.0	ν_4	III
19	A ₁	3	18	A ₂	1	1067.24953	81.2	8.7	ν_4	III
19	E	4	18	E	1	1067.24953	81.2	-2.9	ν_4	III
4	F ₂	6	5	F ₁	2	1067.48803	83.1	-7.3	ν_2	III
13	F ₁	7	12	F ₂	2	1068.09845	92.6	3.1	ν_4	III
18	A ₂	2	17	A ₁	1	1069.65376	88.3	2.0	ν_4	III
18	F ₂	7	17	F ₁	2	1069.68987	76.5	-2.3	ν_4	III
20	F ₂	7	19	F ₁	1	1070.30705	87.1	-2.3	ν_4	III
20	F ₁	6	19	F ₂	1	1070.30705	87.1	0.1	ν_4	III
3	F ₁	5	4	F ₂	1	1071.99964	91.6	0.7	ν_2	III
20	A ₁	3	19	A ₂	1	1076.32595	89.6	5.0	ν_4	III
19	A ₂	3	18	A ₁	1	1077.65775	91.9	-8.8	ν_4	III
16	F ₂	9	15	F ₁	3	1082.45305	95.9	0.8	ν_4	III
16	E	6	15	E	2	1082.72436	96.3	-1.4	ν_4	III
15	A ₂	3	14	A ₁	1	1083.13383	90.1	-5.6	ν_4	III
15	F ₂	9	14	F ₁	2	1083.69828	89.0	-1.5	ν_4	III
22	F ₁	8	21	F ₂	2	1087.67557	96.7	-0.3	ν_4	III
16	F ₂	10	15	F ₁	2	1088.67894	89.0	-6.0	ν_4	III
6	A ₂	2	6	A ₁	1	1092.52864	92.8	-4.9	ν_2	III
3	F ₂	4	3	F ₁	1	1092.69313	93.8	-0.5	ν_2	III
5	F ₂	6	5	F ₁	1	1093.67796	92.7	1.3	ν_2	III
4	F ₂	6	4	F ₁	1	1093.80611	95.1	-0.4	ν_2	III
6	E	5	6	E	1	1094.07925	87.1	-4.4	ν_2	III
8	F ₂	8	8	F ₁	2	1094.19215	96.4	3.5	ν_2	II
6	F ₁	7	6	F ₂	2	1094.24901	93.4	2.7	ν_2	III
9	A ₁	3	9	A ₂	1	1094.37931	93.4	-1.2	ν_2	III
7	F ₁	8	7	F ₂	2	1094.79992	92.9	0.9	ν_2	III
7	F ₁	8	7	F ₂	1	1094.80910	92.0	-1.0	ν_2	III
5	F ₁	7	5	F ₂	1	1094.82573	90.0	2.6	ν_2	III
8	E	6	8	E	2	1095.37358	95.4	0.5	ν_2	III
6	E	6	6	E	1	1095.91087	87.9	-5.3	ν_2	III
10	F ₁	10	10	F ₂	2	1095.93086	94.5	-3.3	ν_2	III
11	A ₁	4	11	A ₂	1	1096.98731	89.4	-7.4	ν_2	III
10	A ₂	4	10	A ₁	1	1097.14889	90.0	-0.9	ν_2	III

Table D.1 – Continued.

<i>J</i>	γ	<i>n</i>	<i>J'</i>	γ'	<i>n'</i>	ν^{exp} , cm^{-1}	Transmittance, %	$\delta \cdot 10^{-4}$, cm^{-1}	Band	Spectra
<i>I</i>		<i>2</i>		<i>3</i>		<i>4</i>		<i>5</i>		<i>7</i>
7	F ₁	10	7	F ₂	1	1097.33065	82.0	0.9	ν_2	III
11	E	8	11	E	1	1097.75577	94.3	1.2	ν_2	III
12	F ₂	13	12	F ₁	2	1098.45270	92.9	-0.3	ν_2	III
13	E	9	13	E	1	1098.57697	95.2	-0.6	ν_2	III
13	F ₂	13	13	F ₁	2	1098.67919	93.8	-3.8	ν_2	III
12	F ₁	13	12	F ₂	2	1098.71889	91.6	0.9	ν_2	III
8	A ₂	4	8	A ₁	1	1098.74955	75.0	-2.3	ν_2	III
8	F ₂	11	8	F ₁	1	1098.80158	77.6	-0.2	ν_2	III
8	E	7	8	E	1	1098.82079	84.0	1.0	ν_2	III
14	A ₂	5	14	A ₁	1	1099.79518	93.1	2.1	ν_2	III
9	F ₂	11	9	F ₁	2	1099.86383	91.9	1.1	ν_2	III
9	A ₂	4	9	A ₁	1	1099.97226	88.5	-5.2	ν_2	III
14	E	10	14	E	2	1100.35030	95.5	2.3	ν_2	III
9	F ₂	12	9	F ₁	1	1100.43337	75.0	0.8	ν_2	III
9	F ₁	12	9	F ₂	1	1100.45859	76.8	1.1	ν_2	III
10	F ₂	13	10	F ₁	2	1101.64211	93.9	0.2	ν_2	III
10	F ₂	13	10	F ₁	1	1101.66123	87.9	5.4	ν_2	III
16	F ₁	16	16	F ₂	2	1101.68722	95.6	-1.2	ν_2	III
10	F ₁	13	10	F ₂	1	1102.22304	75.5	0.4	ν_2	III
10	A ₁	5	10	A ₂	1	1102.23634	78.5	0.5	ν_2	III
11	A ₁	5	11	A ₂	1	1103.38048	90.2	0.4	ν_2	III
18	F ₁	18	18	F ₂	3	1103.86066	96.7	0.2	ν_2	III
18	E	13	18	E	3	1104.05667	93.6	4.0	ν_2	III
12	A ₁	5	12	A ₂	1	1105.13034	94.3	3.8	ν_2	III
12	F ₁	15	12	F ₂	1	1105.44302	89.1	0.6	ν_2	III
12	F ₂	16	12	F ₁	1	1106.11502	62.8	-4.4	ν_2	III
13	F ₂	15	13	F ₁	3	1107.07967	95.8	1.5	ν_2	III
13	F ₂	16	13	F ₁	2	1107.55175	87.5	-0.6	ν_2	III
13	A ₂	6	13	A ₁	1	1107.56114	86.6	1.0	ν_2	III
13	F ₂	17	13	F ₁	1	1108.20616	67.1	-1.8	ν_2	III
13	F ₁	17	13	F ₂	1	1108.20616	67.1	2.1	ν_2	III
14	F ₂	18	14	F ₁	1	1109.73484	86.6	-6.9	ν_2	III
14	F ₁	17	14	F ₂	2	1109.74126	80.7	3.7	ν_2	III
14	A ₁	7	14	A ₂	1	1110.37748	67.1	8.0	ν_2	III
14	E	12	14	E	1	1110.37748	67.1	-8.1	ν_2	III
14	F ₁	18	14	F ₂	1	1110.37748	67.1	-2.8	ν_2	III
15	F ₁	18	15	F ₂	3	1111.57768	94.6	-2.4	ν_2	III
15	F ₂	18	15	F ₁	2	1111.61096	94.2	-2.5	ν_2	III
15	F ₁	19	15	F ₂	2	1112.00907	91.2	1.3	ν_2	III
15	A ₁	6	15	A ₂	1	1112.02049	92.9	1.0	ν_2	III
15	F ₂	19	15	F ₁	1	1112.62007	71.3	-3.2	ν_2	III
15	F ₁	20	15	F ₂	1	1112.62007	71.3	4.3	ν_2	III
16	F ₁	19	16	F ₂	2	1113.97770	95.0	-3.9	ν_2	III
16	E	13	16	E	2	1114.00119	95.1	1.9	ν_2	III
16	E	14	16	E	1	1114.92343	67.1	-2.8	ν_2	III

Table D.1 – Continued.

<i>J</i>	γ	<i>n</i>	<i>J'</i>	γ'	<i>n'</i>	ν^{exp} , cm^{-1}	Transmittance, %	$\delta \cdot 10^{-4}$, cm^{-1}	Band	Spectra
<i>I</i>			<i>2</i>			<i>3</i>	<i>4</i>	<i>5</i>	<i>6</i>	<i>7</i>
16	F ₂	21	16	F ₁	1	1114.92343	67.1	-2.1	ν_2	III
16	A ₂	7	16	A ₁	1	1114.92343	67.1	-0.8	ν_2	III
17	F ₂	22	17	F ₁	1	1117.28043	85.5	4.9	ν_2	III
17	F ₁	22	17	F ₂	1	1117.28043	85.5	-6.9	ν_2	III
18	F ₂	22	18	F ₁	1	1119.14943	97.6	-2.2	ν_2	III
18	F ₁	21	18	F ₂	2	1119.19395	97.6	3.4	ν_2	III
18	F ₁	23	18	F ₂	1	1119.68504	84.3	-1.1	ν_2	III
18	E	16	18	E	1	1119.68504	84.3	1.2	ν_2	III
18	A ₁	8	18	A ₂	1	1119.68504	84.3	-5.6	ν_2	III
19	A ₁	8	19	A ₂	1	1121.70644	96.1	2.4	ν_2	III
19	F ₁	24	19	F ₂	1	1122.13070	94.1	-2.7	ν_2	III
20	F ₂	24	20	F ₁	1	1124.57563	94.1	-4.1	ν_2	III
20	E	16	20	E	1	1124.57563	94.1	-9.5	ν_2	III
20	A ₂	8	20	A ₁	1	1124.57563	94.1	4.6	ν_2	III
6	F ₂	7	5	F ₁	2	1125.33906	92.9	1.8	ν_2	III
6	F ₁	7	5	F ₂	1	1125.82268	94.6	1.0	ν_2	III
21	F ₂	24	21	F ₁	1	1127.07753	97.5	-2.3	ν_2	III
6	F ₂	8	5	F ₁	1	1127.22015	94.8	-0.4	ν_2	III
7	A ₂	3	6	A ₁	1	1131.07777	90.4	0.5	ν_2	III
7	F ₂	8	6	F ₁	1	1131.41408	91.0	-1.8	ν_2	III
8	A ₁	3	7	A ₂	1	1135.10691	96.6	-3.1	ν_2	III
8	F ₂	8	7	F ₁	2	1136.26094	96.5	3.0	ν_2	III
8	F ₂	9	7	F ₁	2	1137.25416	86.6	-2.7	ν_2	III
8	F ₁	9	7	F ₂	2	1137.66092	89.0	-4.2	ν_2	III
8	A ₁	4	7	A ₂	1	1140.18206	94.6	3.1	ν_2	III
8	F ₂	10	7	F ₁	1	1140.40213	94.9	1.0	ν_2	III
9	F ₁	10	8	F ₂	2	1143.22616	89.7	-0.4	ν_2	III
9	E	7	8	E	2	1143.48661	93.9	-1.9	ν_2	III
9	F ₂	10	8	F ₁	2	1143.62482	86.3	0.4	ν_2	III
9	F ₁	11	8	F ₂	1	1146.93567	92.9	1.5	ν_2	III
9	F ₂	11	8	F ₁	1	1147.18947	94.3	4.4	ν_2	III
9	A ₂	4	8	A ₁	1	1147.30485	95.0	-3.4	ν_2	III
10	F ₂	10	9	F ₁	3	1147.53343	95.5	0.6	ν_2	III
10	A ₁	4	9	A ₂	1	1149.12388	87.5	-6.4	ν_2	III
10	F ₂	11	9	F ₁	3	1149.56157	91.3	0.3	ν_2	III
10	A ₂	4	9	A ₁	1	1149.69987	92.1	0.1	ν_2	III
11	F ₂	10	10	F ₁	2	1153.13569	97.2	-2.7	ν_2	III
11	A ₂	4	10	A ₁	1	1153.21008	89.0	-5.8	ν_2	III
10	E	8	9	E	1	1153.86010	96.0	2.8	ν_2	III
10	F ₂	13	9	F ₁	1	1154.23025	95.5	1.3	ν_2	III
11	F ₁	12	10	F ₂	3	1155.35359	90.8	0.1	ν_2	III
11	E	8	10	E	2	1155.50758	92.8	-0.2	ν_2	III
11	F ₂	12	10	F ₁	2	1155.66769	91.4	2.2	ν_2	III
12	F ₂	11	11	F ₁	2	1158.82790	95.8	0.8	ν_2	III
11	F ₁	13	10	F ₂	2	1160.91089	95.2	2.3	ν_2	III

Table D.1 – Continued.

<i>J</i>	γ	<i>n</i>	<i>J'</i>	γ'	<i>n'</i>	ν^{exp} , cm^{-1}	Transmittance, %	$\delta \cdot 10^{-4}$, cm^{-1}	Band	Spectra
<i>I</i>			<i>2</i>			<i>3</i>	<i>4</i>	<i>5</i>	<i>6</i>	<i>7</i>
11	A ₁	5	10	A ₂	1	1161.18023	96.5	2.2	ν_2	III
11	E	9	10	E	1	1161.31320	96.2	1.4	ν_2	III
12	F ₂	13	11	F ₁	3	1161.40498	90.3	-1.8	ν_2	III
12	E	9	11	E	2	1161.60643	94.3	0.5	ν_2	III
12	F ₁	13	11	F ₂	3	1161.71004	88.2	1.4	ν_2	III
13	A ₂	5	12	A ₁	2	1167.38101	91.8	-2.3	ν_2	III
13	F ₂	14	12	F ₁	3	1167.59662	92.4	-0.5	ν_2	III
13	A ₁	5	12	A ₂	1	1167.82655	93.7	-0.3	ν_2	III
12	F ₂	14	11	F ₁	2	1167.89264	94.6	4.2	ν_2	III
12	F ₁	14	11	F ₂	2	1168.06455	94.7	2.7	ν_2	III
12	A ₁	5	11	A ₂	1	1168.17922	95.7	0.9	ν_2	III
12	F ₂	15	11	F ₁	1	1168.51383	95.5	2.7	ν_2	III
14	F ₂	13	13	F ₁	3	1170.16601	97.5	-2.5	ν_2	III
14	F ₂	15	13	F ₁	4	1173.61166	93.8	-1.2	ν_2	III
14	E	10	13	E	2	1173.73131	94.8	1.7	ν_2	III
14	F ₁	15	13	F ₂	3	1173.85549	94.0	-3.0	ν_2	III
13	F ₁	15	12	F ₂	2	1175.13953	96.3	3.1	ν_2	III
13	E	10	12	E	2	1175.17584	96.8	2.9	ν_2	III
13	F ₂	15	12	F ₁	2	1175.32314	96.7	3.8	ν_2	III
13	F ₁	16	12	F ₂	1	1175.42702	95.9	1.8	ν_2	III
15	F ₁	14	14	F ₂	3	1177.57003	97.2	-2.4	ν_2	III
15	F ₁	16	14	F ₂	4	1179.68327	94.3	-0.2	ν_2	III
15	E	11	14	E	3	1179.85294	96.1	-4.3	ν_2	III
15	F ₂	16	14	F ₁	3	1179.93089	94.4	0.9	ν_2	III
14	A ₁	6	13	A ₂	1	1182.46821	96.9	0.7	ν_2	III
14	F ₁	16	13	F ₂	2	1182.51532	97.0	0.8	ν_2	III
14	F ₂	16	13	F ₁	3	1182.56297	96.5	1.3	ν_2	III
14	F ₂	17	13	F ₁	2	1182.78454	96.6	3.3	ν_2	III
14	E	11	13	E	1	1182.79884	97.3	0.8	ν_2	III
16	F ₁	17	15	F ₂	4	1185.87620	96.0	2.5	ν_2	III
16	F ₂	17	15	F ₁	4	1185.97586	95.4	-1.3	ν_2	III
16	A ₂	6	15	A ₁	1	1186.05655	96.1	0.8	ν_2	III
17	F ₁	16	16	F ₂	3	1189.20114	98.9	5.8	ν_2	III
15	F ₂	17	14	F ₁	2	1190.03443	97.4	-0.8	ν_2	III
15	A ₂	6	14	A ₁	1	1190.05968	97.4	2.9	ν_2	III
15	F ₁	18	14	F ₂	2	1190.26245	97.1	2.3	ν_2	III
15	F ₂	18	14	F ₁	1	1190.27908	97.5	2.9	ν_2	III
17	A ₂	6	16	A ₁	2	1190.56513	97.6	-4.2	ν_2	III
17	F ₁	17	16	F ₂	4	1191.42110	98.1	0.8	ν_2	III
17	E	12	16	E	3	1192.00047	96.9	1.0	ν_2	III
17	F ₂	18	16	F ₁	4	1192.11029	96.8	1.1	ν_2	III
18	F ₂	17	17	F ₁	4	1196.47483	97.1	-4.4	ν_2	III
16	F ₂	19	15	F ₁	2	1197.58740	94.3	4.7	ν_2	III
18	F ₂	19	17	F ₁	5	1197.96656	97.1	3.1	ν_2	III
18	E	13	17	E	3	1198.14450	98.2	3.1	ν_2	III

Table D.1 – Continued.

<i>J</i>	γ	<i>n</i>	<i>J'</i>	γ'	<i>n'</i>	$\nu^{\text{exp}},$ cm^{-1}	Transmittance, %	$\delta \cdot 10^{-4},$ cm^{-1}	Band	Spectra
<i>I</i>		<i>2</i>		<i>3</i>		<i>4</i>		<i>5</i>		<i>7</i>
18	F ₁	19	17	F ₂	4	1198.19220	97.6	3.4	ν_2	III
19	F ₁	20	18	F ₂	5	1204.25853	98.2	4.4	ν_2	III
19	A ₁	7	18	A ₂	2	1204.31583	97.9	2.2	ν_2	III
17	A ₂	7	16	A ₁	2	1205.13411	97.6	-5.0	ν_2	III
17	F ₂	19	16	F ₁	3	1205.13411	97.6	1.5	ν_2	III

Table D.2 – Spectroscopic parameters of the v_2/v_4 dyad of the CD₄ molecule.

(v, γ)	(v', γ')	$\Omega (K, nI)$	$^{12}\text{CD}_4, \text{cm}^{-1}$ [84]	$^{13}\text{CD}_4, \text{cm}^{-1}$	$^{13}\text{CD}_4, \text{cm}^{-1}$ [74]
<i>I</i>	2	3	4	5	6
(0000, A ₁)	(0000, A ₁)	2(0,0A ₁)	2.63271835(22)	2.6389325(12)	2.632729(8)
(0000, A ₁)	(0000, A ₁)	4(0,0A ₁)10 ⁵	-2.758924(83)	-2.758924	-2.7635(45)
(0000, A ₁)	(0000, A ₁)	4(4,0A ₁)10 ⁷	-7.45145(13)	-7.45145	-7.4563(4)
(0000, A ₁)	(0000, A ₁)	6(0,0A ₁)10 ¹⁰	7.842(13)	7.842	8.69(90)
(0000, A ₁)	(0000, A ₁)	6(4,0A ₁)10 ¹¹	-1.9056(11)	-1.9056	-1.9577(43)
(0000, A ₁)	(0000, A ₁)	6(6,0A ₁)10 ¹²	-6.3876(90)	-6.3876	-6.1767(87)
(0000, A ₁)	(0000, A ₁)	8(0,0A ₁)10 ¹⁴	-2.337(69)	-2.337	
(0000, A ₁)	(0000, A ₁)	8(4,0A ₁)10 ¹⁶			
(0000, A ₁)	(0000, A ₁)	8(6,0A ₁)10 ¹⁶	-2.802(61)	-2.802	
(0000, A ₁)	(0000, A ₁)	8(8,0A ₁)10 ¹⁷			
(0100, E)	(0100, E)	0(0,0A ₁)	1091.6516918(56)	1091.801144(12)	1091.6619(7)
(0100, E)	(0100, E)	2(0,0A ₁)10 ³	3.110896(55)	2.86032(11)	-0.725(7)
(0100, E)	(0100, E)	2(2,0E)10 ³	-6.64627(17)	-6.87031(19)	-9.987(5)
(0100, E)	(0100, E)	3(3,0A ₂)10 ⁵	-8.2625(51)	-8.1621(29)	-1.66(10)
(0100, E)	(0100, E)	4(0,0A ₁)10 ⁷	1.016(24)	1.016	
(0100, E)	(0100, E)	4(2,0E)10 ⁷	-3.697(17)	-3.697	
(0100, E)	(0100, E)	4(4,0A ₁)10 ⁷	-1.1614(82)	-1.1614	
(0100, E)	(0100, E)	4(4,0E)10 ⁷	1.7659(78)	1.7659	
(0100, E)	(0100, E)	5(3,0A ₂)10 ⁹			
(0100, E)	(0001, F ₁)	1(1,0F ₁)	-5.1543227(23)	-5.0766147(35)	-5.233
(0100, E)	(0001, F ₁)	2(2,0F ₂)10 ²	-1.49348(34)	-1.47603(22)	-1.695(7)
(0100, E)	(0001, F ₁)	3(1,0F ₁)10 ⁵	-4.2580(69)	-4.0097(19)	-6.90(7)
(0100, E)	(0001, F ₁)	3(3,0F ₁)10 ⁵	4.0037(41)	4.2716(19)	1.38(7)
(0100, E)	(0001, F ₁)	3(3,0F ₂)10 ⁵	3.6873(19)	3.9029(11)	-1.64(5)
(0100, E)	(0001, F ₁)	4(2,0F ₂)10 ⁷	-3.7924(37)	-3.7924	
(0100, E)	(0001, F ₁)	4(4,0F ₁)10 ⁷	2.3788(34)	2.3788	
(0100, E)	(0001, F ₁)	4(4,0F ₂)10 ⁷	2.1929(46)	2.1929	
(0100, E)	(0001, F ₁)	5(1,0F ₁)10 ⁹			
(0100, E)	(0001, F ₁)	5(3,0F ₁)10 ¹⁰	8.947(28)	8.947	
(0100, E)	(0001, F ₁)	5(3,0F ₂)10 ⁹	1.4010(19)	1.4010	
(0100, E)	(0001, F ₁)	5(5,0F ₁)10 ⁹	-1.0681(32)	-1.0681	
(0100, E)	(0001, F ₁)	5(5,0F ₁)10 ¹⁰	-5.814(21)	-5.814	
(0100, E)	(0001, F ₁)	5(5,0F ₂)10 ¹⁰			
(0001, F ₂)	(0001, F ₂)	0(0,0A ₁)	997.8711014(46)	989.2502435(70)	989.2509(4)
(0001, F ₂)	(0001, F ₂)	1(1,0F ₁)	3.83980418(95)	4.0296197(13)	4.03241(8)
(0001, F ₂)	(0001, F ₂)	2(0,0A ₁)10 ³	-2.266577(54)	-2.361540(82)	0.004(4)
(0001, F ₂)	(0001, F ₂)	2(2,0E)10 ³			
(0001, F ₂)	(0001, F ₂)	2(2,0F ₂)10 ²	-1.357487(13)	-1.345759(12)	-1.0539(4)
(0001, F ₂)	(0001, F ₂)	3(1,0F ₁)10 ⁴	1.66880(74)	1.67052(41)	0.796(4)
(0001, F ₂)	(0001, F ₂)	3(3,0F ₁)10 ⁴	1.00493(68)	0.99070(38)	0.201(3)
(0001, F ₂)	(0001, F ₂)	4(0,0A ₁)10 ⁷	-6.125(16)	-6.0173(16)	
(0001, F ₂)	(0001, F ₂)	4(2,0E)10 ⁸	7.68(18)	7.68	
(0001, F ₂)	(0001, F ₂)	4(2,0F ₂)10 ⁹			
(0001, F ₂)	(0001, F ₂)	4(4,0A ₁)10 ⁸	5.661(66)	5.661	
(0001, F ₂)	(0001, F ₂)	4(4,0E)10 ⁷	-1.915(12)	-1.8173(17)	
(0001, F ₂)	(0001, F ₂)	4(4,0F ₂)10 ⁷			
(0001, F ₂)	(0001, F ₂)	5(1,0F ₁)10 ⁹	1.0936(17)	1.0936	
(0001, F ₂)	(0001, F ₂)	5(3,0F ₁)10 ¹⁰	5.307(53)	5.307	
(0001, F ₂)	(0001, F ₂)	5(5,0F ₁)10 ⁹	1.2916(63)	1.2916	
(0001, F ₂)	(0001, F ₂)	5(5,1F ₁)10 ⁸			
(0001, F ₂)	(0001, F ₂)	6(0,0A ₁)10 ¹¹	2.467(11)	2.467	
(0001, F ₂)	(0001, F ₂)	6(2,0F ₂)10 ¹²	-4.393(66)	-4.393	
d_{rms}			1.83	2.59	3448

The data in the table are presented using STDS format notations [87]

Table D.3 – Experimental line positions and strengths in the v₂/v₄ dyad of ¹²CD₄.

<i>J</i>	γ	<i>n</i>	<i>J'</i>	γ'	<i>n'</i>	v^{exp} , cm ⁻¹	S_v^{exp} , cm ⁻² · atm ⁻¹	δ , %	Band
<i>I</i>			<i>2</i>			<i>3</i>	<i>4</i>	<i>5</i>	<i>6</i>
21	F ₁	11	22	F ₂	6	883.8316	0.0029	4.4	v ₄
21	E	8	22	E	4	884.0828	0.0018	-2.6	v ₄
21	F ₂	12	22	F ₁	5	884.3305	0.0027	3.1	v ₄
20	A ₁	4	21	A ₂	2	890.1693	0.0044	10.1	v ₄
20	F ₁	11	21	F ₂	5	890.4368	0.0046	0.3	v ₄
20	F ₂	11	21	F ₁	6	890.6932	0.0049	6.0	v ₄
20	A ₂	4	21	A ₁	2	890.9418	0.0038	1.7	v ₄
22	F ₂	13	23	F ₁	5	891.2513	0.0012	2.9	v ₄
22	F ₁	13	23	F ₂	5	892.1703	0.0012	-0.3	v ₄
16	F ₁	5	17	F ₂	2	892.4152	0.0016	-5.1	v ₄
16	F ₂	6	17	F ₁	3	892.4309	0.0017	-1.5	v ₄
22	A ₁	5	23	A ₂	2	893.5006	0.0013	5.4	v ₄
18	F ₂	9	19	F ₁	4	894.2043	0.0010	8.1	v ₄
22	F ₁	14	23	F ₂	4	894.5922	0.0016	8.3	v ₄
17	F ₁	7	18	F ₂	4	894.7152	0.0009	8.2	v ₄
18	A ₂	3	19	A ₁	1	894.7366	0.0010	8.1	v ₄
17	E	5	18	E	3	894.9045	0.0013	12.5	v ₄
19	F ₁	11	20	F ₂	5	896.6932	0.0079	1.0	v ₄
21	F ₂	13	22	F ₁	4	896.6981	0.0021	-3.9	v ₄
19	E	7	20	E	4	896.9652	0.0049	-3.1	v ₄
21	F ₁	12	22	F ₂	5	897.1657	0.0022	-1.7	v ₄
19	F ₂	10	20	F ₁	5	897.2289	0.0073	-3.2	v ₄
16	E	4	17	E	2	897.5391	0.0012	2.2	v ₄
16	F ₁	6	17	F ₂	3	897.5960	0.0020	8.3	v ₄
16	A ₁	3	17	A ₂	1	897.7151	0.0021	-2.1	v ₄
22	A ₂	5	23	A ₁	1	897.7380	0.0013	3.3	v ₄
21	A ₁	4	22	A ₂	2	898.0575	0.0018	-2.5	v ₄
17	F ₁	8	18	F ₂	4	898.5474	0.0023	2.4	v ₄
21	F ₁	13	22	F ₂	4	899.4246	0.0029	12.0	v ₄
15	F ₁	6	16	F ₂	2	899.5440	0.0024	0.5	v ₄
21	E	9	22	E	3	899.7140	0.0018	4.2	v ₄
12	A ₁	1	13	A ₂	1	901.2696	0.0018	7.2	v ₄
16	F ₂	7	17	F ₁	4	901.5461	0.0018	-3.3	v ₄
20	F ₂	12	21	F ₁	5	901.7539	0.0041	7.8	v ₄
22	F ₁	15	23	F ₂	3	901.8883	0.0016	-7.5	v ₄
22	F ₂	16	23	F ₁	2	901.8975	0.0018	1.3	v ₄
21	F ₂	14	22	F ₁	3	902.0732	0.0030	8.1	v ₄
20	E	8	21	E	3	902.0928	0.0028	6.5	v ₄
21	F ₁	14	22	F ₂	3	902.3160	0.0026	-7.2	v ₄
12	F ₁	3	13	F ₂	2	902.5740	0.0011	11.6	v ₄

Table D.3 – Continued.

<i>J</i>	γ	<i>n</i>	<i>J'</i>	γ'	<i>n'</i>	ν^{exp} , cm^{-1}	S_{ν}^{exp} , $\text{cm}^{-2} \cdot \text{atm}^{-1}$	δ , %	Band
<i>I</i>			<i>2</i>			<i>3</i>	<i>4</i>	<i>5</i>	<i>6</i>
20	F ₁	12	21	F ₂	4	902.9338	0.0041	3.0	v ₄
18	F ₂	10	19	F ₁	5	902.9889	0.0124	-1.4	v ₄
18	E	7	19	E	3	903.2709	0.0080	-2.7	v ₄
18	F ₁	10	19	F ₂	5	903.5531	0.0125	2.2	v ₄
16	F ₂	8	17	F ₁	4	904.2583	0.0022	-3.1	v ₄
20	F ₂	13	21	F ₁	4	904.4259	0.0049	9.3	v ₄
16	E	5	17	E	2	904.7910	0.0014	1.4	v ₄
21	E	10	22	E	2	906.0061	0.0019	-9.4	v ₄
21	F ₂	15	22	F ₁	2	906.0190	0.0032	6.1	v ₄
21	A ₂	6	22	A ₁	1	906.0439	0.0027	6.6	v ₄
13	F ₂	4	14	F ₁	1	906.1053	0.0035	0.9	v ₄
13	F ₁	4	14	F ₂	2	906.1114	0.0035	-0.9	v ₄
20	E	9	21	E	2	906.3569	0.0031	1.6	v ₄
20	F ₁	13	21	F ₂	3	906.5560	0.0047	0.8	v ₄
14	F ₁	5	15	F ₂	3	906.5740	0.0033	4.2	v ₄
14	F ₂	5	15	F ₁	2	906.6179	0.0033	-2.7	v ₄
20	A ₁	5	21	A ₂	1	906.8714	0.0040	0.0	v ₄
19	F ₁	12	20	F ₂	4	906.9517	0.0065	-0.2	v ₄
19	E	8	20	E	3	907.5959	0.0043	-2.4	v ₄
19	F ₂	11	20	F ₁	4	908.0897	0.0068	0.2	v ₄
15	A ₂	2	16	A ₁	2	908.8531	0.0049	7.1	v ₄
17	A ₂	4	18	A ₁	2	909.0336	0.0167	1.3	v ₄
17	F ₂	10	18	F ₁	4	909.3288	0.0192	-1.9	v ₄
19	A ₂	4	20	A ₁	2	909.3508	0.0064	3.2	v ₄
17	F ₁	9	18	F ₂	5	909.6282	0.0188	-2.8	v ₄
17	A ₁	3	18	A ₂	2	909.9361	0.0159	-0.7	v ₄
20	F ₁	14	21	F ₂	2	910.1237	0.0047	-7.6	v ₄
20	F ₂	14	21	F ₁	3	910.1781	0.0049	-5.7	v ₄
19	F ₂	12	20	F ₁	3	910.6981	0.0076	-0.1	v ₄
14	A ₂	2	15	A ₁	1	910.8265	0.0018	6.0	v ₄
14	F ₂	6	15	F ₁	3	911.1168	0.0024	2.0	v ₄
19	F ₁	13	20	F ₂	3	911.1420	0.0079	1.9	v ₄
15	A ₁	3	16	A ₂	1	911.1529	0.0014	-5.4	v ₄
14	E	4	15	E	2	911.2697	0.0028	4.7	v ₄
18	A ₁	4	19	A ₂	2	911.9931	0.0088	-1.1	v ₄
18	F ₁	11	19	F ₂	4	912.4723	0.0105	-3.9	v ₄
18	F ₂	11	19	F ₁	4	913.0286	0.0112	0.0	v ₄
13	E	3	14	E	2	913.5310	0.0030	12.6	v ₄
13	F ₂	5	14	F ₁	2	913.5662	0.0045	8.3	v ₄
12	A ₂	1	13	A ₁	1	913.6128	0.0039	4.6	v ₄
12	E	3	13	E	1	913.6286	0.0031	0.2	v ₄
13	A ₂	3	14	A ₁	1	913.6368	0.0046	7.3	v ₄
19	A ₁	5	20	A ₂	1	914.1825	0.0068	-0.6	v ₄

Table D.3 – Continued.

<i>J</i>	γ	<i>n</i>	<i>J'</i>	γ'	<i>n'</i>	ν^{exp} , cm^{-1}	S_{ν}^{exp} , $\text{cm}^{-2} \cdot \text{atm}^{-1}$	δ , %	Band
<i>I</i>			2			3	4	5	6
18	A ₂	4	19	A ₁	1	914.2176	0.0096	0.9	v ₄
19	F ₁	14	20	F ₂	2	914.2917	0.0080	-4.2	v ₄
19	E	9	20	E	2	914.3415	0.0053	-5.3	v ₄
20	A ₂	5	21	A ₁	1	914.6596	0.0047	-1.4	v ₄
14	F ₂	7	15	F ₁	3	914.9007	0.0043	5.8	v ₄
16	F ₂	9	17	F ₁	5	915.2622	0.0297	-1.2	v ₄
18	F ₂	12	19	F ₁	3	915.3560	0.0122	-0.3	v ₄
16	E	6	17	E	3	915.5709	0.0195	-1.0	v ₄
18	E	8	19	E	2	915.6328	0.0082	-0.8	v ₄
16	F ₁	9	17	F ₂	4	915.9042	0.0293	-0.6	v ₄
14	F ₁	7	15	F ₂	3	916.3079	0.0018	-6.5	v ₄
10	F ₂	2	11	F ₁	3	916.4387	0.0018	8.6	v ₄
17	F ₁	10	18	F ₂	4	917.4625	0.0171	-1.9	v ₄
13	F ₂	6	14	F ₁	3	917.4865	0.0019	-8.7	v ₄
10	F ₂	3	11	F ₁	2	917.5680	0.0019	3.6	v ₄
17	E	7	18	E	3	917.8376	0.0115	-3.1	v ₄
13	F ₁	5	14	F ₂	3	917.8920	0.0040	-8.2	v ₄
18	F ₁	12	19	F ₂	3	918.3480	0.0132	0.5	v ₄
18	F ₂	13	19	F ₁	2	918.5270	0.0131	-2.1	v ₄
19	F ₂	13	20	F ₁	2	918.5866	0.0090	-2.8	v ₄
19	F ₁	15	20	F ₂	1	918.5942	0.0098	5.3	v ₄
17	F ₂	11	18	F ₁	3	918.9410	0.0178	-2.2	v ₄
17	F ₁	11	18	F ₂	3	920.1600	0.0195	0.8	v ₄
12	F ₁	4	13	F ₂	2	920.3789	0.0038	-5.9	v ₄
12	F ₂	5	13	F ₁	3	920.4945	0.0061	3.7	v ₄
13	F ₁	6	14	F ₂	3	920.5535	0.0039	8.7	v ₄
11	F ₂	3	12	F ₁	2	921.0214	0.0057	2.2	v ₄
11	F ₁	4	12	F ₂	1	921.0392	0.0063	7.1	v ₄
15	F ₁	9	16	F ₂	4	921.2183	0.0445	0.2	v ₄
15	E	6	16	E	3	921.5599	0.0295	0.3	v ₄
15	F ₂	8	16	F ₁	4	921.9060	0.0433	-0.6	v ₄
17	E	8	18	E	2	922.4616	0.0134	-1.3	v ₄
18	E	9	19	E	1	922.5085	0.0097	-0.6	v ₄
18	F ₁	13	19	F ₂	2	922.5165	0.0145	-0.7	v ₄
18	A ₁	5	19	A ₂	1	922.5321	0.0124	1.1	v ₄
16	F ₂	10	17	F ₁	4	922.5749	0.0270	-0.6	v ₄
17	F ₂	12	18	F ₁	2	922.6034	0.0205	-0.1	v ₄
17	A ₂	5	18	A ₁	1	922.8379	0.0168	-3.0	v ₄
16	E	7	17	E	2	923.4106	0.0188	1.3	v ₄
12	E	4	13	E	2	923.8471	0.0013	-2.6	v ₄
16	F ₁	10	17	F ₂	3	923.9130	0.0282	-0.1	v ₄
12	F ₁	5	13	F ₂	3	924.0859	0.0016	-3.8	v ₄
12	F ₁	5	13	F ₂	2	924.1230	0.0016	1.3	v ₄

Table D.3 – Continued.

<i>J</i>	γ	<i>n</i>	<i>J'</i>	γ'	<i>n'</i>	ν^{exp} , cm^{-1}	S_{ν}^{exp} , $\text{cm}^{-2} \cdot \text{atm}^{-1}$	δ , %	Band
<i>I</i>		2		3		4		5	6
9	F ₁	2	10	F ₂	3	924.1449	0.0023	8.2	v ₄
16	A ₁	4	17	A ₂	1	924.8954	0.0244	-0.9	v ₄
12	A ₁	2	13	A ₂	1	924.9476	0.0088	9.5	v ₄
9	A ₂	1	10	A ₁	1	925.0556	0.0020	4.9	v ₄
12	F ₁	6	13	F ₂	2	926.3131	0.0030	7.9	v ₄
17	F ₂	13	18	F ₁	1	926.4257	0.0221	-1.9	v ₄
17	F ₁	12	18	F ₂	2	926.4555	0.0223	-1.4	v ₄
16	F ₁	11	17	F ₂	2	926.5954	0.0304	-0.7	v ₄
14	A ₁	3	15	A ₂	2	926.8824	0.0552	2.9	v ₄
16	F ₂	11	17	F ₁	3	926.9371	0.0308	-0.9	v ₄
11	A ₁	2	12	A ₂	1	927.0018	0.0037	5.1	v ₄
11	F ₁	5	12	F ₂	2	927.1840	0.0056	10.4	v ₄
14	F ₁	8	15	F ₂	4	927.2227	0.0631	-0.8	v ₄
11	E	3	12	E	2	927.2807	0.0051	6.3	v ₄
12	A ₂	2	13	A ₁	1	927.3156	0.0016	0.4	v ₄
15	A ₂	3	16	A ₁	2	927.4911	0.0333	-1.9	v ₄
14	F ₂	8	15	F ₁	4	927.5902	0.0627	-0.3	v ₄
14	A ₂	3	15	A ₁	1	928.0033	0.0523	-0.4	v ₄
15	F ₂	9	16	F ₁	3	928.0748	0.0412	-0.4	v ₄
10	E	2	11	E	1	928.2987	0.0040	-7.8	v ₄
10	F ₁	3	11	F ₂	2	928.3139	0.0071	4.5	v ₄
10	A ₁	2	11	A ₂	1	928.3438	0.0065	4.3	v ₄
15	F ₁	10	16	F ₂	3	928.6750	0.0425	0.9	v ₄
15	A ₁	4	16	A ₂	1	930.2455	0.0358	-2.0	v ₄
16	A ₂	4	17	A ₁	1	930.3095	0.0286	1.9	v ₄
16	F ₂	12	17	F ₁	2	930.3638	0.0333	-1.5	v ₄
16	E	8	17	E	1	930.3896	0.0230	2.0	v ₄
11	F ₁	6	12	F ₂	3	930.9649	0.0028	2.1	v ₄
15	F ₁	11	16	F ₂	2	930.9735	0.0445	-1.1	v ₄
11	F ₁	6	12	F ₂	2	930.9916	0.0052	6.6	v ₄
15	E	7	16	E	2	931.1892	0.0313	3.2	v ₄
8	A ₁	1	9	A ₂	1	931.7948	0.0018	-7.0	v ₄
13	F ₁	7	14	F ₂	4	932.7452	0.0877	-1.7	v ₄
14	F ₂	9	15	F ₁	3	932.8891	0.0593	-1.0	v ₄
13	E	5	14	E	3	933.0973	0.0588	0.3	v ₄
14	E	6	15	E	2	933.2598	0.0398	-1.8	v ₄
13	F ₂	8	14	F ₁	3	933.5428	0.0866	-1.6	v ₄
10	F ₁	4	11	F ₂	3	933.6582	0.0048	8.1	v ₄
10	F ₂	4	11	F ₁	2	933.9320	0.0075	0.3	v ₄
15	F ₂	10	16	F ₁	2	934.2410	0.0485	-1.0	v ₄
15	F ₁	12	16	F ₂	1	934.3287	0.0490	-0.4	v ₄
14	F ₁	9	15	F ₂	3	934.6638	0.0621	-1.2	v ₄
9	F ₂	3	10	F ₁	1	935.4316	0.0071	3.8	v ₄

Table D.3 – Continued.

<i>J</i>	γ	<i>n</i>	<i>J'</i>	γ'	<i>n'</i>	ν^{exp} , cm^{-1}	S_{ν}^{exp} , $\text{cm}^{-2} \cdot \text{atm}^{-1}$	δ , %	Band
<i>I</i>			2			3	4	5	6
14	F ₂	10	15	F ₁	2	935.4685	0.0647	0.0	v ₄
9	F ₁	3	10	F ₂	2	935.4831	0.0088	5.7	v ₄
10	F ₂	5	11	F ₁	2	936.6703	0.0038	0.4	v ₄
10	E	3	11	E	2	937.0651	0.0026	11.7	v ₄
13	F ₁	8	14	F ₂	3	937.7945	0.0836	-1.4	v ₄
14	E	7	15	E	1	938.1390	0.0459	-0.5	v ₄
14	F ₁	10	15	F ₂	2	938.2086	0.0686	-1.1	v ₄
12	F ₂	7	13	F ₁	4	938.2808	0.1182	-1.9	v ₄
14	A ₁	4	15	A ₂	1	938.3318	0.0576	-0.9	v ₄
12	E	5	13	E	2	938.7007	0.0817	2.3	v ₄
13	E	6	14	E	2	938.8574	0.0575	-0.6	v ₄
12	F ₁	7	13	F ₂	3	939.1252	0.1157	-2.1	v ₄
13	F ₂	9	14	F ₁	2	939.2738	0.0866	-1.6	v ₄
13	A ₂	4	14	A ₁	1	939.9314	0.0750	-0.1	v ₄
9	E	3	10	E	2	940.0538	0.0025	2.1	v ₄
9	F ₂	4	10	F ₁	2	940.2293	0.0042	2.9	v ₄
9	A ₂	2	10	A ₁	1	940.7610	0.0107	1.6	v ₄
13	F ₂	10	14	F ₁	1	942.0337	0.0940	-0.7	v ₄
14	F ₁	11	15	F ₂	1	942.1508	0.0762	-0.8	v ₄
14	F ₂	11	15	F ₁	1	942.1589	0.0746	-3.0	v ₄
13	F ₁	9	14	F ₂	2	942.2205	0.0940	-1.6	v ₄
8	A ₂	1	9	A ₁	1	942.3552	0.0054	-2.9	v ₄
12	A ₁	3	13	A ₂	1	942.4910	0.0935	-2.6	v ₄
9	F ₁	4	10	F ₂	3	942.8448	0.0015	0.6	v ₄
9	F ₁	4	10	F ₂	2	942.8732	0.0013	6.3	v ₄
12	F ₁	8	13	F ₂	2	943.1939	0.1146	-1.6	v ₄
11	A ₂	2	12	A ₁	2	943.4958	0.1305	-1.3	v ₄
12	F ₂	8	13	F ₁	3	943.7559	0.1166	-1.9	v ₄
11	F ₂	6	12	F ₁	3	943.8773	0.1529	-2.7	v ₄
11	F ₁	7	12	F ₂	3	944.3178	0.1521	-2.0	v ₄
11	A ₁	3	12	A ₂	1	944.8949	0.1308	0.0	v ₄
12	A ₂	3	13	A ₁	1	945.7205	0.1028	-1.6	v ₄
13	A ₁	3	14	A ₂	1	945.7973	0.0862	-1.4	v ₄
13	F ₁	10	14	F ₂	1	945.8115	0.1051	0.2	v ₄
13	E	7	14	E	1	945.8184	0.0671	-4.2	v ₄
12	F ₂	9	13	F ₁	2	946.0591	0.1240	-1.9	v ₄
12	E	6	13	E	1	946.1831	0.0845	-0.2	v ₄
8	F ₂	4	9	F ₁	3	946.8744	0.0063	10.1	v ₄
8	F ₂	4	9	F ₁	2	946.8867	0.0033	-1.4	v ₄
11	F ₁	8	12	F ₂	2	947.7297	0.1499	-1.9	v ₄
11	E	5	12	E	2	948.0513	0.1022	-1.1	v ₄
8	E	3	9	E	1	948.1400	0.0011	-0.9	v ₄
10	F ₂	6	11	F ₁	3	948.9261	0.1939	-2.9	v ₄

Table D.3 – Continued.

<i>J</i>	γ	<i>n</i>	<i>J'</i>	γ'	<i>n'</i>	ν^{exp} , cm^{-1}	S_{ν}^{exp} , $\text{cm}^{-2} \cdot \text{atm}^{-1}$	δ , %	Band
<i>I</i>			2			3	4	5	6
10	E	4	11	E	2	949.2956	0.1315	0.1	v ₄
7	F ₁	3	8	F ₂	1	949.3210	0.0096	2.7	v ₄
12	F ₁	9	13	F ₂	1	949.4497	0.1376	-0.9	v ₄
12	F ₂	10	13	F ₁	1	949.4730	0.1364	-2.0	v ₄
11	F ₂	7	12	F ₁	2	949.7518	0.1616	-0.2	v ₄
10	F ₁	6	11	F ₂	3	949.8924	0.1926	-2.7	v ₄
11	F ₁	9	12	F ₂	1	950.1586	0.1601	-2.3	v ₄
19	F ₂	4	19	F ₁	2	951.8772	0.0012	-4.4	v ₄
10	F ₂	7	11	F ₁	2	952.3208	0.1914	-1.8	v ₄
7	F ₁	4	8	F ₂	2	952.6558	0.0018	-4.0	v ₄
7	F ₁	4	8	F ₂	1	952.6658	0.0025	-1.3	v ₄
7	E	2	8	E	2	952.9870	0.0039	9.5	v ₄
11	E	6	12	E	1	953.0860	0.1180	-0.7	v ₄
11	F ₂	8	12	F ₁	1	953.1048	0.1751	-1.9	v ₄
11	A ₂	3	12	A ₁	1	953.1405	0.1459	-2.0	v ₄
10	E	5	11	E	1	953.6413	0.1323	-1.7	v ₄
10	F ₁	7	11	F ₂	2	953.8964	0.1967	-3.3	v ₄
9	F ₁	5	10	F ₂	3	953.9790	0.2354	-3.4	v ₄
10	A ₁	3	11	A ₂	1	954.2677	0.1670	-2.6	v ₄
9	E	4	10	E	2	954.4777	0.1591	-1.6	v ₄
9	F ₂	6	10	F ₁	2	954.9483	0.2333	-2.3	v ₄
9	F ₂	6	10	F ₁	1	954.9669	0.0037	10.3	v ₄
6	E	2	7	E	1	955.7539	0.0037	7.0	v ₄
6	F ₁	2	7	F ₂	2	955.8568	0.0063	-3.3	v ₄
10	F ₁	8	11	F ₂	1	956.7126	0.2147	-3.0	v ₄
9	A ₂	3	10	A ₁	1	956.7228	0.1940	-2.2	v ₄
10	F ₂	8	11	F ₁	1	956.7687	0.2153	-2.9	v ₄
9	F ₂	7	10	F ₁	2	957.5719	0.0026	-2.9	v ₄
9	F ₂	7	10	F ₁	1	957.5905	0.2358	-2.5	v ₄
9	F ₁	6	10	F ₂	2	958.0151	0.2380	-3.6	v ₄
8	A ₁	2	9	A ₂	1	958.7150	0.2322	-3.1	v ₄
6	F ₂	3	7	F ₁	2	958.7928	0.0020	-7.3	v ₄
8	F ₁	5	9	F ₂	2	959.1134	0.2737	-4.2	v ₄
8	F ₂	5	9	F ₁	3	959.5882	0.2769	-1.7	v ₄
9	A ₁	2	10	A ₂	1	960.2790	0.2155	-2.4	v ₄
9	F ₁	7	10	F ₂	1	960.3715	0.2579	-2.9	v ₄
8	A ₂	2	9	A ₁	1	960.3922	0.2360	-1.6	v ₄
9	E	5	10	E	1	960.4119	0.1731	-2.3	v ₄
8	F ₂	6	9	F ₁	2	961.7525	0.2726	-4.0	v ₄
8	E	4	9	E	1	961.9855	0.1902	-0.7	v ₄
15	F ₁	3	15	F ₂	3	962.0107	0.0031	5.4	v ₄
5	F ₂	2	6	F ₁	1	962.1022	0.0031	4.1	v ₄
5	F ₁	2	6	F ₂	2	962.4378	0.0082	10.6	v ₄

Table D.3 – Continued.

<i>J</i>	γ	<i>n</i>	<i>J'</i>	γ'	<i>n'</i>	ν^{exp} , cm^{-1}	S_{ν}^{exp} , $\text{cm}^{-2} \cdot \text{atm}^{-1}$	δ , %	Band
<i>I</i>			2			3	4	5	6
7	F ₁	5	8	F ₂	2	963.6704	0.3072	-5.0	v ₄
8	F ₁	6	9	F ₂	1	963.9278	0.2936	-4.3	v ₄
7	E	3	8	E	2	964.0042	0.2069	-3.0	v ₄
8	F ₂	7	9	F ₁	1	964.0535	0.2925	-5.0	v ₄
14	A ₂	1	14	A ₁	1	964.4434	0.0035	6.5	v ₄
14	F ₂	3	14	F ₁	2	964.4890	0.0034	7.8	v ₄
14	E	2	14	E	2	964.5069	0.0022	10.5	v ₄
7	F ₂	4	8	F ₁	2	964.7615	0.3068	-5.1	v ₄
13	A ₁	1	13	A ₂	1	965.8763	0.0020	8.1	v ₄
7	F ₁	6	8	F ₂	1	965.9432	0.3065	-4.8	v ₄
13	F ₂	2	13	F ₁	3	966.9143	0.0037	-2.6	v ₄
13	F ₁	3	13	F ₂	2	966.9897	0.0026	5.1	v ₄
7	E	4	8	E	1	967.5201	0.2195	-3.2	v ₄
7	F ₂	5	8	F ₁	1	967.6108	0.3224	-5.6	v ₄
7	A ₂	2	8	A ₁	1	967.7539	0.2726	-4.6	v ₄
6	F ₂	4	7	F ₁	2	968.2174	0.3341	-4.0	v ₄
12	F ₁	1	12	F ₂	2	968.5121	0.0016	9.6	v ₄
13	E	2	13	E	1	968.5396	0.0061	8.3	v ₄
13	F ₂	3	13	F ₁	2	968.5437	0.0078	-5.6	v ₄
13	A ₂	2	13	A ₁	1	968.5508	0.0068	0.2	v ₄
4	E	1	5	E	1	968.6528	0.0036	-7.3	v ₄
6	E	3	7	E	1	968.7832	0.2241	-3.4	v ₄
6	F ₁	4	7	F ₂	2	969.1952	0.3299	-4.4	v ₄
6	A ₁	2	7	A ₂	1	969.9986	0.2769	-3.9	v ₄
12	F ₁	3	12	F ₂	1	970.8249	0.0088	-2.4	v ₄
12	F ₂	3	12	F ₁	2	970.8404	0.0092	5.8	v ₄
6	F ₁	5	7	F ₂	1	971.1092	0.3505	-2.8	v ₄
6	F ₂	5	7	F ₁	1	971.3114	0.3485	-4.3	v ₄
11	F ₁	2	11	F ₂	3	971.8735	0.0025	11.3	v ₄
5	A ₂	2	6	A ₁	1	972.4829	0.2877	-3.5	v ₄
5	F ₂	4	6	F ₁	1	972.8792	0.3389	-4.8	v ₄
11	A ₁	1	11	A ₂	1	973.0651	0.0087	6.7	v ₄
11	F ₁	3	11	F ₂	2	973.0956	0.0093	6.2	v ₄
11	E	2	11	E	1	973.1092	0.0059	4.8	v ₄
5	F ₁	3	6	F ₂	2	973.3105	0.3357	-5.1	v ₄
10	A ₂	1	10	A ₁	1	973.9576	0.0042	3.8	v ₄
5	A ₁	1	6	A ₂	1	974.3796	0.2943	-3.9	v ₄
3	F ₁	2	4	F ₂	1	974.5687	0.0027	8.2	v ₄
5	F ₁	4	6	F ₂	1	974.8222	0.3505	-4.4	v ₄
5	E	3	6	E	1	974.9388	0.2371	-3.5	v ₄
10	F ₁	2	10	F ₂	2	975.3079	0.0096	6.3	v ₄
10	F ₂	3	10	F ₁	1	975.3552	0.0072	0.3	v ₄
9	F ₂	1	9	F ₁	2	976.4325	0.0015	-6.5	v ₄

Table D.3 – Continued.

<i>J</i>	γ	<i>n</i>	<i>J'</i>	γ'	<i>n'</i>	ν^{exp} , cm^{-1}	S_{ν}^{exp} , $\text{cm}^{-2} \cdot \text{atm}^{-1}$	δ , %	Band
<i>I</i>			<i>2</i>			<i>3</i>	<i>4</i>	<i>5</i>	<i>6</i>
4	F ₂	3	5	F ₁	2	976.9651	0.3261	-5.1	v ₄
4	E	2	5	E	1	977.2257	0.2238	-1.5	v ₄
21	F ₁	7	21	F ₂	2	977.2821	0.0045	1.0	v ₄
21	F ₂	8	21	F ₁	3	977.2876	0.0042	-6.4	v ₄
9	E	2	9	E	1	977.5087	0.0056	1.0	v ₄
9	F ₂	2	9	F ₁	2	977.5449	0.0073	8.3	v ₄
9	A ₂	1	9	A ₁	1	977.6029	0.0051	0.7	v ₄
4	F ₁	3	5	F ₂	1	978.1265	0.3342	-4.8	v ₄
23	F ₂	8	23	F ₁	3	978.2794	0.0014	-8.4	v ₄
4	F ₂	4	5	F ₁	1	978.5589	0.3355	-4.6	v ₄
8	F ₂	2	8	F ₁	2	979.7716	0.0053	6.3	v ₄
22	F ₂	9	22	F ₁	3	980.2258	0.0025	-7.9	v ₄
22	F ₁	8	22	F ₂	3	980.2487	0.0030	9.1	v ₄
3	F ₁	3	4	F ₂	1	981.0228	0.2925	-4.3	v ₄
16	F ₁	5	16	F ₂	1	981.4863	0.0444	5.8	v ₄
16	F ₂	6	16	F ₁	2	981.4903	0.0396	-5.8	v ₄
3	E	2	4	E	1	981.6837	0.2032	-1.6	v ₄
7	A ₁	1	7	A ₂	1	981.7353	0.0066	3.7	v ₄
12	A ₂	1	12	A ₁	1	981.8729	0.1403	1.9	v ₄
12	F ₂	4	12	F ₁	1	981.8792	0.1760	6.1	v ₄
3	F ₂	2	4	F ₁	1	981.9316	0.2987	-3.8	v ₄
21	E	6	21	E	2	982.1351	0.0029	-8.7	v ₄
21	F ₁	8	21	F ₂	3	982.1417	0.0043	-7.6	v ₄
3	A ₂	1	4	A ₁	1	982.2444	0.2542	-2.2	v ₄
23	F ₁	10	23	F ₂	4	982.5539	0.0013	0.3	v ₄
18	A ₂	2	18	A ₁	1	983.0947	0.0171	4.6	v ₄
18	F ₂	7	18	F ₁	2	983.1060	0.0198	1.9	v ₄
18	E	5	18	E	2	983.1112	0.0129	-0.5	v ₄
15	A ₁	2	15	A ₂	1	983.4034	0.0505	-1.5	v ₄
15	F ₁	6	15	F ₂	2	983.4152	0.0638	3.9	v ₄
15	E	4	15	E	1	983.4211	0.0386	-5.9	v ₄
6	F ₁	1	6	F ₂	2	983.9322	0.0037	-1.8	v ₄
20	F ₁	8	20	F ₂	3	983.9685	0.0081	1.9	v ₄
20	F ₂	8	20	F ₁	3	983.9882	0.0080	7.4	v ₄
11	F ₂	3	11	F ₁	1	984.0548	0.2075	-1.3	v ₄
11	F ₁	4	11	F ₂	1	984.0677	0.2104	0.2	v ₄
22	F ₁	9	22	F ₂	4	984.3938	0.0024	-0.6	v ₄
2	A ₁	1	3	A ₂	1	984.8366	0.1992	-2.2	v ₄
17	F ₂	7	17	F ₁	3	984.9011	0.0308	1.7	v ₄
17	F ₁	6	17	F ₂	2	984.9368	0.0298	0.7	v ₄
14	F ₁	5	14	F ₂	2	985.2531	0.0900	2.9	v ₄
2	F ₁	2	3	F ₂	1	985.2848	0.2287	-7.0	v ₄
2	F ₂	2	3	F ₁	1	985.6156	0.2402	-2.5	v ₄

Table D.3 – Continued.

<i>J</i>	γ	<i>n</i>	<i>J'</i>	γ'	<i>n'</i>	ν^{exp} , cm^{-1}	S_{ν}^{exp} , $\text{cm}^{-2} \cdot \text{atm}^{-1}$	δ , %	Band
<i>I</i>			2			3	4	5	6
19	E	5	19	E	2	985.6980	0.0092	3.9	v ₄
19	A ₂	3	19	A ₁	1	985.8010	0.0111	2.4	v ₄
23	A ₁	4	23	A ₂	2	986.0385	0.0015	-10.8	v ₄
10	E	2	10	E	1	986.1013	0.1755	1.7	v ₄
10	F ₁	3	10	F ₂	1	986.1139	0.2550	-1.4	v ₄
10	A ₁	2	10	A ₂	1	986.1394	0.2123	-1.3	v ₄
16	E	4	16	E	2	986.6065	0.0316	3.4	v ₄
16	F ₁	6	16	F ₂	2	986.6462	0.0437	-2.1	v ₄
16	A ₁	3	16	A ₂	1	986.7282	0.0380	0.8	v ₄
13	E	3	13	E	1	987.0001	0.0816	1.4	v ₄
13	F ₂	5	13	F ₁	2	987.0274	0.1207	0.7	v ₄
13	A ₂	3	13	A ₁	1	987.0839	0.1012	1.4	v ₄
18	F ₁	7	18	F ₂	3	987.3083	0.0221	4.0	v ₄
20	F ₂	9	20	F ₁	4	987.7185	0.0077	0.6	v ₄
20	F ₂	9	20	F ₁	3	987.8265	0.0008	-1.1	v ₄
20	E	6	20	E	3	987.8675	0.0053	2.2	v ₄
9	F ₂	3	9	F ₁	1	987.9975	0.3014	-2.2	v ₄
9	F ₁	3	9	F ₂	1	988.0447	0.2972	-3.3	v ₄
15	F ₂	5	15	F ₁	2	988.1944	0.0671	-0.1	v ₄
15	F ₁	7	15	F ₂	3	988.3524	0.0689	4.5	v ₄
12	F ₁	4	12	F ₂	1	988.6298	0.1611	-0.1	v ₄
17	A ₁	2	17	A ₂	1	988.6606	0.0283	-2.3	v ₄
12	F ₂	5	12	F ₁	2	988.7332	0.1581	-1.1	v ₄
17	F ₁	7	17	F ₂	3	988.9280	0.0319	0.8	v ₄
1	F ₁	1	2	F ₂	1	988.9443	0.1613	1.4	v ₄
19	F ₂	8	19	F ₁	4	989.0115	0.0143	6.2	v ₄
1	E	1	2	E	1	989.1555	0.1111	4.3	v ₄
19	F ₁	9	19	F ₂	5	989.3057	0.0014	-6.7	v ₄
19	F ₁	9	19	F ₂	4	989.4351	0.0130	2.5	v ₄
14	A ₂	2	14	A ₁	1	989.5409	0.0826	0.9	v ₄
8	A ₂	1	8	A ₁	1	989.6844	0.2889	-2.6	v ₄
8	F ₂	3	8	F ₁	1	989.7642	0.3383	-4.2	v ₄
14	F ₂	6	14	F ₁	2	989.7738	0.0937	-0.2	v ₄
8	E	2	8	E	1	989.8066	0.2349	0.3	v ₄
14	E	4	14	E	2	989.9137	0.0626	1.5	v ₄
11	A ₁	2	11	A ₂	1	990.0468	0.1786	1.3	v ₄
20	F ₁	9	20	F ₂	4	990.0764	0.0104	7.1	v ₄
16	F ₁	7	16	F ₂	3	990.1393	0.0495	0.2	v ₄
11	F ₁	5	11	F ₂	2	990.2057	0.2051	-0.9	v ₄
11	E	3	11	E	1	990.2963	0.1396	1.9	v ₄
18	F ₁	8	18	F ₂	4	990.5343	0.0237	8.9	v ₄
16	F ₂	7	16	F ₁	3	990.5616	0.0458	-0.2	v ₄
19	A ₁	4	19	A ₂	2	990.9053	0.0136	0.9	v ₄

Table D.3 – Continued.

<i>J</i>	γ	<i>n</i>	<i>J'</i>	γ'	<i>n'</i>	ν^{exp} , cm^{-1}	S_{ν}^{exp} , $\text{cm}^{-2} \cdot \text{atm}^{-1}$	δ , %	Band
<i>I</i>			2			3	4	5	6
13	F ₂	6	13	F ₁	3	990.9708	0.1349	1.7	v ₄
7	F ₂	2	7	F ₁	1	991.2596	0.3771	-3.7	v ₄
20	F ₂	10	20	F ₁	5	991.2782	0.0066	-12.4	v ₄
15	E	5	15	E	2	991.3093	0.0510	2.1	v ₄
13	F ₁	5	13	F ₂	2	991.3313	0.1203	-3.3	v ₄
7	F ₁	3	7	F ₂	1	991.3952	0.3679	-4.8	v ₄
10	F ₁	4	10	F ₂	2	991.4638	0.2561	-2.4	v ₄
15	F ₂	6	15	F ₁	3	991.5794	0.0741	5.2	v ₄
18	A ₁	3	18	A ₂	2	991.6538	0.0175	3.9	v ₄
10	F ₂	4	10	F ₁	2	991.7007	0.0076	8.2	v ₄
10	F ₂	4	10	F ₁	1	991.7193	0.2557	1.2	v ₄
21	F ₁	10	21	F ₂	5	991.8993	0.0045	-3.3	v ₄
16	A ₂	3	16	A ₁	2	992.0609	0.0480	3.9	v ₄
12	E	4	12	E	2	992.1080	0.1180	-0.8	v ₄
12	F ₁	5	12	F ₂	2	992.3388	0.1762	3.0	v ₄
19	E	6	19	E	3	992.5474	0.0084	-4.7	v ₄
6	E	2	6	E	1	992.5826	0.2716	-1.5	v ₄
0	F ₂	1	1	F ₁	1	992.6059	0.0566	1.2	v ₄
9	E	3	9	E	1	992.6210	0.2127	0.8	v ₄
15	A ₂	2	15	A ₁	1	992.6368	0.0568	0.5	v ₄
17	F ₁	8	17	F ₂	4	992.6454	0.0310	-0.6	v ₄
6	F ₁	2	6	F ₂	1	992.6836	0.3938	-3.9	v ₄
9	F ₂	4	9	F ₁	2	992.7919	0.3051	-1.4	v ₄
18	F ₁	9	18	F ₂	5	992.8468	0.0212	7.3	v ₄
6	A ₁	1	6	A ₂	1	992.9326	0.3305	-2.4	v ₄
13	A ₁	2	13	A ₂	1	992.9856	0.1210	0.6	v ₄
11	F ₂	4	11	F ₁	2	993.0700	0.2242	-2.1	v ₄
12	A ₁	2	12	A ₂	1	993.1557	0.1409	0.3	v ₄
16	F ₂	8	16	F ₁	4	993.2022	0.0445	-0.7	v ₄
16	F ₂	8	16	F ₁	3	993.2736	0.0060	-5.4	v ₄
9	A ₂	2	9	A ₁	1	993.3083	0.2485	-3.1	v ₄
18	F ₂	9	18	F ₁	4	993.4104	0.0229	4.5	v ₄
14	F ₂	7	14	F ₁	3	993.4926	0.0965	0.0	v ₄
8	F ₁	3	8	F ₂	1	993.5876	0.3532	-3.5	v ₄
17	E	6	17	E	3	993.6506	0.0241	9.3	v ₄
5	F ₂	2	5	F ₁	1	993.6758	0.3946	-5.0	v ₄
10	A ₂	2	10	A ₁	1	993.7096	0.2226	-5.9	v ₄
17	E	6	17	E	2	993.7591	0.0022	8.8	v ₄
15	F ₂	7	15	F ₁	4	993.8531	0.0683	-0.2	v ₄
18	A ₂	3	18	A ₁	2	993.8930	0.0198	2.9	v ₄
15	F ₂	7	15	F ₁	3	993.9071	0.0060	8.7	v ₄
13	F ₁	6	13	F ₂	3	993.9559	0.1282	0.2	v ₄
11	F ₁	6	11	F ₂	3	993.9784	0.2189	0.0	v ₄

Table D.3 – Continued.

<i>J</i>	γ	<i>n</i>	<i>J'</i>	γ'	<i>n'</i>	ν^{exp} , cm^{-1}	S_{ν}^{exp} , $\text{cm}^{-2} \cdot \text{atm}^{-1}$	δ , %	Band
<i>I</i>		2		3		4		5	6
5	F ₁	2	5	F ₂	1	994.0095	0.4043	-1.4	v ₄
17	F ₂	9	17	F ₁	5	994.0164	0.0322	-8.3	v ₄
8	F ₂	4	8	F ₁	2	994.1913	0.3428	-4.8	v ₄
7	A ₁	2	7	A ₂	1	994.2300	0.3257	-3.4	v ₄
4	A ₂	1	4	A ₁	1	994.4143	0.3186	-2.7	v ₄
13	E	4	13	E	2	994.4247	0.0929	0.9	v ₄
10	F ₂	5	10	F ₁	2	994.4389	0.2669	-0.6	v ₄
10	F ₂	5	10	F ₁	1	994.4575	0.0116	10.1	v ₄
12	F ₁	6	12	F ₂	3	994.5023	0.1711	-2.0	v ₄
14	E	5	14	E	3	994.5101	0.0635	-7.3	v ₄
12	F ₁	6	12	F ₂	2	994.5289	0.0092	8.1	v ₄
7	F ₁	4	7	F ₂	2	994.7305	0.3780	-5.5	v ₄
4	F ₂	2	4	F ₁	1	994.7419	0.3758	-3.6	v ₄
9	F ₂	5	9	F ₁	3	994.9284	0.3194	-1.5	v ₄
9	F ₂	5	9	F ₁	2	994.9407	0.0074	-3.1	v ₄
4	E	1	4	E	1	994.9676	0.2549	-1.4	v ₄
12	F ₂	6	12	F ₁	3	995.0126	0.1834	-1.0	v ₄
7	E	2	7	E	1	995.0592	0.2619	-2.5	v ₄
11	E	4	11	E	2	995.0694	0.1529	-1.3	v ₄
13	F ₂	7	13	F ₁	4	995.1097	0.1482	2.8	v ₄
6	F ₁	3	6	F ₂	2	995.2008	0.4008	-5.1	v ₄
3	F ₂	1	3	F ₁	1	995.2579	0.3273	-3.9	v ₄
11	F ₂	5	11	F ₁	3	995.3744	0.2334	-1.4	v ₄
9	F ₁	4	9	F ₂	2	995.3991	0.3252	-3.2	v ₄
8	E	3	8	E	2	995.4389	0.2481	-2.0	v ₄
12	A ₂	2	12	A ₁	2	995.4524	0.1560	-1.8	v ₄
10	F ₁	5	10	F ₂	3	995.5659	0.2804	-3.3	v ₄
6	F ₂	3	6	F ₁	1	995.6166	0.4077	-4.9	v ₄
3	F ₁	2	3	F ₂	1	995.6242	0.3167	-7.1	v ₄
5	E	2	5	E	1	995.6698	0.2764	-2.3	v ₄
8	F ₁	4	8	F ₂	2	995.7009	0.3650	-4.8	v ₄
2	E	1	2	E	1	995.7127	0.1760	-0.1	v ₄
9	A ₁	1	9	A ₂	1	995.8312	0.2778	-2.8	v ₄
7	F ₂	3	7	F ₁	2	995.8539	0.4014	-4.0	v ₄
5	F ₂	3	5	F ₁	2	995.8833	0.4071	-4.5	v ₄
2	F ₁	1	2	F ₂	1	995.8951	0.2591	-1.9	v ₄
1	F ₂	1	1	F ₁	1	996.0051	0.1671	-0.2	v ₄
4	F ₁	2	4	F ₂	1	996.0140	0.3786	-5.1	v ₄
6	A ₂	1	6	A ₁	1	996.0599	0.3495	-3.8	v ₄
3	A ₁	1	3	A ₂	1	996.1678	0.2810	-2.1	v ₄
1	A ₂	1	0	A ₁	1	999.4944	0.1448	1.2	v ₄
3	F ₁	3	3	F ₂	1	1002.0782	0.0032	3.5	v ₄
2	F ₂	1	1	F ₁	1	1002.8181	0.2735	-1.7	v ₄

Table D.3 – Continued.

<i>J</i>	γ	<i>n</i>	<i>J'</i>	γ'	<i>n'</i>	ν^{exp} , cm^{-1}	S_{ν}^{exp} , $\text{cm}^{-2} \cdot \text{atm}^{-1}$	δ , %	Band
<i>I</i>			2			3	4	5	6
4	F ₂	3	4	F ₁	1	1003.2807	0.0031	-4.0	v ₄
4	E	2	4	E	1	1003.5406	0.0059	9.7	v ₄
5	F ₂	4	5	F ₁	1	1004.4530	0.0041	2.1	v ₄
5	F ₁	3	5	F ₂	1	1004.8823	0.0111	8.3	v ₄
6	E	3	6	E	1	1005.6117	0.0055	4.3	v ₄
6	F ₁	4	6	F ₂	1	1006.0220	0.0091	4.2	v ₄
3	F ₁	1	2	F ₂	1	1006.0451	0.3530	-4.4	v ₄
3	E	1	2	E	1	1006.0932	0.2430	-1.1	v ₄
8	F ₁	5	8	F ₂	1	1006.4374	0.0041	6.1	v ₄
9	F ₁	5	9	F ₂	2	1006.5334	0.0028	4.3	v ₄
7	F ₂	4	7	F ₁	1	1006.8413	0.0106	0.5	v ₄
11	F ₂	6	11	F ₁	3	1006.8867	0.0015	4.3	v ₄
8	F ₂	5	8	F ₁	2	1006.9051	0.0094	7.9	v ₄
13	F ₂	8	13	F ₁	3	1007.0270	0.0046	2.8	v ₄
9	E	4	9	E	1	1007.0450	0.0055	9.1	v ₄
11	F ₁	7	11	F ₂	3	1007.3312	0.0040	2.3	v ₄
9	F ₂	6	9	F ₁	1	1007.5328	0.0023	-7.4	v ₄
10	F ₁	6	10	F ₂	2	1007.6979	0.0089	-1.1	v ₄
8	A ₂	2	8	A ₁	1	1007.7214	0.0104	6.5	v ₄
11	A ₁	3	11	A ₂	1	1007.9399	0.0084	-0.1	v ₄
7	F ₁	6	7	F ₂	2	1008.0081	0.0060	-3.1	v ₄
7	F ₁	6	7	F ₂	1	1008.0174	0.0135	-2.9	v ₄
8	F ₂	6	8	F ₁	2	1009.0571	0.0093	2.3	v ₄
4	A ₁	1	3	A ₂	1	1009.0862	0.3512	-3.7	v ₄
4	F ₁	1	3	F ₂	1	1009.2080	0.4153	-5.1	v ₄
9	A ₂	3	9	A ₁	1	1009.2702	0.0217	0.9	v ₄
8	E	4	8	E	2	1009.2845	0.0028	3.0	v ₄
4	F ₂	1	3	F ₁	1	1009.3146	0.4157	-5.0	v ₄
10	F ₂	7	10	F ₁	2	1010.0895	0.0129	2.7	v ₄
10	F ₂	7	10	F ₁	1	1010.1081	0.0124	2.4	v ₄
9	F ₂	7	9	F ₁	3	1010.1224	0.0068	8.5	v ₄
9	F ₂	7	9	F ₁	1	1010.1565	0.0108	-1.7	v ₄
9	F ₁	6	9	F ₂	2	1010.5410	0.0031	-1.8	v ₄
9	F ₁	6	9	F ₂	1	1010.5767	0.0153	0.7	v ₄
12	A ₁	3	12	A ₂	1	1010.6991	0.0195	3.3	v ₄
11	F ₁	8	11	F ₂	3	1010.7166	0.0152	3.7	v ₄
11	F ₁	8	11	F ₂	2	1010.7513	0.0091	7.7	v ₄
21	A ₂	5	21	A ₁	2	1010.9104	0.0019	-7.9	v ₄
11	E	5	11	E	2	1011.0290	0.0049	0.0	v ₄
13	F ₁	8	13	F ₂	3	1011.1968	0.0146	4.9	v ₄
20	F ₂	12	20	F ₁	5	1011.2376	0.0034	0.9	v ₄
18	A ₁	4	18	A ₂	2	1011.2459	0.0058	0.5	v ₄
15	A ₂	3	15	A ₁	1	1011.2749	0.0120	-1.0	v ₄

Table D.3 – Continued.

<i>J</i>	γ	<i>n</i>	<i>J'</i>	γ'	<i>n'</i>	ν^{exp} , cm^{-1}	S_{ν}^{exp} , $\text{cm}^{-2} \cdot \text{atm}^{-1}$	δ , %	Band
<i>I</i>		2		3		4		5	6
19	F ₁	12	19	F ₂	5	1011.3236	0.0044	-4.6	v ₄
12	F ₁	8	12	F ₂	2	1011.4097	0.0026	-14.9	v ₄
14	F ₂	9	14	F ₁	3	1011.4810	0.0140	5.8	v ₄
16	F ₂	10	16	F ₁	4	1011.5188	0.0094	-1.5	v ₄
17	F ₁	10	17	F ₂	4	1011.5605	0.0075	-6.1	v ₄
16	F ₂	10	16	F ₁	3	1011.5905	0.0020	6.8	v ₄
10	F ₁	7	10	F ₂	3	1011.6388	0.0027	-10.2	v ₄
10	F ₁	7	10	F ₂	1	1011.6964	0.0131	2.4	v ₄
14	E	6	14	E	2	1011.9038	0.0055	2.2	v ₄
12	F ₂	8	12	F ₁	2	1011.9946	0.0139	4.0	v ₄
10	A ₁	3	10	A ₂	1	1012.0634	0.0128	0.9	v ₄
5	F ₁	1	4	F ₂	1	1012.1358	0.4490	-6.8	v ₄
5	E	1	4	E	1	1012.3596	0.3103	-2.6	v ₄
18	F ₂	11	18	F ₁	3	1012.3896	0.0019	-3.0	v ₄
15	F ₁	10	15	F ₂	4	1012.4194	0.0062	1.9	v ₄
5	F ₂	1	4	F ₁	1	1012.4462	0.4505	-6.1	v ₄
16	E	7	16	E	2	1012.4780	0.0022	-6.1	v ₄
15	F ₁	10	15	F ₂	3	1012.5184	0.0067	4.0	v ₄
21	A ₁	4	21	A ₂	2	1012.5542	0.0016	3.5	v ₄
5	A ₂	1	4	A ₁	1	1012.5731	0.3825	-4.5	v ₄
13	F ₂	9	13	F ₁	4	1012.6394	0.0047	-3.5	v ₄
13	F ₂	9	13	F ₁	2	1012.7350	0.0095	0.6	v ₄
11	F ₂	7	11	F ₁	1	1012.7852	0.0117	1.8	v ₄
16	F ₁	10	16	F ₂	4	1012.8101	0.0046	-3.3	v ₄
16	F ₁	10	16	F ₂	2	1012.9632	0.0037	-0.9	v ₄
17	F ₂	11	17	F ₁	5	1012.9810	0.0049	0.0	v ₄
11	F ₁	9	11	F ₂	1	1013.1870	0.0124	0.6	v ₄
17	F ₂	11	17	F ₁	3	1013.1945	0.0031	-0.7	v ₄
14	F ₁	9	14	F ₂	4	1013.2060	0.0062	1.5	v ₄
13	A ₂	4	13	A ₁	1	1013.3785	0.0105	-11.2	v ₄
12	A ₂	3	12	A ₁	2	1013.8572	0.0040	1.4	v ₄
16	A ₁	4	16	A ₂	1	1013.9085	0.0067	1.6	v ₄
15	A ₁	4	15	A ₂	2	1013.9422	0.0047	-1.5	v ₄
12	F ₂	9	12	F ₁	1	1014.3146	0.0109	7.1	v ₄
15	F ₁	11	15	F ₂	2	1014.8447	0.0065	-3.0	v ₄
15	E	7	15	E	1	1015.0541	0.0049	-2.3	v ₄
6	F ₂	1	5	F ₁	2	1015.0856	0.4639	-6.8	v ₄
6	E	1	5	E	1	1015.1518	0.3181	-3.8	v ₄
6	F ₁	1	5	F ₂	1	1015.5039	0.4692	-4.9	v ₄
6	F ₂	2	5	F ₁	1	1015.6730	0.4727	-4.6	v ₄
15	F ₂	14	16	F ₁	2	1015.7772	0.0018	3.9	v ₂
14	E	7	14	E	1	1016.8254	0.0046	4.5	v ₄
17	F ₂	12	17	F ₁	2	1016.8537	0.0042	4.4	v ₄

Table D.3 – Continued.

<i>J</i>	γ	<i>n</i>	<i>J'</i>	γ'	<i>n'</i>	ν^{exp} , cm $^{-1}$	S_{ν}^{exp} , cm $^{-2} \cdot \text{atm}^{-1}$	δ , %	Band
<i>I</i>			2			3	4	5	6
18	F ₁	12	18	F ₂	2	1017.7794	0.0026	-4.8	v ₄
7	A ₂	1	6	A ₁	1	1017.8888	0.3881	-4.7	v ₄
18	F ₂	13	18	F ₁	1	1017.9490	0.0030	2.5	v ₄
7	F ₂	1	6	F ₁	1	1017.9886	0.4553	-6.9	v ₄
7	F ₁	1	6	F ₂	2	1018.1072	0.4637	-4.8	v ₄
15	F ₁	12	15	F ₂	1	1018.2160	0.0051	1.3	v ₄
7	A ₁	1	6	A ₂	1	1018.5583	0.3848	-4.2	v ₄
7	F ₁	2	6	F ₂	1	1018.7228	0.4540	-6.5	v ₄
7	E	1	6	E	1	1018.7766	0.3106	-4.0	v ₄
19	E	9	19	E	1	1018.9311	0.0013	-3.6	v ₄
19	F ₂	23	20	F ₁	5	1019.1656	0.0019	-15.4	v ₂
19	F ₁	24	20	F ₂	5	1019.2187	0.0016	-1.9	v ₂
16	F ₂	12	16	F ₁	1	1019.4481	0.0038	4.1	v ₄
16	E	8	16	E	1	1019.4729	0.0024	-2.3	v ₄
14	F ₁	13	15	F ₂	2	1020.2725	0.0021	0.6	v ₂
8	F ₂	1	7	F ₁	2	1020.7118	0.4281	-7.1	v ₄
8	E	1	7	E	1	1020.8653	0.2954	-3.1	v ₄
8	F ₁	1	7	F ₂	2	1020.9726	0.4309	-5.9	v ₄
8	A ₁	1	7	A ₂	1	1021.1881	0.3662	-4.1	v ₄
18	F ₂	21	19	F ₁	5	1021.2865	0.0016	-14.2	v ₂
18	A ₁	7	19	A ₂	2	1021.3335	0.0027	2.0	v ₂
18	F ₁	20	19	F ₂	4	1021.3680	0.0025	-7.2	v ₂
18	E	15	19	E	3	1021.5834	0.0016	0.3	v ₂
8	F ₁	2	7	F ₂	1	1021.7602	0.4250	-6.4	v ₄
8	F ₂	2	7	F ₁	1	1021.8512	0.4251	-6.7	v ₄
13	F ₁	12	14	F ₂	1	1023.2315	0.0025	3.6	v ₂
9	F ₁	1	8	F ₂	2	1023.4467	0.3905	-6.1	v ₄
9	E	1	8	E	2	1023.5137	0.2683	-2.8	v ₄
9	F ₂	1	8	F ₁	2	1023.7371	0.3913	-5.1	v ₄
17	F ₁	19	18	F ₂	4	1023.9128	0.0033	-8.7	v ₂
17	E	13	18	E	3	1023.9613	0.0027	-3.7	v ₂
9	F ₁	2	8	F ₂	1	1024.0231	0.3966	-4.0	v ₄
17	F ₁	20	18	F ₂	3	1024.0798	0.0017	-11.2	v ₂
17	F ₁	21	18	F ₂	3	1024.2773	0.0017	-5.0	v ₂
9	E	2	8	E	1	1024.8289	0.2639	-2.7	v ₄
9	F ₂	2	8	F ₁	1	1024.8669	0.3871	-5.2	v ₄
9	A ₂	1	8	A ₁	1	1024.9321	0.3274	-3.9	v ₄
10	A ₁	1	9	A ₂	1	1026.0734	0.2901	-3.8	v ₄
10	F ₁	1	9	F ₂	2	1026.1517	0.3438	-4.9	v ₄
10	F ₂	1	9	F ₁	3	1026.2538	0.3424	-5.1	v ₄
16	F ₂	18	17	F ₁	5	1026.4278	0.0060	-6.3	v ₂
16	E	12	17	E	3	1026.4382	0.0038	0.9	v ₂
10	A ₂	1	9	A ₁	1	1026.5050	0.2899	-2.7	v ₄

Table D.3 – Continued.

<i>J</i>	γ	<i>n</i>	<i>J'</i>	γ'	<i>n'</i>	ν^{exp} , cm^{-1}	S_{ν}^{exp} , $\text{cm}^{-2} \cdot \text{atm}^{-1}$	δ , %	Band
<i>I</i>			2			3	4	5	6
16	F ₂	19	17	F ₁	4	1026.5819	0.0058	1.7	v ₂
10	F ₂	2	9	F ₁	2	1026.7928	0.3458	-3.5	v ₄
16	F ₁	19	17	F ₂	3	1026.8393	0.0038	-4.1	v ₂
10	E	1	9	E	1	1026.8661	0.2368	-0.8	v ₄
10	F ₁	2	9	F ₂	1	1027.8694	0.3379	-4.2	v ₄
10	F ₂	3	9	F ₁	1	1027.9211	0.3381	-4.3	v ₄
11	F ₁	1	10	F ₂	3	1028.7217	0.2931	-3.7	v ₄
11	E	1	10	E	2	1028.8273	0.1993	-1.4	v ₄
11	F ₂	1	10	F ₁	2	1028.9225	0.2901	-4.2	v ₄
12	A ₂	4	13	A ₁	1	1029.1306	0.0027	-3.2	v ₂
15	E	12	16	E	3	1029.1684	0.0060	0.5	v ₂
11	A ₂	1	10	A ₁	1	1029.2129	0.2461	-2.4	v ₄
15	F ₂	18	16	F ₁	3	1029.4945	0.0057	2.4	v ₂
11	F ₂	2	10	F ₁	1	1029.5527	0.2914	-2.8	v ₄
11	F ₁	2	10	F ₂	2	1029.6791	0.2902	-3.2	v ₄
15	A ₁	6	16	A ₂	1	1029.9630	0.0046	-1.7	v ₂
11	A ₁	1	10	A ₂	1	1030.8608	0.2388	-2.5	v ₄
11	F ₁	3	10	F ₂	1	1030.8956	0.2919	-0.8	v ₄
11	E	2	10	E	1	1030.9118	0.1959	-0.2	v ₄
7	A ₁	2	6	A ₂	1	1031.0531	0.0095	-0.8	v ₄
12	F ₂	1	11	F ₁	3	1031.2996	0.2409	-2.7	v ₄
12	E	1	11	E	2	1031.3572	0.1634	-0.8	v ₄
12	F ₁	1	11	F ₂	3	1031.4990	0.2408	-2.2	v ₄
7	F ₁	4	6	F ₂	1	1031.5574	0.0066	-5.3	v ₄
12	F ₂	2	11	F ₁	2	1031.8569	0.2413	-1.7	v ₄
14	F ₁	16	15	F ₂	4	1031.9297	0.0114	-1.7	v ₂
14	F ₂	16	15	F ₁	4	1031.9849	0.0100	-2.7	v ₂
14	F ₂	17	15	F ₁	3	1032.2635	0.0080	-7.2	v ₂
12	E	2	11	E	1	1032.3606	0.1597	-1.2	v ₄
12	F ₁	2	11	F ₂	2	1032.4229	0.2380	-1.8	v ₄
12	A ₁	1	11	A ₂	1	1032.5226	0.1989	-1.6	v ₄
14	F ₂	18	15	F ₁	2	1032.7407	0.0070	1.2	v ₂
11	F ₂	11	12	F ₁	2	1033.7610	0.0030	-7.9	v ₂
13	A ₂	1	12	A ₁	2	1033.8011	0.1611	-1.1	v ₄
12	F ₁	3	11	F ₂	1	1033.8534	0.2378	0.3	v ₄
13	F ₂	1	12	F ₁	3	1033.8600	0.1833	-6.4	v ₄
12	F ₂	3	11	F ₁	1	1033.8738	0.2318	-2.4	v ₄
13	F ₁	1	12	F ₂	3	1033.9373	0.1936	-0.4	v ₄
11	F ₁	11	12	F ₂	1	1033.9832	0.0021	2.2	v ₂
13	A ₁	1	12	A ₂	1	1034.0844	0.1605	-0.6	v ₄
13	F ₁	2	12	F ₂	2	1034.4377	0.1890	-2.0	v ₄
13	E	1	12	E	2	1034.5113	0.1275	-0.8	v ₄
13	F ₁	15	14	F ₂	4	1034.8215	0.0139	-4.5	v ₂

Table D.3 – Continued.

<i>J</i>	γ	<i>n</i>	<i>J'</i>	γ'	<i>n'</i>	ν^{exp} , cm^{-1}	S_{ν}^{exp} , $\text{cm}^{-2} \cdot \text{atm}^{-1}$	δ , %	Band
<i>I</i>			2			3	4	5	6
13	E	10	14	E	3	1034.8648	0.0095	3.4	v ₂
13	F ₂	15	14	F ₁	3	1035.0089	0.0132	2.0	v ₂
13	F ₂	2	12	F ₁	2	1035.1530	0.1870	-1.4	v ₄
13	F ₁	3	12	F ₂	1	1035.2406	0.1861	-2.0	v ₄
13	E	11	14	E	2	1035.5662	0.0059	-2.8	v ₂
8	F ₁	3	7	F ₂	2	1035.6525	0.0018	-0.8	v ₄
8	F ₁	3	7	F ₂	1	1035.6618	0.0121	2.7	v ₄
8	F ₂	4	7	F ₁	1	1036.2711	0.0106	3.7	v ₄
14	F ₂	1	13	F ₁	4	1036.3225	0.1479	-0.9	v ₄
14	E	1	13	E	2	1036.3954	0.0991	-0.1	v ₄
14	F ₁	1	13	F ₂	3	1036.4678	0.1473	-0.5	v ₄
6	F ₂	4	5	F ₁	1	1036.6150	0.0035	8.3	v ₄
13	F ₂	3	12	F ₁	1	1036.7991	0.1761	-5.0	v ₄
13	A ₂	2	12	A ₁	1	1036.8109	0.1522	-1.3	v ₄
14	F ₁	2	13	F ₂	2	1037.0150	0.1454	-0.8	v ₄
14	F ₂	2	13	F ₁	3	1037.1389	0.1479	0.9	v ₄
12	F ₂	14	13	F ₁	4	1037.8553	0.0171	0.2	v ₂
14	A ₂	1	13	A ₁	1	1037.8905	0.1198	-0.1	v ₄
14	F ₂	3	13	F ₁	2	1037.9502	0.1443	0.3	v ₄
14	E	2	13	E	1	1037.9760	0.0962	0.3	v ₄
12	F ₁	14	13	F ₂	3	1038.0415	0.0136	-4.4	v ₂
12	A ₁	5	13	A ₂	1	1038.2013	0.0114	-5.0	v ₂
10	F ₁	10	11	F ₂	2	1038.4350	0.0021	-1.3	v ₂
12	F ₁	15	13	F ₂	2	1038.5062	0.0107	-1.4	v ₂
12	F ₂	15	13	F ₁	3	1038.5601	0.0110	-3.3	v ₂
15	F ₁	1	14	F ₂	4	1038.7915	0.1107	0.0	v ₄
15	E	1	14	E	3	1038.8367	0.0738	0.4	v ₄
15	F ₂	1	14	F ₁	3	1038.9299	0.1110	0.8	v ₄
15	F ₁	2	14	F ₂	3	1039.2977	0.1093	-0.1	v ₄
15	E	2	14	E	2	1039.6365	0.0727	0.9	v ₄
14	F ₁	3	13	F ₂	1	1039.6972	0.1433	2.6	v ₄
15	A ₂	1	14	A ₁	1	1039.8112	0.0905	0.5	v ₄
9	E	3	8	E	1	1039.9411	0.0103	0.1	v ₄
9	F ₂	4	8	F ₁	1	1040.1141	0.0141	0.6	v ₄
9	A ₂	2	8	A ₁	1	1040.6376	0.0112	-0.8	v ₄
15	F ₂	3	14	F ₁	1	1040.6580	0.1055	-0.2	v ₄
15	F ₁	3	14	F ₂	2	1040.6897	0.1063	0.6	v ₄
11	A ₂	5	12	A ₁	2	1041.0003	0.0155	-4.3	v ₂
11	F ₂	13	12	F ₁	3	1041.0834	0.0184	-0.5	v ₂
11	F ₁	13	12	F ₂	3	1041.1793	0.0161	-3.4	v ₂
16	A ₁	1	15	A ₂	2	1041.2076	0.0681	2.3	v ₄
16	F ₁	1	15	F ₂	4	1041.2515	0.0793	-0.3	v ₄
16	F ₂	1	15	F ₁	4	1041.3082	0.0798	1.0	v ₄

Table D.3 – Continued.

<i>J</i>	γ	<i>n</i>	<i>J'</i>	γ'	<i>n'</i>	ν^{exp} , cm^{-1}	S_{ν}^{exp} , $\text{cm}^{-2} \cdot \text{atm}^{-1}$	δ , %	Band
<i>I</i>		2		3		4		5	6
16	A ₂	1	15	A ₁	1	1041.4038	0.0666	0.5	v ₄
11	A ₁	5	12	A ₂	1	1041.4602	0.0118	-4.5	v ₂
11	F ₁	14	12	F ₂	2	1041.6003	0.0127	-2.7	v ₂
16	F ₂	2	15	F ₁	3	1041.7496	0.0785	0.7	v ₄
16	E	1	15	E	2	1041.8130	0.0526	0.6	v ₄
9	E	6	10	E	1	1042.2108	0.0020	-7.4	v ₂
16	F ₁	2	15	F ₂	3	1042.2558	0.0775	0.3	v ₄
11	F ₂	14	12	F ₁	2	1042.3045	0.0077	-0.2	v ₂
11	F ₁	15	12	F ₂	1	1042.3175	0.0075	-0.4	v ₂
16	F ₂	3	15	F ₁	2	1042.3518	0.0773	0.2	v ₄
16	E	2	15	E	1	1043.3632	0.0501	-0.2	v ₄
16	F ₁	3	15	F ₂	2	1043.3720	0.0749	-0.5	v ₄
16	A ₁	2	15	A ₂	1	1043.3888	0.0631	0.5	v ₄
17	F ₁	1	16	F ₂	4	1043.6413	0.0551	-1.0	v ₄
17	E	1	16	E	3	1043.6943	0.0371	0.3	v ₄
17	F ₂	1	16	F ₁	4	1043.7479	0.0547	0.0	v ₄
10	F ₁	4	9	F ₂	1	1044.0254	0.0182	1.3	v ₄
17	A ₂	1	16	A ₁	2	1044.0454	0.0469	2.0	v ₄
17	F ₂	2	16	F ₁	3	1044.2045	0.0542	0.8	v ₄
10	F ₂	4	9	F ₁	1	1044.2852	0.0175	4.8	v ₄
17	F ₁	2	16	F ₂	3	1044.3056	0.0544	0.9	v ₄
10	E	8	11	E	2	1044.4276	0.0130	2.3	v ₂
10	F ₁	12	11	F ₂	3	1044.6831	0.0159	-1.2	v ₂
17	A ₁	1	16	A ₂	1	1044.8284	0.0482	6.6	v ₄
10	F ₂	13	11	F ₁	2	1044.8496	0.0150	-1.7	v ₂
17	F ₁	3	16	F ₂	2	1044.8898	0.0533	0.5	v ₄
17	E	2	16	E	2	1044.9147	0.0361	1.4	v ₄
10	E	9	11	E	1	1045.4586	0.0059	1.1	v ₂
10	F ₁	13	11	F ₂	2	1045.4699	0.0087	0.2	v ₂
10	A ₁	5	11	A ₂	1	1045.4899	0.0076	4.0	v ₂
17	F ₁	4	16	F ₂	1	1046.0465	0.0502	-3.7	v ₄
18	E	1	17	E	3	1046.0717	0.0261	5.1	v ₄
18	F ₁	1	17	F ₂	4	1046.1413	0.0374	-0.1	v ₄
10	A ₂	2	9	A ₁	1	1046.2569	0.0076	3.7	v ₄
18	F ₂	2	17	F ₁	4	1046.4478	0.0378	1.3	v ₄
18	E	2	17	E	2	1046.6976	0.0241	-0.4	v ₄
18	F ₁	2	17	F ₂	3	1046.7508	0.0361	0.5	v ₄
8	F ₁	8	9	F ₂	1	1046.8130	0.0037	2.6	v ₂
18	A ₁	1	17	A ₂	1	1046.8379	0.0306	-0.5	v ₄
8	A ₂	3	9	A ₁	1	1047.4014	0.0048	3.4	v ₂
10	E	3	9	E	1	1047.4184	0.0035	9.7	v ₄
18	F ₁	3	17	F ₂	2	1047.4373	0.0361	1.2	v ₄
18	F ₂	3	17	F ₁	3	1047.4636	0.0360	0.3	v ₄

Table D.3 – Continued.

<i>J</i>	γ	<i>n</i>	<i>J'</i>	γ'	<i>n'</i>	ν^{exp} , cm^{-1}	S_{ν}^{exp} , $\text{cm}^{-2} \cdot \text{atm}^{-1}$	δ , %	Band
<i>I</i>			2			3	4	5	6
9	F ₁	11	10	F ₂	3	1047.8137	0.0209	2.7	v ₂
11	A ₁	2	10	A ₂	1	1047.8425	0.0168	0.9	v ₄
11	E	3	10	E	1	1048.0988	0.0113	-11.9	v ₄
9	A ₂	4	10	A ₁	1	1048.2362	0.0133	-0.2	v ₂
19	A ₂	1	18	A ₁	2	1048.3952	0.0211	1.7	v ₄
19	F ₂	1	18	F ₁	4	1048.4289	0.0246	0.4	v ₄
19	F ₁	1	18	F ₂	5	1048.4722	0.0241	1.2	v ₄
8	F ₁	5	7	F ₂	1	1048.5116	0.0023	8.1	v ₄
19	A ₁	1	18	A ₂	2	1048.5520	0.0212	1.0	v ₄
9	F ₂	12	10	F ₁	1	1048.7360	0.0097	3.6	v ₂
9	F ₁	12	10	F ₂	2	1048.7694	0.0097	0.5	v ₂
19	F ₁	2	18	F ₂	4	1048.8132	0.0239	2.0	v ₄
19	E	1	18	E	3	1048.8580	0.0163	0.0	v ₄
19	F ₂	2	18	F ₁	3	1049.1939	0.0240	1.3	v ₄
19	F ₁	3	18	F ₂	3	1049.2619	0.0237	0.3	v ₄
19	E	2	18	E	2	1049.9867	0.0166	5.3	v ₄
19	F ₂	3	18	F ₁	2	1049.9926	0.0224	-4.5	v ₄
19	A ₂	2	18	A ₁	1	1050.0030	0.0199	2.3	v ₄
20	F ₂	1	19	F ₁	5	1050.7658	0.0154	-0.8	v ₄
20	E	1	19	E	3	1050.8102	0.0106	2.2	v ₄
11	F ₂	4	10	F ₁	2	1050.8386	0.0027	6.1	v ₄
20	F ₁	1	19	F ₂	5	1050.8497	0.0135	-3.9	v ₄
11	F ₂	4	10	F ₁	1	1050.8573	0.0064	-3.6	v ₄
20	A ₁	1	19	A ₂	2	1051.0563	0.0137	3.9	v ₄
20	F ₁	2	19	F ₂	5	1051.0636	0.0022	2.2	v ₄
20	F ₁	2	19	F ₂	4	1051.1930	0.0137	0.1	v ₄
20	F ₂	2	19	F ₁	4	1051.2474	0.0141	-0.5	v ₄
8	A ₁	4	9	A ₂	1	1051.3900	0.0169	1.8	v ₂
8	F ₂	10	9	F ₁	3	1051.6374	0.0156	-1.7	v ₂
20	E	2	19	E	2	1051.7080	0.0103	4.0	v ₄
12	F ₂	5	11	F ₁	1	1051.7666	0.0199	1.1	v ₄
11	F ₁	6	10	F ₂	2	1051.7841	0.0073	5.6	v ₄
8	A ₂	4	9	A ₁	1	1052.1118	0.0083	-4.1	v ₂
8	F ₂	11	9	F ₁	2	1052.1781	0.0099	1.2	v ₂
8	E	7	9	E	1	1052.2019	0.0069	2.2	v ₂
7	A ₂	3	8	A ₁	1	1052.3378	0.0021	-4.7	v ₂
21	F ₁	1	20	F ₂	5	1053.1058	0.0088	-6.2	v ₄
21	E	1	20	E	4	1053.1263	0.0057	1.5	v ₄
21	F ₂	1	20	F ₁	5	1053.1972	0.0084	-4.1	v ₄
21	F ₁	2	20	F ₂	4	1053.3809	0.0099	3.3	v ₄
21	E	2	20	E	3	1053.6108	0.0058	6.2	v ₄
21	F ₂	2	20	F ₁	4	1053.6213	0.0080	5.2	v ₄
9	F ₁	5	8	F ₂	1	1053.8573	0.0059	4.0	v ₄

Table D.3 – Continued.

<i>J</i>	γ	<i>n</i>	<i>J'</i>	γ'	<i>n'</i>	ν^{exp} , cm^{-1}	S_{ν}^{exp} , $\text{cm}^{-2} \cdot \text{atm}^{-1}$	δ , %	Band
<i>I</i>			2			3	4	5	6
12	E	4	11	E	1	1055.1237	0.0059	-1.7	v ₄
7	F ₁	9	8	F ₂	2	1055.2401	0.0163	-1.5	v ₂
13	E	3	12	E	1	1055.2537	0.0131	1.5	v ₄
13	F ₂	5	12	F ₁	1	1055.2828	0.0192	-0.1	v ₄
7	E	6	8	E	2	1055.3088	0.0102	-2.9	v ₂
12	F ₁	5	11	F ₂	3	1055.3257	0.0019	9.6	v ₄
13	A ₂	3	12	A ₁	1	1055.3440	0.0162	1.5	v ₄
12	F ₁	5	11	F ₂	2	1055.3604	0.0079	2.3	v ₄
22	A ₁	1	21	A ₂	2	1055.4067	0.0048	5.0	v ₄
22	F ₁	1	21	F ₂	5	1055.4277	0.0048	-2.2	v ₄
22	A ₂	1	21	A ₁	2	1055.5928	0.0056	7.9	v ₄
22	F ₂	1	21	F ₁	5	1055.6176	0.0035	9.6	v ₄
7	F ₂	9	8	F ₁	2	1055.7113	0.0106	4.5	v ₂
22	F ₁	2	21	F ₂	5	1055.7868	0.0010	-1.4	v ₄
7	F ₁	10	8	F ₂	1	1055.7941	0.0099	0.5	v ₂
7	F ₁	10	8	F ₂	1	1055.7941	0.0101	2.6	v ₂
22	F ₁	2	21	F ₂	4	1056.0214	0.0047	-1.6	v ₄
22	F ₂	3	21	F ₁	4	1056.0464	0.0038	-3.9	v ₄
12	A ₁	2	11	A ₂	1	1056.2007	0.0074	1.9	v ₄
6	F ₁	6	7	F ₂	2	1056.3912	0.0015	4.8	v ₂
6	F ₁	6	7	F ₂	1	1056.4005	0.0031	9.0	v ₂
6	F ₂	7	7	F ₁	1	1057.0372	0.0023	2.8	v ₂
6	E	5	7	E	1	1057.3750	0.0018	6.0	v ₂
12	F ₁	6	11	F ₂	3	1057.5158	0.0020	-6.4	v ₄
6	F ₁	7	7	F ₂	2	1057.5775	0.0009	10.9	v ₂
9	F ₁	6	8	F ₂	2	1057.8550	0.0014	-3.8	v ₄
23	A ₂	1	22	A ₁	2	1057.8727	0.0031	7.0	v ₄
23	F ₂	1	22	F ₁	4	1057.9066	0.0025	-7.8	v ₄
14	F ₁	5	13	F ₂	1	1058.7251	0.0180	1.3	v ₄
14	F ₂	5	13	F ₁	1	1058.7558	0.0185	4.2	v ₄
23	F ₂	3	22	F ₁	3	1059.0036	0.0036	10.6	v ₄
23	F ₁	4	22	F ₂	3	1059.0226	0.0032	10.9	v ₄
6	F ₂	8	7	F ₁	2	1059.1552	0.0144	2.0	v ₂
13	F ₂	6	12	F ₁	2	1059.2094	0.0095	-2.3	v ₄
6	E	6	7	E	1	1059.4550	0.0061	-5.6	v ₂
6	E	6	7	E	1	1059.4550	0.0065	1.8	v ₂
6	F ₁	8	7	F ₂	2	1059.5111	0.0091	0.1	v ₂
13	F ₁	5	12	F ₂	1	1059.5823	0.0092	5.3	v ₄
6	A ₁	3	7	A ₂	1	1059.5877	0.0072	-2.6	v ₂
6	A ₁	3	7	A ₂	1	1059.5877	0.0074	0.0	v ₂
10	E	4	9	E	1	1059.6488	0.0032	4.6	v ₄
5	F ₁	6	6	F ₂	2	1061.6683	0.0009	11.5	v ₂
5	F ₁	6	6	F ₂	1	1061.6735	0.0017	2.4	v ₂

Table D.3 – Continued.

<i>J</i>	γ	<i>n</i>	<i>J'</i>	γ'	<i>n'</i>	ν^{exp} , cm^{-1}	S_{ν}^{exp} , $\text{cm}^{-2} \cdot \text{atm}^{-1}$	δ , %	Band
<i>I</i>			2			3	4	5	6
5	E	4	6	E	1	1061.9094	0.0012	3.0	v ₂
15	A ₁	2	14	A ₂	1	1062.0854	0.0128	-2.1	v ₄
15	F ₁	6	14	F ₂	1	1062.1001	0.0158	1.0	v ₄
15	E	4	14	E	1	1062.1075	0.0098	-6.6	v ₄
5	F ₂	6	6	F ₁	1	1062.1881	0.0014	1.9	v ₂
14	A ₂	2	13	A ₁	1	1062.9880	0.0085	2.2	v ₄
5	A ₂	3	6	A ₁	1	1063.2211	0.0095	1.5	v ₂
14	F ₂	6	13	F ₁	2	1063.2350	0.0097	3.7	v ₄
14	E	4	13	E	1	1063.3829	0.0064	2.7	v ₄
5	F ₂	7	6	F ₁	1	1063.4033	0.0080	-4.7	v ₂
5	F ₂	7	6	F ₁	1	1063.4033	0.0085	1.6	v ₂
5	F ₁	7	6	F ₂	2	1063.4969	0.0076	2.5	v ₂
5	F ₁	7	6	F ₂	2	1063.4969	0.0077	2.7	v ₂
11	A ₂	2	10	A ₁	1	1064.3087	0.0055	3.3	v ₄
10	A ₁	3	9	A ₂	1	1064.5590	0.0022	6.2	v ₄
11	F ₂	6	10	F ₁	1	1064.6967	0.0033	-7.4	v ₄
11	F ₁	7	10	F ₂	2	1065.1368	0.0026	-3.2	v ₄
16	F ₁	5	15	F ₂	1	1065.3736	0.0134	2.0	v ₄
16	F ₂	6	15	F ₁	1	1065.3801	0.0129	-1.5	v ₄
14	F ₁	6	13	F ₂	3	1065.7137	0.0020	8.2	v ₄
4	E	3	5	E	1	1065.7421	0.0002	8.4	v ₂
14	F ₁	6	13	F ₂	2	1065.7506	0.0026	3.6	v ₄
4	F ₁	5	5	F ₂	1	1066.4888	0.0020	2.6	v ₂
15	F ₂	5	14	F ₁	1	1066.8567	0.0087	-2.2	v ₄
14	F ₂	7	13	F ₁	3	1066.9769	0.0032	-4.1	v ₄
15	F ₁	7	14	F ₂	2	1067.0315	0.0090	0.7	v ₄
4	F ₂	6	5	F ₁	2	1067.6056	0.0061	-0.6	v ₂
4	F ₂	6	5	F ₁	2	1067.6056	0.0064	3.1	v ₂
4	E	4	5	E	1	1067.6528	0.0041	2.9	v ₂
4	E	4	5	E	1	1067.6528	0.0038	-3.1	v ₂
12	F ₂	7	11	F ₁	2	1069.5441	0.0048	-5.2	v ₄
15	F ₂	6	14	F ₁	2	1070.2364	0.0029	-1.5	v ₄
16	E	4	15	E	1	1070.4714	0.0051	-2.8	v ₄
16	F ₁	6	15	F ₂	2	1070.5174	0.0082	3.3	v ₄
16	A ₁	3	15	A ₂	1	1070.6162	0.0068	2.3	v ₄
15	A ₂	2	14	A ₁	1	1071.3513	0.0036	2.6	v ₄
3	E	3	4	E	1	1071.3949	0.0012	-0.5	v ₂
3	F ₂	4	4	F ₁	1	1071.6052	0.0008	0.6	v ₂
3	F ₁	5	4	F ₂	1	1072.0203	0.0040	-0.9	v ₂
3	F ₁	5	4	F ₂	1	1072.0203	0.0041	1.6	v ₂
12	A ₁	3	11	A ₂	1	1073.7441	0.0034	4.6	v ₄
17	F ₂	7	16	F ₁	2	1073.9606	0.0065	-2.2	v ₄
16	F ₁	7	15	F ₂	3	1073.9828	0.0038	0.9	v ₄

Table D.3 – Continued.

<i>J</i>	γ	<i>n</i>	<i>J'</i>	γ'	<i>n'</i>	ν^{exp} , cm^{-1}	S_{ν}^{exp} , $\text{cm}^{-2} \cdot \text{atm}^{-1}$	δ , %	Band
<i>I</i>		2		3		4		5	6
17	F ₁	6	16	F ₂	1	1074.0078	0.0069	3.9	v ₄
13	F ₁	7	12	F ₂	2	1074.4469	0.0040	5.1	v ₄
2	A ₁	2	3	A ₂	1	1076.6219	0.0019	2.4	v ₂
18	A ₂	2	17	A ₁	1	1077.3350	0.0047	6.4	v ₄
18	F ₂	7	17	F ₁	2	1077.3563	0.0052	-1.1	v ₄
18	E	5	17	E	1	1077.3670	0.0037	5.2	v ₄
17	A ₁	2	16	A ₂	1	1077.6737	0.0027	-12.0	v ₄
17	F ₁	7	16	F ₂	2	1077.9782	0.0031	-2.6	v ₄
14	F ₁	8	13	F ₂	2	1079.3498	0.0028	0.0	v ₄
14	F ₂	8	13	F ₁	3	1079.7205	0.0019	1.1	v ₄
19	F ₂	6	18	F ₁	1	1080.6441	0.0039	-3.9	v ₄
19	F ₁	8	18	F ₂	2	1080.6524	0.0041	2.1	v ₄
18	F ₂	8	17	F ₁	3	1081.7302	0.0030	-1.1	v ₄
15	E	6	14	E	2	1084.1039	0.0013	7.2	v ₄
14	F ₂	9	13	F ₁	3	1084.9653	0.0013	-2.2	v ₄
14	F ₂	9	13	F ₁	2	1085.0072	0.0014	1.9	v ₄
19	A ₂	3	18	A ₁	1	1085.2474	0.0022	5.8	v ₄
16	F ₂	9	15	F ₁	3	1088.1820	0.0021	0.6	v ₄
20	F ₂	8	19	F ₁	2	1088.5686	0.0020	9.0	v ₄
2	E	2	2	E	1	1092.0320	0.0007	6.4	v ₂
4	E	3	4	E	1	1092.0567	0.0003	-12.6	v ₂
3	F ₁	4	3	F ₂	1	1092.1596	0.0005	2.1	v ₂
2	F ₁	3	2	F ₂	1	1092.2244	0.0006	10.7	v ₂
6	A ₂	2	6	A ₁	1	1092.4214	0.0014	-2.7	v ₂
6	F ₂	6	6	F ₁	1	1092.4906	0.0009	9.1	v ₂
3	F ₂	4	3	F ₁	1	1092.6596	0.0028	0.6	v ₂
7	F ₂	6	7	F ₁	2	1092.6711	0.0013	-3.1	v ₂
4	F ₁	5	4	F ₂	1	1092.8005	0.0007	8.5	v ₂
4	F ₂	5	4	F ₁	1	1093.0426	0.0026	3.0	v ₂
4	F ₂	5	4	F ₁	1	1093.0426	0.0025	-2.9	v ₂
3	F ₁	5	3	F ₂	1	1093.0758	0.0011	0.0	v ₂
5	F ₁	6	5	F ₂	1	1093.2401	0.0008	5.7	v ₂
4	A ₂	2	4	A ₁	1	1093.3149	0.0058	1.0	v ₂
4	A ₂	2	4	A ₁	1	1093.3149	0.0058	1.5	v ₂
5	E	4	5	E	1	1093.4732	0.0020	3.0	v ₂
6	F ₂	7	6	F ₁	1	1093.8473	0.0012	-2.3	v ₂
4	F ₂	6	4	F ₁	1	1093.9213	0.0024	-12.2	v ₂
4	E	4	4	E	1	1093.9677	0.0024	2.1	v ₂
8	F ₁	8	8	F ₂	2	1094.0913	0.0020	-3.4	v ₂
8	F ₁	8	8	F ₂	2	1094.0913	0.0021	0.6	v ₂
6	E	5	6	E	1	1094.2035	0.0026	-9.8	v ₂
6	E	5	6	E	1	1094.2035	0.0030	4.7	v ₂
8	F ₂	8	8	F ₁	2	1094.2819	0.0009	11.6	v ₂

Table D.3 – Continued.

<i>J</i>	γ	<i>n</i>	<i>J'</i>	γ'	<i>n'</i>	ν^{exp} , cm^{-1}	S_{ν}^{exp} , $\text{cm}^{-2} \cdot \text{atm}^{-1}$	δ , %	Band
<i>I</i>			<i>2</i>			<i>3</i>	<i>4</i>	<i>5</i>	<i>6</i>
8	F ₂	8	8	F ₁	1	1094.2996	0.0008	5.4	v ₂
6	F ₁	7	6	F ₂	2	1094.3989	0.0037	2.0	v ₂
9	A ₁	3	9	A ₂	1	1094.4679	0.0030	9.1	v ₂
14	A ₂	4	14	A ₁	1	1094.4851	0.0001	-10.9	v ₂
9	F ₁	9	9	F ₂	2	1094.6123	0.0018	2.2	v ₂
9	E	6	9	E	1	1094.7235	0.0007	1.4	v ₂
8	A ₂	3	8	A ₁	1	1094.7306	0.0037	7.2	v ₂
7	F ₂	8	7	F ₁	1	1094.7806	0.0034	9.6	v ₂
7	F ₂	8	7	F ₁	1	1094.7806	0.0032	3.9	v ₂
5	F ₂	7	5	F ₁	1	1094.9771	0.0056	11.0	v ₂
10	F ₁	9	10	F ₂	3	1094.9984	0.0024	4.1	v ₂
7	F ₁	8	7	F ₂	2	1095.0089	0.0041	8.0	v ₂
5	F ₁	7	5	F ₂	1	1095.0687	0.0069	-0.9	v ₂
5	F ₁	7	5	F ₂	1	1095.0687	0.0070	-0.2	v ₂
10	F ₂	10	10	F ₁	1	1095.1482	0.0003	1.7	v ₂
7	A ₁	3	7	A ₂	1	1095.2225	0.0084	0.4	v ₂
7	A ₁	3	7	A ₂	1	1095.2225	0.0078	-6.5	v ₂
9	F ₂	9	9	F ₁	2	1095.4161	0.0007	-5.1	v ₂
8	F ₂	9	8	F ₁	2	1095.4276	0.0009	-3.8	v ₂
8	F ₂	9	8	F ₁	1	1095.4451	0.0027	3.6	v ₂
8	F ₂	9	8	F ₁	1	1095.4451	0.0027	2.2	v ₂
11	E	7	11	E	2	1095.4787	0.0011	2.4	v ₂
11	F ₂	10	11	F ₁	3	1095.5100	0.0009	-3.9	v ₂
11	F ₂	10	11	F ₁	2	1095.5329	0.0004	-4.4	v ₂
8	E	6	8	E	1	1095.6645	0.0019	1.5	v ₂
8	F ₁	9	8	F ₂	2	1095.8832	0.0003	7.5	v ₂
8	F ₁	9	8	F ₂	1	1095.8929	0.0089	3.5	v ₂
8	F ₁	9	8	F ₂	1	1095.8929	0.0087	1.3	v ₂
6	F ₂	8	6	F ₁	1	1095.9791	0.0011	0.2	v ₂
12	F ₁	11	12	F ₂	2	1095.9863	0.0005	-7.4	v ₂
10	E	7	10	E	2	1096.0503	0.0015	1.8	v ₂
10	E	7	10	E	1	1096.1049	0.0020	2.2	v ₂
10	F ₁	10	10	F ₂	3	1096.1775	0.0005	-6.4	v ₂
10	F ₁	10	10	F ₂	2	1096.2059	0.0023	6.7	v ₂
9	F ₁	10	9	F ₂	1	1096.2675	0.0024	-2.3	v ₂
6	E	6	6	E	1	1096.2836	0.0062	-5.2	v ₂
6	E	6	6	E	1	1096.2836	0.0065	0.3	v ₂
6	F ₁	8	6	F ₂	1	1096.3379	0.0095	0.5	v ₂
6	F ₁	8	6	F ₂	1	1096.3379	0.0098	3.7	v ₂
6	A ₁	3	6	A ₂	1	1096.4108	0.0096	1.5	v ₂
6	A ₁	3	6	A ₂	1	1096.4108	0.0091	-4.2	v ₂
13	F ₁	12	13	F ₂	2	1096.4888	0.0003	10.8	v ₂
9	E	7	9	E	1	1096.5413	0.0048	2.2	v ₂

Table D.3 – Continued.

<i>J</i>	γ	<i>n</i>	<i>J'</i>	γ'	<i>n'</i>	ν^{exp} , cm^{-1}	S_{ν}^{exp} , $\text{cm}^{-2} \cdot \text{atm}^{-1}$	δ , %	Band
<i>I</i>			<i>2</i>			<i>3</i>	<i>4</i>	<i>5</i>	<i>6</i>
9	F ₂	10	9	F ₁	3	1096.6812	0.0021	0.6	v ₂
9	F ₂	10	9	F ₁	3	1096.6812	0.0020	-5.2	v ₂
9	F ₂	10	9	F ₁	2	1096.6935	0.0065	0.0	v ₂
11	F ₂	11	11	F ₁	3	1096.7092	0.0020	2.6	v ₂
11	F ₂	11	11	F ₁	1	1096.7944	0.0025	1.8	v ₂
11	F ₂	11	11	F ₁	1	1096.7944	0.0024	-2.0	v ₂
11	F ₁	11	11	F ₂	2	1096.9696	0.0017	4.7	v ₂
11	F ₁	11	11	F ₂	1	1097.0117	0.0019	2.8	v ₂
10	A ₁	4	10	A ₂	1	1097.0182	0.0017	-0.6	v ₂
12	A ₂	4	12	A ₁	2	1097.2673	0.0023	-3.5	v ₂
10	F ₁	11	10	F ₂	2	1097.2917	0.0050	4.9	v ₂
11	A ₁	4	11	A ₂	1	1097.3720	0.0057	0.2	v ₂
11	A ₁	4	11	A ₂	1	1097.3720	0.0057	-0.4	v ₂
7	E	6	7	E	1	1097.3810	0.0020	-7.1	v ₂
7	E	6	7	E	1	1097.3810	0.0022	1.2	v ₂
12	A ₂	4	12	A ₁	1	1097.3907	0.0017	-5.1	v ₂
12	A ₂	4	12	A ₁	1	1097.3907	0.0018	1.4	v ₂
12	F ₂	12	12	F ₁	3	1097.4462	0.0016	10.6	v ₂
10	F ₂	11	10	F ₁	2	1097.4556	0.0021	1.7	v ₂
10	F ₂	11	10	F ₁	1	1097.4742	0.0056	4.2	v ₂
10	F ₂	11	10	F ₁	1	1097.4742	0.0058	7.3	v ₂
12	F ₂	12	12	F ₁	2	1097.5073	0.0004	3.7	v ₂
12	F ₂	12	12	F ₁	1	1097.5660	0.0020	5.1	v ₂
12	E	8	12	E	2	1097.5950	0.0008	4.3	v ₂
10	A ₂	4	10	A ₁	1	1097.6157	0.0075	0.0	v ₂
10	A ₂	4	10	A ₁	1	1097.6157	0.0073	-2.9	v ₂
12	E	8	12	E	1	1097.6808	0.0012	1.1	v ₂
7	F ₂	9	7	F ₁	1	1097.7910	0.0141	0.8	v ₂
7	F ₂	9	7	F ₁	1	1097.7910	0.0145	3.9	v ₂
7	F ₁	10	7	F ₂	2	1097.8589	0.0012	10.9	v ₂
7	F ₁	10	7	F ₂	1	1097.8683	0.0137	0.4	v ₂
7	F ₁	10	7	F ₂	1	1097.8683	0.0137	0.6	v ₂
13	F ₂	12	13	F ₁	4	1098.0165	0.0018	5.2	v ₂
11	F ₁	12	11	F ₂	2	1098.1067	0.0037	-4.7	v ₂
11	F ₁	12	11	F ₂	2	1098.1067	0.0039	1.7	v ₂
13	F ₂	12	13	F ₁	1	1098.1856	0.0017	5.7	v ₂
12	F ₁	12	12	F ₂	3	1098.1974	0.0007	8.6	v ₂
13	F ₁	13	13	F ₂	2	1098.2076	0.0005	11.9	v ₂
12	F ₁	12	12	F ₂	2	1098.2240	0.0004	2.0	v ₂
12	F ₁	12	12	F ₂	1	1098.2591	0.0050	-4.5	v ₂
12	F ₁	12	12	F ₂	1	1098.2591	0.0053	0.8	v ₂
13	F ₁	13	13	F ₂	1	1098.3307	0.0016	9.1	v ₂
11	F ₂	12	11	F ₁	2	1098.4355	0.0075	0.9	v ₂

Table D.3 – Continued.

<i>J</i>	γ	<i>n</i>	<i>J'</i>	γ'	<i>n'</i>	ν^{exp} , cm^{-1}	S_{ν}^{exp} , $\text{cm}^{-2} \cdot \text{atm}^{-1}$	δ , %	Band
<i>I</i>			2			3	4	5	6
11	F ₂	12	11	F ₁	2	1098.4355	0.0076	2.0	v ₂
14	E	9	14	E	3	1098.6981	0.0007	6.5	v ₂
14	F ₁	13	14	F ₂	4	1098.7286	0.0006	-10.5	v ₂
14	F ₁	13	14	F ₂	3	1098.7752	0.0004	11.8	v ₂
8	F ₁	10	8	F ₂	1	1098.8423	0.0027	4.1	v ₂
14	E	9	14	E	1	1098.9236	0.0009	8.3	v ₂
13	E	9	13	E	2	1099.0076	0.0009	7.6	v ₂
13	E	9	13	E	1	1099.1005	0.0028	2.9	v ₂
13	F ₂	13	13	F ₁	3	1099.1792	0.0016	1.4	v ₂
12	E	9	12	E	2	1099.2333	0.0038	-0.4	v ₂
12	E	9	12	E	2	1099.2333	0.0038	-1.8	v ₂
12	F ₁	13	12	F ₂	3	1099.3155	0.0008	12.5	v ₂
12	F ₁	13	12	F ₂	2	1099.3419	0.0056	-1.0	v ₂
12	F ₁	13	12	F ₂	2	1099.3419	0.0054	-4.7	v ₂
15	F ₂	14	15	F ₁	4	1099.3700	0.0005	8.9	v ₂
15	F ₁	14	15	F ₂	4	1099.3928	0.0003	-5.5	v ₂
15	F ₂	14	15	F ₁	3	1099.4242	0.0004	2.5	v ₂
8	A ₂	4	8	A ₁	1	1099.4411	0.0148	2.4	v ₂
8	F ₂	11	8	F ₁	2	1099.4827	0.0007	4.2	v ₂
8	F ₂	11	8	F ₁	1	1099.5002	0.0171	1.2	v ₂
8	F ₂	11	8	F ₁	1	1099.5002	0.0174	2.8	v ₂
8	E	7	8	E	1	1099.5221	0.0113	-2.7	v ₂
8	E	7	8	E	1	1099.5221	0.0114	-1.4	v ₂
15	F ₂	14	15	F ₁	1	1099.6671	0.0009	-4.7	v ₂
14	F ₁	14	14	F ₂	4	1099.8244	0.0011	4.5	v ₂
13	A ₂	5	13	A ₁	1	1099.9045	0.0021	1.2	v ₂
14	F ₁	14	14	F ₂	2	1099.9613	0.0029	-6.4	v ₂
14	F ₁	14	14	F ₂	2	1099.9613	0.0032	1.6	v ₂
14	F ₂	14	14	F ₁	3	1100.0245	0.0003	6.7	v ₂
13	F ₂	14	13	F ₁	4	1100.0455	0.0003	10.6	v ₂
13	F ₂	14	13	F ₁	3	1100.0993	0.0035	-9.9	v ₂
13	F ₂	14	13	F ₁	3	1100.0993	0.0039	1.1	v ₂
14	F ₂	14	14	F ₁	1	1100.1488	0.0024	0.1	v ₂
14	F ₂	14	14	F ₁	1	1100.1488	0.0023	-4.2	v ₂
13	F ₁	14	13	F ₂	3	1100.1933	0.0006	-4.8	v ₂
13	F ₁	14	13	F ₂	2	1100.2303	0.0045	0.9	v ₂
13	F ₁	14	13	F ₂	2	1100.2303	0.0043	-4.8	v ₂
13	A ₁	5	13	A ₂	1	1100.3276	0.0047	0.5	v ₂
9	F ₁	11	9	F ₂	2	1100.3680	0.0008	6.9	v ₂
14	A ₂	5	14	A ₁	1	1100.4463	0.0045	1.1	v ₂
15	A ₁	5	15	A ₂	2	1100.5627	0.0011	-5.7	v ₂
9	E	8	9	E	1	1100.5732	0.0035	2.2	v ₂
9	E	8	9	E	1	1100.5732	0.0035	2.9	v ₂

Table D.3 – Continued.

<i>J</i>	γ	<i>n</i>	<i>J'</i>	γ'	<i>n'</i>	ν^{exp} , cm^{-1}	S_{ν}^{exp} , $\text{cm}^{-2} \cdot \text{atm}^{-1}$	δ , %	Band
<i>I</i>		2		3		4		5	6
9	F ₂	11	9	F ₁	3	1100.6455	0.0017	12.1	v ₂
9	F ₂	11	9	F ₁	2	1100.6578	0.0051	9.5	v ₂
15	F ₁	15	15	F ₂	4	1100.7000	0.0006	-8.0	v ₂
15	A ₁	5	15	A ₂	1	1100.7540	0.0021	-1.9	v ₂
9	A ₂	4	9	A ₁	1	1100.7836	0.0064	-3.8	v ₂
9	A ₂	4	9	A ₁	1	1100.7836	0.0068	1.9	v ₂
15	F ₁	15	15	F ₂	3	1100.7993	0.0003	4.2	v ₂
15	F ₁	15	15	F ₂	2	1100.8851	0.0022	2.7	v ₂
15	E	10	15	E	1	1100.9697	0.0013	-2.2	v ₂
15	E	10	15	E	1	1100.9697	0.0014	4.9	v ₂
14	F ₂	15	14	F ₁	2	1101.0042	0.0030	0.0	v ₂
14	F ₂	15	14	F ₁	2	1101.0042	0.0029	-3.1	v ₂
14	E	10	14	E	2	1101.1283	0.0021	-3.1	v ₂
14	E	10	14	E	2	1101.1283	0.0020	-9.0	v ₂
17	F ₂	15	17	F ₁	1	1101.1893	0.0005	5.4	v ₂
14	F ₁	15	14	F ₂	3	1101.2404	0.0042	-3.5	v ₂
14	F ₁	15	14	F ₂	3	1101.2404	0.0045	3.0	v ₂
9	F ₂	12	9	F ₁	1	1101.3019	0.0191	-0.2	v ₂
9	F ₂	12	9	F ₁	1	1101.3019	0.0192	0.5	v ₂
9	F ₁	12	9	F ₂	1	1101.3309	0.0195	-0.4	v ₂
9	F ₁	12	9	F ₂	1	1101.3309	0.0197	0.9	v ₂
15	F ₂	15	15	F ₁	2	1101.4552	0.0039	0.5	v ₂
15	F ₂	15	15	F ₁	2	1101.4552	0.0040	2.8	v ₂
16	F ₁	15	16	F ₂	1	1101.7016	0.0017	-0.9	v ₂
16	F ₂	16	16	F ₁	2	1101.7723	0.0014	-3.7	v ₂
15	E	11	15	E	2	1102.1331	0.0021	-0.9	v ₂
15	E	11	15	E	2	1102.1331	0.0021	-4.3	v ₂
10	F ₂	12	10	F ₁	1	1102.1733	0.0003	-8.8	v ₂
15	F ₂	16	15	F ₁	3	1102.2089	0.0033	1.9	v ₂
10	E	8	10	E	2	1102.2137	0.0012	0.1	v ₂
16	E	11	16	E	2	1102.4289	0.0018	-7.1	v ₂
10	F ₁	12	10	F ₂	2	1102.4888	0.0070	2.0	v ₂
10	F ₁	12	10	F ₂	2	1102.4888	0.0064	-6.6	v ₂
16	F ₁	16	16	F ₂	2	1102.5082	0.0025	0.3	v ₂
16	F ₁	16	16	F ₂	2	1102.5082	0.0024	-2.6	v ₂
10	F ₂	13	10	F ₁	2	1102.6182	0.0022	1.0	v ₂
10	F ₂	13	10	F ₁	1	1102.6368	0.0064	1.1	v ₂
16	F ₁	17	16	F ₂	3	1103.0664	0.0022	0.6	v ₂
16	F ₂	17	16	F ₁	3	1103.1612	0.0026	6.8	v ₂
16	A ₂	6	16	A ₁	2	1103.2304	0.0023	3.1	v ₂
16	A ₂	6	16	A ₁	2	1103.2304	0.0022	-0.3	v ₂
10	E	9	10	E	1	1103.2612	0.0134	0.3	v ₂
10	E	9	10	E	1	1103.2612	0.0133	-0.6	v ₂

Table D.3 – Continued.

<i>J</i>	γ	<i>n</i>	<i>J'</i>	γ'	<i>n'</i>	ν^{exp} , cm^{-1}	S_{ν}^{exp} , $\text{cm}^{-2} \cdot \text{atm}^{-1}$	δ , %	Band
<i>I</i>			<i>2</i>			<i>3</i>	<i>4</i>	<i>5</i>	<i>6</i>
10	F ₁	13	10	F ₂	1	1103.2699	0.0194	-4.0	v ₂
10	F ₁	13	10	F ₂	1	1103.2699	0.0207	2.5	v ₂
10	A ₁	5	10	A ₂	1	1103.2856	0.0176	3.0	v ₂
10	A ₁	5	10	A ₂	1	1103.2856	0.0167	-2.0	v ₂
17	F ₂	17	17	F ₁	3	1103.4187	0.0019	-1.5	v ₂
17	F ₂	17	17	F ₁	3	1103.4187	0.0019	-2.9	v ₂
17	F ₁	17	17	F ₂	3	1103.4289	0.0002	3.0	v ₂
18	F ₂	17	18	F ₁	1	1103.4516	0.0008	4.7	v ₂
18	F ₁	17	18	F ₂	2	1103.4846	0.0008	-1.3	v ₂
17	F ₁	17	17	F ₂	2	1103.5084	0.0016	1.3	v ₂
17	F ₁	17	17	F ₂	2	1103.5084	0.0016	-0.2	v ₂
17	A ₁	6	17	A ₂	1	1103.7768	0.0023	3.7	v ₂
17	F ₁	18	17	F ₂	3	1104.0242	0.0016	-4.3	v ₂
11	F ₂	13	11	F ₁	3	1104.0929	0.0003	5.5	v ₂
17	E	12	17	E	2	1104.1111	0.0010	-4.2	v ₂
11	F ₁	13	11	F ₂	3	1104.1927	0.0019	-6.7	v ₂
11	F ₁	13	11	F ₂	3	1104.1927	0.0021	5.0	v ₂
17	F ₂	18	17	F ₁	4	1104.2004	0.0019	-0.3	v ₂
17	F ₂	18	17	F ₁	4	1104.2004	0.0019	-2.9	v ₂
11	F ₁	13	11	F ₂	2	1104.2274	0.0007	9.8	v ₂
19	F ₁	18	19	F ₂	2	1104.3561	0.0005	3.8	v ₂
19	A ₁	6	19	A ₂	1	1104.3969	0.0005	9.1	v ₂
18	E	12	18	E	2	1104.4109	0.0007	-0.2	v ₂
18	F ₂	18	18	F ₁	2	1104.4154	0.0013	8.2	v ₂
18	A ₂	6	18	A ₁	1	1104.4230	0.0012	-5.3	v ₂
11	A ₁	5	11	A ₂	1	1104.5052	0.0063	-4.6	v ₂
11	A ₁	5	11	A ₂	1	1104.5052	0.0067	1.7	v ₂
11	F ₁	14	11	F ₂	3	1104.5871	0.0014	-1.7	v ₂
11	F ₁	14	11	F ₂	2	1104.6219	0.0072	-0.6	v ₂
11	E	9	11	E	1	1104.6554	0.0055	1.1	v ₂
11	E	9	11	E	1	1104.6554	0.0056	3.4	v ₂
18	F ₁	18	18	F ₂	3	1104.8675	0.0019	6.7	v ₂
18	F ₁	18	18	F ₂	3	1104.8675	0.0016	-12.7	v ₂
19	F ₂	18	19	F ₁	5	1105.0385	0.0002	3.1	v ₂
18	E	13	18	E	3	1105.1631	0.0009	0.0	v ₂
18	F ₁	19	18	F ₂	4	1105.2071	0.0013	-5.5	v ₂
20	F ₁	18	20	F ₂	1	1105.2786	0.0004	6.3	v ₂
19	F ₁	19	19	F ₂	3	1105.3228	0.0008	8.2	v ₂
11	F ₂	14	11	F ₁	1	1105.3378	0.0192	-2.4	v ₂
11	F ₂	14	11	F ₁	1	1105.3378	0.0197	0.2	v ₂
11	F ₁	15	11	F ₂	1	1105.3460	0.0193	-2.4	v ₂
11	F ₁	15	11	F ₂	1	1105.3460	0.0195	-1.4	v ₂
19	F ₂	19	19	F ₁	3	1105.9393	0.0012	12.7	v ₂

Table D.3 – Continued.

<i>J</i>	γ	<i>n</i>	<i>J'</i>	γ'	<i>n'</i>	ν^{exp} , cm^{-1}	S_{ν}^{exp} , $\text{cm}^{-2} \cdot \text{atm}^{-1}$	δ , %	Band
<i>I</i>			2			3	4	5	6
19	E	13	19	E	2	1105.9494	0.0008	-3.7	v ₂
20	F ₁	19	20	F ₂	2	1106.3147	0.0005	-0.6	v ₂
12	F ₁	14	12	F ₂	1	1106.3295	0.0005	3.8	v ₂
20	E	13	20	E	2	1106.3769	0.0004	7.0	v ₂
12	A ₁	5	12	A ₂	1	1106.4094	0.0034	0.3	v ₂
12	A ₁	5	12	A ₂	1	1106.4094	0.0034	-0.1	v ₂
12	F ₁	15	12	F ₂	3	1106.6955	0.0007	0.3	v ₂
12	F ₁	15	12	F ₂	2	1106.7222	0.0003	-4.7	v ₂
12	F ₂	15	12	F ₁	3	1106.7377	0.0004	-10.8	v ₂
12	F ₁	15	12	F ₂	1	1106.7572	0.0076	0.0	v ₂
12	F ₁	15	12	F ₂	1	1106.7572	0.0072	-5.7	v ₂
12	F ₂	15	12	F ₁	2	1106.7988	0.0086	0.2	v ₂
12	F ₂	15	12	F ₁	2	1106.7988	0.0078	-9.4	v ₂
20	F ₁	20	20	F ₂	3	1107.0532	0.0008	0.8	v ₂
20	A ₂	7	20	A ₁	2	1107.2651	0.0008	1.6	v ₂
21	F ₁	21	21	F ₂	3	1107.8829	0.0002	-0.7	v ₂
3	F ₁	4	2	F ₂	1	1107.9528	0.0010	0.8	v ₂
21	F ₂	22	21	F ₁	5	1108.3674	0.0004	3.5	v ₂
13	F ₂	15	13	F ₁	3	1108.4932	0.0024	5.4	v ₂
13	F ₁	16	13	F ₂	3	1108.5781	0.0018	8.5	v ₂
13	F ₁	16	13	F ₂	2	1108.6151	0.0020	-1.1	v ₂
13	F ₁	16	13	F ₂	2	1108.6151	0.0020	-2.8	v ₂
13	E	11	13	E	1	1109.0354	0.0053	2.9	v ₂
13	E	11	13	E	1	1109.0354	0.0052	1.5	v ₂
13	F ₂	16	13	F ₁	2	1109.0451	0.0077	-1.4	v ₂
13	F ₂	16	13	F ₁	2	1109.0451	0.0076	-2.1	v ₂
13	A ₂	6	13	A ₁	1	1109.0607	0.0069	-2.1	v ₂
13	A ₂	6	13	A ₁	1	1109.0607	0.0065	-8.9	v ₂
22	A ₂	8	22	A ₁	2	1109.4736	0.0003	4.8	v ₂
22	F ₁	23	22	F ₂	4	1109.6845	0.0002	0.5	v ₂
14	F ₂	17	14	F ₁	3	1110.8555	0.0010	12.8	v ₂
14	A ₂	6	14	A ₁	1	1110.8598	0.0021	1.0	v ₂
14	F ₂	17	14	F ₁	2	1110.9205	0.0023	1.2	v ₂
14	F ₂	17	14	F ₁	2	1110.9205	0.0023	0.7	v ₂
14	E	11	14	E	2	1110.9350	0.0018	-2.0	v ₂
15	E	12	15	E	2	1113.0685	0.0004	-0.5	v ₂
15	A ₂	6	15	A ₁	1	1113.0810	0.0014	5.1	v ₂
15	F ₂	18	15	F ₁	4	1113.2573	0.0004	6.3	v ₂
15	F ₁	18	15	F ₂	3	1113.3518	0.0027	-1.2	v ₂
15	F ₂	18	15	F ₁	2	1113.3651	0.0023	1.3	v ₂
15	F ₂	18	15	F ₁	2	1113.3651	0.0023	1.6	v ₂
4	A ₁	2	3	A ₂	1	1113.4655	0.0023	3.1	v ₂
4	A ₁	2	3	A ₂	1	1113.4655	0.0023	2.3	v ₂

Table D.3 – Continued.

<i>J</i>	γ	<i>n</i>	<i>J'</i>	γ'	<i>n'</i>	ν^{exp} , cm^{-1}	S_{ν}^{exp} , $\text{cm}^{-2} \cdot \text{atm}^{-1}$	δ , %	Band
<i>I</i>			2			3	4	5	6
15	E	13	15	E	1	1113.8372	0.0043	4.8	v ₂
15	F ₁	19	15	F ₂	2	1113.8420	0.0057	-5.8	v ₂
15	A ₁	6	15	A ₂	1	1113.8511	0.0049	1.1	v ₂
4	F ₁	5	3	F ₂	1	1113.8559	0.0018	-3.9	v ₂
4	F ₁	5	3	F ₂	1	1113.8559	0.0018	-5.1	v ₂
4	F ₂	5	3	F ₁	1	1114.0970	0.0015	8.6	v ₂
4	F ₂	6	3	F ₁	1	1114.9757	0.0003	2.8	v ₂
16	F ₂	19	16	F ₁	4	1115.5258	0.0007	8.9	v ₂
16	F ₂	19	16	F ₁	3	1115.5974	0.0005	-8.7	v ₂
16	A ₁	7	16	A ₂	1	1115.8327	0.0023	3.7	v ₂
16	F ₁	19	16	F ₂	2	1115.8895	0.0022	2.8	v ₂
16	E	13	16	E	2	1115.9109	0.0014	1.2	v ₂
16	E	13	16	E	2	1115.9109	0.0014	-3.7	v ₂
16	F ₂	20	16	F ₁	2	1116.3446	0.0045	-8.1	v ₂
16	F ₂	20	16	F ₁	2	1116.3446	0.0050	2.2	v ₂
16	F ₁	20	16	F ₂	1	1116.3540	0.0042	-12.6	v ₂
16	F ₁	20	16	F ₂	1	1116.3540	0.0047	-1.1	v ₂
17	E	13	17	E	2	1118.1511	0.0005	5.5	v ₂
17	F ₁	20	17	F ₂	3	1118.2112	0.0006	-7.9	v ₂
17	F ₁	21	17	F ₂	2	1118.4880	0.0016	1.1	v ₂
17	F ₂	20	17	F ₁	3	1118.5233	0.0017	-0.2	v ₂
17	F ₂	20	17	F ₁	3	1118.5233	0.0016	-2.3	v ₂
5	F ₁	6	4	F ₂	1	1119.5516	0.0035	5.0	v ₂
5	F ₁	6	4	F ₂	1	1119.5516	0.0034	2.9	v ₂
5	E	4	4	E	1	1119.7881	0.0021	1.5	v ₂
5	F ₂	6	4	F ₁	1	1120.0740	0.0021	4.2	v ₂
5	F ₂	6	4	F ₁	1	1120.0740	0.0021	4.0	v ₂
5	A ₂	3	4	A ₁	1	1121.1083	0.0019	4.4	v ₂
18	A ₂	7	18	A ₁	1	1121.1826	0.0011	-2.3	v ₂
18	F ₂	22	18	F ₁	2	1121.2005	0.0010	-2.5	v ₂
18	E	15	18	E	2	1121.2156	0.0007	12.2	v ₂
18	F ₁	22	18	F ₂	2	1121.5292	0.0027	0.3	v ₂
18	F ₁	22	18	F ₂	2	1121.5292	0.0025	-5.3	v ₂
19	F ₁	22	19	F ₂	3	1123.6059	0.0006	2.2	v ₂
19	F ₂	22	19	F ₁	2	1123.8775	0.0009	-3.2	v ₂
19	F ₁	24	19	F ₂	3	1124.0975	0.0002	3.1	v ₂
6	E	4	5	E	1	1124.1052	0.0011	4.5	v ₂
19	E	15	19	E	1	1124.1346	0.0006	-1.5	v ₂
19	F ₁	23	19	F ₂	2	1124.1511	0.0012	0.9	v ₂
19	A ₁	8	19	A ₂	1	1124.1710	0.0016	-1.5	v ₂
19	F ₁	25	19	F ₂	1	1124.6908	0.0030	3.9	v ₂
19	F ₂	24	19	F ₁	1	1124.6942	0.0027	-4.3	v ₂
6	F ₂	7	5	F ₁	2	1125.4175	0.0055	1.7	v ₂

Table D.3 – Continued.

<i>J</i>	γ	<i>n</i>	<i>J'</i>	γ'	<i>n'</i>	ν^{exp} , cm^{-1}	S_{ν}^{exp} , $\text{cm}^{-2} \cdot \text{atm}^{-1}$	δ , %	Band
<i>I</i>			<i>2</i>			<i>3</i>	<i>4</i>	<i>5</i>	<i>6</i>
6	F ₂	7	5	F ₁	2	1125.4175	0.0057	4.8	v ₂
6	E	5	5	E	1	1125.7672	0.0025	-5.8	v ₂
6	E	5	5	E	1	1125.7672	0.0027	2.4	v ₂
6	F ₁	7	5	F ₂	1	1125.9707	0.0037	2.5	v ₂
6	F ₁	7	5	F ₂	1	1125.9707	0.0036	0.5	v ₂
20	A ₁	8	20	A ₂	1	1126.3011	0.0005	-1.2	v ₂
20	F ₁	22	20	F ₂	2	1126.3112	0.0003	4.4	v ₂
20	F ₁	23	20	F ₂	1	1126.8350	0.0009	-8.3	v ₂
20	F ₂	24	20	F ₁	2	1126.9050	0.0008	-2.7	v ₂
20	A ₂	8	20	A ₁	1	1127.2829	0.0015	-5.7	v ₂
20	F ₂	25	20	F ₁	1	1127.3135	0.0017	-2.5	v ₂
20	E	17	20	E	1	1127.3218	0.0012	-2.4	v ₂
6	F ₂	8	5	F ₁	1	1127.5529	0.0031	10.9	v ₂
7	F ₂	6	6	F ₁	1	1129.4950	0.0007	1.3	v ₂
7	F ₁	7	6	F ₂	2	1129.5510	0.0018	8.6	v ₂
21	F ₂	25	21	F ₁	1	1129.9302	0.0010	-3.2	v ₂
21	F ₁	25	21	F ₂	1	1129.9519	0.0010	-3.4	v ₂
7	F ₂	7	6	F ₁	1	1130.5708	0.0009	-0.3	v ₂
7	A ₂	3	6	A ₁	1	1131.2084	0.0071	2.8	v ₂
7	A ₂	3	6	A ₁	1	1131.2084	0.0069	0.1	v ₂
7	F ₂	8	6	F ₁	1	1131.5907	0.0058	-1.3	v ₂
7	F ₂	8	6	F ₁	1	1131.5907	0.0059	0.8	v ₂
7	F ₁	8	6	F ₂	2	1131.8304	0.0050	11.5	v ₂
7	A ₁	3	6	A ₂	1	1132.0456	0.0040	1.8	v ₂
7	A ₁	3	6	A ₂	1	1132.0456	0.0038	-2.3	v ₂
22	E	17	22	E	1	1132.6067	0.0004	2.4	v ₂
7	F ₁	9	6	F ₂	2	1134.1364	0.0009	0.4	v ₂
7	F ₁	9	6	F ₂	1	1134.1417	0.0027	-1.8	v ₂
7	E	6	6	E	1	1134.2096	0.0023	3.5	v ₂
8	E	5	7	E	1	1134.9727	0.0008	4.3	v ₂
8	E	5	7	E	1	1134.9727	0.0008	1.6	v ₂
8	F ₁	7	7	F ₂	2	1134.9899	0.0013	-4.6	v ₂
8	F ₁	7	7	F ₂	2	1134.9899	0.0013	-2.0	v ₂
8	A ₁	3	7	A ₂	1	1135.0274	0.0020	3.1	v ₂
23	F ₂	25	23	F ₁	1	1135.2501	0.0005	2.9	v ₂
8	F ₁	8	7	F ₂	2	1136.1661	0.0006	4.7	v ₂
8	F ₁	8	7	F ₂	1	1136.1760	0.0002	-1.9	v ₂
8	F ₂	8	7	F ₁	2	1136.3481	0.0019	0.2	v ₂
8	F ₂	8	7	F ₁	1	1136.3617	0.0002	5.7	v ₂
8	F ₂	9	7	F ₁	2	1137.4936	0.0074	0.6	v ₂
8	F ₂	9	7	F ₁	2	1137.4936	0.0067	-9.5	v ₂
8	E	6	7	E	1	1137.7156	0.0048	0.4	v ₂
8	E	6	7	E	1	1137.7156	0.0051	5.1	v ₂

Table D.3 – Continued.

<i>J</i>	γ	<i>n</i>	<i>J'</i>	γ'	<i>n'</i>	ν^{exp} , cm^{-1}	S_{ν}^{exp} , $\text{cm}^{-2} \cdot \text{atm}^{-1}$	δ , %	Band
<i>I</i>		2		3		4		5	6
8	F ₁	9	7	F ₂	2	1137.9578	0.0046	-4.1	v ₂
8	F ₁	9	7	F ₂	2	1137.9578	0.0049	0.7	v ₂
8	F ₁	9	7	F ₂	1	1137.9671	0.0014	-1.8	v ₂
9	F ₂	8	8	F ₁	2	1140.4545	0.0012	-8.3	v ₂
9	F ₁	8	8	F ₂	1	1140.4776	0.0019	3.7	v ₂
8	A ₁	4	7	A ₂	1	1140.7834	0.0038	1.1	v ₂
8	A ₁	4	7	A ₂	1	1140.7834	0.0038	2.1	v ₂
8	F ₁	10	7	F ₂	2	1140.9072	0.0012	-1.2	v ₂
8	F ₁	10	7	F ₂	1	1140.9165	0.0027	-0.3	v ₂
8	F ₁	10	7	F ₂	1	1140.9165	0.0027	2.8	v ₂
8	F ₂	10	7	F ₁	1	1141.0341	0.0036	5.1	v ₂
8	F ₂	10	7	F ₁	1	1141.0341	0.0034	-0.5	v ₂
9	F ₁	9	8	F ₂	2	1141.9264	0.0011	1.8	v ₂
9	F ₁	9	8	F ₂	1	1141.9364	0.0007	4.0	v ₂
9	E	6	8	E	2	1142.0225	0.0018	0.9	v ₂
9	F ₁	10	8	F ₂	2	1143.5458	0.0089	0.9	v ₂
9	F ₁	10	8	F ₂	2	1143.5458	0.0088	-0.1	v ₂
9	E	7	8	E	2	1143.8403	0.0042	0.8	v ₂
9	E	7	8	E	2	1143.8403	0.0039	-7.8	v ₂
9	F ₂	10	8	F ₁	2	1143.9981	0.0069	1.3	v ₂
9	F ₂	10	8	F ₁	2	1143.9981	0.0070	2.6	v ₂
9	F ₂	10	8	F ₁	1	1144.0157	0.0005	9.1	v ₂
10	A ₂	3	9	A ₁	1	1145.9337	0.0012	8.9	v ₂
10	F ₂	9	9	F ₁	2	1145.9499	0.0015	3.4	v ₂
10	E	6	9	E	1	1145.9564	0.0011	-4.9	v ₂
10	E	6	9	E	1	1145.9564	0.0012	0.5	v ₂
10	F ₁	9	9	F ₂	2	1147.5527	0.0010	3.2	v ₂
10	F ₂	10	9	F ₁	3	1147.6799	0.0023	3.2	v ₂
9	E	8	8	E	1	1147.8933	0.0020	1.3	v ₂
9	F ₂	11	8	F ₁	1	1147.9800	0.0033	4.4	v ₂
9	F ₂	11	8	F ₁	1	1147.9800	0.0032	2.8	v ₂
9	A ₂	4	8	A ₁	1	1148.1129	0.0030	0.0	v ₂
9	A ₂	4	8	A ₁	1	1148.1129	0.0029	-5.4	v ₂
10	E	7	9	E	1	1148.6175	0.0006	8.1	v ₂
10	F ₁	10	9	F ₂	2	1148.7318	0.0010	-1.0	v ₂
10	F ₁	10	9	F ₂	1	1148.7675	0.0004	1.3	v ₂
10	A ₁	4	9	A ₂	1	1149.5137	0.0083	-2.9	v ₂
10	A ₁	4	9	A ₂	1	1149.5137	0.0085	-0.3	v ₂
10	F ₁	11	9	F ₂	2	1149.8175	0.0076	-0.8	v ₂
10	F ₁	11	9	F ₂	2	1149.8175	0.0077	-0.2	v ₂
10	F ₁	11	9	F ₂	1	1149.8533	0.0005	8.5	v ₂
10	F ₂	11	9	F ₁	3	1150.0061	0.0066	0.4	v ₂
10	F ₂	11	9	F ₁	3	1150.0061	0.0061	-6.9	v ₂

Table D.3 – Continued.

<i>J</i>	γ	<i>n</i>	<i>J'</i>	γ'	<i>n'</i>	ν^{exp} , cm $^{-1}$	S_{ν}^{exp} , cm $^{-2} \cdot \text{atm}^{-1}$	δ , %	Band
<i>I</i>			2			3	4	5	6
10	F ₂	11	9	F ₁	2	1150.0183	0.0010	2.3	v ₂
10	A ₂	4	9	A ₁	1	1150.1630	0.0065	3.1	v ₂
10	A ₂	4	9	A ₁	1	1150.1630	0.0063	-0.1	v ₂
11	F ₂	9	10	F ₁	1	1151.4347	0.0014	5.4	v ₂
11	F ₁	10	10	F ₂	2	1151.4431	0.0016	2.3	v ₂
11	F ₁	10	10	F ₂	2	1151.4431	0.0015	-3.0	v ₂
11	E	7	10	E	2	1153.2646	0.0010	3.8	v ₂
11	F ₂	10	10	F ₁	2	1153.3015	0.0016	2.2	v ₂
11	F ₂	10	10	F ₁	1	1153.3201	0.0005	12.5	v ₂
11	A ₂	4	10	A ₁	1	1153.3901	0.0030	-0.6	v ₂
11	F ₂	11	10	F ₁	2	1154.5007	0.0006	6.3	v ₂
11	F ₂	11	10	F ₁	1	1154.5192	0.0006	8.8	v ₂
10	F ₂	12	9	F ₁	3	1154.7052	0.0006	0.0	v ₂
11	F ₁	11	10	F ₂	3	1154.7122	0.0017	2.5	v ₂
10	F ₂	12	9	F ₁	2	1154.7174	0.0038	1.1	v ₂
10	F ₂	12	9	F ₁	2	1154.7174	0.0038	0.7	v ₂
10	E	8	9	E	1	1154.7809	0.0027	-8.9	v ₂
10	E	8	9	E	1	1154.7809	0.0030	1.9	v ₂
10	F ₁	12	9	F ₂	1	1155.0504	0.0028	1.3	v ₂
10	F ₂	13	9	F ₁	1	1155.2027	0.0032	2.0	v ₂
11	F ₁	12	10	F ₂	3	1155.8491	0.0078	-0.5	v ₂
11	F ₁	12	10	F ₂	3	1155.8491	0.0079	0.9	v ₂
11	F ₁	12	10	F ₂	2	1155.8774	0.0003	7.6	v ₂
11	F ₁	12	10	F ₂	1	1155.9068	0.0003	-3.8	v ₂
11	E	8	10	E	2	1156.0240	0.0049	-6.4	v ₂
11	E	8	10	E	2	1156.0240	0.0052	-1.4	v ₂
11	F ₂	12	10	F ₁	2	1156.2041	0.0062	0.1	v ₂
11	F ₂	12	10	F ₁	2	1156.2041	0.0066	5.1	v ₂
11	F ₂	12	10	F ₁	1	1156.2227	0.0012	-2.9	v ₂
12	F ₁	10	11	F ₂	2	1156.9337	0.0013	0.8	v ₂
12	A ₁	4	11	A ₂	1	1156.9395	0.0011	-1.7	v ₂
12	F ₁	11	11	F ₂	3	1158.9731	0.0014	-0.6	v ₂
12	F ₂	11	11	F ₁	2	1159.0262	0.0023	1.6	v ₂
12	F ₂	11	11	F ₁	2	1159.0262	0.0021	-9.0	v ₂
12	F ₂	12	11	F ₁	3	1160.4555	0.0009	8.6	v ₂
12	F ₂	12	11	F ₁	2	1160.4783	0.0010	0.4	v ₂
12	E	8	11	E	2	1160.5729	0.0016	1.5	v ₂
12	E	8	11	E	2	1160.5729	0.0015	0.1	v ₂
12	E	8	11	E	1	1160.6106	0.0005	0.8	v ₂
12	F ₁	12	11	F ₂	2	1161.2455	0.0005	-4.8	v ₂
12	F ₁	12	11	F ₂	1	1161.2876	0.0005	10.5	v ₂
11	A ₂	5	10	A ₁	1	1161.8132	0.0033	-4.6	v ₂
11	A ₂	5	10	A ₁	1	1161.8132	0.0035	0.5	v ₂

Table D.3 – Continued.

<i>J</i>	γ	<i>n</i>	<i>J'</i>	γ'	<i>n'</i>	ν^{exp} , cm^{-1}	S_{ν}^{exp} , $\text{cm}^{-2} \cdot \text{atm}^{-1}$	δ , %	Band
<i>I</i>			<i>2</i>			<i>3</i>	<i>4</i>	<i>5</i>	<i>6</i>
11	F ₂	13	10	F ₁	2	1161.8842	0.0007	1.9	v ₂
11	F ₂	13	10	F ₁	1	1161.9029	0.0033	1.1	v ₂
11	F ₂	13	10	F ₁	1	1161.9029	0.0033	-0.1	v ₂
12	F ₂	13	11	F ₁	3	1161.9872	0.0077	-1.8	v ₂
12	F ₂	13	11	F ₁	3	1161.9872	0.0081	2.7	v ₂
11	F ₁	13	10	F ₂	2	1161.9983	0.0035	-6.3	v ₂
11	F ₁	13	10	F ₂	2	1161.9983	0.0036	-1.1	v ₂
12	E	9	11	E	2	1162.2110	0.0040	0.1	v ₂
12	E	9	11	E	2	1162.2110	0.0041	3.5	v ₂
12	E	9	11	E	1	1162.2489	0.0007	1.4	v ₂
11	A ₁	5	10	A ₂	1	1162.3009	0.0021	1.6	v ₂
12	F ₁	13	11	F ₂	3	1162.3288	0.0066	-1.1	v ₂
12	F ₁	13	11	F ₂	3	1162.3288	0.0069	3.5	v ₂
11	F ₁	14	10	F ₂	2	1162.3928	0.0003	9.3	v ₂
11	E	9	10	E	2	1162.4037	0.0003	2.7	v ₂
13	F ₂	11	12	F ₁	2	1162.4305	0.0010	-6.3	v ₂
13	F ₁	11	12	F ₂	1	1162.4356	0.0011	1.1	v ₂
11	E	9	10	E	1	1162.4580	0.0020	5.8	v ₂
11	E	9	10	E	1	1162.4580	0.0019	4.6	v ₂
13	A ₁	4	12	A ₂	1	1164.6668	0.0011	-1.1	v ₂
13	F ₁	12	12	F ₂	2	1164.7046	0.0014	-1.5	v ₂
13	F ₁	12	12	F ₂	2	1164.7046	0.0015	-0.3	v ₂
13	E	8	12	E	2	1164.7175	0.0012	-5.3	v ₂
13	F ₂	12	12	F ₁	3	1166.2476	0.0008	0.6	v ₂
13	F ₁	13	12	F ₂	3	1166.3970	0.0015	1.4	v ₂
13	F ₁	13	12	F ₂	3	1166.3970	0.0014	-2.1	v ₂
13	F ₁	13	12	F ₂	2	1166.4235	0.0013	1.1	v ₂
13	E	9	12	E	2	1167.2684	0.0006	3.7	v ₂
13	F ₂	13	12	F ₁	2	1167.4179	0.0007	-3.8	v ₂
14	A ₂	4	13	A ₁	1	1167.9322	0.0007	-7.8	v ₂
13	A ₂	5	12	A ₁	2	1168.0412	0.0061	-4.1	v ₂
13	A ₂	5	12	A ₁	2	1168.0412	0.0063	-1.4	v ₂
13	F ₂	14	12	F ₁	3	1168.2768	0.0060	-0.3	v ₂
13	F ₂	14	12	F ₁	3	1168.2768	0.0061	1.3	v ₂
13	F ₂	14	12	F ₁	2	1168.3381	0.0005	-4.9	v ₂
13	F ₁	14	12	F ₂	3	1168.4195	0.0051	-9.7	v ₂
13	F ₁	14	12	F ₂	3	1168.4195	0.0056	-0.8	v ₂
13	F ₁	14	12	F ₂	2	1168.4461	0.0005	2.9	v ₂
13	F ₁	14	12	F ₂	1	1168.4813	0.0003	9.2	v ₂
13	A ₁	5	12	A ₂	1	1168.5357	0.0049	-4.7	v ₂
13	A ₁	5	12	A ₂	1	1168.5357	0.0051	-1.0	v ₂
12	F ₂	14	11	F ₁	2	1169.1187	0.0035	0.1	v ₂
12	E	10	11	E	2	1169.2052	0.0003	-6.1	v ₂

Table D.3 – Continued.

<i>J</i>	γ	<i>n</i>	<i>J'</i>	γ'	<i>n'</i>	ν^{exp} , cm^{-1}	S_{ν}^{exp} , $\text{cm}^{-2} \cdot \text{atm}^{-1}$	δ , %	Band
<i>I</i>			2			3	4	5	6
12	E	10	11	E	1	1169.2432	0.0020	6.6	v ₂
12	E	10	11	E	1	1169.2432	0.0018	-4.9	v ₂
12	F ₁	14	11	F ₂	3	1169.2814	0.0002	-1.0	v ₂
12	F ₁	14	11	F ₂	2	1169.3159	0.0030	-0.8	v ₂
12	F ₁	14	11	F ₂	2	1169.3159	0.0027	-11.0	v ₂
12	A ₁	5	11	A ₂	1	1169.4544	0.0031	-0.5	v ₂
12	A ₁	5	11	A ₂	1	1169.4544	0.0029	-9.3	v ₂
12	F ₁	15	11	F ₂	1	1169.7857	0.0021	0.0	v ₂
12	F ₁	15	11	F ₂	1	1169.7857	0.0021	-0.4	v ₂
12	F ₂	15	11	F ₁	1	1169.8322	0.0023	-1.8	v ₂
14	F ₁	12	13	F ₂	3	1170.3664	0.0002	0.6	v ₂
14	F ₁	12	13	F ₂	2	1170.4033	0.0012	1.6	v ₂
14	F ₂	13	13	F ₁	3	1170.4180	0.0015	-0.5	v ₂
14	E	9	13	E	2	1172.1391	0.0006	-1.4	v ₂
14	F ₁	13	13	F ₂	3	1172.1775	0.0009	-1.5	v ₂
14	F ₁	13	13	F ₂	2	1172.2146	0.0006	-7.1	v ₂
14	A ₁	5	13	A ₂	1	1172.2820	0.0024	1.9	v ₂
14	F ₁	14	13	F ₂	3	1173.2733	0.0003	8.3	v ₂
14	F ₁	14	13	F ₂	2	1173.3104	0.0006	1.4	v ₂
14	F ₂	14	13	F ₁	4	1173.4551	0.0011	0.2	v ₂
14	F ₂	14	13	F ₁	3	1173.5087	0.0006	1.7	v ₂
14	F ₂	14	13	F ₁	2	1173.5507	0.0003	9.0	v ₂
14	A ₂	5	13	A ₁	1	1173.8935	0.0011	6.5	v ₂
14	F ₂	15	13	F ₁	4	1174.3698	0.0052	0.5	v ₂
14	F ₂	15	13	F ₁	4	1174.3698	0.0056	6.4	v ₂
14	F ₂	15	13	F ₁	3	1174.4238	0.0002	2.5	v ₂
14	F ₂	15	13	F ₁	2	1174.4655	0.0003	5.9	v ₂
14	E	10	13	E	2	1174.5045	0.0035	-0.8	v ₂
14	E	10	13	E	2	1174.5045	0.0035	-2.2	v ₂
14	F ₁	15	13	F ₂	3	1174.6427	0.0047	-1.0	v ₂
14	F ₁	15	13	F ₂	3	1174.6427	0.0048	1.4	v ₂
14	F ₁	15	13	F ₂	2	1174.6797	0.0005	6.8	v ₂
15	E	9	14	E	2	1176.1155	0.0007	-7.6	v ₂
15	F ₂	13	14	F ₁	2	1176.1224	0.0011	-0.4	v ₂
15	A ₂	5	14	A ₁	1	1176.1335	0.0010	-4.7	v ₂
13	F ₁	15	12	F ₂	2	1176.5233	0.0027	0.4	v ₂
13	F ₁	15	12	F ₂	2	1176.5233	0.0026	-1.0	v ₂
13	E	10	12	E	2	1176.5667	0.0019	0.4	v ₂
13	F ₂	15	12	F ₁	2	1176.7319	0.0023	-1.1	v ₂
13	F ₁	16	12	F ₂	1	1176.8660	0.0029	-0.9	v ₂
13	F ₁	16	12	F ₂	1	1176.8660	0.0028	-1.3	v ₂
13	E	11	12	E	1	1177.2890	0.0012	-0.4	v ₂
13	F ₂	16	12	F ₁	1	1177.3006	0.0019	3.4	v ₂

Table D.3 – Continued.

<i>J</i>	γ	<i>n</i>	<i>J'</i>	γ'	<i>n'</i>	ν^{exp} , cm^{-1}	S_{ν}^{exp} , $\text{cm}^{-2} \cdot \text{atm}^{-1}$	δ , %	Band
<i>I</i>		2		3		4		5	6
13	F ₂	16	12	F ₁	1	1177.3006	0.0019	6.2	v ₂
13	A ₂	6	12	A ₁	1	1177.3209	0.0015	-5.9	v ₂
13	A ₂	6	12	A ₁	1	1177.3209	0.0016	3.8	v ₂
15	F ₂	14	14	F ₁	3	1178.0160	0.0009	-2.6	v ₂
15	F ₁	14	14	F ₂	3	1178.0808	0.0017	5.6	v ₂
15	F ₁	15	14	F ₂	4	1179.3412	0.0005	-6.8	v ₂
15	F ₁	15	14	F ₂	3	1179.3877	0.0007	1.4	v ₂
15	E	10	14	E	3	1179.4308	0.0009	-0.9	v ₂
15	E	10	14	E	2	1179.4956	0.0005	-4.1	v ₂
15	F ₂	15	14	F ₁	2	1180.0583	0.0005	-1.8	v ₂
15	F ₂	15	14	F ₁	1	1180.1174	0.0005	1.2	v ₂
15	F ₁	16	14	F ₂	4	1180.5284	0.0045	-1.5	v ₂
15	F ₁	16	14	F ₂	4	1180.5284	0.0043	-5.2	v ₂
15	E	11	14	E	3	1180.7122	0.0025	2.4	v ₂
15	E	11	14	E	3	1180.7122	0.0026	7.6	v ₂
15	E	11	14	E	2	1180.7772	0.0004	-1.6	v ₂
15	F ₂	16	14	F ₁	3	1180.8008	0.0040	-2.4	v ₂
15	F ₂	16	14	F ₁	3	1180.8008	0.0039	-4.4	v ₂
16	F ₁	14	15	F ₂	3	1181.8321	0.0009	1.3	v ₂
16	F ₂	14	15	F ₁	2	1181.8448	0.0009	6.8	v ₂
16	F ₂	15	15	F ₁	3	1183.9248	0.0008	1.0	v ₂
16	E	10	15	E	2	1183.9333	0.0008	-1.3	v ₂
14	A ₁	6	13	A ₂	1	1184.0021	0.0019	-1.4	v ₂
14	A ₁	6	13	A ₂	1	1184.0021	0.0019	1.9	v ₂
14	F ₁	16	13	F ₂	2	1184.0569	0.0018	-14.5	v ₂
14	F ₁	16	13	F ₂	2	1184.0569	0.0020	-1.7	v ₂
14	F ₂	16	13	F ₁	3	1184.1152	0.0020	-12.0	v ₂
14	F ₂	16	13	F ₁	3	1184.1152	0.0022	0.5	v ₂
14	A ₂	6	13	A ₁	1	1184.3068	0.0015	5.0	v ₂
14	A ₂	6	13	A ₁	1	1184.3068	0.0015	8.9	v ₂
14	F ₂	17	13	F ₁	2	1184.3817	0.0021	1.1	v ₂
14	F ₂	17	13	F ₁	2	1184.3817	0.0023	9.7	v ₂
14	E	11	13	E	1	1184.4041	0.0015	-2.2	v ₂
16	F ₁	15	15	F ₂	4	1185.2874	0.0005	1.4	v ₂
16	F ₂	16	15	F ₁	4	1185.3652	0.0007	-3.2	v ₂
16	F ₂	16	15	F ₁	3	1185.4193	0.0009	-2.0	v ₂
16	E	11	15	E	2	1186.1757	0.0004	0.6	v ₂
16	F ₁	16	15	F ₂	4	1186.1944	0.0005	1.0	v ₂
16	A ₁	6	15	A ₂	2	1186.5952	0.0034	2.2	v ₂
16	A ₁	6	15	A ₂	2	1186.5952	0.0032	-3.1	v ₂
16	F ₁	17	15	F ₂	4	1186.8109	0.0029	-5.2	v ₂
16	F ₁	17	15	F ₂	4	1186.8109	0.0029	-2.7	v ₂
16	F ₁	17	15	F ₂	3	1186.9098	0.0003	3.4	v ₂

Table D.3 – Continued.

<i>J</i>	γ	<i>n</i>	<i>J'</i>	γ'	<i>n'</i>	ν^{exp} , cm^{-1}	S_{ν}^{exp} , $\text{cm}^{-2} \cdot \text{atm}^{-1}$	δ , %	Band
<i>I</i>			<i>2</i>			<i>3</i>	<i>4</i>	<i>5</i>	<i>6</i>
16	F ₂	17	15	F ₁	4	1186.9238	0.0030	-1.2	v ₂
16	F ₂	17	15	F ₁	4	1186.9238	0.0030	-2.0	v ₂
16	A ₂	6	15	A ₁	1	1187.0141	0.0026	-3.9	v ₂
16	A ₂	6	15	A ₁	1	1187.0141	0.0027	-1.6	v ₂
17	A ₁	5	16	A ₂	1	1187.5471	0.0006	6.6	v ₂
17	F ₁	15	16	F ₂	2	1187.5604	0.0006	1.8	v ₂
17	F ₂	15	16	F ₁	4	1189.7142	0.0002	-11.5	v ₂
17	F ₂	15	16	F ₁	3	1189.7858	0.0006	-4.7	v ₂
17	F ₁	16	16	F ₂	3	1189.7921	0.0008	-1.6	v ₂
17	E	11	16	E	3	1191.2875	0.0003	-7.3	v ₂
17	F ₂	16	16	F ₁	4	1191.2942	0.0005	0.5	v ₂
17	A ₂	6	16	A ₁	2	1191.3551	0.0012	-3.8	v ₂
17	F ₂	16	16	F ₁	3	1191.3658	0.0004	2.3	v ₂
15	F ₁	17	14	F ₂	3	1191.6345	0.0018	4.5	v ₂
15	F ₁	17	14	F ₂	3	1191.6345	0.0017	0.4	v ₂
15	E	12	14	E	2	1191.7124	0.0010	5.2	v ₂
15	F ₂	17	14	F ₁	2	1191.7458	0.0016	-1.6	v ₂
15	A ₂	6	14	A ₁	1	1191.7955	0.0017	-0.6	v ₂
15	A ₂	6	14	A ₁	1	1191.7955	0.0019	6.6	v ₂
15	F ₁	18	14	F ₂	2	1192.0304	0.0015	-6.1	v ₂
17	F ₂	17	16	F ₁	3	1192.3083	0.0003	5.8	v ₂
17	F ₁	17	16	F ₂	4	1192.3261	0.0008	0.7	v ₂
17	F ₁	17	16	F ₂	3	1192.4208	0.0003	1.6	v ₂
15	A ₁	6	14	A ₂	1	1192.5331	0.0008	2.2	v ₂
17	A ₁	6	16	A ₂	1	1192.7898	0.0007	1.0	v ₂
17	F ₁	18	16	F ₂	4	1192.9214	0.0020	-4.1	v ₂
17	E	12	16	E	3	1193.0251	0.0014	-10.7	v ₂
17	E	12	16	E	3	1193.0251	0.0015	-3.8	v ₂
17	F ₂	18	16	F ₁	4	1193.1443	0.0022	-0.4	v ₂
17	F ₂	18	16	F ₁	4	1193.1443	0.0022	-1.7	v ₂
18	F ₁	15	17	F ₂	2	1193.2798	0.0004	-10.6	v ₂
18	F ₂	16	17	F ₁	3	1193.2883	0.0004	-2.4	v ₂
18	E	11	17	E	2	1195.6467	0.0004	7.5	v ₂
18	F ₁	16	17	F ₂	3	1195.6546	0.0005	-3.6	v ₂
18	A ₁	6	17	A ₂	1	1195.6688	0.0005	-0.1	v ₂
18	F ₁	17	17	F ₂	4	1197.2587	0.0005	-1.8	v ₂
18	F ₂	17	17	F ₁	4	1197.3049	0.0009	8.6	v ₂
18	F ₂	18	17	F ₁	5	1198.3329	0.0004	7.0	v ₂
18	E	12	17	E	3	1198.3369	0.0005	4.9	v ₂
18	F ₂	18	17	F ₁	4	1198.4202	0.0002	-2.5	v ₂
18	E	12	17	E	2	1198.4453	0.0002	-0.5	v ₂
18	F ₁	18	17	F ₂	3	1198.9989	0.0003	-0.2	v ₂
19	F ₂	16	18	F ₁	2	1199.0109	0.0003	7.3	v ₂

Table D.3 – Continued.

<i>J</i>	γ	<i>n</i>	<i>J'</i>	γ'	<i>n'</i>	ν^{exp} , cm^{-1}	S_{ν}^{exp} , $\text{cm}^{-2} \cdot \text{atm}^{-1}$	δ , %	Band
<i>I</i>			<i>2</i>			<i>3</i>	<i>4</i>	<i>5</i>	<i>6</i>
19	A ₂	6	18	A ₁	1	1199.0187	0.0003	10.4	v ₂
18	F ₂	19	17	F ₁	5	1199.0584	0.0016	-5.0	v ₂
18	F ₂	19	17	F ₁	5	1199.0584	0.0017	-3.2	v ₂
18	F ₁	18	17	F ₂	2	1199.0783	0.0003	7.6	v ₂
18	E	13	17	E	3	1199.2447	0.0009	2.8	v ₂
18	F ₁	19	17	F ₂	4	1199.3051	0.0016	-3.9	v ₂
16	F ₂	18	15	F ₁	3	1199.3476	0.0012	-2.8	v ₂
16	E	12	15	E	2	1199.3607	0.0009	9.4	v ₂
16	F ₂	19	15	F ₁	2	1199.4681	0.0014	0.3	v ₂
16	F ₁	18	15	F ₂	3	1199.4732	0.0010	-2.1	v ₂
16	A ₁	7	15	A ₂	1	1199.7208	0.0010	-4.6	v ₂
16	F ₁	19	15	F ₂	2	1199.7606	0.0010	-1.7	v ₂
16	E	13	15	E	1	1199.7759	0.0006	-7.9	v ₂
16	F ₂	20	15	F ₁	1	1200.2344	0.0007	-3.0	v ₂
16	F ₁	20	15	F ₂	1	1200.2414	0.0007	-6.4	v ₂
19	F ₂	17	18	F ₁	3	1201.5086	0.0004	-3.8	v ₂
19	F ₁	17	18	F ₂	3	1201.5358	0.0004	4.1	v ₂
19	A ₁	6	18	A ₂	2	1203.2185	0.0003	-11.9	v ₂
19	E	12	18	E	3	1203.2671	0.0003	-6.8	v ₂
19	F ₁	18	18	F ₂	4	1203.2751	0.0004	6.5	v ₂
19	F ₁	19	18	F ₂	5	1204.3283	0.0004	-7.4	v ₂
19	F ₂	18	18	F ₁	4	1204.4024	0.0004	-1.7	v ₂
19	F ₁	19	18	F ₂	4	1204.4303	0.0004	2.9	v ₂
20	F ₁	17	19	F ₂	3	1204.7351	0.0002	7.5	v ₂
20	F ₂	17	19	F ₁	2	1204.7432	0.0002	-2.9	v ₂
19	F ₂	20	18	F ₁	4	1205.3681	0.0007	-3.1	v ₂
19	F ₁	20	18	F ₂	5	1205.4411	0.0010	1.4	v ₂
19	A ₁	7	18	A ₂	2	1205.5099	0.0009	-0.3	v ₂
17	F ₂	19	16	F ₁	3	1207.1364	0.0008	-3.3	v ₂
17	F ₁	19	16	F ₂	2	1207.1758	0.0004	-9.3	v ₂
17	F ₁	20	16	F ₂	3	1207.2031	0.0002	2.2	v ₂
17	E	13	16	E	2	1207.2185	0.0007	2.2	v ₂
17	F ₁	20	16	F ₂	2	1207.2613	0.0004	-3.4	v ₂
17	A ₁	7	16	A ₂	1	1207.3690	0.0005	-1.1	v ₂
17	F ₁	21	16	F ₂	1	1207.5590	0.0006	6.7	v ₂
17	F ₂	20	16	F ₁	2	1207.5826	0.0007	-0.3	v ₂
20	F ₂	19	19	F ₁	4	1209.2295	0.0003	-8.2	v ₂
20	F ₁	18	19	F ₂	4	1209.2381	0.0002	-14.1	v ₂
20	F ₁	19	19	F ₂	5	1210.3657	0.0003	-3.2	v ₂
20	A ₁	7	19	A ₂	2	1210.3772	0.0004	-6.7	v ₂
20	F ₁	19	19	F ₂	4	1210.4951	0.0002	2.9	v ₂
20	F ₂	20	19	F ₁	5	1211.0526	0.0007	-6.9	v ₂
20	F ₂	21	19	F ₁	5	1211.5390	0.0003	4.2	v ₂

Table D.3 – Continued.

<i>J</i>	γ	<i>n</i>	<i>J'</i>	γ'	<i>n'</i>	ν^{exp} , cm^{-1}	S_{ν}^{exp} , $\text{cm}^{-2} \cdot \text{atm}^{-1}$	δ , %	Band
<i>I</i>			<i>2</i>			<i>3</i>	<i>4</i>	<i>5</i>	<i>6</i>
20	E	14	19	E	3	1211.5494	0.0004	-3.0	v ₂
20	F ₁	21	19	F ₂	5	1211.6628	0.0006	-1.4	v ₂
18	F ₁	20	17	F ₂	3	1214.9130	0.0004	-7.8	v ₂
18	A ₁	7	17	A ₂	1	1214.9184	0.0007	2.0	v ₂
18	F ₂	21	17	F ₁	4	1214.9331	0.0005	0.4	v ₂
18	F ₁	20	17	F ₂	2	1214.9923	0.0004	8.0	v ₂
18	F ₂	20	17	F ₁	3	1215.0142	0.0006	0.9	v ₂
18	A ₂	7	17	A ₁	1	1215.4230	0.0005	10.0	v ₂
18	F ₂	22	17	F ₁	2	1215.4508	0.0004	7.6	v ₂
21	F ₁	21	20	F ₂	5	1217.1293	0.0005	0.9	v ₂
19	F ₁	21	18	F ₂	3	1222.7611	0.0004	-2.4	v ₂
19	A ₂	8	18	A ₁	1	1222.8368	0.0004	8.9	v ₂

Temperature is 293.85 K.

Table D.4 – Experimental values of absolute line strengths of the ν_4 band of $^{13}\text{CD}_4$.

J	γ	n	J'	γ'	n'	ν^{exp} , cm^{-1}	S_{ν}^{exp} , $\text{cm}^{-2} \cdot \text{atm}^{-1}$	δ , %
<i>I</i>			<i>2</i>			<i>3</i>	<i>4</i>	<i>5</i>
12	A ₁	3	13	A ₂	1	935.3257	0.0884	-6.6
12	F ₁	8	13	F ₂	2	936.0153	0.1130	-0.9
11	F ₂	6	12	F ₁	3	937.0744	0.1475	-3.0
11	F ₁	7	12	F ₂	3	937.4677	0.1470	-2.4
11	A ₁	3	12	A ₂	1	938.0068	0.1238	-2.2
11	F ₁	8	12	F ₂	2	940.4317	0.1493	0.2
10	F ₂	6	11	F ₁	3	941.9400	0.1874	-2.6
12	F ₂	10	13	F ₁	1	942.0550	0.1295	-1.9
10	E	4	11	E	2	942.2592	0.1262	-0.7
11	F ₁	9	12	F ₂	1	942.7511	0.1566	-0.4
10	F ₁	6	11	F ₂	3	942.8084	0.1812	-5.4
11	E	6	12	E	1	945.5674	0.1093	-3.0
11	F ₂	8	12	F ₁	1	945.5845	0.1694	0.2
10	F ₁	7	11	F ₂	2	946.3998	0.1987	1.8
10	A ₁	3	11	A ₂	1	946.7399	0.1605	-2.3
9	F ₁	5	10	F ₂	3	946.7905	0.2299	-1.7
9	E	4	10	E	2	947.2355	0.1549	-0.4
9	F ₂	6	10	F ₁	2	947.6529	0.2192	-5.2
10	F ₁	8	11	F ₂	1	949.0921	0.2060	-1.7
10	F ₂	8	11	F ₁	1	949.1429	0.2181	3.8
9	A ₂	3	10	A ₁	1	949.1691	0.1846	-3.8
9	F ₂	7	10	F ₁	1	950.0054	0.2317	-0.6
9	F ₁	6	10	F ₂	2	950.3963	0.2357	-0.3
8	A ₁	2	9	A ₂	1	951.3546	0.2266	-1.1
8	F ₁	5	9	F ₂	2	951.7007	0.2682	-1.9
8	F ₂	5	9	F ₁	3	952.1200	0.2629	-3.1
9	A ₁	2	10	A ₂	1	952.5627	0.2120	1.4
9	F ₁	7	10	F ₂	1	952.6454	0.2444	-2.8
9	E	5	10	E	1	952.6820	0.1609	-4.2
8	A ₂	2	9	A ₁	1	952.8673	0.2207	-3.9
8	F ₂	6	9	F ₁	2	954.0399	0.2903	6.1
7	F ₁	5	8	F ₂	2	956.0924	0.2953	-4.3
8	F ₂	7	9	F ₁	1	956.2192	0.2814	-3.2
7	E	3	8	E	2	956.3792	0.1994	-2.4
7	F ₂	4	8	F ₁	2	957.0713	0.3061	-0.7
7	F ₁	6	8	F ₂	1	958.0975	0.3491	12.0
7	F ₂	5	8	F ₁	1	959.6804	0.3193	-0.9
7	A ₂	2	8	A ₁	1	959.8098	0.2664	-1.2
6	F ₂	4	7	F ₁	2	960.4611	0.3317	0.2
6	E	3	7	E	1	960.9665	0.2147	-2.8
6	A ₁	2	7	A ₂	1	962.0292	0.2683	-2.4

Table D.4 – Continued.

<i>J</i>	γ	<i>n</i>	<i>J'</i>	γ'	<i>n'</i>	ν^{exp} , cm^{-1}	S_{ν}^{exp} , $\text{cm}^{-2} \cdot \text{atm}^{-1}$	δ , %
<i>I</i>			2			3	4	5
6	F ₁	5	7	F ₂	1	963.0879	0.3284	-3.9
6	F ₂	5	7	F ₁	1	963.2707	0.3642	5.7
5	A ₂	2	6	A ₁	1	964.5778	0.2967	4.8
5	F ₂	4	6	F ₁	1	964.9241	0.3327	-1.6
5	F ₁	3	6	F ₂	2	965.3044	0.3490	3.7
5	A ₁	1	6	A ₂	1	966.2997	0.2849	-1.4
5	F ₁	4	6	F ₂	1	966.6885	0.3416	-1.3
4	F ₂	3	5	F ₁	2	968.8714	0.3153	-3.1
4	F ₁	3	5	F ₂	1	969.9266	0.3272	-1.1
4	F ₂	4	5	F ₁	1	970.3115	0.3315	0.0
3	E	2	4	E	1	973.3854	0.1991	2.2
12	A ₂	1	12	A ₁	1	974.5451	0.1382	3.6
12	F ₂	4	12	F ₁	1	974.5529	0.1670	4.3
12	E	3	12	E	1	974.5568	0.1115	4.5
15	A ₁	2	15	A ₂	1	975.6463	0.0494	-4.4
15	F ₁	6	15	F ₂	2	975.6648	0.0679	9.0
11	F ₂	3	11	F ₁	1	976.5529	0.2269	10.5
2	F ₁	2	3	F ₂	1	976.8822	0.2336	1.2
10	E	2	10	E	1	978.4244	0.1779	6.5
10	F ₁	3	10	F ₂	1	978.4386	0.2654	6.1
10	A ₁	2	10	A ₂	1	978.4678	0.2196	5.6
13	F ₂	5	13	F ₁	2	979.1067	0.1169	-1.8
9	F ₂	3	9	F ₁	1	980.1477	0.2886	-2.6
9	F ₁	3	9	F ₂	1	980.1993	0.2992	1.3
12	F ₁	4	12	F ₂	1	980.5981	0.1536	-3.4
12	F ₂	5	12	F ₁	2	980.7208	0.1604	1.7
8	A ₂	1	8	A ₁	1	981.6661	0.2765	-2.6
14	F ₂	6	14	F ₁	2	981.7247	0.0908	-2.0
8	F ₂	3	8	F ₁	1	981.7494	0.3602	6.1
8	E	2	8	E	1	981.7939	0.2213	-1.6
13	F ₂	6	13	F ₁	3	982.7968	0.1217	-5.9
7	F ₂	2	7	F ₁	1	983.0856	0.3823	2.2
13	F ₁	5	13	F ₂	2	983.1829	0.1245	1.1
7	F ₁	3	7	F ₂	1	983.2228	0.3569	-3.5
6	A ₁	1	6	A ₂	1	984.6141	0.3267	0.9
13	A ₁	2	13	A ₂	1	984.6416	0.1278	10.3
9	A ₂	2	9	A ₁	1	984.9775	0.2489	0.2
8	F ₁	3	8	F ₂	1	985.1359	0.3795	7.9
5	F ₂	2	5	F ₁	1	985.2349	0.3870	-1.7
4	A ₂	1	4	A ₁	1	985.8846	0.3172	2.6
9	F ₁	4	9	F ₂	2	986.8379	0.3107	-2.6
8	E	3	8	E	2	986.8459	0.2234	-7.4
3	F ₁	2	3	F ₂	1	986.9742	0.3290	2.5

Table D.4 – Continued.

<i>J</i>	γ	<i>n</i>	<i>J'</i>	γ'	<i>n'</i>	v^{exp} , cm^{-1}	S_{ν}^{exp} , $\text{cm}^{-2} \cdot \text{atm}^{-1}$	δ , %
<i>I</i>			2			3	4	5
9	A ₁	1	9	A ₂	1	987.2221	0.2554	-5.7
3	A ₁	1	3	A ₂	1	987.4551	0.2844	5.0
3	F ₁	1	2	F ₂	1	997.0997	0.3540	1.9
3	E	1	2	E	1	997.1434	0.2315	0.0
4	F ₁	1	3	F ₂	1	1000.2013	0.4246	3.1
5	A ₂	1	4	A ₁	1	1003.4893	0.3780	0.3
6	F ₂	1	5	F ₁	2	1005.9935	0.4651	-0.5
7	A ₂	1	6	A ₁	1	1008.7639	0.3999	4.1
7	F ₂	1	6	F ₁	1	1008.8585	0.4574	-0.5
7	F ₁	1	6	F ₂	2	1008.9702	0.4547	-1.0
7	F ₁	2	6	F ₂	1	1009.5453	0.4880	6.1
7	E	1	6	E	1	1009.5945	0.2939	-4.0
8	F ₁	1	7	F ₂	2	1011.8032	0.4925	12.3
8	F ₁	2	7	F ₂	1	1012.5440	0.4566	5.9
9	F ₁	1	8	F ₂	2	1014.2630	0.3887	-0.8
9	E	2	8	E	1	1015.5753	0.2596	0.5
9	F ₂	2	8	F ₁	1	1015.6106	0.4172	7.0
10	F ₂	1	9	F ₁	3	1017.0436	0.3448	1.1
10	A ₂	1	9	A ₁	1	1017.2859	0.2834	0.3
10	F ₂	2	9	F ₁	2	1017.5648	0.3403	0.1
10	E	1	9	E	1	1017.6353	0.2189	-3.6
10	F ₂	3	9	F ₁	1	1018.6338	0.3404	0.9
11	F ₁	1	10	F ₂	3	1019.4960	0.2784	-3.4
11	F ₂	1	10	F ₁	2	1019.6923	0.3283	12.6
11	A ₂	1	10	A ₁	1	1019.9800	0.2326	-2.9
11	F ₂	2	10	F ₁	1	1020.3078	0.2814	-1.4
11	F ₁	2	10	F ₂	2	1020.4312	0.2832	-0.8
11	F ₁	3	10	F ₂	1	1021.5883	0.2842	0.5
11	E	2	10	E	1	1021.6037	0.1894	0.4
12	F ₂	1	11	F ₁	3	1022.0558	0.2258	-3.9
12	F ₁	1	11	F ₂	3	1022.2512	0.2381	1.9
12	E	2	11	E	1	1023.1012	0.1499	-3.0
12	A ₁	1	11	A ₂	1	1023.2631	0.1910	-1.2
12	F ₁	3	11	F ₂	1	1024.5325	0.2201	-4.0
12	F ₂	3	11	F ₁	1	1024.5526	0.2245	-2.1
13	F ₁	2	12	F ₂	2	1025.1846	0.1814	-1.3
13	F ₂	2	12	F ₁	2	1025.8849	0.1823	0.2
13	F ₁	3	12	F ₂	1	1025.9759	0.1715	-6.2
14	A ₁	1	13	A ₂	1	1027.5375	0.1131	-3.9
14	F ₁	2	13	F ₂	2	1027.7547	0.1448	3.2
14	A ₂	1	13	A ₁	1	1028.6177	0.1202	4.0
14	F ₂	3	13	F ₁	2	1028.6830	0.1509	8.2
15	F ₂	1	14	F ₁	3	1029.6365	0.1012	-3.6

Table D.4 – Continued.

<i>J</i>	γ	<i>n</i>	<i>J'</i>	γ'	<i>n'</i>	ν^{exp} , cm $^{-1}$	S_{ν}^{exp} , cm $^{-2} \cdot \text{atm}^{-1}$	δ , %
<i>I</i>			<i>2</i>			<i>3</i>	<i>4</i>	<i>5</i>
15	F ₂	2	14	F ₁	2	1030.4452	0.1020	-1.6
15	A ₂	1	14	A ₁	1	1030.5627	0.0951	9.1
15	F ₂	3	14	F ₁	1	1031.3931	0.1144	10.7
15	F ₁	3	14	F ₂	2	1031.4297	0.0994	-2.8

Temperature is 293.85 K.

Table D.5 – Effective dipole parameters $p_{v_l\gamma_l,v_u\gamma_u}^{\Omega K(K,n\Gamma_r)}$ of the moment of the CD₄ molecule.

(v_u, Γ_u)	$(Q, K, n\Gamma)$	¹² CD ₄ , D	¹³ CD ₄ , D
<i>I</i>	2	3	4
(0001, F_1)	(0, 0, A_1)	0.088707(29)	0.086582(38)
	(1, 1, F_1) 10^3	0.15368(92)	0.15336
	(2, 0, A_1) 10^5	-0.2413(41)	-0.2413
	(2, 2, F_2) 10^5	-0.1570(32)	-0.1570
(0100, E)	(1, 1, F_1) 10^4	0.5054(30)	0.5054
	(2, 2, F_2) 10^5	-0.1148(16)	-0.1148
d_{rms}		4.79 %	4.21 %

Table D.6 – Spectroscopic parameters of the $v_1 + v_2$ band of SiF₄ molecule.

Level	(v, γ)	(v', γ')	$\Omega (K, n\Gamma)$	Value, cm ⁻¹
<i>I</i>	2	3	4	5
GS	(0000, A ₁)	(0000, A ₁)	2(0,0A ₁)	0.13778054(57)
	(0000, A ₁)	(0000, A ₁)	4(0,0A ₁)10 ⁷	-0.4138(03)
	(0000, A ₁)	(0000, A ₁)	4(4,0A ₁)10 ⁸	-0.336051(05)
	(0000, A ₁)	(0000, A ₁)	6(0,0A ₁)10 ¹³	-0.2102(62)
	(0000, A ₁)	(0000, A ₁)	6(4,0A ₁)10 ¹⁴	0.214(86)
	(0000, A ₁)	(0000, A ₁)	6(6,0A ₁)10 ¹⁵	0.353(87)
	(0000, A ₁)	(0000, A ₁)	8(0,0A ₁)10 ¹⁶	0.101(54)
	(0000, A ₁)	(0000, A ₁)	8(4,0A ₁)10 ¹⁸	0.115(72)
	(0000, A ₁)	(0000, A ₁)	8(6,0A ₁)10 ¹⁹	0.36(24)
	(0000, A ₁)	(0000, A ₁)	8(8,0A ₁)10 ¹⁹	-0.544(04)
v ₁	(1000, A ₁)	(1000, A ₁)	0(0,0A ₁)	800.66566(20)
	(1000, A ₁)	(1000, A ₁)	2(0,0A ₁)10 ³	-0.15877(75)
	(1000, A ₁)	(1000, A ₁)	4(0,0A ₁)10 ⁹	0.67(08)
	(1000, A ₁)	(1000, A ₁)	4(4,0A ₁)10 ¹⁰	0.469(99)
v ₂	(0100, E)	(0100, E)	0(0,0A ₁)	264.219525(37)
	(0100, E)	(0100, E)	2(0,0A ₁)10 ³	-0.143083(55)
	(0100, E)	(0100, E)	2(2,0E)10 ⁴	-0.46789(32)
	(0100, E)	(0100, E)	3(3,0A ₂)10 ⁶	0.14181(26)
	(0100, E)	(0100, E)	4(0,0A ₁)10 ⁹	0.3910(69)
	(0100, E)	(0100, E)	4(2,0E)10 ⁹	-0.1008(99)
	(0100, E)	(0100, E)	4(4,0A ₁)10 ¹⁰	0.3535(32)
	(0100, E)	(0100, E)	4(4,0E)10 ¹⁰	-0.774(58)
	(0100, E)	(0100, E)	5(3,0A ₂)10 ¹²	0.322(58)
v ₁ + v ₂	(1100, E)	(1100, E)	0(0,0A ₁)	-2.40189(89)
	(1100, E)	(1100, E)	2(0,0A ₁)10 ⁵	7.50(11)
	(1100, E)	(1100, E)	2(2,0E)10 ⁵	5.21(12)
	(1100, E)	(1100, E)	3(3,0A ₂)10 ⁷	-1.918(27)
	(1100, E)	(1100, E)	4(0,0A ₁)10 ⁹	3.14(29)
	(1100, E)	(1100, E)	4(2,0E)10 ¹⁰	
	(1100, E)	(1100, E)	4(4,0A ₁)10 ¹⁰	-4.97(60)
	(1100, E)	(1100, E)	4(4,0E)10 ¹⁰	
$d_{\text{rms}} \cdot 10^{-3}$, cm ⁻¹		0.398		

Table D.7 – Spectroscopic band parameters $v_1 + v_2 + v_4$ of SiF₄ molecule.

Level	(v, γ)	(v', γ')	$\mathcal{Q}(K, n\Gamma)$	Value, cm ⁻¹
<i>I</i>	2	3	4	5
GS	(0000, A ₁)	(0000, A ₁)	2(0,0A ₁)	0.13778054(57)
	(0000, A ₁)	(0000, A ₁)	4(0,0A ₁)10 ⁷	-0.4138(03)
	(0000, A ₁)	(0000, A ₁)	4(4,0A ₁)10 ⁸	-0.336051(05)
	(0000, A ₁)	(0000, A ₁)	6(0,0A ₁)10 ¹³	-0.2102(62)
	(0000, A ₁)	(0000, A ₁)	6(4,0A ₁)10 ¹⁴	0.214(86)
	(0000, A ₁)	(0000, A ₁)	6(6,0A ₁)10 ¹⁵	0.353(87)
	(0000, A ₁)	(0000, A ₁)	8(0,0A ₁)10 ¹⁶	0.101(54)
	(0000, A ₁)	(0000, A ₁)	8(4,0A ₁)10 ¹⁸	0.115(72)
	(0000, A ₁)	(0000, A ₁)	8(6,0A ₁)10 ¹⁹	0.36(24)
	(0000, A ₁)	(0000, A ₁)	8(8,0A ₁)10 ¹⁹	-0.544(04)
v ₁	(1000, A ₁)	(1000, A ₁)	0(0,0A ₁)	800.66566(20)
	(1000, A ₁)	(1000, A ₁)	2(0,0A ₁)10 ³	-0.15877(75)
	(1000, A ₁)	(1000, A ₁)	4(0,0A ₁)10 ⁹	0.67(08)
	(1000, A ₁)	(1000, A ₁)	4(4,0A ₁)10 ¹⁰	0.469(99)
v ₂	(0100, E)	(0100, E)	0(0,0A ₁)	264.219525(37)
	(0100, E)	(0100, E)	2(0,0A ₁)10 ³	-0.143083(55)
	(0100, E)	(0100, E)	2(2,0E)10 ⁴	-0.46789(32)
	(0100, E)	(0100, E)	3(3,0A ₂)10 ⁶	0.14181(26)
	(0100, E)	(0100, E)	4(0,0A ₁)10 ⁹	0.3910(69)
	(0100, E)	(0100, E)	4(2,0E)10 ⁹	-0.1008(99)
	(0100, E)	(0100, E)	4(4,0A ₁)10 ¹⁰	0.3535(32)
	(0100, E)	(0100, E)	4(4,0E)10 ¹⁰	-0.774(58)
	(0100, E)	(0100, E)	5(3,0A ₂)10 ¹²	0.322(58)
v ₄	(0001, F ₂)	(0001, F ₂)	0(0,0A ₁)	388.433275(29)
	(0001, F ₂)	(0001, F ₂)	1(1,0F ₁)10 ¹	-0.275717(17)
	(0001, F ₂)	(0001, F ₂)	2(0,0A ₁)10 ³	0.168545(22)
	(0001, F ₂)	(0001, F ₂)	2(2,0E)10 ³	-0.117473(42)
	(0001, F ₂)	(0001, F ₂)	2(2,0F ₂)10 ⁴	0.55406(41)
	(0001, F ₂)	(0001, F ₂)	3(1,0F ₁)10 ⁶	-0.11535(25)
	(0001, F ₂)	(0001, F ₂)	3(3,0F ₁)10 ⁶	-0.20262(12)
	(0001, F ₂)	(0001, F ₂)	4(0,0A ₁)10 ⁹	-0.2638(35)
	(0001, F ₂)	(0001, F ₂)	4(2,0E)10 ⁹	-0.1842(37)
	(0001, F ₂)	(0001, F ₂)	4(2,0F ₂)10 ¹⁰	0.787(42)
	(0001, F ₂)	(0001, F ₂)	4(4,0A ₁)10 ¹⁰	-0.1291(76)
	(0001, F ₂)	(0001, F ₂)	4(4,0E)10 ¹⁰	0.821(30)
	(0001, F ₂)	(0001, F ₂)	4(4,0F ₂)10 ¹⁰	0.189(21)
v ₁ + v ₂	(1100, E)	(1100, E)	0(0,0A ₁)	-0.240182(85)
	(1100, E)	(1100, E)	2(0,0A ₁)10 ⁵	0.7515(92)
	(1100, E)	(1100, E)	2(2,0E)10 ⁵	0.5265(93)
	(1100, E)	(1100, E)	3(3,0A ₂)10 ⁷	-0.1918(22)
	(1100, E)	(1100, E)	4(0,0A ₁)10 ⁹	0.298(27)
	(1100, E)	(1100, E)	4(2,0E)10 ¹⁰	-0.11(19)
	(1100, E)	(1100, E)	4(4,0A ₁)10 ¹⁰	-0.524(76)
	(1100, E)	(1100, E)	4(4,0E)10 ¹⁰	0.75(12)
v ₁ + v ₄	(1001, F ₂)	(1001, F ₂)	0(0,0A ₁)	0.891585
	(1001, F ₂)	(1001, F ₂)	1(1,0F ₁)10 ²	0.2397

Table D.7 – Continued.

	(1001, F_2)	(1001, F_2)	$2(0,0A_1)10^4$	0.1627(18)
	(1001, F_2)	(1001, F_2)	$2(2,0E)10^4$	-0.1108(32)
	(1001, F_2)	(1001, F_2)	$2(2,0F_2)10^5$	0.221(44)
	(1001, F_2)	(1001, F_2)	$3(1,0F_1)10^7$	0.1054(80)
$v_2 + v_4$	(0101, F_1)	(0101, F_1)	$0(0,0A_1)$	0.42552(33)
	(0101, F_1)	(0101, F_1)	$1(1,0F_1)10^3$	0.699(26)
	(0101, F_1)	(0101, F_1)	$2(0,0A_1)10^4$	0.1878(99)
	(0101, F_1)	(0101, F_1)	$2(2,0E)10^5$	-0.268(92)
	(0101, F_1)	(0101, F_1)	$2(2,0F_2)10^5$	-0.89(10)
	(0101, F_1)	(0101, F_1)	$3(1,0F_1)10^7$	0.882(85)
	(0101, F_1)	(0101, F_1)	$4(0,0A_1)10^7$	-0.1169(23)
	(0101, F_1)	(0101, F_1)	$4(2,0E)10^8$	-0.547(21)
	(0101, F_1)	(0101, F_1)	$4(4,0E)10^8$	-0.159(15)
	(0101, F_1)	(0101, F_1)	$4(4,0F_2)10^8$	0.449(22)
	(0101, F_1)	(0101, F_2)	$1(1,0F_1)10^3$	-0.655(26)
	(0101, F_1)	(0101, F_2)	$2(2,0E)10^4$	-0.1564(63)
	(0101, F_1)	(0101, F_2)	$3(1,0F_1)10^6$	-0.2671(53)
	(0101, F_1)	(0101, F_2)	$4(2,0E)10^8$	-0.270(11)
	(0101, F_1)	(0101, F_2)	$4(4,0E)10^8$	0.281(12)
	(0101, F_1)	(0101, F_2)	$4(4,0F_2)10^9$	-0.253(60)
	(0101, F_2)	(0101, F_2)	$0(0,0A_1)$	0.64666(16)
	(0101, F_2)	(0101, F_2)	$1(1,0F_1)10^2$	-0.1190(14)
	(0101, F_2)	(0101, F_2)	$2(0,0A_1)10^4$	-0.1783(72)
	(0101, F_2)	(0101, F_2)	$2(2,0E)10^4$	-0.1425(82)
	(0101, F_2)	(0101, F_2)	$2(2,0F_2)10^5$	0.611(72)
	(0101, F_2)	(0101, F_2)	$3(1,0F_1)10^6$	0.1369(56)
	(0101, F_2)	(0101, F_2)	$4(2,0E)10^8$	-0.243(17)
	(0101, F_2)	(0101, F_2)	$4(4,0E)10^8$	0.275(16)
$v_1 + v_2 + v_4$	(1101, F_1)	(1101, F_1)	$0(0,0A_1)$	0.9649(20)
	(1101, F_1)	(1101, F_1)	$1(1,0F_1)$	-0.585(24)
	(1101, F_1)	(1101, F_1)	$2(0,0A_1)10^2$	0.194(44)
	(1101, F_1)	(1101, F_1)	$2(2,0F_2)10^4$	-0.420(60)
	(1101, F_1)	(1101, F_1)	$3(1,0F_1)10^4$	-0.292(15)
	(1101, F_1)	(1101, F_1)	$3(1,0F_1)10^5$	-0.1148(94)
	(1101, F_1)	(1101, F_2)	$1(1,0F_1)10^2$	0.135(13)
	(1101, F_1)	(1101, F_2)	$2(2,0E)10^4$	0.163(24)
	(1101, F_1)	(1101, F_2)	$3(3,0A_2)10^6$	0.94034(48)
	(1101, F_2)	(1101, F_2)	$0(0,0A_1)$	-0.1040(49)
	(1101, F_2)	(1101, F_2)	$1(1,0F_1)10^2$	-0.420(32)
	(1101, F_2)	(1101, F_2)	$2(0,0A_1)10^4$	-0.228(48)
	(1101, F_2)	(1101, F_2)	$2(2,0F_2)10^4$	-0.208(54)
	(1101, F_2)	(1101, F_2)	$3(1,0F_1)10^6$	0.221(13)
$d_{\text{rms}} \cdot 10^{-3}, \text{cm}^{-1}$	0.429			

Table D.8 – Spectroscopic parameters of the $v_1 + v_3$ band of SiF₄ molecule.

Lvl	(v, γ)	(v', γ')	$\mathcal{Q} (K, n\Gamma)$	²⁸ SiF ₄ , cm ⁻¹	²⁹ SiF ₄ , cm ⁻¹	³⁰ SiF ₄ , cm ⁻¹
<i>I</i>	2	3	4	5	6	7
GS	(0000, A ₁)	(0000, A ₁)	2(0,0A ₁)	0.13778054(14)	0.13778094(13)	
	(0000, A ₁)	(0000, A ₁)	4(0,0A ₁)10 ⁷	-0.4138(11)	-0.4218(31)	
	(0000, A ₁)	(0000, A ₁)	4(4,0A ₁)10 ⁸	-0.336051(68)	-0.340228(70)	
	(0000, A ₁)	(0000, A ₁)	6(0,0A ₁)10 ¹³	-0.2102(26)		
	(0000, A ₁)	(0000, A ₁)	6(4,0A ₁)10 ¹⁴	0.214(23)		
	(0000, A ₁)	(0000, A ₁)	6(6,0A ₁)10 ¹⁵	0.353(49)		
	(0000, A ₁)	(0000, A ₁)	8(0,0A ₁)10 ¹⁶	0.101(17)		
	(0000, A ₁)	(0000, A ₁)	8(4,0A ₁)10 ¹⁸	0.115(13)		
	(0000, A ₁)	(0000, A ₁)	8(6,0A ₁)10 ¹⁹	0.36(18)		
	(0000, A ₁)	(0000, A ₁)	8(8,0A ₁)10 ¹⁹	-0.544(74)		
v_1	(1000, A ₁)	(1000, A ₁)	0(0,0A ₁)	800.66566(11)		
	(1000, A ₁)	(1000, A ₁)	2(0,0A ₁)10 ³	-0.15877(24)		
	(1000, A ₁)	(1000, A ₁)	4(0,0A ₁)10 ⁹	0.67(11)		
	(1000, A ₁)	(1000, A ₁)	4(4,0A ₁)10 ¹⁰	0.469(70)		
v_3	(0010, F ₂)	(0010, F ₂)	0(0,0A ₁)	1031.544438(65)	1022.575194(94)	1014.164534(80)
	(0010, F ₂)	(0010, F ₂)	1(1,0F ₁)	0.31312443(17)	0.307421(10)	0.301736(67)
	(0010, F ₂)	(0010, F ₂)	2(0,0A ₁)10 ³	-0.29725(13)	-0.29208(30)	-0.28761(25)
	(0010, F ₂)	(0010, F ₂)	2(2,0E)10 ³	0.2531815(74)	0.24735(46)	0.24274(26)
	(0010, F ₂)	(0010, F ₂)	2(2,0F ₂)10 ⁴	-0.996048(77)	-0.9656(53)	-0.9396(36)
	(0010, F ₂)	(0010, F ₂)	3(1,0F ₁)10 ⁶	0.10540(54)	0.1037(68)	0.1018(32)
	(0010, F ₂)	(0010, F ₂)	3(3,0F ₁)10 ⁷	-0.246(14)	-0.246	-0.246
	(0010, F ₂)	(0010, F ₂)	4(2,0E)10 ⁸	-0.574(32)	-0.574(86)	-0.479(28)
	(0010, F ₂)	(0010, F ₂)	4(2,0F ₂)10 ⁸	0.626(32)	0.631(88)	0.631
	(0010, F ₂)	(0010, F ₂)	4(4,0A ₁)10 ¹⁰	0.871(60)	0.871	0.871
	(0010, F ₂)	(0010, F ₂)	4(4,0E)10 ⁸	0.920(48)	0.920	0.920
	(0010, F ₂)	(0010, F ₂)	4(4,0F ₂)10 ⁸	0.671(36)	0.671	0.671
	(0010, F ₂)	(0010, F ₂)	5(1,0F ₁)10 ¹¹	-0.989(40)	-0.989	-0.989
	(0010, F ₂)	(0010, F ₂)	5(3,0F ₁)10 ¹¹	-0.198(61)	-0.198	-0.198
	(0010, F ₂)	(0010, F ₂)	5(5,0F ₁)10 ¹¹	0.471(68)	0.471	0.471
	(0010, F ₂)	(0010, F ₂)	5(5,1F ₁)10 ¹¹	-0.913(57)	-0.913	-0.913
	(0010, F ₂)	(0010, F ₂)	6(0,0A ₁)10 ¹²	-0.132(13)	-0.132	-0.132
	(0010, F ₂)	(0010, F ₂)	6(2,0E)10 ¹²	-0.1462(98)	-0.1462	-0.1462
	(0010, F ₂)	(0010, F ₂)	6(2,0F ₂)10 ¹²	0.144(10)	0.144	0.144
	(0010, F ₂)	(0010, F ₂)	6(4,0A ₁)10 ¹⁴	-0.826(79)	-0.484	-0.484
	(0010, F ₂)	(0010, F ₂)	6(4,0E)10 ¹²	0.240(15)	0.240	0.240
	(0010, F ₂)	(0010, F ₂)	6(4,0F ₂)10 ¹²	0.174(11)	0.174	0.174
$v_1 + v_3$	(1010, F ₂)	(1010, F ₂)	0(0,0A ₁)	-3.855453(66)	-3.94525(20)	-4.00663(17)
	(1010, F ₂)	(1010, F ₂)	1(1,0F ₁)10 ²	-2.9117(45)	-2.553(22)	-2.366(11)
	(1010, F ₂)	(1010, F ₂)	2(0,0A ₁)10 ⁵	-1.472(85)	-1.320(68)	-1.278(43)
	(1010, F ₂)	(1010, F ₂)	2(2,0E)10 ⁵	3.368(42)	2.16(42)	2.16
	(1010, F ₂)	(1010, F ₂)	2(2,0F ₂)10 ⁴	-1.258(14)	-1.072(73)	-1.036(82)
	(1010, F ₂)	(1010, F ₂)	3(1,0F ₁)10 ⁷	-1.296(88)	1.25(17)	1.25
	(1010, F ₂)	(1010, F ₂)	3(3,0F ₁)10 ⁷	1.646(69)	1.646	1.646
	(1010, F ₂)	(1010, F ₂)	4(0,0A ₁)10 ⁹	5.33(22)	5.33	5.33
	(1010, F ₂)	(1010, F ₂)	4(2,0F ₂)10 ⁹	-4.06(21)	-4.06	-4.06
$d_{\text{rms}} \cdot 10^{-3}, \text{cm}^{-1}$				0.563	0.665	0.478

Table D.9 – Spectroscopic parameters of the $\nu_1 + \nu_4$ band of SiF₄ molecule.

Level	(v, γ)	(v', γ')	$\Omega (K, n\Gamma)$	Value, cm ⁻¹
<i>I</i>	2	3	4	5
GS	(0000, A ₁)	(0000, A ₁)	2(0,0A ₁)	0.13778054(14)
	(0000, A ₁)	(0000, A ₁)	4(0,0A ₁)10 ⁷	-0.4138(11)
	(0000, A ₁)	(0000, A ₁)	4(4,0A ₁)10 ⁸	-0.336051(68)
	(0000, A ₁)	(0000, A ₁)	6(0,0A ₁)10 ¹³	-0.2102(26)
	(0000, A ₁)	(0000, A ₁)	6(4,0A ₁)10 ¹⁴	0.214(23)
	(0000, A ₁)	(0000, A ₁)	6(6,0A ₁)10 ¹⁵	0.353(49)
	(0000, A ₁)	(0000, A ₁)	8(0,0A ₁)10 ¹⁶	0.101(17)
	(0000, A ₁)	(0000, A ₁)	8(4,0A ₁)10 ¹⁸	0.115(13)
	(0000, A ₁)	(0000, A ₁)	8(6,0A ₁)10 ¹⁹	0.36(18)
	(0000, A ₁)	(0000, A ₁)	8(8,0A ₁)10 ¹⁹	-0.544(74)
ν_1	(1000, A ₁)	(1000, A ₁)	0(0,0A ₁)	800.66566(11)
	(1000, A ₁)	(1000, A ₁)	2(0,0A ₁)10 ³	-0.15877(24)
	(1000, A ₁)	(1000, A ₁)	4(0,0A ₁)10 ⁹	0.67(11)
	(1000, A ₁)	(1000, A ₁)	4(4,0A ₁)10 ¹⁰	0.469(70)
ν_4	(0001, F ₂)	(0001, F ₂)	0(0,0A ₁)	388.433275(29)
	(0001, F ₂)	(0001, F ₂)	1(1,0F ₁)10 ¹	-0.275717(17)
	(0001, F ₂)	(0001, F ₂)	2(0,0A ₁)10 ³	0.168545(22)
	(0001, F ₂)	(0001, F ₂)	2(2,0E)10 ³	-0.117473(42)
	(0001, F ₂)	(0001, F ₂)	2(2,0F ₂)10 ⁴	0.55406(41)
	(0001, F ₂)	(0001, F ₂)	3(1,0F ₁)10 ⁶	-0.11535(25)
	(0001, F ₂)	(0001, F ₂)	3(3,0F ₁)10 ⁶	-0.20262(12)
	(0001, F ₂)	(0001, F ₂)	4(0,0A ₁)10 ⁹	-0.2638(35)
	(0001, F ₂)	(0001, F ₂)	4(2,0E)10 ⁹	-0.1842(37)
	(0001, F ₂)	(0001, F ₂)	4(2,0F ₂)10 ¹⁰	0.787(42)
	(0001, F ₂)	(0001, F ₂)	4(4,0A ₁)10 ¹⁰	-0.1291(76)
	(0001, F ₂)	(0001, F ₂)	4(4,0E)10 ¹⁰	0.821(30)
	(0001, F ₂)	(0001, F ₂)	4(4,0F ₂)10 ¹⁰	0.189(21)
$\nu_1 + \nu_4$	(1001, F ₂)	(1001, F ₂)	0(0,0A ₁)	0.891585(83)
	(1001, F ₂)	(1001, F ₂)	1(1,0F ₁)10 ²	0.2397(34)
	(1001, F ₂)	(1001, F ₂)	2(0,0A ₁)10 ⁴	1.628(18)
	(1001, F ₂)	(1001, F ₂)	2(2,0E)10 ⁴	-1.109(32)
	(1001, F ₂)	(1001, F ₂)	2(2,0F ₂)10 ⁵	2.21(44)
	(1001, F ₂)	(1001, F ₂)	3(1,0F ₁)10 ⁷	1.054(80)
$d_{\text{rms}} \cdot 10^{-3}$, cm ⁻¹		0.417		

Table D.10 – Spectroscopic parameters of the $v_2 + v_3$ band of SiF₄ molecule.

Level	(v, γ)	(v', γ')	$\Omega (K, n\Gamma)$	Value, cm ⁻¹
<i>I</i>	2	3	4	5
GS	(0000, A ₁)	(0000, A ₁)	2(0,0A ₁)	0.13778054(14)
	(0000, A ₁)	(0000, A ₁)	4(0,0A ₁)10 ⁷	-0.4138(11)
	(0000, A ₁)	(0000, A ₁)	4(4,0A ₁)10 ⁸	-0.336051(68)
	(0000, A ₁)	(0000, A ₁)	6(0,0A ₁)10 ¹³	-0.2102(26)
	(0000, A ₁)	(0000, A ₁)	6(4,0A ₁)10 ¹⁴	0.214(23)
	(0000, A ₁)	(0000, A ₁)	6(6,0A ₁)10 ¹⁵	0.353(49)
	(0000, A ₁)	(0000, A ₁)	8(0,0A ₁)10 ¹⁶	0.101(17)
	(0000, A ₁)	(0000, A ₁)	8(4,0A ₁)10 ¹⁸	0.115(13)
	(0000, A ₁)	(0000, A ₁)	8(6,0A ₁)10 ¹⁹	0.36(18)
	(0000, A ₁)	(0000, A ₁)	8(8,0A ₁)10 ¹⁹	-0.544(74)
v_2	(0100, E)	(0100, E)	0(0,0A ₁)	264.219525(37)
	(0100, E)	(0100, E)	2(0,0A ₁)10 ³	-0.143083(55)
	(0100, E)	(0100, E)	2(2,0E)10 ⁴	-0.46789(32)
	(0100, E)	(0100, E)	3(3,0A ₂)10 ⁶	0.14181(26)
	(0100, E)	(0100, E)	4(0,0A ₁)10 ⁹	0.3910(69)
	(0100, E)	(0100, E)	4(2,0E)10 ⁹	-0.1008(99)
	(0100, E)	(0100, E)	4(4,0A ₁)10 ¹⁰	0.3535(32)
	(0100, E)	(0100, E)	4(4,0E)10 ¹⁰	-0.774(58)
	(0100, E)	(0100, E)	5(3,0A ₂)10 ¹²	0.322(58)
v_3	(0010, F ₂)	(0010, F ₂)	0(0,0A ₁)	1031.544438(65)
	(0010, F ₂)	(0010, F ₂)	1(1,0F ₁)	0.31312443(17)
	(0010, F ₂)	(0010, F ₂)	2(0,0A ₁)10 ³	-0.29725(13)
	(0010, F ₂)	(0010, F ₂)	2(2,0E)10 ³	0.2531815(74)
	(0010, F ₂)	(0010, F ₂)	2(2,0F ₂)10 ⁴	-0.996048(77)
	(0010, F ₂)	(0010, F ₂)	3(1,0F ₁)10 ⁶	0.10540(54)
	(0010, F ₂)	(0010, F ₂)	3(3,0F ₁)10 ⁷	-0.246(14)
	(0010, F ₂)	(0010, F ₂)	4(2,0E)10 ⁸	-0.574(32)
	(0010, F ₂)	(0010, F ₂)	4(2,0F ₂)10 ⁸	0.626(32)
	(0010, F ₂)	(0010, F ₂)	4(4,0A ₁)10 ¹⁰	0.871(60)
	(0010, F ₂)	(0010, F ₂)	4(4,0E)10 ⁸	0.920(48)
	(0010, F ₂)	(0010, F ₂)	4(4,0F ₂)10 ⁸	0.671(36)
	(0010, F ₂)	(0010, F ₂)	5(1,0F ₁)10 ¹¹	-0.989(40)
	(0010, F ₂)	(0010, F ₂)	5(3,0F ₁)10 ¹¹	-0.198(61)
	(0010, F ₂)	(0010, F ₂)	5(5,0F ₁)10 ¹¹	0.471(68)
	(0010, F ₂)	(0010, F ₂)	5(5,1F ₁)10 ¹¹	-0.913(57)
	(0010, F ₂)	(0010, F ₂)	6(0,0A ₁)10 ¹²	-0.132(13)
	(0010, F ₂)	(0010, F ₂)	6(2,0E)10 ¹²	-0.1462(98)
	(0010, F ₂)	(0010, F ₂)	6(2,0F ₂)10 ¹²	0.144(10)
	(0010, F ₂)	(0010, F ₂)	6(4,0A ₁)10 ¹⁴	-0.826(79)
	(0010, F ₂)	(0010, F ₂)	6(4,0E)10 ¹²	0.240(15)
	(0010, F ₂)	(0010, F ₂)	6(4,0F ₂)10 ¹²	0.174(11)
$v_2 + v_3$	(0110, F ₁)	(0110, F ₁)	0(0,0A ₁)	-3.0661(27)
	(0110, F ₁)	(0110, F ₁)	1(1,0F ₁)10 ²	0.2079(20)
	(0110, F ₁)	(0110, F ₁)	3(1,0F ₁)10 ⁷	-1.24(16)
	(0110, F ₁)	(0110, F ₁)	3(3,0F ₁)10 ⁶	-1.31(16)
	(0110, F ₁)	(0110, F ₁)	4(2,0F ₂)10 ⁹	0.289(25)

Table D.10 – Continued.

	(0110, F_1)	(0110, F_2)	$1(1,0F_1)10^3$	0.307(86)
	(0110, F_1)	(0110, F_2)	$2(2,0F_2)10^5$	0.595(31)
	(0110, F_1)	(0110, F_2)	$3(1,0F_1)10^7$	-0.123(30)
	(0110, F_1)	(0110, F_2)	$3(3,0A_2)10^8$	0.867(67)
	(0110, F_2)	(0110, F_2)	$0(0,0A_1)$	-1.84054(13)
	(0110, F_2)	(0110, F_2)	$1(1,0F_1)10^2$	0.6149(16)
	(0110, F_2)	(0110, F_2)	$2(2,0F_2)10^4$	-0.123(49)
	(0110, F_2)	(0110, F_2)	$3(1,0F_1)10^6$	0.126(16)
$d_{\text{rms}} \cdot 10^{-3}, \text{cm}^{-1}$	0.445			

Table D.11 – Spectroscopic parameters of the $v_2 + v_4$ band of the SiF₄ molecule.

Level	(v, γ)	(v', γ')	$\mathcal{Q} (K, n\Gamma)$	Value, cm ⁻¹
<i>I</i>	2	3	4	5
GS	(0000, A ₁)	(0000, A ₁)	2(0,0A ₁)	0.13778054(14)
	(0000, A ₁)	(0000, A ₁)	4(0,0A ₁)10 ⁷	-0.4138(11)
	(0000, A ₁)	(0000, A ₁)	4(4,0A ₁)10 ⁸	-0.336051(68)
	(0000, A ₁)	(0000, A ₁)	6(0,0A ₁)10 ¹³	-0.2102(26)
	(0000, A ₁)	(0000, A ₁)	6(4,0A ₁)10 ¹⁴	0.214(23)
	(0000, A ₁)	(0000, A ₁)	6(6,0A ₁)10 ¹⁵	0.353(49)
	(0000, A ₁)	(0000, A ₁)	8(0,0A ₁)10 ¹⁶	0.101(17)
	(0000, A ₁)	(0000, A ₁)	8(4,0A ₁)10 ¹⁸	0.115(13)
	(0000, A ₁)	(0000, A ₁)	8(6,0A ₁)10 ¹⁹	0.36(18)
	(0000, A ₁)	(0000, A ₁)	8(8,0A ₁)10 ¹⁹	-0.544(74)
v_2	(0100, E)	(0100, E)	0(0,0A ₁)	264.219525(37)
	(0100, E)	(0100, E)	2(0,0A ₁)10 ³	-0.143083(55)
	(0100, E)	(0100, E)	2(2,0E)10 ⁴	-0.46789(32)
	(0100, E)	(0100, E)	3(3,0A ₂)10 ⁶	0.14181(26)
	(0100, E)	(0100, E)	4(0,0A ₁)10 ⁹	0.3910(69)
	(0100, E)	(0100, E)	4(2,0E)10 ⁹	-0.1008(99)
	(0100, E)	(0100, E)	4(4,0A ₁)10 ¹⁰	0.3535(32)
	(0100, E)	(0100, E)	4(4,0E)10 ¹⁰	-0.774(58)
	(0100, E)	(0100, E)	5(3,0A ₂)10 ¹²	0.322(58)
	(0001, F ₂)	(0001, F ₂)	0(0,0A ₁)	388.433275(29)
v_4	(0001, F ₂)	(0001, F ₂)	1(1,0F ₁)10 ¹	-0.275717(17)
	(0001, F ₂)	(0001, F ₂)	2(0,0A ₁)10 ³	0.168545(22)
	(0001, F ₂)	(0001, F ₂)	2(2,0E)10 ³	-0.117473(42)
	(0001, F ₂)	(0001, F ₂)	2(2,0F ₂)10 ⁴	0.55406(41)
	(0001, F ₂)	(0001, F ₂)	3(1,0F ₁)10 ⁶	-0.11535(25)
	(0001, F ₂)	(0001, F ₂)	3(3,0F ₁)10 ⁶	-0.20262(12)
	(0001, F ₂)	(0001, F ₂)	4(0,0A ₁)10 ⁹	-0.2638(35)
	(0001, F ₂)	(0001, F ₂)	4(2,0F ₂)10 ¹⁰	0.787(42)
	(0001, F ₂)	(0001, F ₂)	4(4,0A ₁)10 ¹⁰	-0.1291(76)
	(0001, F ₂)	(0001, F ₂)	4(4,0E)10 ¹⁰	0.821(30)
	(0001, F ₂)	(0001, F ₂)	4(4,0F ₂)10 ¹⁰	0.189(21)
	(0101, F ₁)	(0101, F ₁)	0(0,0A ₁)	0.42553(33)
$v_2 + v_4$	(0101, F ₁)	(0101, F ₁)	1(1,0F ₁)10 ³	0.700(26)
	(0101, F ₁)	(0101, F ₁)	2(0,0A ₁)10 ⁴	0.1879(99)
	(0101, F ₁)	(0101, F ₁)	2(2,0E)10 ⁵	-0.268(92)
	(0101, F ₁)	(0101, F ₁)	3(1,0F ₁)10 ⁷	0.883(85)
	(0101, F ₁)	(0101, F ₁)	4(0,0A ₁)10 ⁷	-0.1169(23)
	(0101, F ₁)	(0101, F ₁)	4(2,0E)10 ⁸	-0.547(21)
	(0101, F ₁)	(0101, F ₁)	4(4,0E)10 ⁸	-0.159(15)
	(0101, F ₁)	(0101, F ₁)	4(4,0F ₂)10 ⁸	0.450(22)
	(0101, F ₁)	(0101, F ₂)	1(1,0F ₁)10 ³	-0.655(26)
	(0101, F ₁)	(0101, F ₂)	2(2,0E)10 ⁴	-0.1565(63)
	(0101, F ₁)	(0101, F ₂)	3(1,0F ₁)10 ⁶	-0.2672(53)
	(0101, F ₁)	(0101, F ₂)	4(2,0E)10 ⁸	-0.271(11)
	(0101, F ₁)	(0101, F ₂)	4(4,0E)10 ⁸	0.282(12)
	(0101, F ₁)	(0101, F ₂)	4(4,0F ₂)10 ⁹	-0.253(60)

Table D.11 – Continued.

	(0101, F_2)	(0101, F_2)	0(0,0 A_1)	0.64666(16)
	(0101, F_2)	(0101, F_2)	1(1,0 F_1)10 ²	-0.1191(14)
	(0101, F_2)	(0101, F_2)	2(0,0 A_1)10 ⁴	-0.1784(72)
	(0101, F_2)	(0101, F_2)	2(2,0 E)10 ⁴	-0.1425(82)
	(0101, F_2)	(0101, F_2)	2(2,0 F_2)10 ⁵	0.612(72)
	(0101, F_2)	(0101, F_2)	3(1,0 F_1)10 ⁶	0.1369(56)
	(0101, F_2)	(0101, F_2)	4(2,0 E)10 ⁸	-0.243(17)
	(0101, F_2)	(0101, F_2)	4(4,0 E)10 ⁸	0.275(16)
$d_{\text{rms}} \cdot 10^{-3}, \text{cm}^{-1}$	0.382			

Table D.12 – Spectroscopic parameters of the $v_3 + v_4$ band of SiF₄ molecule.

Level	(v, γ)	(v', γ')	$\mathcal{Q}(K, n\Gamma)$	Value, cm ⁻¹
<i>I</i>	2	3	4	5
GS	(0000, A ₁)	(0000, A ₁)	2(0,0A ₁)	0.13778054(14)
	(0000, A ₁)	(0000, A ₁)	4(0,0A ₁)10 ⁻⁷	-0.4138(11)
	(0000, A ₁)	(0000, A ₁)	4(4,0A ₁)10 ⁻⁸	-0.336051(68)
	(0000, A ₁)	(0000, A ₁)	6(0,0A ₁)10 ⁻¹³	-0.2102(26)
	(0000, A ₁)	(0000, A ₁)	6(4,0A ₁)10 ⁻¹⁴	0.214(23)
	(0000, A ₁)	(0000, A ₁)	6(6,0A ₁)10 ⁻¹⁵	0.353(49)
	(0000, A ₁)	(0000, A ₁)	8(0,0A ₁)10 ⁻¹⁶	0.101(17)
	(0000, A ₁)	(0000, A ₁)	8(4,0A ₁)10 ⁻¹⁸	0.115(13)
	(0000, A ₁)	(0000, A ₁)	8(6,0A ₁)10 ⁻¹⁹	0.36(18)
	(0000, A ₁)	(0000, A ₁)	8(8,0A ₁)10 ⁻¹⁹	-0.544(74)
v_3	(0010, F ₂)	(0010, F ₂)	0(0,0A ₁)	1031.544438(65)
	(0010, F ₂)	(0010, F ₂)	1(1,0F ₁)	0.31312443(17)
	(0010, F ₂)	(0010, F ₂)	2(0,0A ₁)10 ³	-0.29725(13)
	(0010, F ₂)	(0010, F ₂)	2(2,0E)10 ³	0.2531815(74)
	(0010, F ₂)	(0010, F ₂)	2(2,0F ₂)10 ⁴	-0.996048(77)
	(0010, F ₂)	(0010, F ₂)	3(1,0F ₁)10 ⁶	0.10540(54)
	(0010, F ₂)	(0010, F ₂)	3(3,0F ₁)10 ⁷	-0.246(14)
	(0010, F ₂)	(0010, F ₂)	4(2,0E)10 ⁸	-0.574(32)
	(0010, F ₂)	(0010, F ₂)	4(2,0F ₂)10 ⁸	0.626(32)
	(0010, F ₂)	(0010, F ₂)	4(4,0A ₁)10 ¹⁰	0.871(60)
	(0010, F ₂)	(0010, F ₂)	4(4,0E)10 ⁸	0.920(48)
	(0010, F ₂)	(0010, F ₂)	4(4,0F ₂)10 ⁸	0.671(36)
	(0010, F ₂)	(0010, F ₂)	5(1,0F ₁)10 ¹¹	-0.989(40)
	(0010, F ₂)	(0010, F ₂)	5(3,0F ₁)10 ¹¹	-0.198(61)
	(0010, F ₂)	(0010, F ₂)	5(5,0F ₁)10 ¹¹	0.471(68)
	(0010, F ₂)	(0010, F ₂)	5(5,1F ₁)10 ¹¹	-0.913(57)
	(0010, F ₂)	(0010, F ₂)	6(0,0A ₁)10 ¹²	-0.132(13)
	(0010, F ₂)	(0010, F ₂)	6(2,0E)10 ¹²	-0.1462(98)
	(0010, F ₂)	(0010, F ₂)	6(2,0F ₂)10 ¹²	0.144(10)
	(0010, F ₂)	(0010, F ₂)	6(4,0A ₁)10 ¹⁴	-0.826(79)
	(0010, F ₂)	(0010, F ₂)	6(4,0E)10 ¹²	0.240(15)
	(0010, F ₂)	(0010, F ₂)	6(4,0F ₂)10 ¹²	0.174(11)
v_4	(0001, F ₂)	(0001, F ₂)	0(0,0A ₁)	388.433275(29)
	(0001, F ₂)	(0001, F ₂)	1(1,0F ₁)10 ¹	-0.275717(17)
	(0001, F ₂)	(0001, F ₂)	2(0,0A ₁)10 ³	0.168545(22)
	(0001, F ₂)	(0001, F ₂)	2(2,0E)10 ³	-0.117473(42)
	(0001, F ₂)	(0001, F ₂)	2(2,0F ₂)10 ⁴	0.55406(41)
	(0001, F ₂)	(0001, F ₂)	3(1,0F ₁)10 ⁶	-0.11535(25)
	(0001, F ₂)	(0001, F ₂)	3(3,0F ₁)10 ⁶	-0.20262(12)
	(0001, F ₂)	(0001, F ₂)	4(0,0A ₁)10 ⁹	-0.2638(35)
	(0001, F ₂)	(0001, F ₂)	4(2,0F ₂)10 ¹⁰	0.787(42)
$v_3 + v_4$	(0011, A ₁)	(0011, A ₁)	0(0,0A ₁)	-0.5210(26)
	(0011, A ₁)	(0011, A ₁)	2(0,0A ₁)10 ²	0.1185(70)
	(0011, A ₁)	(0011, A ₁)	4(0,0A ₁)10 ⁶	-0.2279(48)
	(0011, A ₁)	(0011, A ₁)	4(4,0A ₁)10 ⁷	-0.212(16)
	(0011, A ₁)	(0011, E)	2(2,0E)10 ³	0.185(33)

Table D.12 – Continued.

(0011, A ₁)	(0011, E)	$4(2,0E)10^7$	-0.157(25)
(0011, A ₁)	(0011, E)	$4(4,0E)10^8$	0.434(89)
(0011, A ₁)	(0011, F ₁)	$1(1,0F_1)10^2$	-0.682(42)
(0011, A ₁)	(0011, F ₁)	$3(1,0F_1)10^5$	0.394(85)
(0011, A ₁)	(0011, F ₁)	$3(3,0F_1)10^5$	0.164(20)
(0011, A ₁)	(0011, F ₁)	$4(4,0F_1)10^7$	-0.223(21)
(0011, A ₁)	(0011, F ₂)	$2(2,0F_2)10^3$	0.415(29)
(0011, A ₁)	(0011, F ₂)	$3(3,0F_2)10^5$	0.119(33)
(0011, E)	(0011, E)	$0(0,0A_1)$	-0.258662(30)
(0011, E)	(0011, E)	$3(3,0A_2)10^6$	0.169(25)
(0011, E)	(0011, F ₂)	$1(1,0F_1)10^2$	-0.191(84)
(0011, E)	(0011, F ₂)	$4(4,0F_1)10^8$	0.204(57)
(0011, F ₁)	(0011, F ₁)	$0(0,0A_1)$	-0.110913(34)
(0011, F ₁)	(0011, F ₁)	$1(1,0F_1)10^2$	-0.1852(93)
(0011, F ₁)	(0011, F ₁)	$2(0,0A_1)10^3$	-0.378(34)
(0011, F ₁)	(0011, F ₁)	$2(2,0E)10^3$	0.448(49)
(0011, F ₁)	(0011, F ₁)	$2(2,0F_2)10^3$	0.939(59)
(0011, F ₁)	(0011, F ₁)	$4(2,0E)10^8$	-0.159(60)
(0011, F ₁)	(0011, F ₂)	$1(1,0F_1)10^2$	0.1273(39)
(0011, F ₁)	(0011, F ₂)	$2(2,0E)10^5$	-0.185(13)
(0011, F ₁)	(0011, F ₂)	$2(2,0F_2)10^3$	-0.129(16)
(0011, F ₁)	(0011, F ₂)	$4(2,0F_2)10^8$	0.175(34)
(0011, F ₂)	(0011, F ₂)	$0(0,0A_1)$	-0.136510(24)
(0011, F ₂)	(0011, F ₂)	$1(1,0F_1)10^2$	-0.1166(71)
(0011, F ₂)	(0011, F ₂)	$3(1,0F_1)10^6$	-0.136(25)
(0011, F ₂)	(0011, F ₂)	$3(3,0F_1)10^6$	-0.179(24)
(0011, F ₂)	(0011, F ₂)	$4(0,0A_1)10^8$	0.426(52)
(0011, F ₂)	(0011, F ₂)	$4(2,0F_2)10^8$	0.549(79)
$d_{\text{rms}} \cdot 10^{-3}, \text{cm}^{-1}$	0.633		

The work is devoted to obtaining new high-precision information by studying high-resolution spectra of molecules of the spherical and asymmetric top type, as well as developing new and improving existing methods for analyzing the spectra of molecules in non-singlet electronic states. The study of rotational and vibrational-rotational spectra of polyatomic molecules in the gas phase has long been of fundamental importance for determining the exact molecular geometry in various vibrational states, for obtaining information on the internal force field, vibrational-rotational interaction parameters, dipole moments, calculating thermodynamic functions and, in general, for obtaining information on the relationship between the structure and physical properties of the molecule. In this work, the analysis of the positions of vibrational-rotational spectra lines of combination bands of the SiF₄, CD₄, C₂D₄, ClO₂ molecules and their isotopologues was performed for the first time. The inverse spectroscopic problem was solved for the studied bands. The obtained sets of spectroscopic parameters allow reproducing the values of excited energy levels with an accuracy not worse than the experiment. Using the obtained spectroscopic parameters of the combination bands of the SiF₄ molecule and the XTDS software package, the calculation of the line positions was performed for the first time and theoretical spectra of the "hot" bands of this molecule, up to the 14th polyad, were calculated. In addition, new high-precision spectra of the SiH₄ molecule were obtained and analysed to improve the data on the dipole moment parameters.

La thèse est consacrée à l'obtention de nouvelles informations de haute précision par l'étude de spectres à haute résolution de molécules de type sphérique et asymétrique, ainsi qu'au développement de nouvelles méthodes et à l'amélioration des méthodes existantes pour l'analyse des spectres de molécules dans des états électroniques non singlés. L'étude des spectres rotationnels et ro-vibrationnels des molécules polyatomiques en phase gazeuse est depuis longtemps d'une importance fondamentale pour déterminer la géométrie moléculaire exacte dans différents états vibrationnels, pour obtenir des informations sur le champ de force interne, les paramètres d'interaction vibrationnelle-rotationnelle, les moments dipolaires, pour calculer les fonctions thermodynamiques et, en général, pour obtenir des informations sur la relation entre la structure et les propriétés physiques de la molécule. Dans ce travail, l'analyse des positions des raies spectrales vibrationnelles-rotationnelles des bandes de combinaison des molécules SiF₄, CD₄, C₂D₄, ClO₂ et de leurs isotopologues a été réalisée pour la première fois. Le problème spectroscopique inverse a été résolu pour les bandes étudiées. Les ensembles de paramètres spectroscopiques obtenus permettent de reproduire les valeurs des niveaux d'énergie excités avec une précision qui n'est pas inférieure à l'expérimentale. En utilisant les paramètres spectroscopiques obtenus pour les bandes combinées de la molécule SiF₄ et le progiciel XTDS, le calcul des positions des raies a été effectué pour la première fois et les spectres théoriques des bandes « chaudes » de cette molécule, jusqu'à la 14^{ème} polyade, ont été calculés. De plus, de nouveaux spectres de haute précision de la molécule SiH₄ ont été obtenus et analysés pour améliorer les données sur les paramètres du moment dipolaire.